

**Flanders**  
State of  
the Art

20\_079\_1  
FH reports

# MOZES – Research on the Morphological Interaction between the Sea bottom and the Belgian Coastline

Working year 1

DEPARTMENT  
MOBILITY &  
PUBLIC  
WORKS

[www.flandershydraulics.be](http://www.flandershydraulics.be)

# MOZES – Research on the Morphological Interaction between the Sea bottom and the Belgian Coastline

Working year 1

Dujardin, A.; Houthuys, R.; Nnafie, A.; Röbbke, B.; van der Werf, J.; de Swart, H.E.; Biernaux, V.;  
De Maerschalck, B.; Dan, S.; Verwaest, T.

### Legal notice

Flanders Hydraulics is of the opinion that the information and positions in this report are substantiated by the available data and knowledge at the time of writing.  
 The positions taken in this report are those of Flanders Hydraulics and do not reflect necessarily the opinion of the Government of Flanders or any of its institutions.  
 Flanders Hydraulics nor any person or company acting on behalf of Flanders Hydraulics is responsible for any loss or damage arising from the use of the information in this report.

### Copyright and citation

© The Government of Flanders, Department of Mobility and Public Works, Flanders Hydraulics 2023  
 D/2023/3241/076

This publication should be cited as follows:

**Dujardin, A.; Houthuys, R.; Nnafie, A.; Röbbke, B.; van der Werf, J.; de Swart, H.E.; Biernaux, V.; De Maerschalc, B.; Dan, S.; Verwaest, T.** (2023). MOZES – Research on the Morphological Interaction between the Sea bottom and the Belgian Coastline: Working year 1. Version 4.0. FH Reports, 20\_079\_1. Flanders Hydraulics: Antwerp

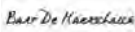
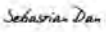
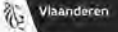
Reproduction of and reference to this publication is authorised provided the source is acknowledged correctly.

### Document identification

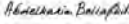
|                    |   |  |                 |
|--------------------|---|--|-----------------|
| Customer:          | Flanders Hydraulics / Coastal Division  | Ref.:  | WL2023R20_079_1 |
| Keywords (3-5):    | Coastal Morphology, Sediment Transport  |  |                 |
| Knowledge domains: | Hydraulics and Sediment > Morphology > Erosion / Sedimentation > Literature and desktop study<br>Hydraulics and Sediment > Morphology > Erosion / Sedimentation > Numerical modelling |  |                 |
| Text (p.):         | 155   | Appendices (p.):                                     | 6               |
| Confidential:      | <input checked="" type="checkbox"/> No  | <input checked="" type="checkbox"/> Available online |                 |

|            |  |
|------------|--|
| Author(s): | Dujardin, A.; Houthuys, R.; Nnafie, A.; Röbbke, B. |
|------------|--|

### Control

|                 | Name               | Signature  |
|-----------------|--------------------|--|
| Reviser(s):     | De Maerschalc, B.; | Getekend door: Bart De Maerschalc (Sig)<br>Getekend op: 2023-03-31 14:53:09 +02:0<br>Reden: Ik keur dit document goed<br>   |
|                 | Dan, S.            | Getekend door: Sebastian Dan (Signature)<br>Getekend op: 2023-03-31 12:38:50 +02:0<br>Reden: Ik keur dit document goed<br>  |
| Project leader: | Verwaest, T.       | Getekend door: Toon Verwaest (Signature)<br>Getekend op: 2023-03-31 12:26:00 +02:0<br>Reden: Ik keur dit document goed<br>  |

### Approval

|                   |               |   |
|-------------------|---------------|---|
| Head of Division: | Bellafkih, K. | Getekend door: Abdelkarim Bellafkih (Sign)<br>Getekend op: 2023-03-31 10:41:38 +02:0<br>Reden: Ik keur dit document goed<br> |
|-------------------|---------------|---|



# Abstract

*The MOZES-project (**M**Orfolgische interactie kustnabije **Z**Eebodem en **S**trand) focuses on the morphological interaction between the nearshore seabed (inner shelf) and the shoreline of the Belgian coast on time scales of months to centuries. The knowledge gained in this project aims to improve system understanding of the regional morphodynamics, which is essential for an efficient coastal management.*

*This report describes the progress of four subtasks (called Work Packages, WP) of the first working year. WP1 involves data collection to expand the overall covering of the historic elevation dataset of the Belgian coast. WP2 addresses the coupled shelf-shoreline long-term morphodynamics (10-100 years) by developing new idealized morphodynamic models. WP3 investigates the hypothesis of natural feeding of the beach by sediment transport over shoreface-connected sand ridges (sfc) using complex process-based numerical models (Delft3D Flexible-Mesh FlemCo model, openTELEMAC Scaldis-Coast model). Finally, WP4 addresses effects of the observed deepening of nearshore tidal channels on beach erosion and beach nourishments.*

*WP1: Inner shelf, nearshore bathymetric and beach topographic maps of the mid-1980s have newly been vectorized and converted to DEMs, showing the situation just after the extension of the Zeebrugge harbour breakwaters. Another DEM was built for the year 1866: a coastline without harbour breakwaters and three sfc (Trapegeer – Broersbank – Den Oever; Stroombank; and Wenduinebank – Paardenmarkt), as opposed to only the first one nowadays.*

*WP2: A new idealized morphodynamic shelf model was developed, which is capable of reproducing ridges that resemble the sfc observed on the Long-Island shelf (New York, USA), which were used to validate this new model. Furthermore, an existing shelf-shoreline coupled model, which was designed for the Long-Island micro-tidal coast, was modified so that it is more representative for the Belgium coast. Preliminary results are promising, but still many adjustments are needed in the two models (inclusion of tides, waves and sea-level rise, using more realistic bathymetry,...), which are suggested key topics for the next working year.*

*WP3: Preliminary results from the complex morphological models for years 1866 and 2015 indicate landward sediment transport over the nearshore parts of sfc towards the beaches. Further research is needed to examine whether this landward directed sediment indeed nourishes the beaches (called natural feeding). Moreover, the interaction of tide and waves relevant for this landward directed has to be investigated in more detail.*

*WP4: Analysis of the large-scale morphological changes between 1984 – 1987 and 2022 showed a landwards and northeastwards movement of the sfc and the tidal channels that separate these ridges from the coastline. A deepening of those channels is observed, although doubts on the vertical accuracy of the 1980's map prohibited the execution of reliable volume balances. An analysis of beach and shoreface nourishment intensity showed that storm events, changes in (safety) policy or nourishment method and other human factors are the main drivers behind nourishment intensity and obscure a possible correlation with the deepening of nearshore tidal channels.*

# Contents

|  |      |
|--|------|
| Abstract .....   | III  |
| Contents .....   | IV   |
| List of tables.....  | VII  |
| List of figures .....  | VIII |
| List of abbreviations .....  | XII  |
| Introduction.....  | 1    |
| 1 Data Acquisition.....  | 6    |
| 1.1 Vectorising pre-2000 maps of beach, shoreface and inner shelf..... | 6    |
| 1.1.1 Context and aim .....  | 6    |
| 1.1.2 Preparatory research about the content and information .....     | 6    |
| 1.1.3 Preparatory research about projection and units.....             | 8    |
| 1.1.4 List of available maps .....                                     | 9    |
| 1.1.5 Outsourcing of the vectorisation work.....                       | 15   |
| 1.1.6 Preparation of the outsourcing .....                             | 16   |
| 1.1.7 Control of the delivery.....                                     | 17   |
| 1.1.8 Progress of the vectorisation work.....                          | 17   |
| 1.1.9 Further processing: construction of DEMs.....                    | 17   |
| 1.2 Use of GIS in coastal morphology.....                              | 21   |
| 1.3 Chart series "Vlaamse Banken" .....                                | 22   |
| 1.3.1 Digitisation within QUEST4D .....                                | 22   |
| 1.3.2 Additional data from the Stessels 1866 map .....                 | 30   |
| 1.3.3 Creating the TIN.....  | 30   |
| 1.3.4 Converting MLWS to TAW and NAP .....                             | 32   |
| 1.3.5 Creating and exporting the DEM .....                             | 33   |
| 1.4 Exploration of other historic data .....                           | 35   |
| 1.4.1 MOW – ATO – Dienst Fotogrammetrie - Topografie.....              | 35   |
| 1.4.2 Vakgroep Archeologie UGent .....                                 | 36   |
| 1.4.3 INBO.....  | 37   |
| 2 Modelling coupled shelf-shoreline long-term morphodynamics.....      | 38   |
| 2.1 Introduction.....  | 38   |
| 2.1.1 Geographical setting.....  | 38   |
| 2.1.2 Research question .....  | 39   |

|       |  |     |
|-------|--|-----|
| 2.2   | Morphodynamic shelf model .....  | 41  |
| 2.2.1 | Model description.....   | 41  |
| 2.2.2 | Methodology .....  | 42  |
| 2.2.3 | Results and discussion .....   | 44  |
| 2.3   | Coupled shelf-shoreline model.....   | 49  |
| 2.3.1 | Coupled Model .....  | 49  |
| 2.3.2 | Methodology .....  | 50  |
| 2.3.3 | Results and discussion .....   | 51  |
| 2.4   | Summary and outlook .....  | 55  |
| 3     | Research on natural feeding of the beach over shoreface-connected ridges .....                     | 56  |
| 3.1   | Introduction.....  | 56  |
| 3.2   | Study area.....  | 56  |
| 3.3   | Methodology .....  | 59  |
| 3.3.1 | The FM-FlemCo model .....  | 59  |
| 3.3.2 | SedTRAILS analysis.....  | 69  |
| 3.3.3 | The Telemac Scaldis-Coast model .....  | 71  |
| 3.4   | Results .....  | 77  |
| 3.4.1 | Sediment transport.....  | 77  |
| 3.4.2 | SedTRAILS .....  | 81  |
| 3.4.3 | Sediment transport in Scaldis-Coast.....   | 87  |
| 3.5   | Discussion .....   | 90  |
| 3.6   | Conclusions.....   | 91  |
| 4     | Effect of gradual deepening of nearshore tidal channels on beach erosion.....                      | 93  |
| 4.1   | Literature quick-scan on the morphological evolution of the Belgian shelf and coastline.....       | 93  |
| 4.1.1 | Evolution of the Belgian shelf and coastline since the last ice age .....                          | 93  |
| 4.1.2 | Geology of the sand banks on the Belgian shelf .....   | 103 |
| 4.1.3 | Evolution of the Coastal Banks and nearshore tidal gullies since the 16 <sup>th</sup> century..... | 106 |
| 4.1.4 | Summary.....   | 113 |
| 4.2   | Data analysis for the Belgian coast.....   | 114 |
| 4.2.1 | Large-scale morphological change of the inner shelf between 1984-87 and 2022 .....                 | 114 |
| 4.2.2 | Study of the (beach) nourishments at the Belgian coast since the 1980's .....                      | 123 |
| 4.2.3 | Study of cross-shore profiles since the year 2000.....   | 129 |
| 4.3   | Literature review and data analysis for the Dutch coast.....                                       | 135 |
| 4.3.1 | Introduction.....  | 135 |
| 4.3.2 | Quick scan of nourishments and morphological evolution of channels along the Dutch coast           | 135 |

|              |   |     |
|--------------|---|-----|
| 4.3.3        | Oostgat case study.....   | 141 |
| 4.4          | Conclusion .....  | 144 |
| 5            | Conclusions and outlook .....   | 146 |
| 5.1          | Data acquisition .....  | 146 |
| 5.2          | Modelling long-term morphodynamics.....   | 146 |
| 5.3          | Natural feeding of the beach.....   | 147 |
| 5.4          | Effects of gradual deepening of nearshore tidal channels on beach erosion and nourishment intensities ..... | 148 |
| 6            | References.....   | 150 |
| Appendix 1   | Documents on the outsourced vectorization work.....   | A1  |
| Appendix 2   | Supplementary info on the setup of the longterm morphodynamic models.....                                   | A2  |
| Appendix 2.1 | Supplementary info on §2.2 (WP 2, Activity 1) .....   | A2  |
| Appendix 2.2 | Supplementary info on §2.3 (WP 2, Activity 2) .....   | A3  |
| Appendix 2.3 | Adjustments in the Delft3D model code .....   | A6  |

## List of tables

|  |     |
|--|-----|
| Table 1 – List of abbreviations.....   | XII |
| Table 2 – List of available beach maps, scale 1/1000.....  | 9   |
| Table 3 – List of available nearshore maps, scale 1/5000.....  | 12  |
| Table 4 – List of available inner shelf maps, scale 1/20,000. ....   | 14  |
| Table 5 – Progress of the outsourced vectorisation work.....   | 18  |
| Table 6 – DEMs made of vectorised data.....  | 19  |
| Table 7 – Largest and overall residual errors while georeferencing. ....   | 28  |
| Table 8 – Observed errors in location of georeferenced landmarks on the map. ....  | 28  |
| Table 9 – Files used to generate the Stessels 1866 DEMs.....   | 33  |
| Table 10 – Size, spatial resolution and number of cells of the three employed wave grids.....  | 61  |
| Table 11 – Data sources used to create the model bathymetry of the Delft3D Flexible Mesh-Flemish Coast Model. ....   | 62  |
| Table 12 – Overview of selected model parameter settings and essential features of the FM-FlemCo model and comparison with the Telemac Scaldis-Coast model (Wang et al., 2021; Kolokythas et al., 2020 & 2021). .... | 64  |
| Table 13 – Definition of the coastal morphologic zones according to Houthuys et al. (2022). ....   | 124 |
| Table 14 – Overview of the physical and numerical parameters of the coupled shelf-shoreline model. ....  | A5  |

# List of figures

Figure 1 – Map of the research area, present day (2021) en 19<sup>th</sup> century (1866) situation..... 2

Figure 2 – 2 m-DEM of vectorised survey Spring 1983 between Blankenberge and Zeebrugge..... 20

Figure 3 – 2 m-DEM of vectorised survey Spring 1983 between Zeebrugge and Zwin..... 20

Figure 4 – 2 m-DEM of vectorised survey Spring 1985 between Zeebrugge and Zwin..... 20

Figure 5 – Mosaic 10 m-DEM of 1984, 1986 and 1987 inner shelf surveys. Sections in thin pink lines. .... 21

Figure 6 – Georeferencing the “kaart Stessels 1866” in ArcMap..... 23

Figure 7 – Quality of the georeferenced map. .... 24

Figure 8 – Accuracy of the paper map drawing at Oostende (background: CartoWeb.be (NGI, 2022a))..... 25

Figure 9 – Example of a erroneous isobath:..... 26

Figure 10 – Example of non-matching isobath and depth point at the Northern tip of the Buiten Ratel sandbank: ..... 26

Figure 11 – Example of a fold in the map, resulting in dislocation of the isobaths and gridlines..... 27

Figure 12 – Example of anomalies in the digitization by Janssens et al. (2012)..... 29

Figure 13 – vectorised isobaths on the Stessels map..... 30

Figure 14 – Initial TIN based on isobaths and depth points only. .... 31

Figure 15 – Resulting TIN based on isobaths, depth points and ridge and trough lines (shown in green),.... 31

Figure 16 – Conversion grid of GLLWS to TAW for Vlaamse Banken, ..... 32

Figure 17 – Conversion grid of LAT to NAP for the southern North Sea ..... 32

Figure 18 – Map of the research area. .... 38

Figure 19 – Schematic view of the Trowbridge (1995) mechanism. .... 39

Figure 20 – Block diagram showing the steps toward the design of the new coupled shelf-shoreline morphodynamic model. .... 40

Figure 21 – Model structure and study area ..... 41

Figure 22 – Setup of the idealised morphodynamic shelf model..... 41

Figure 23 – Results of run series "Flow over topography", ..... 44

Figure 24 – Results of run series “Initial erosion and deposition”, ..... 45

Figure 25 – Results of run series “Long-term shelf morphodynamics”: bed evolution. .... 46

Figure 26 – Results of run series “Long-term shelf morphodynamics”: sand ridge properties. .... 47

Figure 27 – Results of run series “Long-term shelf morphodynamics”: evolution of a shallower bed..... 48

Figure 28 – Coupled shelf-shoreline model..... 49

Figure 29 – Setup of run series "Couple-Exp*i*", *i* = 0,1,2,3'. .... 51

Figure 30 – Results of run series "Couple-Exp*i*", *i* = 0,1,2,3' (bathymetry)..... 52

Figure 31 – Results of run series "Couple-Exp*i*", *i* = 0,1,2,3' (shoreline evolution). .... 53

Figure 32 – Results of run series "Couple-Exp*i*",  $i = 0,1,2,3'$  (spatial distribution of wave energy density). 54

Figure 33 – Study area..... 58

Figure 34 – Bathymetry of the Belgian coast and the Western Scheldt mouth of the year 1866. .... 58

Figure 35 – Sedimentary composition of the seabed of the eastern Belgian coast and the adjacent Western Scheldt estuary mouth ..... 59

Figure 36 – Model domain and computational flow grid of the Delft3D Flexible Mesh-Flemish Coast Model. .... 60

Figure 37 – Overall and nested computational wave grids of the Delft3D Flexible Mesh-Flemish Coast Model. .... 61

Figure 38 – Comparison of the longshore sediment transport, ..... 67

Figure 39 – Comparison of the longshore sediment transport, ..... 68

Figure 40 – Flow chart of the SedTRAILS modelling methodology. .... 71

Figure 41 – Characteristic element sizes of the Scaldis-Coast TELEMAC2D base grid. .... 74

Figure 42 – Element size determination based on the local gradient of maximum velocity magnitude by use of GMSH Size Field options..... 74

Figure 43 – Mesh layout of the Scaldis-Coast wave propagation model (TOMAWAC)..... 75

Figure 44 – Overview of the bathymetric data for the model domain ..... 75

Figure 45 – Roughness field (Manning’s law) on the computational domain of Scaldis-Coast model. .... 76

Figure 46 – Longshore sediment transport, ..... 78

Figure 47 – Longshore sediment transport, ..... 78

Figure 48 – Cross-shore component of the year-averaged sediment transport simulated by Scaldis-Coast. 80

Figure 49 – Cross-shore component of the year-averaged sediment transport simulated by Scaldis-Coast at 750 m offshore. .... 81

Figure 50 – Results of a preliminary SedTRAILS analysis for the Belgian coast,..... 83

Figure 51 – Results of a preliminary SedTRAILS analysis for the Belgian coast,..... 83

Figure 52 – Results of a preliminary SedTRAILS analysis for the area of the sand ridge Trapegeer-Broersbank-Den Oever..... 84

Figure 53 – Results of a preliminary SedTRAILS analysis for the area of the sand ridge Stroombank..... 85

Figure 54 – Results of a preliminary SedTRAILS analysis for the area of the sand ridge (Wenduinebank-)Paardenmarkt..... 86

Figure 55 – Results of a preliminary SedTRAILS analysis for the Belgian coast performed for FM-FlemCo model Run038o ..... 87

Figure 56 – Residual sediment transport streamlines at Trapegeer – Broersbank – Den Oever, as simulated by Scaldis-Coast..... 88

Figure 57 – Residual sediment transport streamlines at Stroombank, Groote Rede and Wenduinebank, as simulated by Scaldis-Coast. .... 89

Figure 58 – Residual sediment transport streamlines at Paardenmarkt, as simulated by Scaldis-Coast. .... 89

Figure 59 – Belgian coastline around 10,450 cal BP..... 95

Figure 60 – Belgian coastline around 9,500 cal BP..... 96

|  |     |
|--|-----|
| Figure 61 – Belgian coastline around 8,000 cal BP. ....  | 97  |
| Figure 62 – Belgian coastline around 7500 cal BP.....  | 98  |
| Figure 63 – Belgian coastline between 5000 and 2800 cal BP. ....   | 99  |
| Figure 64 – Paleogeographic reconstruction of the Belgian shelf between 5000 and 2800 cal BP. ....                             | 100 |
| Figure 65 – Paleographic reconstruction of the Belgian coast between 2800 cal BP and 550 cal BP (1400 AD).<br>.....            | 102 |
| Figure 66 – Isopach map of seismic unit U7 (Mathys, 2009),.....  | 103 |
| Figure 67 – Position of the sandbanks with respect to former coastlines. ....  | 105 |
| Figure 68 – Georeferenced bathymetric charts dating from 1866, 1908, 1938 en 1969 in the Potje gully –<br>Trapegeer area. .... | 107 |
| Figure 69 – Morphologic evolution of the Potje gully and Den Oever shoreface-connected sand ridge. ....                        | 108 |
| Figure 70 – Evolution of the Kleine Rede (gully) and Stroombank.....   | 109 |
| Figure 71 – Morphologic evolution of the Kleine Rede gully and Stroombank sand ridge.....                                      | 109 |
| Figure 72 – Evolution of the Groote Rede (gully) and Stroombank. ....  | 110 |
| Figure 73 – Morphologic evolution of the Groote Rede gully between Oostende and Zeebrugge.....                                 | 111 |
| Figure 74 – Georeferenced bathymetric charts in the Paardenmarkt - Appelzak area. ....   | 112 |
| Figure 75 – Morphologic evolution of the Appelzak (gully) and Paardenmarkt sand ridge.....                                     | 113 |
| Figure 76 – Elevation difference map of the overlap area between the 1984/7 and the 2022 bathymetric<br>maps. ....             | 117 |
| Figure 77 – West coast: Contour line shift (top) and elevation difference (bottom) between 1987 and 2022.<br>.....             | 118 |
| Figure 78 – Middle coast: Contour line shift (top) and elevation difference (bottom) between 1984 and 2022.<br>.....           | 120 |
| Figure 79 – De Haan to Zeebrugge: Contour line shift (top) and elevation difference (bottom) between 1984/6<br>and 2022.....   | 121 |
| Figure 80 – East coast: : Contour line shift (top) and elevation difference (bottom) between 1986 and 2022.<br>.....           | 122 |
| Figure 81 – Coastal sections and stretches along the Belgian coast (Vandebroek et al., 2017). ....                             | 124 |
| Figure 82 – Nourishment intensity at the Belgian coast, per stretch from 1979 until 2019.....                                  | 125 |
| Figure 83 – Nourishment intensity at the Belgian coast, per stretch from 1979 until 2019.....                                  | 126 |
| Figure 84 – Morfologic evolution of the Potje gully and shoreface west of Koksijde.....  | 130 |
| Figure 85 – Morfologic evolution of the Kleine Rede gully and shoreface at Middelkerke.....                                    | 130 |
| Figure 86 – Morfologic evolution of the Kleine Rede gully and shoreface at Oostende.....                                       | 131 |
| Figure 87 – Morfologic evolution of the Kleine Rede gully and shoreface 600 m east of Oostends eastern<br>breakwater. ....     | 131 |
| Figure 88 - Morfologic evolution of the Grote Rede gully and shoreface at De Haan. ....  | 132 |
| Figure 89 – Morfologic evolution of the Grote Rede gully and shoreface at Wenduine. ....                                       | 132 |
| Figure 90 – Morfologic evolution of the Grote Rede gully and shoreface east of Blankenberge marina.....                        | 133 |

Figure 91 – Morfologic evolution of the Appelzak gully and shoreface at Knokke-Zoute. .... 133

Figure 92 – Morfologic evolution of the Paardenmarkt sand ridge, Appelzak gully and shoreface in front of the Zwin. .... 134

Figure 93 – Nourishments in the area of Terschelling, Ameland and Schiermonnikoog (The Netherlands). 136

Figure 94 – Nourishments in the area of Vlieland, Texel and North-Holland (The Netherlands). .... 137

Figure 95 – Nourishments in the area of South-Holland (The Netherlands)..... 138

Figure 96 – Nourishments in the area of the Dutch Delta. .... 139

Figure 97 – On- and offshore topography in the area of the Oostgat channel east of Zeebrugge (The Netherlands) and location of the five bed level transects illustrated in Figure 98 to Figure 100. .... 140

Figure 98 – Measured bed levels along the JARKUS-transects 2165 (top) and 2255 (bottom) located in the Oostgat channel (Zeeland, The Netherlands) in the period 1970 to 2022. The dark yellow area illustrates the minimum, the light grey area the maximum bed level through all illustrated measurements. The bright yellow area illustrates the most recent, i.e. the 2022 bathymetry. .... 142

Figure 99 – Measured bed levels along the JARKUS-transects 2349 (top) and 2499 (bottom) located in the Oostgat channel (Zeeland, The Netherlands) in the period 1970 to 2022. The dark yellow area illustrates the minimum, the light grey area the maximum bed level through all illustrated measurements. The bright yellow area illustrates the most recent, i.e. the 2022 bathymetry. .... 143

Figure 100 – Measured bed levels along the JARKUS-transect 2597 located in the Oostgat channel (Zeeland, The Netherlands) in the period 1970 to 2022. The dark yellow area illustrates the minimum, the light grey area the maximum bed level through all illustrated measurements. The bright yellow area illustrates the most recent, i.e. the 2022 bathymetry..... 144

Figure 101 – Schematic view of the structure of the coupled shelf-shoreline model. .... A3

Figure 102 – Setup of the coupled shelf-shoreline model. .... A4

## List of abbreviations

Table 1 – List of abbreviations.

|       |   |
|-------|---|
| BeSPO | Belgian Science Policy Office   |
| DEM   | Digital Elevation Model   |
| dm    | decimeter   |
| FH    | Flanders Hydraulics   |
| GLLWS | Gemiddeld Laag Laag Water Springtij = Mean Low Low Water Spring tide  |
| HHWS  | High High Water Spring tide   |
| LAT   | Lowest Astronomical Tide  |
| LLWS  | Low Low Water Spring tide   |
| MLWS  | Mean Low Water Spring tide  |
| MLLWS | Mean Low Low Water Spring tide  |
| MOZES | <b>MO</b> rfolgische interactie kustnabije <b>ZE</b> ebodem en <b>Str</b> and   |
| NAP   | Normaal Amsterdams Peil, the Dutch vertical topographical reference level ( = Amsterdam Ordnance Datum; equivalent to mean sea level) |
| SB    | single-beam echosounding  |
| SBO   | Strategische Basis Onderzoek  |
| sdcr  | shoreface-detached sand ridge   |
| sfcr  | shoreface-connected sand ridge  |
| TAW   | Tweede Algemene Waterpassing, the Belgian vertical topographical reference level  |
| TIN   | triangulated irregular network  |
| TKI   | Topconsortium voor Kennis en Innovatie (Nederland)  |
| tsr   | tidal sand ridge  |
| VLIZ  | Vlaams Instituut voor de Zee (Flanders Marine Institute)  |

# Introduction

The Flanders Hydraulics MOZES-project (**MO**rfolgische interactie kustnabije **ZE**ebodem en **Str**and) focuses on the morphological interaction between the nearshore seabed and the shoreline of the Belgian (Flemish) coast on time scales from months to centuries. The knowledge gained in this project aims at an improvement of the system understanding of the regional morphodynamics, which is essential for an efficient coastal management.

Within the MOZES-project, Flanders Hydraulics (FH) is collaborating together with Antea Group (international consultant), the Utrecht University and the Dutch research institute Deltares. The project was granted for one year and started in 2022. It is three times extendable for another year, resulting in a maximum duration of four years. At the start of the project 4 research topics were formulated:

- Data acquisition:
  - Digitize/georeference/vectorize older depth soundings Vlaamse Hydrografie (since 1960). Selection of prioritized areas and/or periods in time.
  - Digitize/georeference/vectorize Eurosense maps (1/1000, 1/5000) predating the year 2000.
  - Exploration of other data sources, including beach and shoreface nourishments.
- Development of an idealized morphodynamic model, capable of simulating the long-term evolution of near-shore tidal gullies and (shoreface-connected) sand ridges. Slow changes in the hydro-meteo climate should not be neglected.

Areas of interest are the morphological systems of (i) Potje gully – Trapegeer/Broersbank/Den Oever sand ridges, (ii) Kleine Rede gully – Stroombank sand ridge and (iii) Grote Rede gully – Wenduine sand ridge and Appelzak gully – Paardenmarkt sand ridge. All three locations showed shoreface-connected sand ridges in the 19<sup>th</sup> century (cfr. Stessels map 1866), but nowadays only the Potje gully – Trapegeer/Broersbank/Den Oever system remains attached to the shore. Stroombank has been cut by the access channel to the harbour of Oostende, and the 19<sup>th</sup> century Wenduinebank/Paardenmarkt system changed drastically since the development of the harbour of Zeebrugge at the beginning of the 20<sup>th</sup> century and its extension in the 1980's (Figure 1).
- Test the hypothesis of natural feeding of the shoreline by sediment transport over the shoreface-connected ridges with available process based numerical models. Comparison of 19<sup>th</sup> century and present day situation.
- Study the effect of the gradual deepening of near-shore tidal gullies during the last decades on the nourishment intensity to maintain the shoreline at its position. Research can be done by data analysis and/or numerical modelling, priority research areas might be defined and sea level rise should be taken into account.

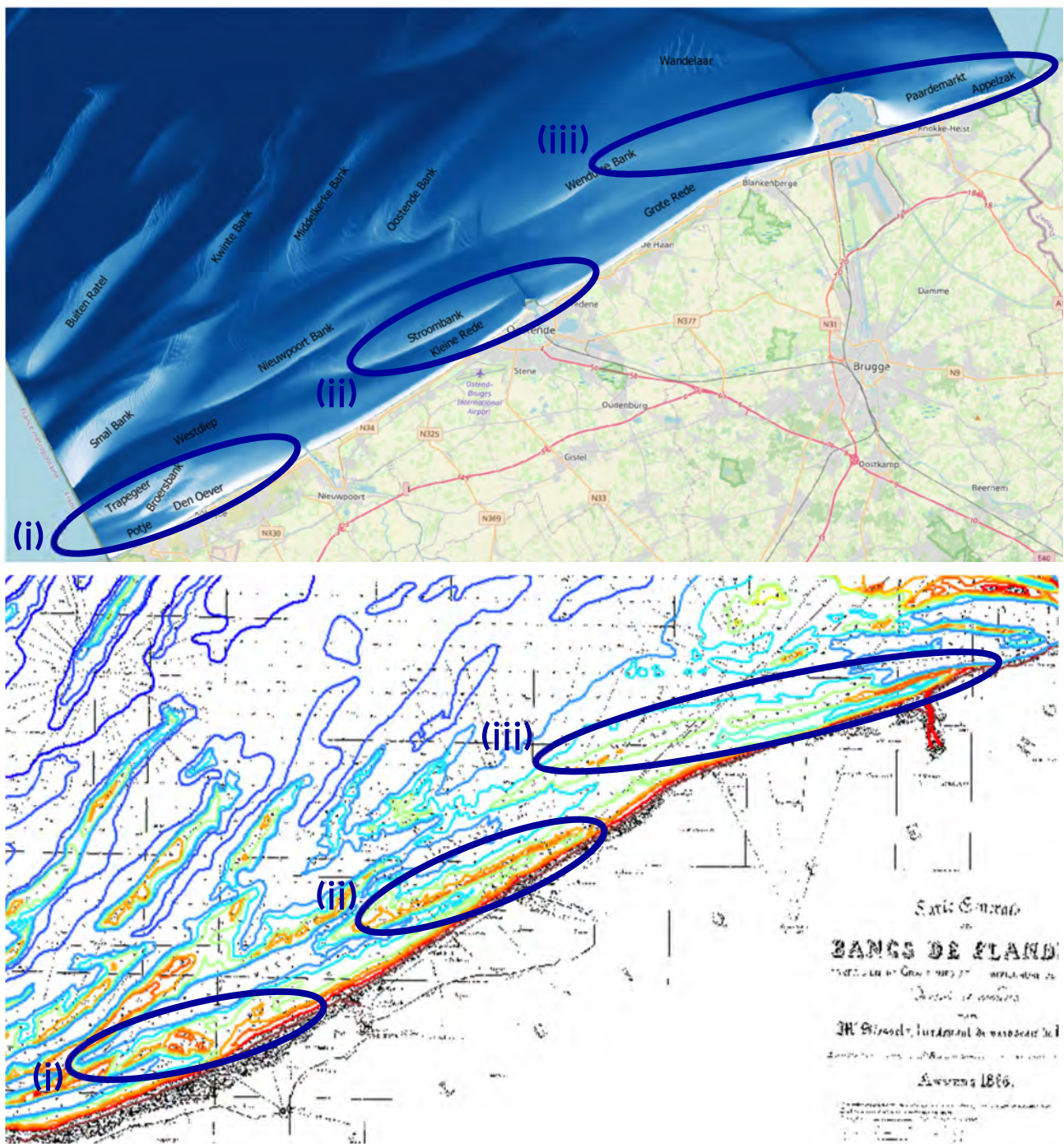


Figure 1 – Map of the research area, present day (2021) en 19<sup>th</sup> century (1866) situation.

The 4 research topics were detailed into 4 Work Packages for the first working year as follows:

### 1. Data acquisition

Work Package 1 aims at gathering as much data as possible which can be of interest to answer the research questions within the MOZES-project. The focus lies on collecting old bathymetric and topographic data that were not yet available in a vectorized format in order to make DEMs covering the whole area of interest at specific times (e.g. 1866 before the construction of the coastal harbours, or late 1980's after the extension of Zeebrugge). These data can be used as inputs for the numerical models and will assist in the research on the morphological evolution of the nearshore gullies and sand ridges on a time-scale of decades. Several subtasks were defined:

- a. Vectorizing Eurosense data preceding the year 2000  
Scans of (paper) maps covering the whole coastal area for certain years are available at Vlaamse Hydrografie. Beach maps have a typical scale of 1/1000 and shoreface maps a scale of 1/5000.
- b. Vectorizing depth soundings Vlaamse Hydrografie  
Scans of (paper) maps covering the nearshore zone (scale 1/20.000) are available at Vlaamse Hydrografie. The area extending from the French till the Dutch border and ca. 10 km seawards from the shore, are covered by three maps called: Zuydcoote – Westende, Westende – De Haan and Wielingen – Scheur.
- c. Vectorizing maps Vlaamse Banken (Stessels, 1866)  
The 1866 map of the Vlaamse Banken (called the Stessels map) has already been scanned, georeferenced and (partly) vectorized within the Quest4D-project. A quality control and analysis of the induced errors will be carried out before vectorizing the remaining data of the map.
- d. Exploration of other old data  
Inventory potentially interesting data to study the morphological evolution of the coastline over the past decades. These data might be lists of beach/shoreface nourishments, old topographic maps, old navigation charts, aerial photographs for photogrammetry purposes, oblique aerial pictures, old beach profiles, dune vegetation maps, ...
- e. Set up of a project-GIS database  
A GIS database containing all relevant data gathered within the MOZES-project will be set up in dialogue with FH's GIS manager.

Tasks a. and b. of this Work Package are outsourced. The choice of zones and periods in times is defined in agreement with the other Work Packages within the MOZES-project. Quality control and interpretation of the delivered data is done by the MOZES-project team.

### 2. Modelling of long-term morphodynamics of shoreface-connected sand ridges

Work Package 2 consists of the development of an idealized numerical model set which is capable of simulating the slow morphodynamics (time scales of tens and hundreds of years) of coastal-attached sandbanks and channels. This model set is based on an idealized representation of the Belgian coastal zone (schematized tide, wind and waves, bottom, coastline, etc.). It is important to note that these idealized model instruments are mainly intended to increase understanding of the system behavior. An important benchmark here is that this instrumentation must be able to reproduce the typical large-scale characteristics of coastal-attached sandbanks (correct dimensions and orientations of the banks/channels in relation to the coastline, etc.). As soon as this modeling tool can simulate these banks/channels, it will be subsequently (time permitting) linked to a coastline model to study the morphodynamic interaction between the banks/channels with the coastline.

In this first working year, the focus is mainly on the development of the idealized model in such a way that it can be used for general research and management questions. These developments will also need to prove that the model set can be used in case studies for specific areas like (parts of) the Belgian coast in later working years of the MOZES-project. For example, the current state of the Belgian coast could be compared to the situation before the development of the Flemish coastal ports (1866).

### **3. Research on natural feeding of the beach over shoreface-connected sand ridges**

With detailed process based morphological models, sediment transport calculations are performed based on the present day bathymetry (situation with 1 shoreface-connected sand ridge, namely Trapegeer – Broersbank – Den Oever) and the bathymetry of 1860/1866 (situation with 3 shoreface-connected sand ridges, namely (i) Trapegeer – Broersbank – Den Oever, (ii) Stroombank and (iii) Wenduine Bank – Paardenmarkt). This makes it possible to compare the sediment transport paths before the development of the coastal ports with the sediment transport paths in the present situation, and to test the hypothesis of the natural feeding of the coastline through sediment transport over the shoreface-connected sand ridges.

Already existing morphological models of the Flemish Coast, which are suitable for the sediment transport calculations, are the Delft3D Flexible Mesh Flemish Coast (FlemCo) model (Röbke *et al.* 2020, Grasmeijer *et al.*, 2020) and the Telemac Scaldis-Coast model (Kolokythas *et al.*, 2020). In the MOZES-project, the FlemCo model is further developed and calibrated with a focus on longitudinal sediment transports of the Flemish coast and possibly additionally with a focus on a hindcast period (e.g. ca. 1984 – 1994).

The 19<sup>th</sup> century bathymetry, consisting of the 1866 map of the Flemish Banks (Vlaamse Banken) and bathymetric recordings of the Western Scheldt from 1860 is being built into both morphological models. After all, the morphological changes in the mouth of the Western Scheldt might have an important impact on the hydrodynamics in the estuary area (Vlakte van de Raan, Oostgat, Appelzak). The same hydrodynamic boundary conditions are applied in the sediment transport calculations for both the current situation and the 1860-1866 period. Possible changes in wave climate due to climate change are neglected, however sea level rise is taken into account (adjustment of the A0 component in the model).

Finally, it is important to note that within this first working year, the aim is mainly to gain insight into the results to be expected from the different models and their reliability, rather than to define the best morphological model. Furthermore, the application of three different model approaches (Scaldis-Coast, FlemCo and soon also the idealized model) provides additional insight into the (un)certainty of the models, based on the variety of answers to the research questions.

### **4. Effect of gradual deepening of nearshore tidal channels on beach erosion and beach nourishments**

Literature review and data analysis provide an initial assessment of the morphological evolution of the nearshore tidal gullies and (shoreface-connected) sand ridges on a time scale of decades to centuries. Hotspots in shoreface and beach nourishment intensity are defined. Combination of the observed morphological evolution and the conducted nourishment intensities can give an insight on the effects of the (observed) gradual deepening of the nearshore tidal channels on the intensity of nourishments needed to sustain the coastline at its present location. Further research can then be focused on the most problematic zones along the Belgian coast.

The literature review will include a search for analogue cases in other areas around the world (e.g. northern France, The Netherlands, USA Long Island).

In a next phase, after the literature review and the data-analysis, it will be possible to use numerical models to investigate the impact of the deepening of the gullies on the hydrodynamics and sediment transport. This can be done by either introducing a (schematized) deepening of the gullies or by comparing a situation in the past (e.g. 1986, after the extension of the harbour of Zeebrugge) with the present day situation.

Each of these Work Packages is reported in detail below in the subsequent chapters.

# 1 Data Acquisition

A thorough study of the relationship between nearshore large bedforms and the evolution of the coast requires good-quality historic bathymetric and topographic data of the nearshore and shore area over the past decades, even centuries. This Work Package 1 of the MOZES project attempts to collect, inventory and make available an overall covering historic elevation dataset of the Belgian coast in the currently used digital formats. As large quantities of data are available, a selection is made of data most valuable for the work in the first project year.

## 1.1 Vectorising pre-2000 maps of beach, shoreface and inner shelf

### 1.1.1 Context and aim

The morphological state and evolution of the Flemish coast is excellently documented by annual, often biannual surveys since 2000. Altimetric and volumetric trends of morphological change have been detected and quantified, and morphological processes have been proposed to describe and explain coherent patterns (Houthuys *et al.*, 2022). It was attempted to single out natural from man-induced morphological change, but this proved to be very difficult as the amount of interaction, mainly dredging and sand nourishment, was very high during the last two decades.

Due to the repetitive character of the work involved, it was decided to source the actual vectorisation work out. Our task is to select and prepare the maps to be vectorised, to control this work and to further process the digital information into DEMs.

### 1.1.2 Preparatory research about the content and information

#### Beach and dune foot maps

These 1/1000 maps, "situatieplannen", were routinely made by Eurosense on commission of "Dienst der Kust" (predecessor of Afdeling Kust) since the late 1970s till 2004. Not all maps ever produced have been retrieved. The maps are the processed result of stereophotogrammetric survey flights done at a low flight altitude during low water, using a stabilised small aircraft equipped with a professional vertical photo camera with a wide-angle photographic lens. They were stereoscopically elaborated in elevation contours and points. Because of their large scale, a single survey flight of the Flemish coast is represented in a set of 43 adjacent map sheets. They are usually based on a survey flight performed on a single day in the time span of one or two hours.

They show:

- a) fixed reference marks and texts: frame, coordinate grid, legend, caption page with information on the survey, section boundaries and numbers, scale, north arrow, ...
- b) fixed planimetric elements: seawall top, streets, buildings, stakes on the beach, ...
- c) variable planimetric elements: contour of groins on the beach, seawall toe line, osier hedges, ...
- d) variable altimetric elements: elevation contour lines (full lines every metre and dashed lines every half metre), elevation points (mostly fixed marks used for orienting the stereo couples)

The altimetric elements (d) are the basic information needed to produce elevation models. In order to control gaps in the spatial coverage with information, it is also useful to obtain outlines of the groins and seawalls. They can be filled with the elevation of these elements copied from the earliest available DEM.

The elevation contours can be provided as 2D polyline shapefiles with the elevation stored in a numeric attribute field. The elevation points can be provided as 2D point shapefiles with the elevation stored likewise. Points are mass input and 2D contour lines are hard-line input for the GIS elevation surface building tool. The groin and seawall outlines can be made available as 2D polylines lacking elevation information.

The maps' reference system is Lambert 1972. All elevation information is in Z MOW. More recently, elevation data in coastal monitoring is being processed in TAW. The conversion is:  $Z (TAW) = Z (MOW) - 0.11 \text{ m}$ .

### Nearshore maps

These 1/5000 maps, "vooroeverlodingen", were routinely made by Eurosense on commission of "Dienst der Kust" (predecessor of Afdeling Kust) since the late 1980s till about 2000. Not all maps ever produced have been retrieved. The maps are the processed result of single-beam (SB) echosoundings of the nearshore area done during high water. Most of the soundings were done using a dedicated hovercraft that could perform measurements in very shallow water. They were cartographically reported by selected depth points arranged in tracks perpendicular to the coastline. A single echosounding survey of the Flemish coast is represented in a set of 8 adjacent map sheets. They are usually based on surveys conducted during 10 to 15 survey days that may, due to limiting conditions, be separated by several weeks in a single measurement campaign.

They show:

- a) fixed reference marks and texts: frame, coordinate grid, caption page with information on the survey, location names, scale, north arrow, ...  
Observations from about 1970 to 2000 are relatively extensive and systematic, yet they have not been preserved in digital form. Surveys used to be converted into contour lines and depth points and were stored as paper maps. The information in them is detailed and accurate enough to endeavour to vectorise it and derive digital elevation models (DEMs). They will then considerably extend our time series of DEMs since 2000.
- b) fixed planimetric elements: schematised street axes, groin outlines, seawall top, ...
- c) variable altimetric elements: depth points and manually interpolated depth contour lines every metre

The depth points of (c) are the basic information needed to produce elevation models. The depth contour lines represent an interpretation that is considered unnecessary for the production of DEMs comparable to the DEMs that are still made today based on nearshore SB echosoundings.

The elevation points can be provided as 2D point shapefiles with the elevation stored in a numeric field attribute. Points are then mass input for the GIS elevation surface building tool.

The maps' reference system is UTM31 based on ED50. All depth information is in dm with respect to Z MOW. More recently, depth data in coastal monitoring is being processing in TAW. The conversion is:  $Z (TAW) = Z (MOW) - 0.11 \text{ m}$ . Negative depths represent elevation in dm on the beach.

### Inner shelf maps

These 1/20,000 maps, "kustnabije lodingen", were routinely made by the Hydrographic Service of Dienst der Kust (Coastal Division) since the late 1950s. The survey programme continues today. Until the 1990s, only paper maps are preserved as the processed result of single-beam (SB) echosoundings of the inner shelf area. Most of the surveys were done during high water using a dedicated hydrographic vessel and often using shallow speedboats that could perform measurements in very shallow water. They were cartographically reported by selected depth points arranged in tracks perpendicular to the local overall slope gradient. A complete echosounding survey of the Flemish inner shelf is represented in a set of 3 adjacent map sheets. They are usually based on surveys conducted during several survey days that may, due to limiting conditions, be separated by several weeks or months in a single measurement campaign covering one survey sheet.

The maps show:

- a) fixed reference marks and texts: frame, coordinate grid, caption page with information on the survey, location names, navigation marks, wrecks, scale, north arrow, ...
- b) fixed planimetric elements: schematised seawall, harbours dams, groins, ...
- c) variable altimetric elements: depth points and manually interpolated depth contour lines every metre

The depth points of (c) are the basic information needed to produce elevation models. The depth contour lines represent an interpretation that is considered unnecessary for the production of DEMs comparable to the DEMs that are still made today based on nearshore SB echosoundings.

The elevation points can be provided as 2D point shapefiles with the elevation stored in a numeric field attribute. Points are then mass input for the GIS elevation surface building tool.

The maps' reference system is UTM31 based on ED50. All depth information is in dm, most usually with respect to the local mean LLWS-surface (H-surface). Conversion rasters to convert this depth to elevations in TAW are available at the Hydrographic Service and at FH. Negative depths represent elevation in dm on the beach.

### 1.1.3 Preparatory research about projection and units

All maps show locations using a coordinate system which allows to integrate the data represented in the map with other geographic data layers. In geographic information, two common types of coordinate systems are used: geographic coordinate systems that use coordinates on a globe or sphere, and projected coordinate systems that project maps of the earth's spherical surface onto a two-dimensional Cartesian coordinate plane.

Some of the maps used in this project show gridlines or crosses marking geographical coordinates, but all show marks indicating either the projected system UTM31 based on ED50 or the Belgian Lambert 1972 system. The program cConvert provided by the National Geographic Institute (<https://www.ngi.be/website/hulpmiddelen-voor-transformatie-van-coordinaten/>) can be used to convert coordinates from one system to another.

All maps used in this project have been scanned into digital images by Coastal Division during the previous years. The image files can be displayed in GIS. In order to project them in the coordinate system used in our coastal research (i.e., Belgian Lambert 1972), they must be georeferenced. The Desktop ArcGIS used allows to perform a georeferencing procedure, that must be applied once in order to obtain a transformation that is then automatically adopted for the georeferenced image file.

The method of georeferencing applied to the images is Spline transformation based on several tens of control points distributed over the image area.

Scanning of maps that were rolled up or folded, produces locally correct geometry in parts of the map that however are overall ill aligned. It is thought that either a 3<sup>rd</sup> order polynomial or a spline transformation based on a sufficiently large number of control points thus produce a good result of the georeferencing procedure. In this project around 50, sometimes up to almost 100, coordinate marks are available in the image, and often, due to the distortion of the scanned originals, they are all needed for creating links in order to obtain a high-quality georeferenced image using the Spline transformation, which ensures optimal local geometrical accuracy.

After the links have been placed, the transformation information is stored in an auxiliary file .AUX.XML using the Update Georeferencing command. The original raster dataset is not changed. For use in other GIS or CAD packages, the image must be permanently transformed into a new, warped image. This can be done using the Rectify command, or by exporting the map to a geotiff file. It's a time demanding process that produces large files. It is not done routinely, only on demand of a subcontractor.

## 1.1.4 List of available maps

Table 2 to Table 4 list the available image files of beach maps (Eurosense), nearshore maps (Eurosense) and inner shelf maps (Hydrographic Service). These image files are available at Coastal Division and a copy is placed at this location on FH's fileservers:

[P:\20\\_079\\_MorfoInteract\3\\_Uitvoering\Deeltaak1\\_DataAcquisition\OudeKaarten\PlanscansKust](P:\20_079_MorfoInteract\3_Uitvoering\Deeltaak1_DataAcquisition\OudeKaarten\PlanscansKust).

Table 2 – List of available beach maps, scale 1/1000.

| Map and name of scan file                  | Date of survey | Coverage  | Remarks                            |
|--|----------------|---|------------------------------------|
| SIT_1983_0_OOST01.jpg (-OOST13)            | 04/02/1983     | Blankenb. - Cadzand                                 | 1 <sup>st</sup> available coverage |
| SIT_1983_0_MIDD01.jpg (-MIDD07)            | 04/02/1983     | Bredene - Wenduine                                  | 1 <sup>st</sup> available coverage |
| SIT_1983_1_MIWE01.jpg (-MIWE33)            | 18/05/1983     | De Panne – Blankenb.                                | 1 <sup>st</sup> complete coverage  |
| SIT_1983_1_OOST01.jpg (-OOST13)            | 18/05/1983     | Blankenb. - Cadzand                                 |                                    |
| SIT_1984_1_MIWE01.jpg (-MIWE33)            | 21/03/1984     | De Panne – Blankenb.                                | N° 10, 11, 12 missing              |
| SIT_1984_1_OOST01.jpg (-OOST13)            | 21/03/1984     | Blankenb. - Cadzand                                 |                                    |
| SIT_1984_2_OOST01.jpg (-OOST13)            | 30/10/1984     | Blankenb. - Cadzand                                 |                                    |
| SIT_1985_1_MIWE01.jpg (-MIWE33)            | 24/04/1985     | De Panne – Blankenb.                                |                                    |
| SIT_1985_1_OOST01.jpg (-OOST13)            | 24/04/1985     | Blankenb. - Cadzand                                 |                                    |
| SIT_1985_2_OOST07.jpg (-OOST10)            | 30/01/1986     | Knokke-Zoute - Lekkerbek                            | Special survey                     |
| SIT_1986_1_MIWE01.jpg (-MIWE33)            | 29/05/1986     | De Panne – Blankenb.                                |                                    |
| SIT_1986_1_OOST01.jpg (-OOST13)            | 26/05/1986     | Blankenb. - Cadzand                                 |                                    |
| SIT_1986_2_OOST01.jpg (-OOST13)            | 25/09/1986     | Blankenb. - Cadzand                                 |                                    |
| SIT_1987_1_MIWE01.jpg (-MIWE33)            | 18/04/1987     | De Panne – Blankenb.                                |                                    |
| SIT_1987_1_OOST01.jpg (-OOST13)            | 18/04/1987     | Blankenb. - Cadzand                                 |                                    |
| SIT_1987_2_MIWE01.jpg (-MIWE07, MIWE24-31) | 9/12/1987      | De Panne – Oostduinkerke;<br>Bredene – Blankenberge |                                    |
| SIT_1987_2_OOST01.jpg (-OOST13)            | 9/12/1987      | Blankenb. - Cadzand                                 |                                    |
| SIT_1988_1_MIWE01.jpg (-MIWE33)            | 23/04/1988     | De Panne – Blankenb.                                |                                    |
| SIT_1988_1_OOST01.jpg (-OOST13)            | 23/04/1988     | Blankenb. - Cadzand                                 |                                    |

|  |            |   |                      |
|--|------------|---|----------------------|
| SIT_1988_2_MIWE01.jpg (-MIWE07, MIWE24-33) | 1/10/1988  | De Panne – Oostduinkerke;<br>Bredene – Blankenberge | Scans with stripes   |
| SIT_1988_2_OOST01.jpg (-OOST13)            | 1/10/1988  | Blankenb. - Cadzand                                 |                      |
| SIT_1989_1_MIWE01.jpg (-MIWE33)            | 9/04/1989  | De Panne – Blankenb.                                | N° 01 and 17 missing |
| SIT_1989_1_OOST01.jpg (-OOST13)            | 9/04/1989  | Blankenb. - Cadzand                                 |                      |
| SIT_1989_2_MIWE01.jpg (-MIWE07, MIWE24-33) | 22/10/1989 | De Panne – Oostduinkerke;<br>Bredene – Blankenberge |                      |
| SIT_1989_2_OOST01.jpg (-OOST13)            | 22/10/1989 | Blankenb. - Cadzand                                 |                      |
| SIT_1990_0_MIWE01.jpg (-MIWE33)            | 16/03/1990 | De Panne – Blankenb.                                | After storm          |
| SIT_1990_0_OOST01.jpg (-OOST13)            | 16/03/1990 | Blankenb. - Cadzand                                 | After storm          |
| SIT_1990_1_OOST01.jpg (-OOST13)            | 27/05/1990 | Blankenb. - Cadzand                                 |                      |
| SIT_1990_2_MIWE01.jpg (-MIWE07, MIWE24-33) | 12/10/1990 | De Panne – Oostduinkerke;<br>Bredene – Blankenberge |                      |
| SIT_1990_2_OOST01.jpg (-OOST13)            | 12/10/1990 | Blankenb. - Cadzand                                 |                      |
| SIT_1991_0_MIWE25.jpg (-MIWE28)            | 7/03/1991  | De Haan   | Special survey       |
| SIT_1991_1_MIWE01.jpg (-MIWE33)            | 19/05/1991 | De Panne – Blankenb.                                | N° 11 missing        |
| SIT_1991_1_OOST01.jpg (-OOST13)            | 19/05/1991 | Blankenb. - Cadzand                                 |                      |
| SIT_1991_2_MIWE01.jpg (-MIWE07, MIWE24-33) | 27/10/1991 | De Panne – Oostduinkerke;<br>Bredene – Blankenberge |                      |
| SIT_1991_2_OOST01.jpg (-OOST13)            | 27/10/1991 | Blankenb. - Cadzand                                 |                      |
| SIT_1992_1_MIWE01.jpg (-MIWE33)            | 8/04/1992  | De Panne – Blankenb.                                |                      |
| SIT_1992_1_OOST01.jpg (-OOST13)            | 8/04/1992  | Blankenb. - Cadzand                                 |                      |
| SIT_1992_2_MIWE26.jpg (-MIWE27)            | 11/06/1992 | De Haan   | Special survey       |
| SIT_1992_3_MIWE01.jpg (-MIWE07, MIWE24-33) | 4/11/1992  | De Panne – Oostduinkerke;<br>Bredene – Blankenberge |                      |
| SIT_1992_3_OOST01.jpg (-OOST13)            | 4/11/1992  | Blankenb. - Cadzand                                 |                      |
| SIT_1993_1_MIWE01.jpg (-MIWE33)            | 30/04/1993 | De Panne – Blankenb.                                |                      |
| SIT_1993_1_OOST01.jpg (-OOST13)            | 30/04/1993 | Blankenb. - Cadzand                                 |                      |
|  | 7/01/1994  | De Panne – Blankenb.                                | All plans missing    |

|  |            |   |                   |
|--|------------|---|-------------------|
|  | 7/01/1994  | Blankenb. - Cadzand                                 | All plans missing |
| SIT_1994_1_MIWE01.jpg (-MIWE33)            | 1/06/1994  | De Panne – Blankenb.                                |                   |
| SIT_1994_1_OOST01.jpg (-OOST13)            | 1/06/1994  | Blankenb. - Cadzand                                 |                   |
| SIT_1994_2_MIWE01.jpg (-MIWE07, MIWE24-33) | 10/10/1994 | De Panne – Oostduinkerke;<br>Bredene – Blankenberge |                   |
| SIT_1994_2_OOST01.jpg (-OOST13)            | 10/10/1994 | Blankenb. - Cadzand                                 |                   |
| SIT_1995_1_MIWE01.jpg (-MIWE33)            | 22/05/1995 | De Panne – Blankenb.                                |                   |
| SIT_1995_1_OOST01.jpg (-OOST13)            | 22/05/1995 | Blankenb. - Cadzand                                 |                   |
| SIT_1995_2_MIWE21.jpg (-MIWE33)            | 12/11/1995 | Oostende – Blankenb.                                |                   |
| SIT_1996_1_MIWE01.jpg (-MIWE33)            | 27/03/1996 | De Panne – Blankenb.                                |                   |
| SIT_1996_1_OOST01.jpg (-OOST13)            | 27/03/1996 | Blankenb. - Cadzand                                 |                   |
| SIT_1996_2_KUST01.jpg (-KUST43)            | 14/01/1997 | Complete coast                                      |                   |

Table 3 – List of available nearshore maps, scale 1/5000.

| Map and name of scan file | Date of survey      | Coverage  | Remarks  |
|---------------------------|---------------------|---|--|
| VO_1986_0_(2maps).jpg     | 27/01, 22/03/1986   | Knokke-Zoute  |  |
| VO_1986_1_(2maps).jpg     | 6/05 to 3/06/1986   | Heist to Cadzand                                      | 1 <sup>st</sup> coverage Heist-Cadz.   |
| VO_1986_2_(2maps).jpg     | 29/09 to 17/10/1986 | Heist to Cadzand                                      |  |
| VO_1987_1_(3maps).jpg     | 28/04 to 12/06/1987 | Blankenb. to Cadzand                                  | 1 <sup>st</sup> coverage Blankenb.   |
| VO_1987_2_(4maps).jpg     | 17/09 to 5/11/1987  | De Haan to Cadzand                                    | 1 <sup>st</sup> coverage De Haan   |
| VO_1987_2_(1map).jpg      | 20 to 22/10/1987    | De Panne to Oostdk.                                   | 1 <sup>st</sup> coverage DP-Oostd.   |
| VO_1988_1_(3maps).jpg     | 28/04 to 20/05/1988 | Blankenb. to Cadzand                                  |  |
| VO_1988_2_(4maps).jpg     | 21/09 to 4/11/1988  | De Haan to Cadzand                                    |  |
| VO_1988_2_(1map).jpg      | 8 to 10/11/1988     | De Panne to Oostdk.                                   |  |
| VO_1989_1_(3maps).jpg     | 2 to 19/05/1989     | Blankenb. to Cadzand                                  |  |
| VO_1989_2_(4maps).jpg     | 19/09 to 3/11/1989  | De Haan to Cadzand                                    |  |
| VO_1989_2_(1map).jpg      | 28 and 29/11/1989   | De Panne to Oostdk.                                   |  |
| VO_1990_0_maart1990.jpg   | 13 and 14/03/1990   | De Haan   |  |
| VO_1990_1_(3maps).jpg     | 18 to 22/06/1990    | Blankenb. to Cadzand                                  |  |
| VO_1990_2_(4maps).jpg     | 17/09 to 23/10/1990 | De Haan to Cadzand                                    |  |
| VO_1990_2_(1map).jpg      | 5/11 to 5/12/1990   | De Panne to Oostdk.                                   |  |
| VO_1991_1_(3maps).jpg     | 22 to 31/05/1991    | Blankenb. to Cadzand                                  |  |
| VO_1991_2_(4maps).jpg     | 27/09 to 9/12/1991  | De Haan to Cadzand                                    |  |
| VO_1992_1_(7maps).jpg     | 1/04 to 23/06/1992  | Complete coast  | 1 <sup>st</sup> complete coverage<br>Sheet Oostdk-Middk<br>missing, use<br>"koppeling" |
| VO_1992_1_(2maps).jpg     | 1 and 2/04/1992     | France Littoral Est:<br>Dunkerque – Belgian<br>border | In UTM31 and Z MOW   |
| VO_1992_2_(3maps).jpg     | 30/10 to 8/12/1992  | Blankenb. to Cadzand                                  |  |

|  |                          |   |                                   |
|--|--------------------------|---|-----------------------------------|
| VO_1993_1_(7maps).jpg                                  | 22/03 to 22/06/1993      | De Panne – Westende and Oostende – Cadz.                |                                   |
| VO_1993_1_(2maps).jpg                                  | 1 and 2/06/1993          | France Littoral Est: Dunkerque – Belgian border         | In UTM31 and Z MOW                |
| VO_1993_2_(5maps).jpg                                  | 29/09 to 5/11/1993       | Middelkerke – De Haan and Heist – Cadzand               |                                   |
| VO_1993_strm_(4maps).jpg                               | 23/11/1993 to 9/02/1994  | De Panne – Oostdk. and Oostende – Zeebrugge             |                                   |
| VO_1994_1_(8maps).jpg                                  | 19/04 to 20/06/1994      | Complete coast  |                                   |
| VO_1994_2_(6maps).jpg                                  | 19/09 to 5/11/1994       | De Panne – Oostduink. and Oostende – Cadz.              |                                   |
| VO_1995_1_(6maps).jpg                                  | 19/04 to 21/06/1995      | Nieuwprtt. – Westende and Oostende – Cadz.              |                                   |
| VO_1995_2_(3maps).jpg                                  | 18/09 to 10/10/1995      | Oostende – Wenduine and Blankenberge                    |                                   |
| VO_1996_1_(8maps).jpg                                  | 4/03 to 11/06/1996       | Complete coast  |                                   |
| VO_1996_2_(8maps).jpg                                  | 16/09/1996 to 25/01/1997 | Complete coast except sections 106-111                  |                                   |
| VO_1997_1_(8maps).jpg                                  | 24/03 to 30/05/1997      | Complete coast  | Already available in digital form |
| VO_1997_2_(7maps).jpg                                  | 16/09 to 15/10/1997      | Nieuwpoort – Sint-Laureinsstrand and Oostende - Cadzand | Already available in digital form |
| 1998-2000 (50 maps): already available in digital form |                          |   |                                   |

Table 4 – List of available inner shelf maps, scale 1/20,000.

| Map and name of scan file   | Date of survey        | Coverage                   | Remarks  |
|-----------------------------|-----------------------|----------------------------|--|
| Wie-sch1960.pdf             | May-August 1960       | Wielingen-Scheur           | Sparse points on lines   |
| Wie-sch1961.pdf             | April-June 1961       | Wielingen-Scheur           | Sparse points on lines   |
| Wie-sch1962.pdf             | June-October 1962     | Wielingen-Scheur           | Sparse points on lines   |
| Wie-sch1962a.pdf (b)        | 1964 to 1967          | Wielingen-Scheur           | Sparse dispersed points and lines (plan b) with two details (plan a) |
| Wie-sch 64-67plan1.pdf (-5) | 1964 to 1967          | Wielingen-Scheur           | Sparse dispersed points<br>Five scans of same plan                   |
| Dh-cadz1966.pdf             | Illisible             | De Haan-Cadzand            | Illisible  |
| Wie-sch1968.pdf             | May-August 1968       | Wielingen-Scheur           | Sparse disperse points, incomplete coverage                          |
| Wie-sch1976.pdf             | May-September 1976    | Wielingen-Scheur           | Sparse dispersed points  |
| Wie-sch1986.pdf             | April-August 1986     | Wielingen-Scheur           | Points on lines  |
| Wie-sch1988.pdf             | March-June 1988       | Wielingen-Scheur           | Points on lines  |
| Wie-sch1990.pdf             | February-April 1990   | Wielingen-Scheur           | Points on lines  |
| Wie-sch1992.pdf             | February-April 1992   | Wielingen-Scheur           | Points on lines  |
| Wie-sch1994.pdf             | August 1994           | Wielingen-Scheur           | Points on lines  |
| Wie-sch1996.pdf             | Apr-Jun and Oct 1996  | Wielingen-Scheur           | Points on lines  |
| Wie-sch1998.pdf             | Jan-Apr and Sep 1998  | Wielingen-Scheur           | Points on lines  |
| Wie-sch2000.pdf             | Jan, Apr and Nov 2000 | Wielingen-Scheur           | Points on lines  |
| West-dh69.pdf               | May-September 1969    | Westende-De Haan           | Sparse dispersed points  |
| Ost-dh74-75.pdf             | June-October 1974     | Oostende-De Haan (p1)      | Sparse dispersed points  |
| Ost-dh74-75plan2.pdf        | June-September 1975   | Westende-Oostende (part 2) | Sparse dispersed points  |
| West-dh1979.pdf             | May-October 1979      | Westende-De Haan           | Sparse dispersed points  |
| West-dh1984.pdf             | March-May 1984        | Westende-De Haan           | Points on lines  |

|                 |                       |                    |                         |
|-----------------|-----------------------|--------------------|-------------------------|
| West-dh1989.pdf | April-June 1989       | Westende-De Haan   | Points on lines         |
| West-dh1993.pdf | February-March 1993   | Westende-De Haan   | Points on lines         |
| West-dh1997.pdf | October-Novbr 1997    | Westende-De Haan   |                         |
| ZUYWE_1967.pdf  | April-Sept 1967       | Zuydcoote-Westende | Sparse dispersed points |
| ZUYWE_1973.pdf  | July-October 1973     | Zuydcoote-Westende | Sparse dispersed points |
| ZUYWE_1978.pdf  | May-October 1978      | Zuydcoote-Westende | Sparse dispersed points |
| ZUYWE_1983.pdf  | June-October 1983     | Zuydcoote-Westende | Points on lines         |
| ZUYWE_1987.pdf  | March-June 1987       | Zuydcoote-Westende | Points on lines         |
| ZUYWE_1991.pdf  | March-April 1991      | Zuydcoote-Westende | Points on lines         |
| ZUYWE_1997.pdf  | Feb-Apr and Sep 1997  | Zuydcoote-Westende | Points on lines         |
| ZUYWE_2003.pdf  | Apr, Jun and Oct 2003 | Zuydcoote-Westende | Already in database?    |
| ZUYWE_2006.pdf  | January-July 2006     | Zuydcoote-Westende | Already in database?    |
| ZUYWE_2009.pdf  | February-April 2009   | Zuydcoote-Westende | Already in database?    |

### 1.1.5 Outsourcing of the vectorisation work

In view of the repetitive character of the vectorisation work, it was decided to outsource it in accordance with the MOZES project specifications. Terms of reference were made with the work specifications, the quality standards and the selection criteria of candidate subcontractors. The complete terms of reference are added in Appendix 1.

The selection of the service providers is based on the following principles:

- (1) price – 30 points
- (2) time in which a certain amount of work will be delivered – 30 points
- (3) quality of the work – 40 points:
  - (a) completeness – 15 points
  - (b) geometric accuracy – 10 points
  - (c) elevation accuracy – 10 points
  - (d) structure of the delivered files – 5 points

The subscribers were asked to deliver the vectorisation result of one scanned map of each of the map types of this project: SIT\_1985\_1\_OOST10.jpg for the beach maps, VO\_1982\_1\_8616.jpg for the nearshore maps and wie-sch1986.jpg for the inner shelf maps.

An invitation was sent on 16 June 2022 to Messelis Design (Lauwe), Sparks bvba (Sint-Pieters-Leeuw), GIM (Leuven), UGent and Vives (Kortrijk). The quotations were awaited by the 8<sup>th</sup> of July 2022. Only one subscription was received, by Sparks bvba. After this date, HoWest and Hogeschool Zeeland additionally expressed their interest.

The selection of the subcontractor was done according to section 4 of the work specifications (see Annex 1). The subscriber Sparks bvba fulfilled the selection criteria (see selection report in Annex 2) and was awarded the vectorisation work of project year 1.

#### 1.1.6 Preparation of the outsourcing

These tasks are common to the selection of service providers and the acceptance of deliveries:

#### Selection of the work package

In the tender stage, a test delivery was asked from the candidate service providers. The test involves the production of a vectorisation delivery according to the specifications of the tender documents, for one map of each type:

- beach map: SIT\_1985\_1\_OOST10.jpg
- nearshore map: VO\_1986\_1\_8616.tif
- inner shelf map: wie-sch1986.jpg

The maps were rather large, to give candidates an idea of the processing work involved. These three maps can immediately serve as they are in the TKI ShorelineS focus area Knokke.

Requested deliveries were ordered in packages of about 10 maps, which in view of the foreseen budget could be repeated 4 times in the first project year. The selection of the deliveries was discussed among the MOZES team. A first priority was the TKI ShorelineS study area from Zeebrugge to Zwin, survey before the first (1986) maintenance replenishment, i.e. Spring 1985. This was complemented by the first available nearshore survey of the area (Spring 1986) and an inner shelf bathymetric map of the same time (1986). Next came the vectorisation of the Spring 1983 survey (the first survey that covers the entire beach). And a survey of the inner shelf, in or close to 1983. The further progress is listed in Table 5.

#### Georeferencing

Most of the scanned beach maps have at the time of scanning been georeferenced using a 1<sup>st</sup> order polynomial affine transformation based on four control points. This is adequate for a quick visual inspection of the contents, but not sufficient for the accuracy required in this project, as the original paper maps were rolled or folded and are thus distorted. The nearshore maps and inner shelf maps have not even this basic georeferencing. Therefore, the maps of each vectorisation work package have to be georeferenced according to the method explained in §1.1.3. As this georeferencing is crucial for the accuracy of the result, it is done in this project before sending the images out for the vectorisation work.

#### Evaluation of vectorisation work by VLIZ

In the framework of the SBO CREST project, task "Recovery of existing data", VLIZ has vectorised elevation contours in beach maps 1 (Westhoek), 8 (Groenendijk), 17 and 18 (Mariakerke) of each spring survey over the period 1983-1996 (total of 14 surveys). These data can be downloaded as shapefiles from VLIZ Marine Data Archive: <https://mda.vliz.be/archive.php> sub CREST, 9\_Topography, Altimetry-Eurosense. The shapefiles contain:

- elevation contours every 0.5 m on the beach and every 1 m in the dune part
- they have carefully been digitised with a node density of about 4 to 5 points per metre along the lines
- the outlines of groins and seawall have not been digitised
- the features contain an attribute "hoogte\_m", which is the elevation in m like in the maps, i.e. with reference to the Z MOW datum

With respect to available planimetric reference elements, planimetric deviations vary from 0 to 2.5 m. The deviation is often systematically 2 to 2.5 m to the south. It is thought to have been occasioned by an insufficiently locally applied georeferencing. Apparently, the 1<sup>st</sup> order polynomial affine transformation based on four control points was used. Because 2 m is the raster resolution of the DEMs used in our database, it seems appropriate to redo the few sheets in the current vectorisation effort using the more elaborated 3<sup>rd</sup> order or spline georeferencing adopted now.

#### 1.1.7 Control of the delivery

Georeferenced plan packages, vectorisation work deliveries and the control reports can be found here: [P:\20\\_079\\_MorfoInteract\3\\_Uitvoering\Deeltaak1\\_DataAcquisition\OudeKaarten\VectorisatieKustplannen](P:\20_079_MorfoInteract\3_Uitvoering\Deeltaak1_DataAcquisition\OudeKaarten\VectorisatieKustplannen) in subfolders "plannen" (georeferenced plan packages sent out) and "lev" (delivery and report). The control and acceptance of each delivery of the vectorisation work is done according to section 5 of the work specifications (see Appendix 1). The most stringent control is a check on numeric elevation outliers which can result from errors when introducing the map elevation in the numeric elevation field. Typically, values of "null" or "zero" can occur, and values that deviate with an order of magnitude due to typing or automatic number recognition errors. They are easily detected using a TIN and will show as isolated peaks or pits. If only a few of these are present in the delivery, they can be quickly corrected and there is then no need of a redelivery.

#### 1.1.8 Progress of the vectorisation work

Table 5 provides an overview of the work progress.

#### 1.1.9 Further processing: construction of DEMs

For the study of morphological change through time, Digital Elevation Models (DEMs) are needed of each available survey. They allow to make visual change maps, elevation change maps and calculate volume changes per area of interest, such as sections, groups of sections or even larger areas. In line with the existing DEMs at FH, ESRI rasters are produced with the same spatial resolution that are used in coastal morphology studies: 2 m resolution for beach and dune surveys and 10 m resolution for nearshore and inner shelf surveys.

The following workflow is followed:

- control of the area covered with elevation data
- make a TIN of the spatial elevation features. Elevation points are fed as mass points with the elevation attribute as height source. Contour lines are fed as hard break lines with the elevation attribute as height source. The TIN is clipped to the TIN delineation area to avoid extrapolations.
- interpolate a raster with cell size 2 m for data derived from beach maps and 10 m for data derived from nearshore maps and inner shelf maps.

Specific steps according to data type:

- beach and dune foot maps
  - the surveys have elevation points or contour lines with reference to ZMOW. In the vectorisation delivery shapefiles, a field is added in the attribute table with the elevation in TAW (this is obtained using Field Calculator with the expression " $= [\text{hoogte}] - 0.11$ ").
  - supplement uncovered areas (inside groins, seawall) with more recent available data. This supposes no change has occurred since the processed survey on the structures, which is certainly the case for the large majority of the structures. Even in the case of a change, this remains the best strategy to avoid interpolations through the groins as a flat area.
  - add some breaklines (e.g. in troughs and along bar crests, between elevation points on the seawall) to avoid spurious interpolations.

Table 5 – Progress of the outsourced vectorisation work.

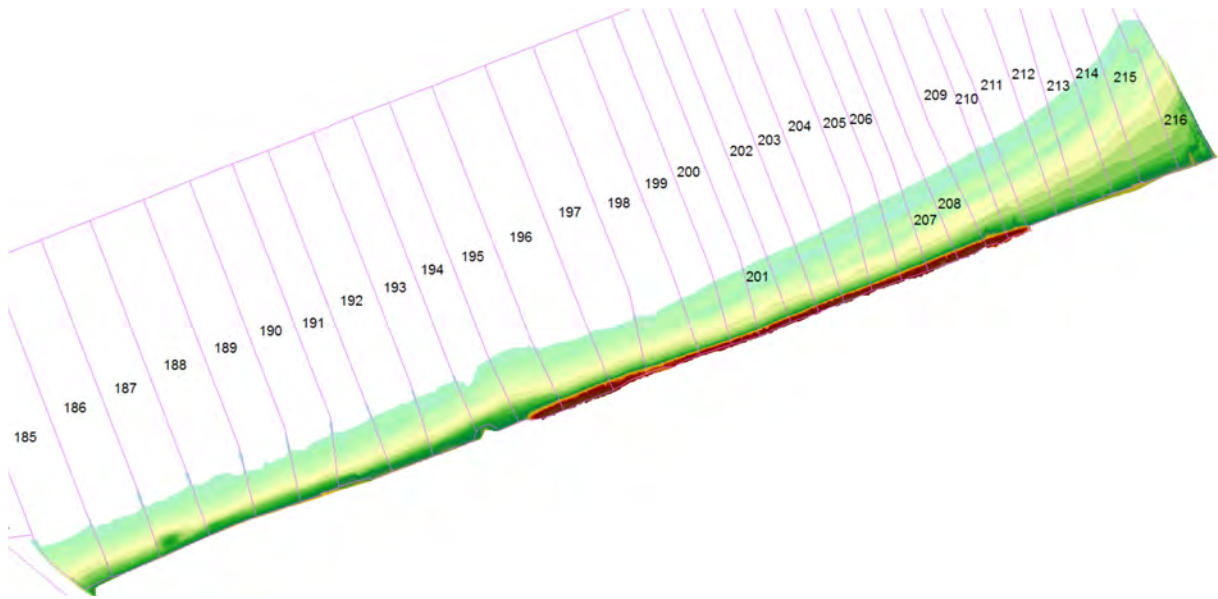
| Work package    | Sheets   | Date commissioned | Date of delivery | Date of acceptance |
|-----------------|--|-------------------|------------------|--------------------|
| Selection stage | A typical beach map:<br>SIT_1985_1_OOST10.jpg (1 sheet)<br><br>A typical nearshore map:<br>VO_1986_1_8616.jpg (1 sheet)<br><br>A typical inner shelf map:<br>wie-sch1986.jpg (1 sheet) | 16/06/2022        | 8/07/2022        | 12/07/2022         |
| Deelopdracht 1  | SIT_1985_1_OOST05 – 09, OOST11;<br>SIT_1983_1_OOST05 – 08 (10 sheets) and ZUYWE_1987 en west-dh1984 (2 sheets)   | 20/07/2022        | 22/08/2022       | 29/08/2022         |
| Deelopdracht 2  | SIT_1983_1_OOST09 – 11; OOST03 – 04; MIWE28 – 32 (10 sheets)   | 5/09/2022         | 10/10/2022       | 11/10/2022         |
| Deelopdracht 3  | SIT_1983_1_MIWE01 – 09;<br>VO_1987_2_87130   | 14/10/2022        | 14/11/2022       | 16/11/2022         |
| Deelopdracht 4  | SIT_1983_1_MIWE10 – 20   | 21/11/2022        |                  |                    |
| Deelopdracht 5  | SIT_1983_1_MIWE21 – 27   | (soon)            |                  |                    |

- nearshore maps
  - the surveys have elevation points with reference to Z MOW. In the vectorisation delivery shapefiles, a field is added in the attribute table with the elevation in TAW (this is obtained using Field Calculator with the expression "= [hoogte] – 0.11").
- inner shelf maps
  - the inner shelf maps are in dm below GLLWS (= "H"). In the point shapefiles, a field is added to contain the elevation in m GLLWS; this is calculated from the field "Hoogte" using Field Calculator. This elevation is input to a TIN and then a 10 m-raster in GLLWS. The latter is then converted to TAW using Raster Calculator with the following expression: "[current raster] - "gllws\_to\_taw\_vlaamsebanken\_I72.tif"
  - a mosaic raster in TAW of entire project area using three neighbouring surveys of successive years is produced. If a gap is present between the rasters, an auxiliary raster is first made from a TIN interpolating the survey points around the gap. The mosaic preserves the cell values of the most recent survey in overlapping areas.

The following DEMs (Table 6) have been made and are available on [P:\20\\_079\\_MorfoInteract\3\\_Uitvoering\Deeltaak1\\_DataAcquisition\DEMs](P:\20_079_MorfoInteract\3_Uitvoering\Deeltaak1_DataAcquisition\DEMs). The rasters are in ESRI raster format. They are referenced in Lambert72 and, while the source maps are either in Z MOW or GLLWS, they have been converted to TAW before making the DEMs. For the datum conversion GLLWS to TAW, use has been made of gllws\_to\_taw\_vlaamsebanken\_I72.tif, a conversion raster borrowed from aMT available at FH on <G:\Masterarchief\cnv>.

Table 6 – DEMs made of vectorised data.

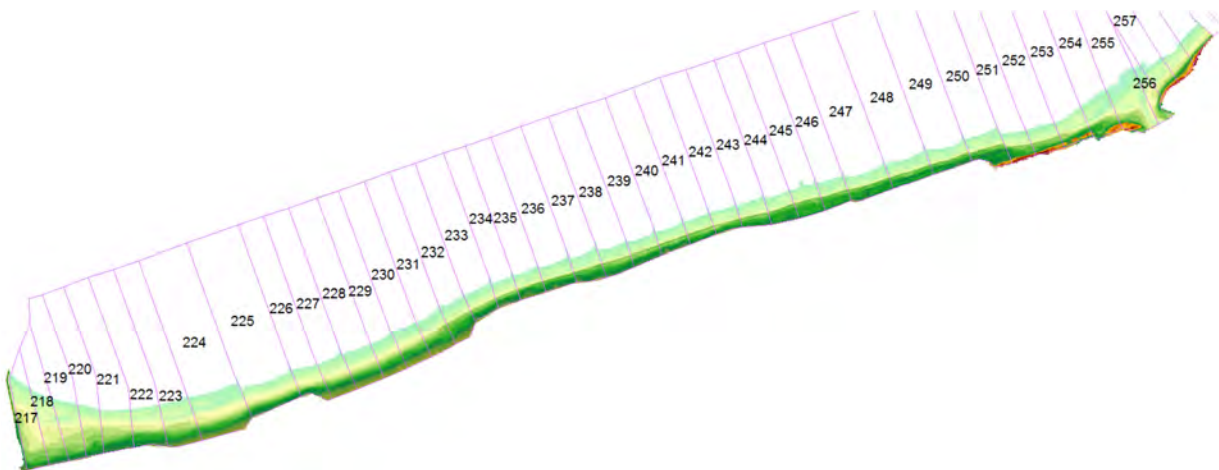
| Topic                                    | Source of data               | DEM           | Area                      |
|--|------------------------------|---------------|---------------------------|
| Beach and dune foot maps (cell size 2 m) | SIT_1983_1_MIWE01-09.jpg     | (soon)        | De Panne to Nieuwpoort    |
|  | SIT_1983_1_MIWE10-20.jpg     | (soon)        | Nieuwprt to Oostende      |
|  | SIT_1983_1_MIWE21-31.jpg     | (soon)        | Oostende to Wenduine      |
|  | SIT_1983_1_MIWE31-OOST04.jpg | G_1983_1D     | Blankenberge to Zeebr.    |
|  | SIT_1983_1_OOST05-11.jpg     | G_1983_1E     | From Heist to Zwin        |
|  | SIT_1985_1_OOST05-11.jpg     | G_1985_1_Knok | From Heist to Zwin        |
| Nearshore maps (cell size 10 m)          | VO_1987_2_87130              | (soon)        | De Panne to Oostduinkerke |
|  | VO_1986_1_8616.jpg           | G_1986V1_Knok | From Heist to Zwin        |
| Inner shelf maps (cell size 10 m)        | Wie-sch1986.pdf              | G_WS1986_TAW  | Inner shelf eastern part  |
|  | West-dh1984.pdf              | G_WD1984_TAW  | Inner shelf central part  |
|  | ZUYWE_1987.pdf               | G_ZW1987_TAW  | Inner shelf western part  |
|  | Mosaic 1984-1987             | G_KN84_87_TAW | Complete inner shalf      |



---

Figure 2 – 2 m-DEM of vectorised survey Spring 1983 between Blankenberge and Zeebrugge.

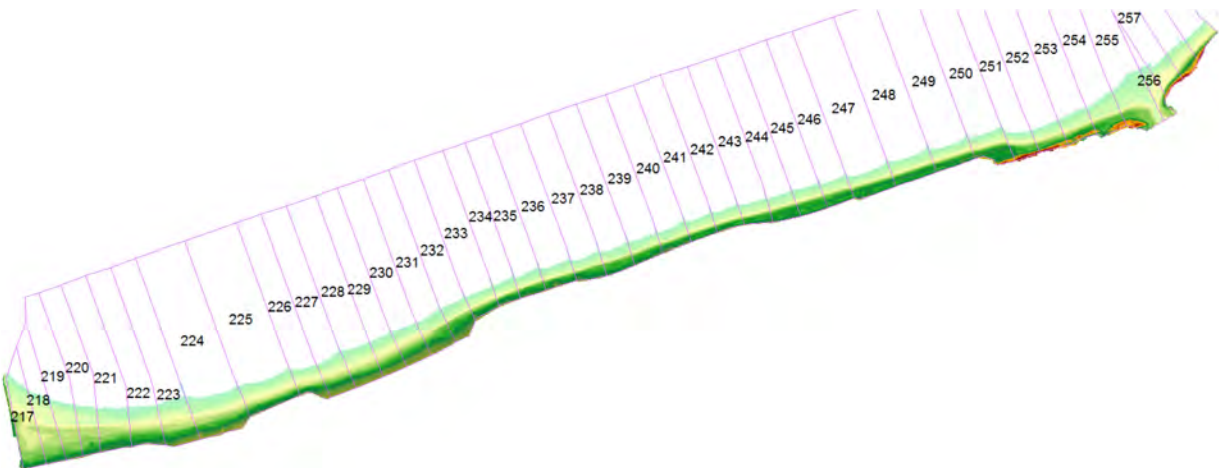
---



---

Figure 3 – 2 m-DEM of vectorised survey Spring 1983 between Zeebrugge and Zwin.

---



---

Figure 4 – 2 m-DEM of vectorised survey Spring 1985 between Zeebrugge and Zwin.

---

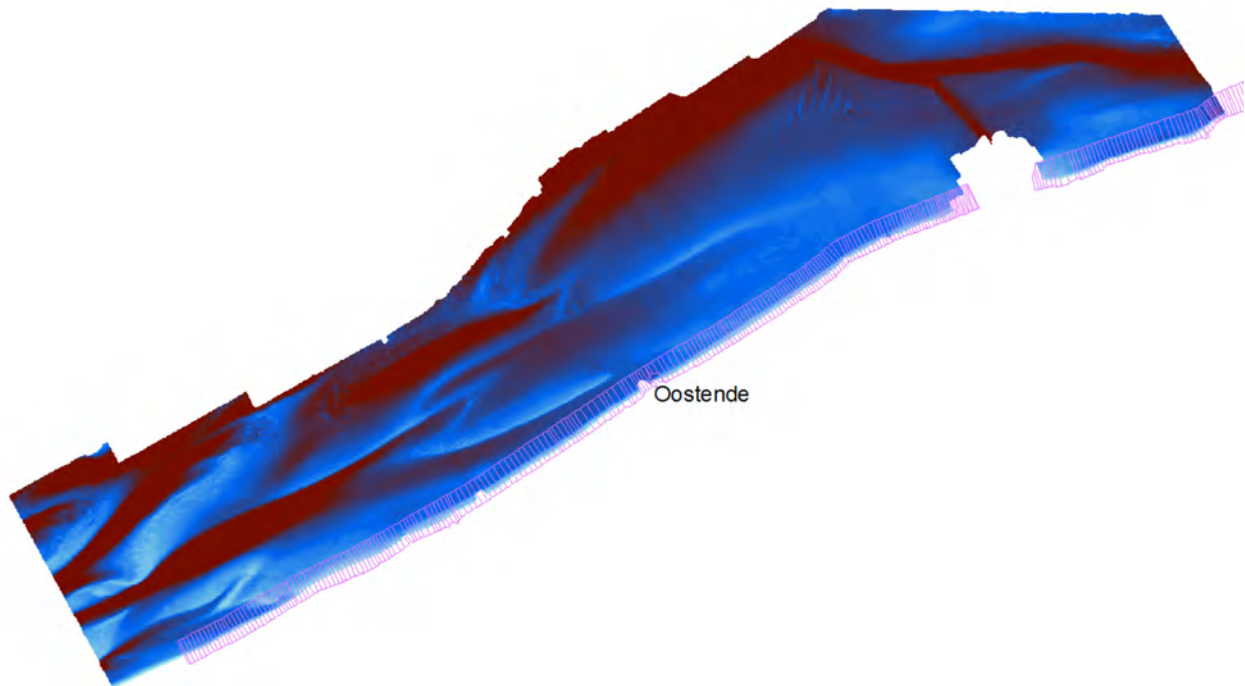


Figure 5 – Mosaic 10 m-DEM of 1984, 1986 and 1987 inner shelf surveys. Sections in thin pink lines. Elevations range from 0 to about -15 m TAW.

## 1.2 Use of GIS in coastal morphology

Since the early 1980s, an informal tradition of processing coastal surveys in GIS for the purpose of coastal morphological studies has been established. It involved dividing the Belgian coast in fixed coastal sections, making maps, elevation difference maps, plotting average profiles per coastal section and computing volume differences with respect to a first survey in three, later five elevation slices per coastal section. Processing new coastal surveys allows to establish decadal morphological evolution and trends (*sensu* Houthuys *et al.*, 2022). It is useful to document and standardise this tradition so that the context and quality of data through time can be evaluated and continuity in future coastal survey processing is safeguarded. Currently, most of the processing has been done in ESRI's Desktop ArcMap version 10.x. Proper documentation of the processing steps will allow implementation in other environments, such as the open-source QGIS package.

A "user's guide for coastal morphology GIS processing" is being prepared during the current Mozes project. It contains dedicated information with respect to basic settings, projection systems used and conversions, useful base layers, standard display of data, georeferencing of images, vector data and editing them, making terrain surfaces using TINs and rasters (to be continued; the document grows along with the project). It can be found here: [P:\20\\_079\\_MorfoInteract\3\\_Uitvoering\Deeltaak1\\_DataAcquisition\ArcGIS\Documentatie](P:\20_079_MorfoInteract\3_Uitvoering\Deeltaak1_DataAcquisition\ArcGIS\Documentatie) and is named "ArcGIS technieken Mozes\_v05.docx".

## 1.3 Chart series "Vlaamse Banken"

Within the framework of Quest4D (Van Lancker *et al.*, 2012), the bathymetric information present in some small-scale (about 1/100,000) navigation charts of the series called "Vlaamse banken" were digitised: 1866, 1901 – 1908, 1938, 1959 – 1969.

Here the quality and reuse of the so-called "kaart Stessels 1866", officially "Carte Générale des Bancs de Flandres compris entre Gravelines et l'embouchure de l'Escaut", is addressed. The paper map was scanned as a tiff-file and georeferenced in ArcMap (Janssens *et al.*, 2012). For the analyses to be conducted for the MOZES study (Verwaest *et al.*, 2021) the quality of this digitisation exercise had to be checked and additional bathymetric information was vectorised.

### 1.3.1 Digitisation within QUEST4D

#### Methodology

The process of digitization is described in detail by Janssens *et al.* (2012), and is briefly resumed in this section. Figure 6 shows the georeferenced scan (tiff-file) on top of the topographic map of Belgium (NGI, 2022a); the red numbers indicate the cross-hairs on the paper-map for which a Belgian Lambert72 coordinate was computed. In ArcMap the geographic map coordinates and the corresponding Lambert72 coordinates are stored in a link-table.

The paper map shows geographical coordinates (degrees latitude and longitude), with the longitude in respect to the meridian of Paris. Nowadays, the meridian of Greenwich is commonly used to express longitude in geographical coordinate systems. In order to correlate the longitude shown on the map to Greenwich, a translation of  $+2^{\circ}20'14,025''$  was applied.

In 1866 the latitude of an offshore location was determined from stellar measurements and/or solar altitude, while the longitude was calculated as the deviation from a known position, based on estimated speed, heading and elapsed time. These coordinates were then drawn directly onto the map. Janssens *et al.* (2012) used the software PCTrans (courtesy of the Royal Netherlands Navy) to transform the geographic map coordinates to Belgian Lambert72. Both the geographic map coordinates and the corresponding Belgian Lambert72 coordinates were fed to the link-table in ArcMap. The "Adjust" option within the link-table was used to fit the tiff-file to the Belgian Lambert72 coordinates. This option combines a polynomial fit with TIN-interpolation, in order to achieve the optimal fit on both global and local scale. This option causes the most distortion off the tiff image and is also known as "rubbersheeting".

Janssens *et al.* (2012) found that using the Hayford BERE parameter-set to conduct the transformation from geographical map coordinates to Belgian Lambert72 yielded the best results, when comparing the georeferenced tiff to orthophotos in ArcMap. However they did not report the residual errors from the georeferencing, nor the precise number of the resulting errors they observed. Based on the figures they show, the order of magnitude of the resulting error seems to be 100 m. They do report that adding additional landmarks (e.g. church towers) to the link table did not yield to a better fit (Figure 7).

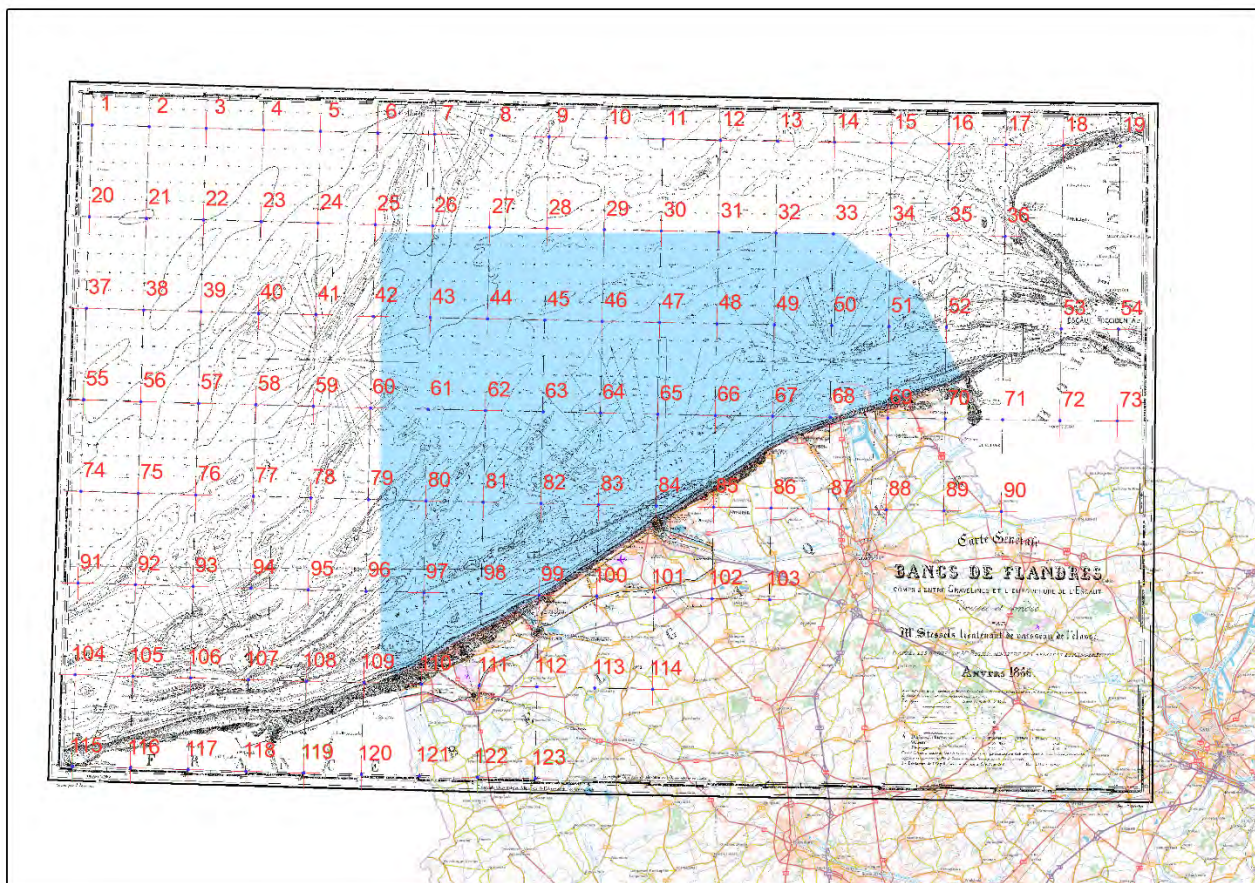


Figure 6 – Georeferencing the “kaart Stessels 1866” in ArcMap.

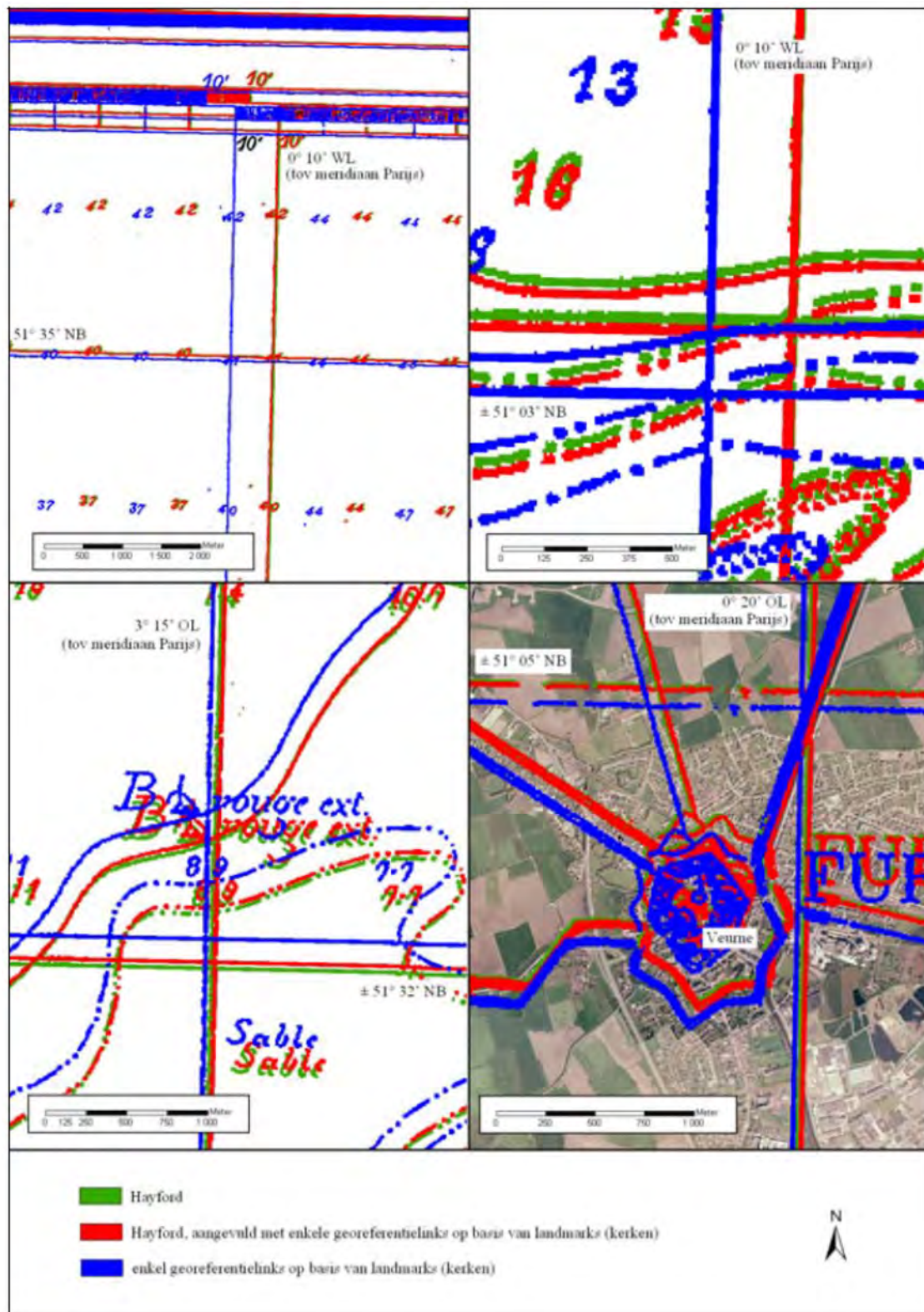


Figure 7 – Quality of the georeferenced map.

Based on 123 coordinates in the link-tabel (green), 123 coordinates and additional landmarks (red) and solely on landmarks (blue).

## Quality check

### Accuracy of the paper map

In 1866 the latitude of an offshore location was determined from stellar measurements and/or solar altitude, while the longitude was calculated as the deviation from a known position, based on estimated speed, heading and elapsed time. These coordinates were then drawn directly onto the map.

Depth soundings were conducted with a weighted rope. This can be quite accurate in calm water, but is heavily influenced when marine currents are strong. Furthermore the isobaths are an interpretation of the drawer, based on scarce measurement points. Unlike in onland topography, the features of the landscape (valleys, convex/concave slopes) cannot be observed directly in the murky waters of the North Sea.

Finally there is the accuracy of the drawing itself. The line thickness itself is at least 2 pixels of the scan, sometimes up to 6 pixels (20 to 60 m in reality). It appears that some points were located and drawn much more precise than others. E.g. in Oostende at Fort Napoleon there's 40 m error in the georeferenced tiff, while the canal Oostende – Brugge shows an offset up to 260 m (Figure 8). Furthermore erroneously drawn isobaths (Figure 9) and non-matching isobaths and depth points (Figure 10) were found on the map.

Folding of the paper map (Figure 11), as well as the scanning itself can have produced deformation in the resulting tiff-file. Therefore “rubbersheeting” needs to be applied when georeferencing the scanned map (see below: Accuracy of the Georeferencing).



Figure 8 – Accuracy of the paper map drawing at Oostende (background: CartoWeb.be (NGI, 2022a)).



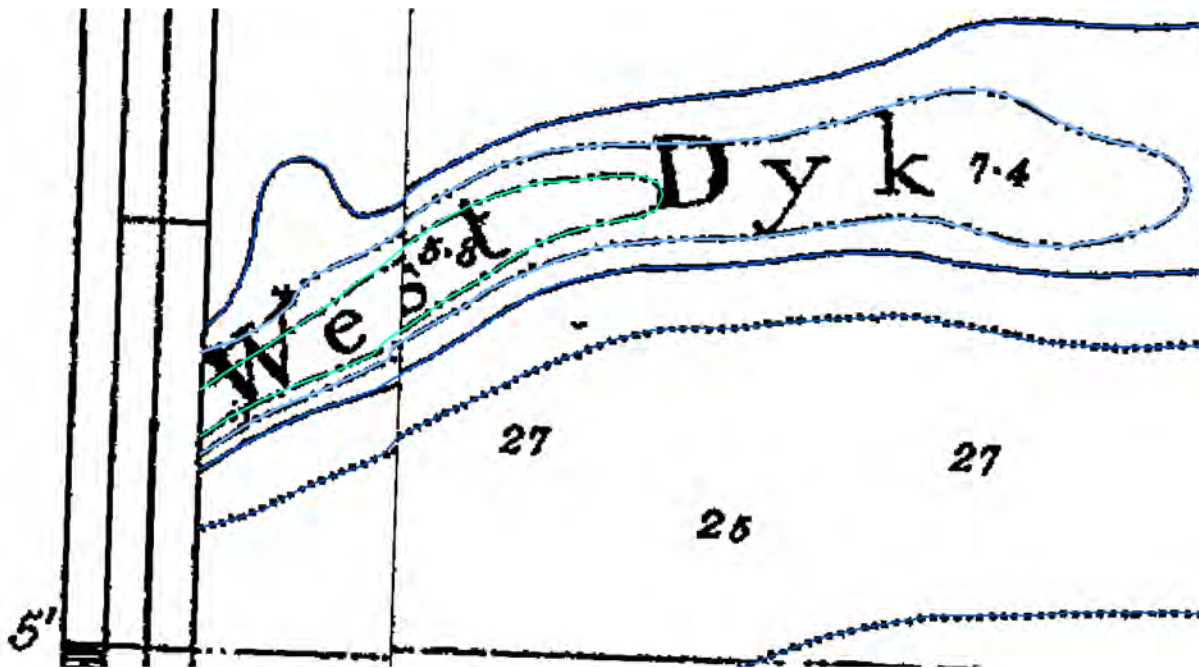


Figure 11 – Example of a fold in the map, resulting in dislocation of the isobaths and gridlines.

### Error induced by the Coordinate Transformation

Janssens *et al.* (2012) used the software PCTrans from the Royal Netherlands Navy (2022) to transform the geographic map coordinates to Belgian Lambert72 coordinates. This transformation could also be done with other software packages like cConvert (NGI, 2022b), SuperTrans (Deltares, 2021) or even within ArcMap itself.

A test with the packages mentioned above showed that differences up to 30 m can occur when transforming the same set of coordinates. This can be explained by the fact that some transformations take into account the height above the geoid and others do not. cConvert for instance gives both options and so does SuperTrans, depending on the chosen EPSG-codes<sup>1</sup>. This shows the importance of using identical transformation parameter settings.

### Accuracy of the Georeferencing

Based on the link-table attached to the geo-tiff in ArcMap, we were able to retrieve which points on the map were used to compute the “Adjust” fit (Figure 6). A total of 123 points was used; the largest residual errors are shown in Table 7, the other 116 points have an error of 0 due to the “Adjust” fit. All points with a residual error are located on the West and SouthWest borders of the paper map.

On the paper map sightlines are drawn to 9 landmarks: the lighthouses of Gravelines, Raversijde and Westkapelle (former church tower); the church towers of Lefferinckoucke, Veurne, Middelkerke, Gistel and Middelburg and the belfry of Brugge.

<sup>1</sup> EPSG Geodetic Parameter Dataset (also EPSG registry) is a public registry of geodetic datums, spatial reference systems, Earth ellipsoids, coordinate transformations and related units of measurement. Originally created by European Petroleum Survey Group (EPSG). Each entity is assigned an EPSG code between 1024-32767, along with a standard machine-readable well-known text (WKT) representation. The dataset is actively maintained by the IOGP Geomatics Committee (Wikipedia, 2022).

Table 8 shows the observed errors of these landmarks when comparing the georeferenced tiff to recent topographic maps and orthofoto's.

Table 7 – Largest and overall residual errors while georeferencing.  
The 116 points with an error equal to zero are not listed.

| Link                     | Residual_x [m] | Residual_y [m] | Residual [m] |
|--------------------------|----------------|----------------|--------------|
| 1                        | -8.301         | 2.834          | 8.771        |
| 55                       | -16.887        | -15.477        | 22.906       |
| 74                       | -17.521        | -13.084        | 21.867       |
| 115                      | -26.574        | -19.922        | 33.212       |
| 119                      | 55.063         | -14.266        | 56.881       |
| 120                      | 21.618         | -4.459         | 22.073       |
| 122                      | -35.231        | -15.780        | 38.603       |
| 123                      | -40.171        | -26.513        | 48.132       |
| <b>Total RMSE Error:</b> |                |                | <b>8.886</b> |

Table 8 – Observed errors in location of georeferenced landmarks on the map.

| Location               | Remarks   | Map Stessels  |               | Topographic Map |               | $\Delta x$ [m] | $\Delta y$ [m] | Error [m] |
|------------------------|---|---------------|---------------|-----------------|---------------|----------------|----------------|-----------|
|                        |   | x [Lambert72] | y [Lambert72] | x [Lambert72]   | y [Lambert72] |                |                |           |
| lighthouse Gravelines  | phare de Gravelines Petit-Fort Philippe: build in 1843                            | -8661         | 190543        | -8577           | 190592        | -84            | -49            | 97        |
| church Lefferinckoucke | Lefferinckoucke-village no longer has a church                                    |               |               | -               | -             |                |                |           |
| church Veurne          | Sint-Niklaaskerk: tower was build in 12th - 13th century                          |               |               |                 |               |                |                |           |
|                        | Sint-Walburgakerk was rebuild in 13th -14th century, without a tower              | 30403         | 197301        | 30468           | 197164        | -65            | 137            | 152       |
| church Middelkerke     | rebuild in 1919 - 1921, the tower originates from 1681                            | 41695         | 209416        | 41742           | 209437        | -47            | -21            | 51        |
| lighthouse Raversijde  | were probably demolished in 1914  |               |               | -               | -             |                |                |           |
| church Gistel          | rebuild in 1853 - 1867, the tower originates from the 17th century                | 52001         | 206273        | 51976           | 206203        | 25             | 70             | 74        |
| belfry Brugge          | build in 1240, segments added to the tower in 1487 and 1822                       | 70097         | 211618        | 70056           | 211527        | 41             | 91             | 100       |
| lighthouse Westkapelle | Westkapelle het Hoge Licht: former church (1470), converted to lighthouse in 1802 |               |               |                 |               |                |                |           |
|                        | after a fire in 1831 only the tower/lighthouse was restored                       | 86103         | 246959        | 86039           | 247026        | 64             | -67            | 93        |
| church Middelburg      | Abbey tower "Lange Jan", build in 14th century                                    | 97645         | 243611        | 97637           | 243598        | 8              | 13             | 15        |
| Total RMSE Error:      |   |               |               |                 |               |                |                | 92        |

### Anomalies in the digitized data

The -8 m GLWS isobath was digitized as a polygon by Janssens *et al.* (2012). At some locations this has produced erroneous connections between isobaths; e.g. over the Bol de Knocke and over the most shallow part of the historical Paardenmarkt (Figure 12). In order to produce a DEM combining all isobaths and individual sample points on the map, the polygons need to be transformed to polylines and the erroneous connections need to be removed.



### 1.3.2 Additional data from the Stessels 1866 map

The 0, 2, 4, 6, 10, 20 and 30 m MLWS isobaths were vectorised; at the same time some missing 8 m MLWS isobaths were added. Additionally, the 5.5 and 7 m MLWS isobaths (Vlakte van de Raan and Appelzak, see Figure 9) and the dunefoot were digitised. Adding the dunefoot was necessary in order to enable to implement the beach slope in the Scaldis-Coast and FlemCo models for 1866. The dunefoot height was estimated at +5.4 m MLWS (5 m TAW), based on current day observations.

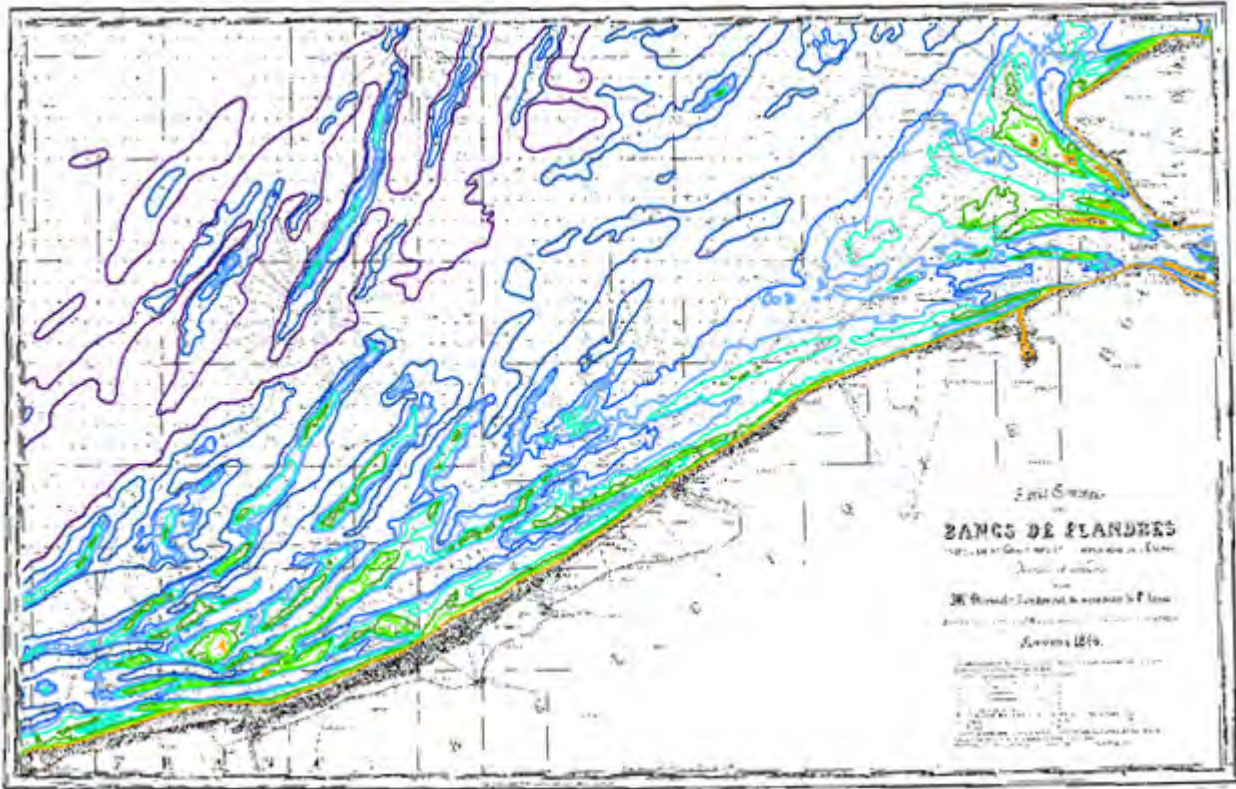


Figure 13 – vectorised isobaths on the Stessels map.

### 1.3.3 Creating the TIN

After digitising these isobaths, a TIN was created. In an iterative process, ridge and trough lines were manually drawn and the TIN was recalculated in order to improve its quality. During this process some misplaced depth points and/or erroneous depth values, digitised by Janssens *et al.* (2012), were found and corrected.

Comparison of the initial TIN, based solely on the isobaths and depth points (Figure 14), and the resulting TIN after addition of ridge and trough lines and the correction of some depth points (Figure 15), shows clearly a more natural representation of the bathymetry, with smoother slopes, less isolated depth points and more continuous ridges and troughs.

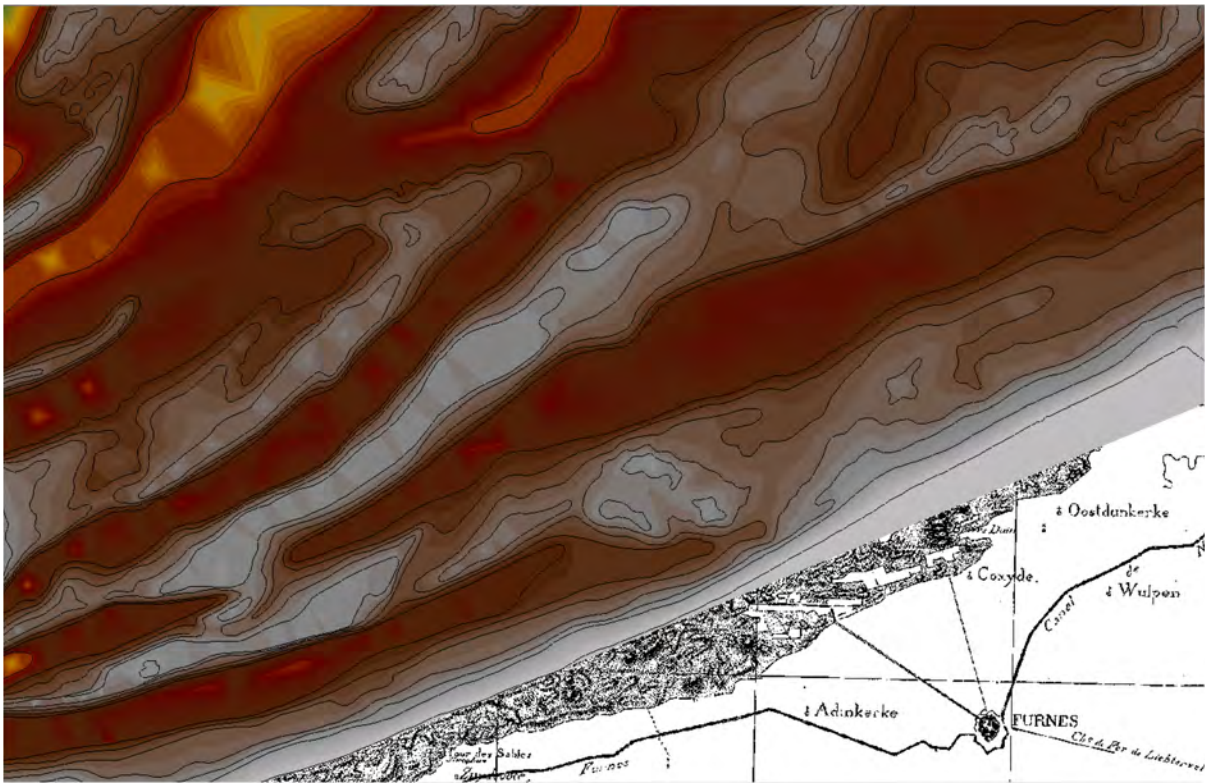


Figure 14 – Initial TIN based on isobaths and depth points only.  
Zoom on the area around Trapegeer, Hills and Smal Bank.

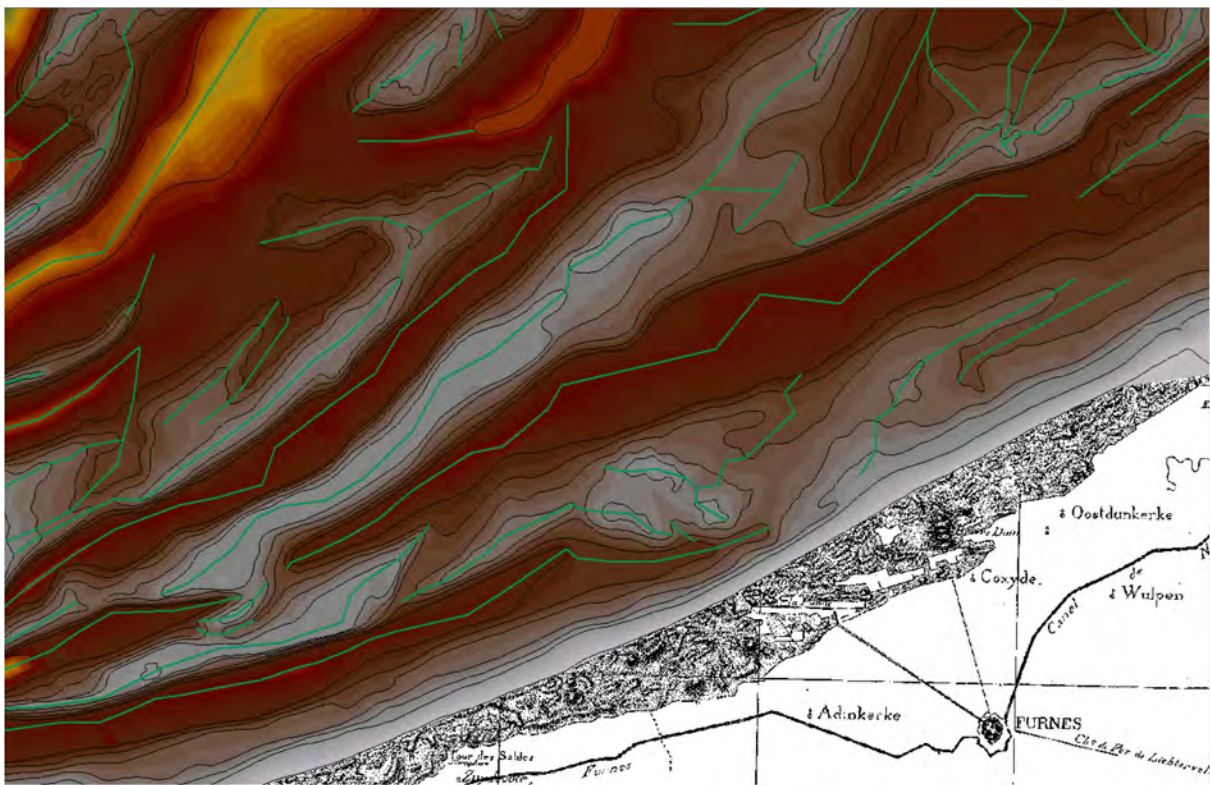


Figure 15 – Resulting TIN based on isobaths, depth points and ridge and trough lines (shown in green),  
for the same area as shown in Figure 14.

### 1.3.4 Converting MLWS to TAW and NAP

The GIS cell at FH has several tidal reduction grids available to convert tide dependent depths like LAT and MLLWS to a vertical reference like TAW. However, due to different reduction methods used in Flanders and the Netherlands, a break in the conversion values is observed at the border. To obtain a smooth transition an interpolation in the overlapping zone should be applied (Figure 16). Also these grids do not cover the whole area of the Stessels Map, nor the computational domains of Scaldis-Coast and FlemCo.

Subsequently, a conversion grid for the whole North Sea was obtained from the GIS cell of the Maritime Access Division (Figure 17). Obviously, this grid does not show any line artefacts, but it is only available for conversion from LAT to NAP. Given the accuracy of the paper map (see §1.3.1 – Quality check), we conclude that the error introduced by assuming depth values in LAT instead of MLWS is smaller (maximum 15 cm at Nieuwpoort) than the possible errors introduced by interpolating several reduction grids. For the conversion from NAP to TAW a constant value of 2.333 m is used.

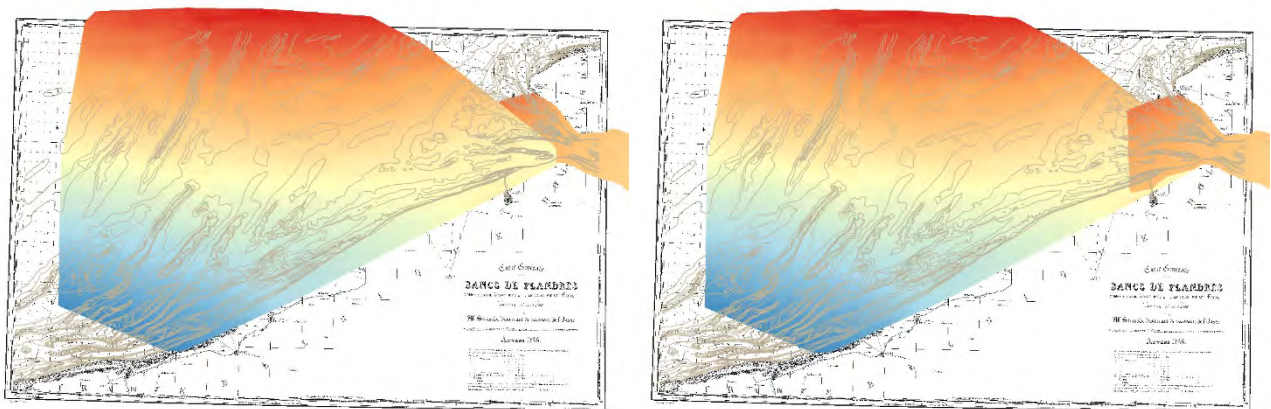


Figure 16 – Conversion grid of GLLWS to TAW for Vlaamse Banken, shown on top of the grid for Westerschelde (left), and vice-versa (right).

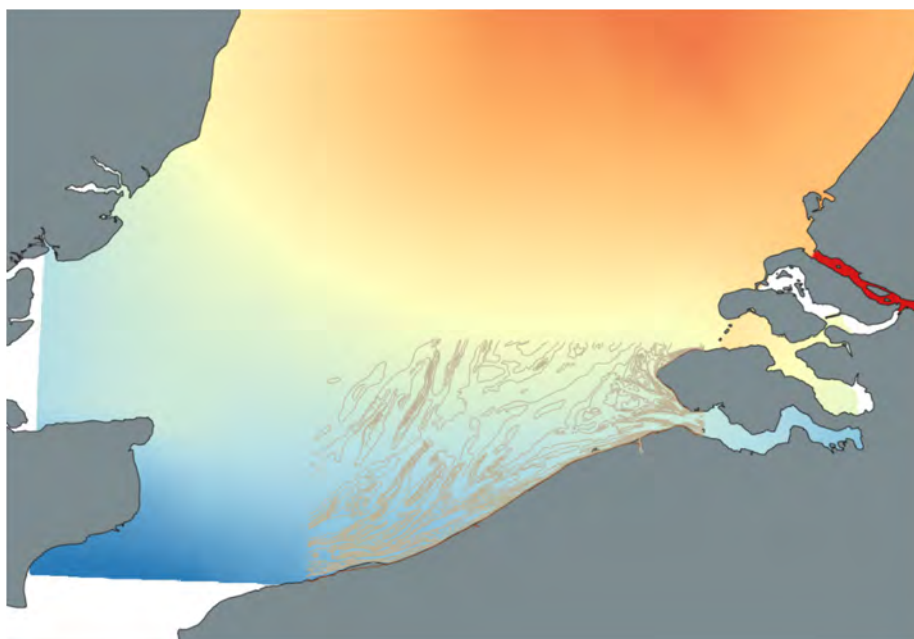


Figure 17 – Conversion grid of LAT to NAP for the southern North Sea (source: Maritime Access Division GIS-server Z:\GISdata\frame\bth\verticale\_transformatiegrids\_alle\_projectiesystemen\RD.gdb)

### 1.3.5 Creating and exporting the DEM

From the resulting TIN, obtained after several iterations of correcting misplaced depth points and/or erroneous depth values and adding ridge and trough lines, a raster needs to be generated in order to be able to convert the MLWS values from the TIN to a fixed horizontal reference level like TAW (or NAP) for further analysis and modelling.

All rasters generated within the project need to have the same origin in order to be able to combine them. This origin is set in ArcMAP in the Geoprocessing > Environment Settings > Processing Extent menu, by defining a Snap Raster. The snap raster to be used, can be found in the MOZES project folder [p:\20\\_079-MorfoInteract\3\\_Uitvoering\Deeltaak1\\_DataAcquisition\ArcGIS\snapraster](p:\20_079-MorfoInteract\3_Uitvoering\Deeltaak1_DataAcquisition\ArcGIS\snapraster).

For geographic and volumetric analysis purposes like conducted by Houthuys *et al.* (2022) a 10x10 m raster was generated from the TIN. This file proved to be difficult to handle in the pre-processing software of the numerical models (Delft FM and openTELEMAC); therefore a second raster was created with a 20x20 m mesh size. Both raster files were thereafter converted from MLWS to NAP using the conversion raster shown in Figure 17. Conversion to TAW was subsequently done by adding an offset of 2.333 m.

Table 9 lists all files used and created in the process of generating the DEM's to be used for further analysis and numerical modelling. All files can be retrieved in the MOZES project folder [p:\20\\_079-MorfoInteract\3\\_Uitvoering\Deeltaak1\\_DataAcquisition\ArcGIS\DigitalisatieStessels](p:\20_079-MorfoInteract\3_Uitvoering\Deeltaak1_DataAcquisition\ArcGIS\DigitalisatieStessels), unless stated otherwise in Table 9.

Table 9 – Files used to generate the Stessels 1866 DEMs.

| Name   | File Type                   | Data Type   | Remark  |
|--|-----------------------------|-------------|---|
| 1866_Bancs-de-Flanders.tif                   | Geotiff                     | Source data | Scan of the Stessels map, georeferenced by Janssens <i>et al.</i> (2012) within the QUEST4D project                             |
| 1866_points.shp                              | Shape, geometry type: Point | Edited      | Individual depth points, corrected from the "1866_points.shp" file by Janssens <i>et al.</i> (2012)                             |
| 1866_polylines_Merged2.shp                   | Shape, geometry type: Line  | Created     | Digitised lines from the geotiff Polylines for 30, 20, 10, 8, 7, 6, 5.5, 5, 4, 2 and 0 m isobath and dunefoot                   |
| 1866_RidgeTroughLines.shp                    | Shape, geometry type: Line  | Created     | Interpretation of the ridge and trough lines, based on isobaths shape and individual depth points. Polylines without Z-values.  |
| 1866_tin05                                   | TIN                         | Created     | Constrained Delaunay TIN, based on individual depth points and digitised isobaths   |
| 1866_RidgeTroughLines_InterpolateShape05.shp | Shape, geometry type: Line  | Created     | The file "1866_tin05" is used to interpolate the Z-values on the ridge and trough lines defined in "1866_RidgeTroughLines.shp". |
| 1866_tin15_constrained                       | TIN                         | Created     | Constrained Delaunay TIN, based on individual depth points, digitised isobaths and interpreted ridge and trough lines           |

|  |                       |   |  |
|--|-----------------------|---|--|
| snapraster   | ESRI GRID<br>(raster) | Source data<br>(environment<br>setting) | p:\20_079-<br>MorfoInteract\3_Uitvoering\<br>Deeltaak1_DataAcquisition\<br>ArcGIS\snapraster\  |
| g_stes_glws10  | ESRI GRID<br>(raster) | Created                                 | 10x10 m raster created from<br>"1866_tin14_constrained"  |
| g_stes_glws20  | ESRI GRID<br>(raster) | Created                                 | 20x20 m raster created from<br>"1866_tin14_constrained"  |
| LAT_NAP_NED_RD<br>(shortened name:<br>g_latnap_orig) | ESRI GRID<br>(raster) | Source data                             | 200x200 m conversion grid from LAT<br>to NAP in Dutch RDnew coordinates<br>(Figure 17)   |
| g_latnap_L72r  | ESRI GRID<br>(raster) | Created                                 | 10x10 m conversion grid from LAT to<br>NAP; interpolated and transformed<br>to Lambert 72 from the original<br>"LAT_NAP_NED_RD" raster |
| g_stess_taw10  | ESRI GRID<br>(raster) | Created                                 | 10x10 DEM in Lambert72 and TAW<br>"g_stes_glws10"-<br>"g_latnap_L72r"+2.333  |
| g_stess_nap20  | ESRI GRID<br>(raster) | Created                                 | 20x20 DEM in Lambert72 and NAP<br>"g_stes_glws10"- "g_latnap_L72r"   |
| g_stess_rdnap  | ESRI GRID<br>(raster) | Created                                 | 20x20 DEM in RDnew and NAP<br>coordinate transformation of<br>"g_stess_nap20"  |
| 1866_all_rdnap20.asc                                 | ESRI ASCII raster     | Created                                 | ascii export from "g_stess_rdnap"<br>conversion tool "Raster to ASCII"   |

## 1.4 Exploration of other historic data

### 1.4.1 MOW – ATO – Dienst Fotogrammetrie - Topografie

The Flemish Department Mobiliteit, Openbare Werken en Waterwegen (MOW) has in its Algemene Technische Ondersteuning (ATO) a cell for Photogrammetry and Topography, based in the Ferraris Building in Brussels. Steven Muylaert en Kris Van Molle received the MOZES team on 28/04/2022 for an explorative visit.

We obtain a copy of the original high-resolution (300 dpi) scans of the **Minister Map 1950-1970** at scale 1/5000, map sheets 5 – 7 – 11 – 12 that cover the coast. It is placed here in the project folder: [P:\20\\_079\\_MorfoInteract\3\\_Uitvoering\Deeltaak1\\_DataAcquisition\OudeKaarten\Ministerkaart1950-1970Kust](P:\20_079_MorfoInteract\3_Uitvoering\Deeltaak1_DataAcquisition\OudeKaarten\Ministerkaart1950-1970Kust).

The scanned images are jpg format. They are not georeferenced but contain Lambert (pre-1972?) reference marks that allow georeferencing. The maps were stereophotogrammetrically obtained from middle-scale (order of 1/10,000) vertical black and white aerial photographs. The date of update is present in the lower right of the image. The map sheets don't cover the Belgian coast completely. Their main type of information relevant for the MOZES project is that they mapped the coastal dunes using elevation contours with 1 metre interval. Other topographic maps don't contain this information. Information on the beach is more frugal: a low-water line (probably LLWS mark), a high-water line (probably HHWS mark), the seawalls and groins. The latter are shown using two outlines: the part that emerges from the sand and the covered groin base.

The cell has a large collection of vertical black-and-white aerial photographs. The file [P:\20\\_079\\_MorfoInteract\3\\_Uitvoering\Deeltaak1\\_DataAcquisition\OudeKaarten\20220420\\_databaseLuchtfotoATO.xlsx](P:\20_079_MorfoInteract\3_Uitvoering\Deeltaak1_DataAcquisition\OudeKaarten\20220420_databaseLuchtfotoATO.xlsx) is a list of all photo series in the archive. The archive covers the Flemish territory with photos dating from 1930 to 1998. Potentially interesting photos for the MOZES project have been highlighted in colour. Records that have a map sheet number in column G have been used to produce the Minister Map and are not highlighted. All photos that cover that territory of the city of Oostende have been scanned by the city administration. We receive a copy of the scans; it is located [P:\20\\_079\\_MorfoInteract\3\\_Uitvoering\Deeltaak1\\_DataAcquisition\OudeKaarten\LuchtfotosOostende1952](P:\20_079_MorfoInteract\3_Uitvoering\Deeltaak1_DataAcquisition\OudeKaarten\LuchtfotosOostende1952). The file **AAA\_hulpblad\_cijfers.pdf** gives an overview of these and the records have been highlighted in blue in column F of **20220420\_databaseLuchtfotoATO.xlsx**. The 8 July 1952 is potentially interesting as a reference not long before the February 1953 inundations. They have a 60% sideways overlap and have probably been used for the Minister Map. The scans are sharp but often geometrically distorted. The beach is about 2 cm wide in the photos with sea level between middle tide and high tide.

The other parts of the Flemish coast have been briefly visited on 28/04/2022 (marked in yellow in **20220420\_databaseLuchtfotoATO.xlsx**) (due to limited time, others have not been visited, they are marked in orange).

Many of the photos are at a small scale, they are sharp and most have sideways overlap. They could potentially be elaborated stereoscopically, though this would be an enormous task. Some general remarks:

- the photos of the series "verkeerstellingen" seem the most interesting for our project. They were made in July 1968. They are at a large scale. The beach is often 7 cm wide on the photos. There is a large sideways overlap. Most are negatives, which in principle are not lent out. Of some, positives are also present. The coverage remains to be checked, but at least large parts of the resorts have been photographed several times during the month of July 1968.
- another series "vlotters" or "stromingen" is not of interest: the beach is insufficiently exposed and the large surface of sea makes rectifying the images an impossible task.

This photo archive is shortly after our visit closed for inventory. It will afterwards move to a new location.

#### 1.4.2 Vakgroep Archeologie UGent

The department of Archaeology of Ghent University (UGent) recently published a book "*De Kust 4 augustus 1945*" (Stichelbaut *et al.*, 2021). It contains a complete series of large-scale oblique black-and-white aerial photos covering the Flemish coast at low tide. These aerial photos allow to potentially map the high-water mark, erosion scars, dune foot, coastal defence works, etc.

Rik Houthuys and Anne-Lise Montreuil visited the principal author, dr. Birger Stichelbaut ([birger.stichelbaut@ugent.be](mailto:birger.stichelbaut@ugent.be)) on 9 August 2022. Dr. B. Stichelbaut is a postdoc researcher and specialises in valorising old aerial photos for archaeological purposes. He is in close cooperation with the Provinces and museums such as In Flanders Fields ([www.inflandersfields.be](http://www.inflandersfields.be)), the Royal Military Museum Brussels ([https://warheritage.be/language\\_selection\\_page?destination=/node/1](https://warheritage.be/language_selection_page?destination=/node/1)) and Atlantikwall Raversyde ([www.raversyde.be/nl/atlantikwall-raversyde](http://www.raversyde.be/nl/atlantikwall-raversyde)). His work however depends on external project funding.

B. Stichelbaut is also the principal author of the book "*De oorlog vanuit de lucht. 1914-1918: het front in België*" (Stichelbaut & Chielens, 2013) which has been added to FH's library.

The aerial photos of the coast areas available at the research unit in Gent belong to the following sets:

1. World War 1 vertical aerial photographs: they all together probably cover almost the entire coast. The actual coverage inventory is in progress, but it is clear the frontline part was covered most. The sorties were at several dates. Often the photos are at a large scale, have stereoscopic overlap and have been made at low tide. However, they are often blurry and show few recognisable ground points because of the war destructions. An indication of the photo quality can be found in Stichelbaut & Chielens (2013). The photos have been scanned and georectifying is ongoing. Later this year, probably in November 2022, a geoportal will be operational where the coverage and metadata can freely be consulted ([www.luchtfoto1914-1918.be](http://www.luchtfoto1914-1918.be)). The photos are owned by the Royal Military Museum Brussels (contact via [info@warheritage.be](mailto:info@warheritage.be)). The research unit scanned (almost) all photos of the Belgian coastal area. They are digitally available after a purchase or an agreement with the Museum.
2. A series of about 250 oblique aerial black-and-white photographs covering the Belgian coast from France to The Netherlands made on 4 August 1945 (see Stichelbaut *et al.*, 2021, which however reproduced only about 80 of these photos). The photos were made by the American Air Force and reside in a New York based archive. The UGent researchers visited the collection there and were allowed to scan them at high resolution from microfilm negatives. The B/W photos have been processed to enhance the contrast. They can be used for mapping morphological features on the beach as they provide an excellent view from above the sea towards the seawall and sea fronting dunes. They would probably not be suitable for 3D elaboration. The research unit asks something in return for delivering them: either a joint publication or a purchase.
3. A series of vertical aerial photographs including (parts of) the beach from 1944, taken at diverse times. They are at a small scale and would probably yield poorer resolution elevation models. The researchers already rectified some of these using 7-12 ground control points in ArcMap's Georeferencing environment (using the "projective transformation") and further processed them into a photo mosaic.

Most of these photos can also be purchased from a commercial provider (e.g. NCAP in Edinburgh, <https://ncap.org.uk/>, with an online search function) at about €60 per photo (digital, but otherwise unprocessed, image). Possibly, a deal between governments could be concluded, contact: [ncap@hes.scot](mailto:ncap@hes.scot). The photos don't contain technical specifications about height, orientation or lens. The scale can be derived by identifying ground control points on recent geographical data layers. They have often sideways overlap and could be elaborated in elevation models if enough ground control points can be identified and further using computer-aided block adjustment. This would however be a costly and specialised job. If a terrain model could be established, it would also be interesting for the research group at UGent.

Birger further indicated an interesting set of ground-based photos, taken in 1944 by the German army, on the beach looking at the war defences, that covers the Belgian coast. They are available at the Atlantikwall Raversyde museum (further to be explored).

#### 1.4.3 INBO

INBO (Instituut voor Natuur- en Bosonderzoek) (contact: [sam.provoost@inbo.be](mailto:sam.provoost@inbo.be)) researches the natural ecosystem of the coastal dunes and advises the Flemish Government on coastal management. Some reports from INBO address the historical and recent morphological evolution of parts of the coastal dunes.

INBO also has digital information which they are willing to share. One set is a shapefile Hoogte westkust 50.shp made by Sam Provoost (see [p:\20\\_079-MorfolInteract\3\\_Uitvoering\Deeltaak1\\_DataAcquisition\OudeKaarten\Ministerkaart1950-1970Kust\](p:\20_079-MorfolInteract\3_Uitvoering\Deeltaak1_DataAcquisition\OudeKaarten\Ministerkaart1950-1970Kust\)). He vectorised dune elevation contour lines of the western part of the coast of the 1950s Minister Map. The shapefile contains polygons every metre of the non-built part of the dunes between the French border and Nieuwpoort. The elevation (like in the maps, probably in TAW) is stored in an attribute "Hoogte" (this contains only values ending in .5, as the elevation is interpreted as the average elevation of the slice defined by the lower bounding contour line of each polygon and the following one, one metre higher). The projection system is Lambert (like in the maps, probably compatible with Lambert 1972). The polygon can be converted to polylines and the elevation can be restored by subtracting 0.5 m from the altitude attribute.

## 2 Modelling coupled shelf-shoreline long-term morphodynamics

### 2.1 Introduction

#### 2.1.1 Geographical setting

The Belgium inner shelf is characterized by the presence of a field of rhythmic sand ridges, which are aligned highly oblique with respect to the shoreline, i.e., their seaward ends are shifted several kilometres southwest with respect to their landward ends (Figure 18, panel a). These so-called shoreface-connected sand ridges (sfc) have alongshore crest-to-crest distances of 10-20 km, are 15-20 km long, 2-3 km wide, up to 6 m high (panel b) and they have an alongshore migration speed of several meters per year in the north-east direction (in accordance with the residual tidal current and primary direction of the wind and wave-driven flow on the Belgium shelf (Baeye *et al.*, 2010; Verwaest *et al.*, 2011)). Such ridges are also observed on other inner sandy shelves where frequent storms occur, such as those of the Dutch coast (Van de Meene *et al.*, 1996), Germany (Antia, 1996), the East Coast of United States (Duane *et al.*, 1972; Swift and Freeland, 1978) and Argentina (Parker *et al.*, 1982). Noticeably, crests of sfc are oriented persistently up-current with respect to the local storm-driven alongshore current, which, in the case of the Belgium shelf, is directed predominantly to the northeast. Indeed, observations have revealed that sfc evolve in stormy conditions, during which the joint action of high waves and strong currents causes erosion and transport of sediment at the bottom (Swift *et al.*, 1978; Parker *et al.*, 1982). The formation of sfc has been explained by Trowbridge (1995) and the mechanism is described in Figure 19 (see also the review by Ribas *et al.*, 2015).

Besides an alongshore migration, analysis of historical bathymetric data of the Belgium shelf (see §4.1) reveals that sfc migrate also landward, at rates in the order of meters per year. As these ridges affect the onshore wave propagation and consequently patterns of wave breaking and refraction in the nearshore, the onshore migration of the sfc might have significant impacts on the adjacent shoreline.

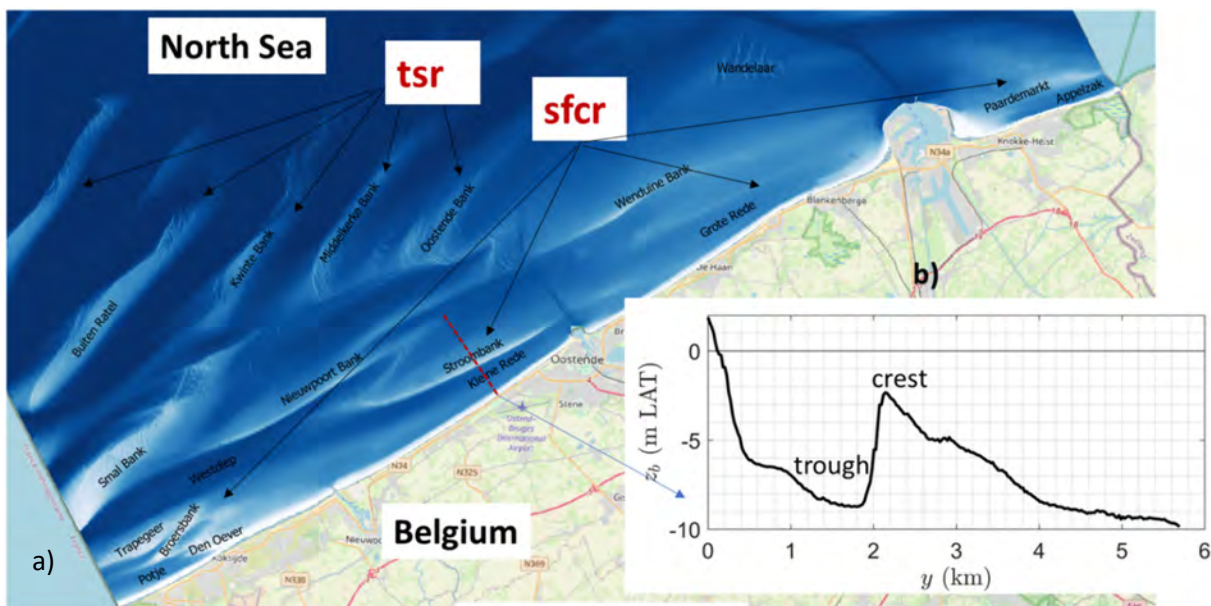


Figure 18 – Map of the research area.

a) Bathymetric map (LAT, m) of observed fields of shoreface-connected sand ridges (sfc) and the more offshore located tidal sand ridges (tsr) on the Belgium shelf. b) Bathymetric profile along a transect over the ridge "Stroombank".

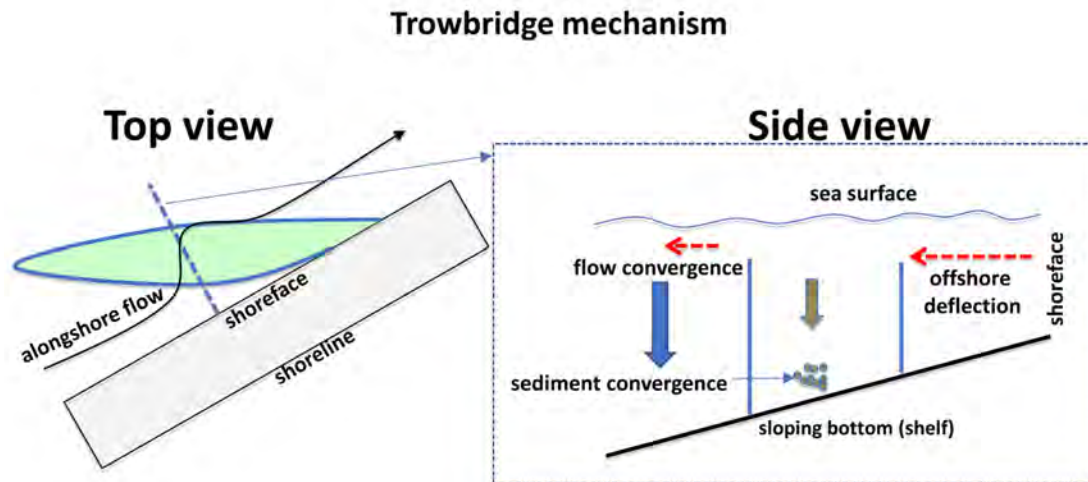


Figure 19 – Schematic view of the Trowbridge (1995) mechanism.

A ridge that is up-current aligned with respect to the alongshore storm-driven flow causes an offshore deflection of this flow due to mass conservation. The offshore sloping bathymetry of the inner shelf causes the flow to converge. Since sediment transport is assumed to be proportional to the current, convergence of sediment occurs over the ridge as well, resulting in ridge growth. Offshore decreasing wave stirring increases the sediment convergence, thereby enhancing growth. A down-current oriented ridge will not grow because divergence of sediment would occur over its crest due to onshore flow deflection. This mechanism explains why only up-current oriented ridges are observed in the field. Note that further offshore on the Belgium shelf (Figure 18), tidal sand ridges (tsr) are present, which have a different orientation compared to that of sfc and whose formation mechanism is due to tides (Huthnance, 1982). See also the review by Vittori & Blondeaux (2022).

### 2.1.2 Research question

The overall aim of subtask 2 (Work Package 2, WP2) of the MOZES project is to investigate the impacts of onshore migrating sfc on the Belgium shoreline. To this end, the shelf and shoreline areas will be studied in conjunction with each other by developing a new idealized model tool that couples a morphodynamic shelf model to a morphodynamic shoreline evolution model (coupled shelf-shoreline model). The strategy how to set up this new tool is outlined in Figure 20. An existing coupled shelf-shoreline model will serve as a starting point, which was developed by the Utrecht University (IMAU) and UPC Barcelona (Nnafie *et al.*, 2021). This model was established by coupling a shelf model (Delft3D-SWAN) to a shoreline evolution model (Q2Dmorfo). One major drawback in the coupled model of Nnafie *et al.* (2021) was that the shelf model was morphostatic, i.e., the bottom was not allowed to evolve during the model simulations. This is because their shelf model was not capable of self-developing sfc when starting from an initially flat bed. Instead, a synthetic field of morphostatic sfc was artificially placed on the shelf, which provided a forcing template for the morphodynamic development of the shoreline. Other drawbacks are that the model 1) is designed for the situation of the Long-Island coastal zone, 2) it does not account for tides and 3) it considers waves that come from one direction only.

This chapter describes the activities of the first year within subtask 2 (Work Package 2, WP2) of the MOZES project, which are based on the strategy depicted in Figure 20. These activities were:

1. to develop an idealized morphodynamic shelf model (Delft3D-SWAN) that simulates self-developing sfc on the Belgium shelf (Activity 1); and
2. to use the model of Nnafie *et al.* (2021) to obtain preliminary ideas about potential impacts of the onshore migration of sfc on the evolution of the Belgium shoreline at timescales of decades (Activity 2).

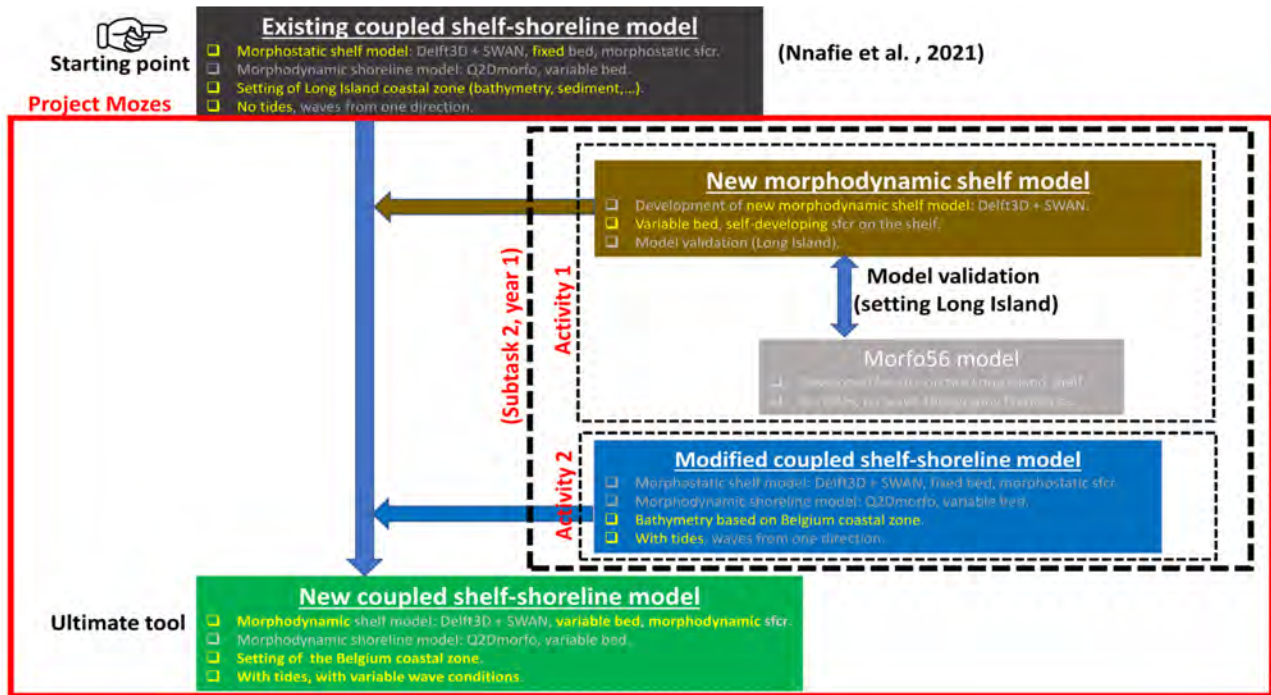


Figure 20 – Block diagram showing the steps toward the design of the new coupled shelf-shoreline morphodynamic model. Main differences between this new model and the existing models are indicated in yellow text. The two activities within subtask 2 of Work Package 2 (WP2) in the first year of the Mozes project are also shown.

With regard to Activity 1, it should be stressed that this was quite challenging, as so far, no such numerical model exists. An exception seems to be the numerical model Morfo56, but this model has no tides and it crudely simplifies waves, which makes it not suitable for use in this research. The new shelf model was validated by 1) comparing its simulated hydrodynamics and sediment transport with those of Morfo56, which has been successfully applied to Long-Island micro-tidal shelf (New York, USA, Figure 21b, Nnafie *et al.*, 2014b); and by 2) comparing its simulated ridges with observations on the Long-Island shelf.

As for Activity 2, the coupled model of Nnafie *et al.* (2021) was modified such that 1) its background topography is more representative for the Belgium coast and 2) it contains tides.

The structure of the remainder of this chapter is as following. Sections 2.2 and 2.3 provide extended summaries of the setups and the results of, respectively, the new morphodynamic shelf model (Activity 1) and the modified coupled shelf-shoreline model (Activity 2). Further details are given in Appendix 2. Finally, Section 2.4 gives a summary and outlook.

## 2.2 Morphodynamic shelf model

This section describes the setup of the new morphodynamic shelf model and its validation by testing its capability to reproduce 1) an offshore deflection of the flow (and sediment transport) over the crests of a field of ridges and an onshore deflection over their troughs, in agreement with the growth mechanism of Trowbridge (1995) (benchmark 1); and to reproduce 2) self-developing ridges on the shelf that have similar gross characteristics (orientation, alongshore spacing, evolving time scales, height and migration rates) as those of observed sfc (benchmark 2). For this validation, the new shelf model uses the model equations and configuration of model Morfo56, which has been successfully applied to Long-Island micro-tidal shelf and where waves predominantly come from one direction (Nnafie *et al.*, 2014b).

### 2.2.1 Model description

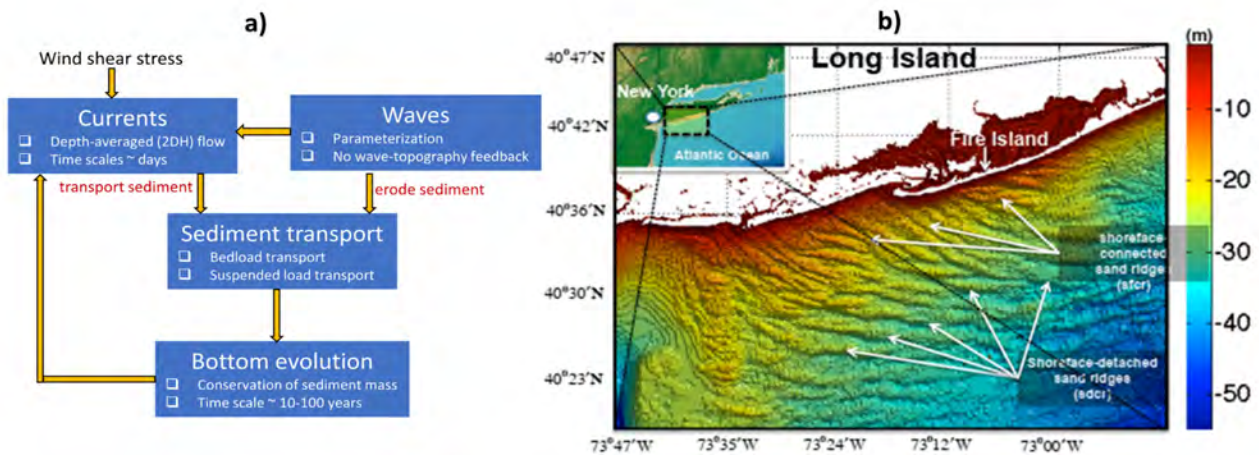


Figure 21 – Model structure and study area

a) Feedbacks between the model components. b) Bathymetric maps of the Long Island shelf, showing a field of sfc and the more offshore located sdc (shoreface-detached sand ridges). Figure adopted from the work by Nnafie *et al.* (2014b).

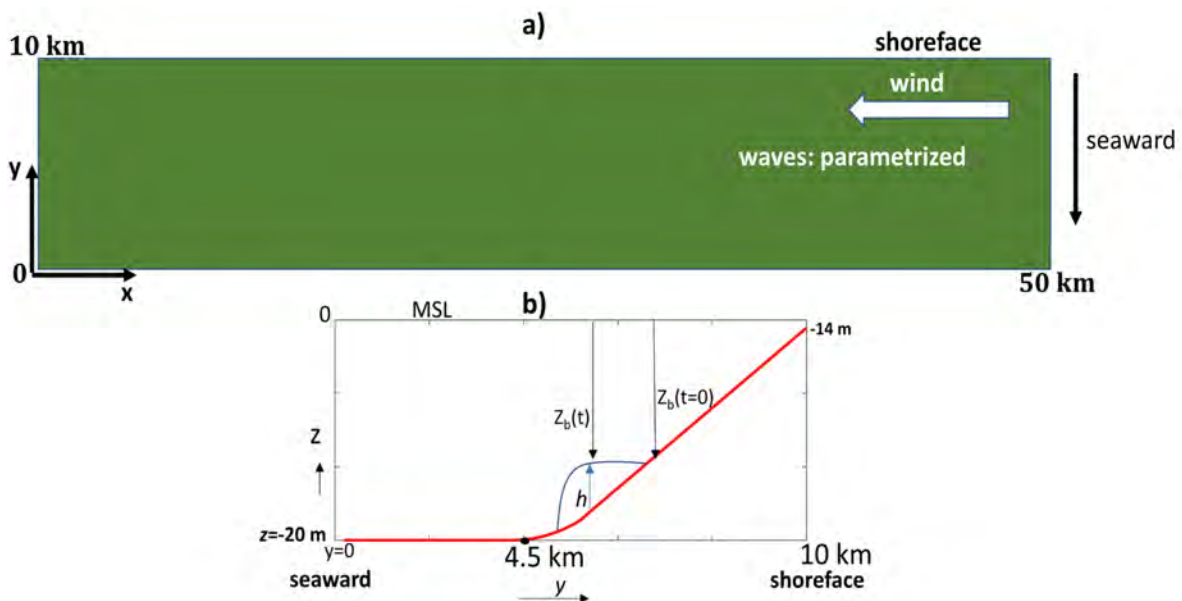


Figure 22 – Setup of the idealised morphodynamic shelf model.

Top (a) and side (b) views of the model domain. For the explanation of the symbols see the text.

The Delft3D (D3D) software package (depth-averaged, 2DH) is used for the development of the morphodynamic shelf model. For this validation, new formulations (bed-shear stress, wind stress, wave parametrization, Bailard's transport, bed slope) were implemented as new options in the D3D code.

The shelf model uses a rectangular model domain, with  $x$ - $y$  pointing in the along- and cross-shore directions, respectively. Note that a positive  $y$  indicates a shoreward direction (Figure 22). Coordinate  $z$  denotes a vertical position, while  $z_b(x, y, t)$  marks the position of the bed-level, positive downward (panel b). Perturbations in bed-level  $z_b(x, y, t)$  with respect to its initial value ( $z_b(x, y, 0)$ ) are represented by  $h$  (positive upward), i.e.,  $h(x, y, t) = z_b(x, y, t) - z_b(x, y, 0)$ . The following bed-shear stress formulation is used, which is derived by assuming stormy conditions:

$$\vec{\tau}_b = \rho r_0 u_{rms} \vec{v}, \quad (1)$$

with  $\rho$  the density of water,  $r_0$  a drag coefficient,  $u_{rms}$  the root-mean-square (rms) amplitude of the wave orbital velocity at the bottom and  $\vec{v}$  the velocity vector with  $x$ - $y$  components ( $u, v$ ). Rms amplitude  $u_{rms}$  is computed using the parametrization of Calvete *et al.* (2001), which neglects the feedbacks between the changing depth and  $u_{rms}$  (Equation A1 in Appendix 2.1). As for sediment transport, the transport formulations of Bailard (1981) are used, which account for bedload ( $\vec{q}_b$ ) and suspended load transport ( $\vec{q}_s$ ):

$$\vec{q}_{tot} = \vec{q}_b + \vec{q}_s = \left[ \nu_b u_{rms}^2 + \frac{\delta D}{\hat{u}^3} u_{rms}^3 \right] \vec{v} - [\nu_b \lambda_b u_{rms}^3 + \lambda_s u_{rms}^5] \vec{\nabla} h. \quad (2)$$

Here,

- $\nu_b$  is a coefficient of the bedload transport,
- $\lambda_b$  and  $\lambda_s$  are bedslope parameters for bedload and suspended load transport, respectively,
- $D$  is the total water depth,  $\hat{u}$  is a calibration velocity and  $\delta$  is the (scaled) layer thickness of the suspended sediment in the water column.

Note that the terms containing gradient  $\vec{\nabla} h$  in Equation 2 represent bed-slope induced sediment transport over bottom perturbations  $h$ . A view of the structure of the new morphodynamic shelf model is depicted in Figure 21a. Waves exert a shear stress at the bottom, thereby eroding sediments from this bottom. Subsequently, these sediments are transported by current  $\vec{v}$ , which is induced by a wind-shear stress  $\vec{\tau}_w$  representative for stormy conditions. The divergence or convergence of sediment transport  $\vec{q}_{tot}$  determines changes in bed-level  $z_b$ , which influence the current.

### 2.2.2 Methodology

The rectangular model domain has dimensions  $50 \times 10$  km. The chosen initial bed-level profile (Figure 22b), is uniform in the alongshore direction (exact expression is given in Appendix 2.1). At the landward side ( $y = 10$  km), depth is 14 m, and it increases linearly in the seaward direction (negative  $y$ -direction) over a distance of 5.5 km, after which it remains constant (20 m). See also the Appendix. The model is forced with a wind stress  $\vec{\tau}_w$  that acts along the coast (in the negative  $x$ -direction, value is  $-0.4 \text{ Nm}^{-2}$ ). Furthermore, at the lateral boundary conditions, Neumann conditions (in both the water level and sediment transport) are imposed, while at the offshore boundary a water level of 0 m is prescribed. As for the numerical parameters, mesh sizes of the computational grid are 200 m in both the cross-shore and alongshore directions, while time step is 0.1 minutes.

Three series of experiments have been performed with the shelf model. In the first series (“Flow over topography”), a field of artificial sfcf was placed on the shelf. In these series different heights of the sfcf, time steps, grid sizes and horizontal eddy viscosities were considered. The resulting changes in the flow and sediment transport fields over the artificial sfcf were quantified. According to the growth mechanism described by Trowbridge (1995) the presence of the ridges should induce an offshore deflection of the flow (and consequently the sediment transport) over the crests and an onshore deflection over the troughs (benchmark 1).

As an initial step toward the simulation of shelf morphodynamics, the initial erosion and deposition patterns over the artificial sfcf were examined in the second series (“Initial erosion and deposition”). These patterns, which were obtained by computing divergence  $-\vec{\nabla} \cdot \vec{q}_{tot}$ , indicate the tendency of the ridges to either grow or decay. If deposition (erosion) takes place in the crest (trough) areas, the ridges will grow, otherwise they will decay. Besides growth, ridge migration may also occur as a result of the storm-driven current. Migration takes place if the location of maximal deposition is slightly shifted with respect the location of maximum height of the crests.

Finally, in the third series (“Long-term shelf morphodynamics”), the long-term morphodynamic evolution of the shelf was addressed by activating the bed-level evolution. Different grid sizes, time steps and numerical schemes were considered. Initially, small-scale random bottom perturbations with a root-mean square height of 10 cm were superimposed on the background sloping bathymetry. These perturbations contain various patterns at different length scales. The mechanism proposed by Trowbridge (1995) will subsequently cause the bottom pattern that initially has the fastest growth rates to dominate after some time. After that stage, when ridges have attained considerable height, they will nonlinearly interact with each other and typically attain a finite height (see e.g. Nnafie *et al.*, 2014a). To reduce computation time, a morphological acceleration factor of 400 is used. This is justified because the morphodynamic timescale is much longer (order of years) than the hydrodynamic timescale (order of hours to days). The experiment was run for a maximum period of 1500 years. The expectation was that the model simulate shelf-developing bedforms with gross characteristics that resemble those of observed sfcf on the Long-Island shelf (benchmark 2). The characteristics of the simulated bedforms were analysed in terms of their root-mean-square (rms) height  $||h||$ , global growth rate  $\sigma$ , global migration speed  $V_m$  and their longshore dominant spacing (wavelength). Definitions of these quantities are given in Appendix 2.1.

## 2.2.3 Results and discussion

## Flow over topography

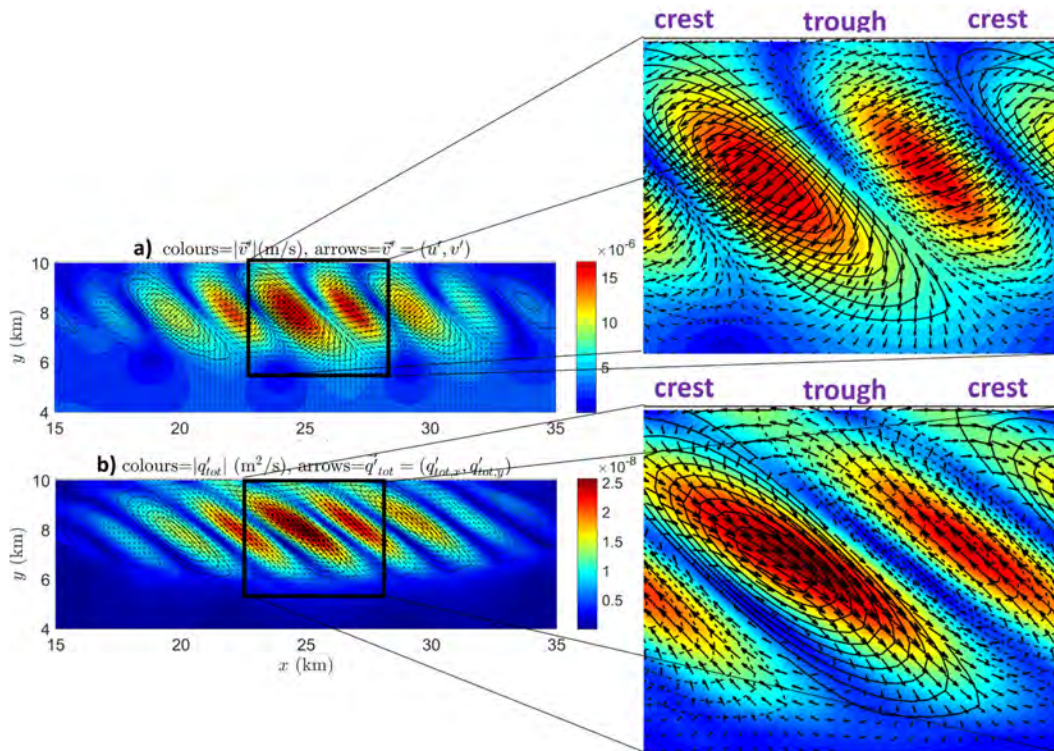


Figure 23 – Results of run series "Flow over topography", in the case of using the "Flooding" scheme with a horizontal eddy viscosity of  $\nu = 1 \cdot 10^{-6} \text{m}^2\text{s}^{-1}$ .

a) Magnitude  $|\vec{v}'|$  (colours) of perturbed flow vector  $\vec{v}'$  (arrows).

b) As in a), but for the perturbed sediment transport vector  $\vec{q}'_{tot}$ . These quantities are defined as  $\vec{v}' = \vec{v} - \langle \vec{v} \rangle$  and  $\vec{q}'_{tot} = \vec{q}_{tot} - \langle \vec{q}_{tot} \rangle$ , respectively. Here, brackets  $\langle \cdot \rangle$  denote an alongshore averaging. Zoom-ins are shown in the right panels.

Results from these run series are presented in Figure 23, which shows the perturbed flow and sediment transport fields,  $\vec{v}' = \vec{v} - \langle \vec{v} \rangle$  and  $\vec{q}'_{tot} = \vec{q}_{tot} - \langle \vec{q}_{tot} \rangle$ , respectively. Here, brackets  $\langle \cdot \rangle$  denote an alongshore averaging. This figure clearly demonstrates the capability of the model to reproduce the offshore (onshore) deflection of flow and transport fields over crests (troughs) of the artificial ridges. **This demonstration of the Trowbridge (1995) growth mechanism is considered as a first milestone.**

This first milestone was achieved after a long search into the D3D numerical schemes and after many additional experiments. Results displayed in Figure 23 were obtained when combining the "Flooding" scheme with a very small horizontal eddy viscosity ( $\nu = 1 \cdot 10^{-6} \text{m}^2\text{s}^{-1}$ ; molecular viscosity). For the default numerical scheme of Delft3D (so-called "Cyclic" scheme), as well as for the "Waqua" scheme, the model was not capable of simulating the offshore (onshore) deflection of the flow and sediment transport over crest (troughs) of the ridges. A further analysis of the model results revealed that the "Cyclic" and "Waqua" schemes, which discretize the horizontal advection terms in the momentum equations, are too diffusive to accurately resolve changes in the advection terms caused by the presence of the artificial ridges. Results from additional experiments showed that reducing time step ( $\Delta t$ ) and viscosity  $\nu$  and/or imposing a larger amplitude sfcf did not significantly improve the accuracy of the two model schemes.

### Initial erosion and deposition

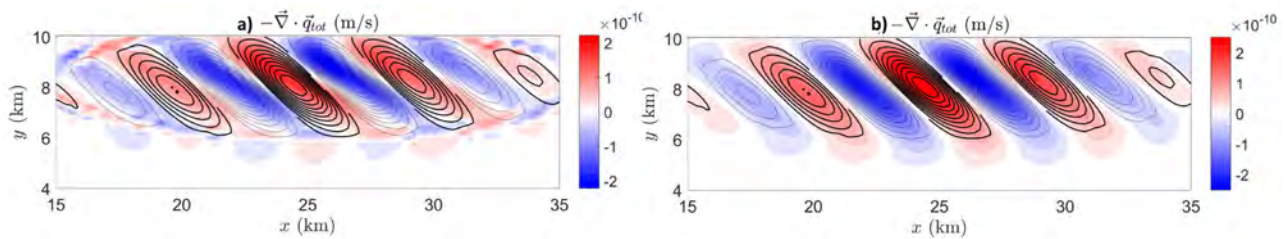


Figure 24 – Results of run series “Initial erosion and deposition”,

- a) Initial erosion (blue colours) and deposition patterns (red) in the cases of the using the D3D default staggering scheme for depth. Crests and troughs are indicated by thick solid and thin dashed lines, respectively. These patterns were obtained by computing divergence  $-\vec{\nabla} \cdot \vec{q}_{tot}$ .
- b) As in a), but using a new staggering scheme, which uses depth at the  $u, v$  velocity nodes for the calculation of sediment transport  $\vec{q}_{tot}$ .

From Figure 24 it is seen that the shelf model correctly simulates that deposition and erosion take place in the crest and trough areas. However, small-scale erosion and sedimentation patterns appear around the crests and troughs, which are attributed to numerical instabilities. The accuracy of the model results improves when increasing the grid resolution by factor of 2. After a long dive into the model code, it turned out that these instabilities were caused by an incorrect staggering of depth in the D3D code when computing the sediment transport, viz., depth at the water level nodes is used instead of the  $u, v$  velocity nodes. The D3D codes was then adjusted such that the depth at the  $u, v$  velocity nodes was used in the calculation of the sediment transport (as is the case in Morfo56). This adjustment solved the problem of numerical instabilities (Figure 24b), **which is considered as a second milestone**.

### Long-term shelf morphodynamics

Results from experiment "Long-term shelf morphodynamics" are presented in Figure 25, which shows snapshots of bottom perturbations  $h(x, y, t)$  in the first 1000 years. Initially, mode scale selection takes place: bottom modes that do not have the most-preferred topographic wavelength (alongshore spacing) will decay over time, and only the mode with this specific wavelength will eventually remain (Figure 25 from panel a to panel b). Once the latter mode emerges (after a couple of hundreds of years), coast-oblique ridges with an alongshore wavelength of about 2.6 km develop across the shelf, whose height exponential increases over time (Figure 25 from panel b to panel d).

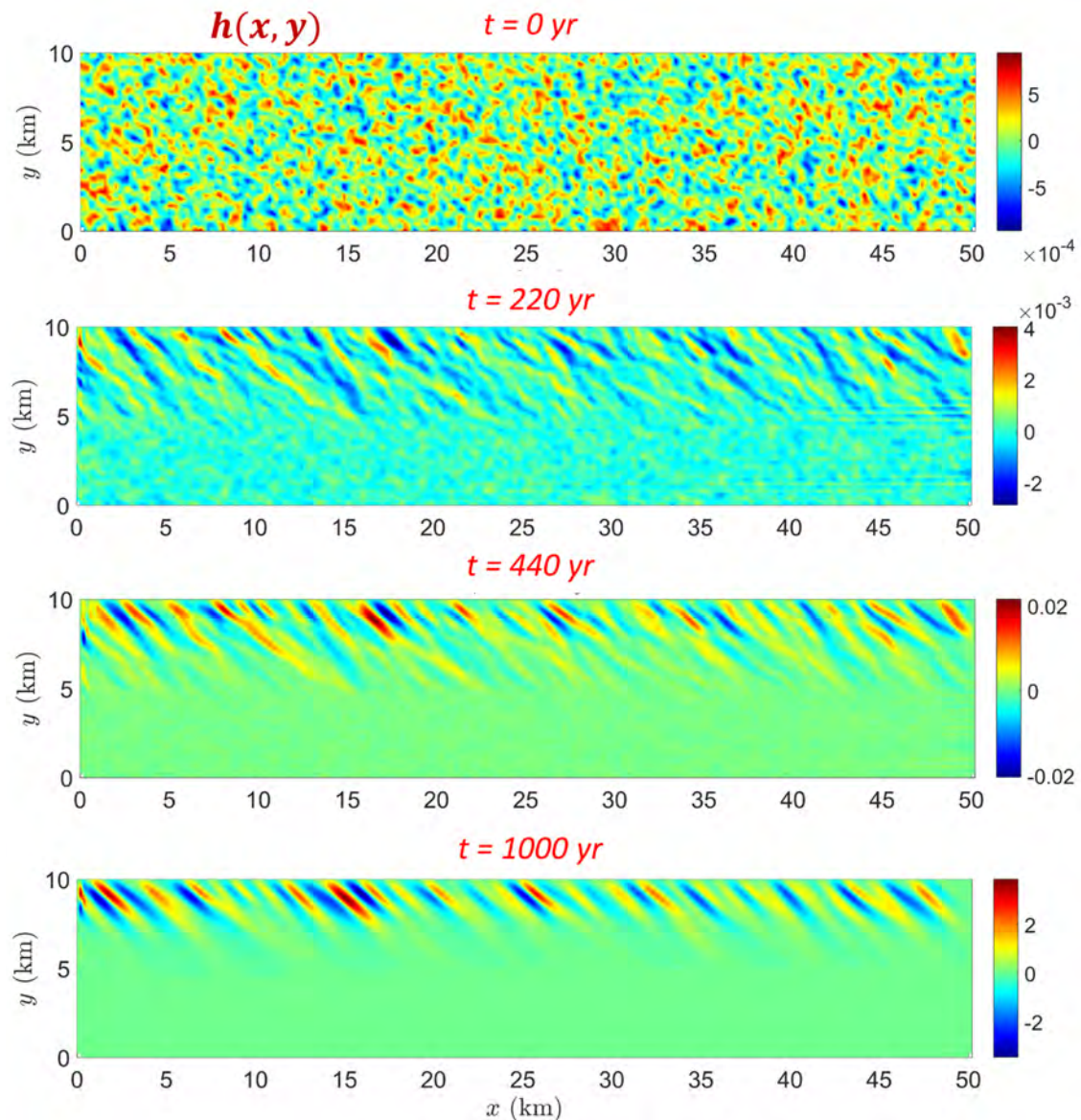


Figure 25 – Results of run series “Long-term shelf morphodynamics”: bed evolution.

a-c) Snapshots of bottom perturbations  $h(x, y, t)$  at different points in time, as computed by the morphodynamic shelf model. Model was run starting from random bottom perturbations with rms height of 10 cm. A morphological acceleration factor of 400 was used.

The latter is seen from panel a of Figure 26, which shows rms height  $\|h\|$  of bedforms versus time. From Figure 26 it further appears that the simulated ridges grow on centennial time scales ( $= \sigma^{-1}$ , panel b) with heights (crest-to-trough distance) of several meters (a) and they migrate at rates  $V_m$  of about -2.5 m/y in the downstream direction (negative  $x$ ) as a result of the storm-driven currents (panel c). These characteristics of the simulated ridges resemble those of observed sfc on the Long-Island shelf. On long time scales ( $t > 1000$  years) strong non-linear interactions take place, causing the growth rate and migration to decrease. Note that for  $t > 1300$  years, model blows up due to numerical instabilities, which is a phenomenon that was also reported by previous studies on sfc on the Long-Island shelf. These instabilities might be due to the absence of wave-topography feedbacks or sea-level rise, which are considered important topics for year 2 of the MOZES project. Also note that boundary effects might affect model results on long time scales, as a result of the collision of alongshore migrating ridges against the left lateral boundary. This collision can be avoided by implementing periodic boundary conditions at the lateral boundaries (as is the case in Morfo56), which is also considered a topic of future code improvements.

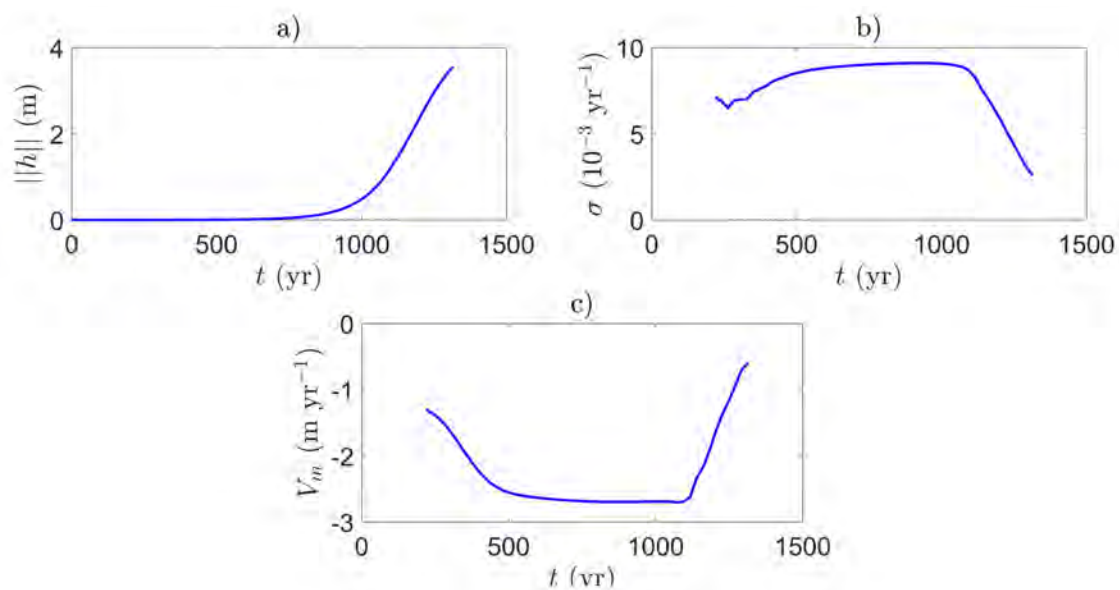


Figure 26 – Results of run series “Long-term shelf morphodynamics”: sand ridge properties. a-c) Rms height  $\|h\|$  (a), global growth rate  $\sigma$  (b) and migration  $V_m$  (c) of the ridges versus time.

One of the main differences between the Long-Island and Belgium shelves is that the latter is shallower compared with the former one. To explore how a difference in depth would affect the characteristics of the simulated ridges, experiment "Long-term shelf morphodynamics" was repeated, but with the difference that the depth is much shallower (Figure 27, top panel). Due to enhanced morphological changes for smaller depths, the morphological acceleration factor was set to a smaller value (100). Snapshots of bottom perturbations obtained from this additional experiment are presented Figure 27. Compared with the Long-Island shelf, the ridges now grow much quicker (order of 10 years), migrate much faster (order of 10 m/y), have smaller wavelengths ( $\sim 2$  km) and they have a smaller offshore extent. To be able to compare with observed sfc on the Belgium shelf, still many adjustments in the shelf model must be carried out, of which the most important ones are the inclusion of tides, waves, sea-level rise and the use of a more realistic bathymetry. These adjustments are key topics of future research.

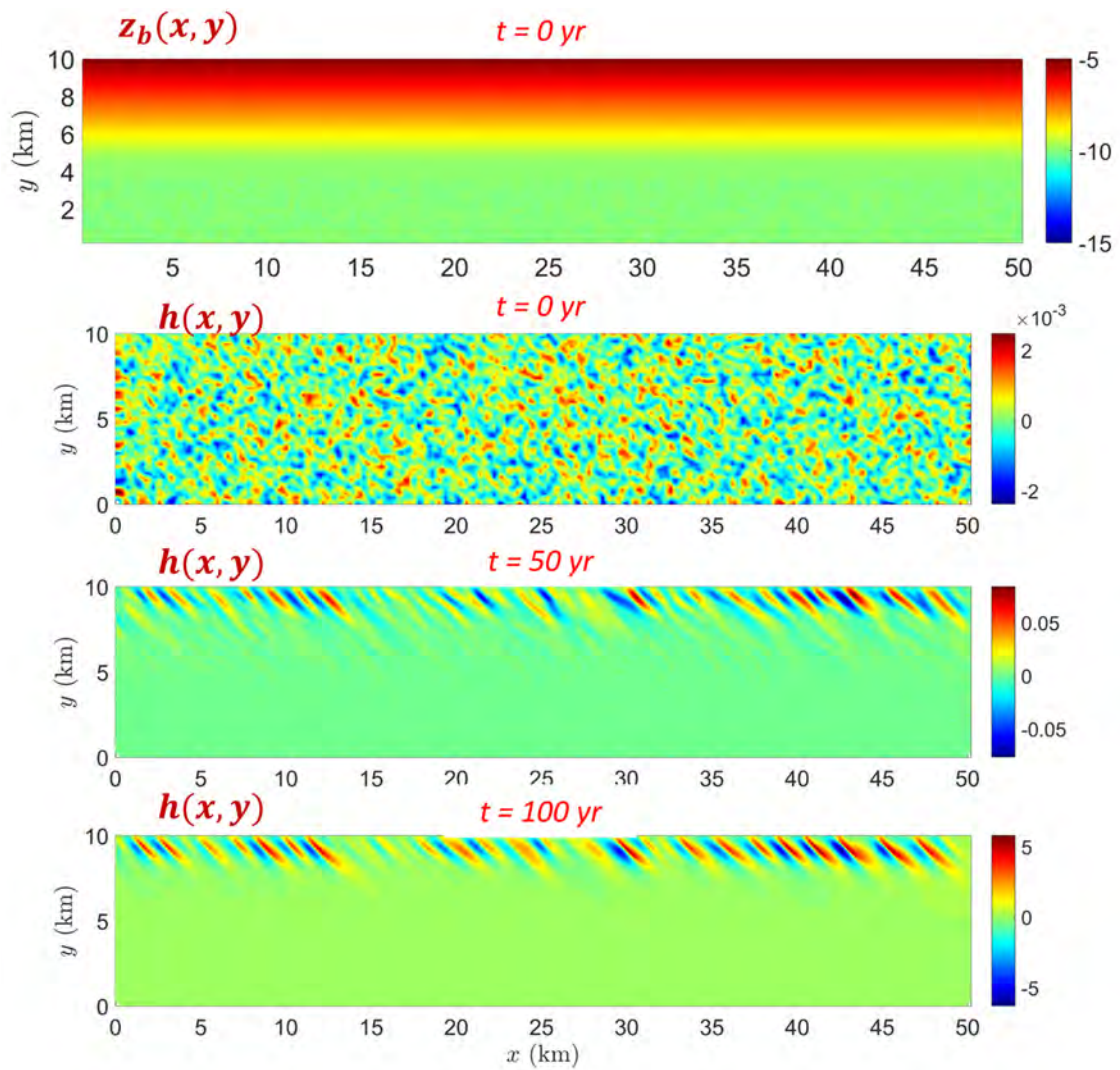


Figure 27 – Results of run series “Long-term shelf morphodynamics”: evolution of a shallower bed. As in Figure 25, but for a shallower depth (top panel). A morphological amplification of 100 was used.

## 2.3 Coupled shelf-shoreline model

To explore potential impacts of the observed onshore migration of sfcf on the Belgium shelf on the evolution of the adjacent shoreline and nearshore zone, simulations were carried out with an existing shelf-shoreline model system (Nnafie *et al.*, 2021), but modified such that it uses the background bathymetry based on that of the Belgium shelf and it accounts for tides (see Figure 20). The next section briefly describes the model. For a more detailed description, the reader is referred to Appendix 2.2.

### 2.3.1 Coupled Model

The coupled model distinguishes between processes on the shelf ( $x_1 \leq x \leq x_L$ ,  $0 \leq y \leq y_L$ ), in the nearshore zone ( $0 \leq x \leq x_2$ ,  $0 \leq y \leq y_L$ ) and in a coupling zone ( $x_1 \leq x \leq x_2$ ) between shelf and nearshore zone (see Figure 28).

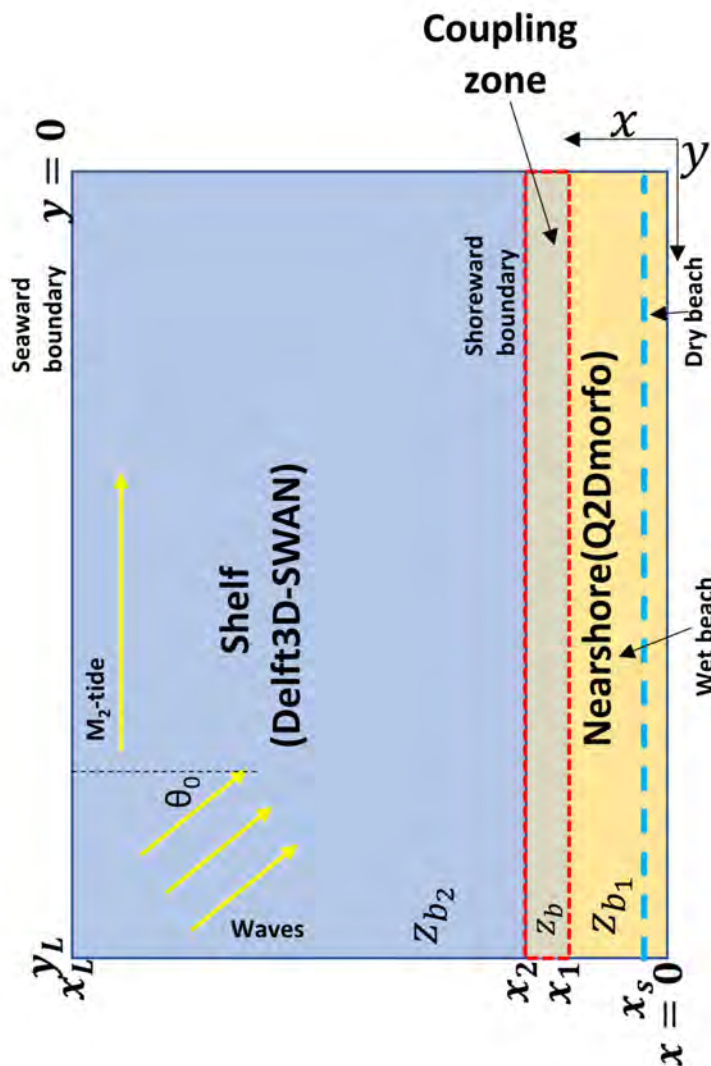


Figure 28 – Coupled shelf-shoreline model.

Domains of the shelf ( $x_1 \leq x \leq x_L$ ,  $0 \leq y \leq y_L$ ) and shoreline models ( $0 \leq x \leq x_2$ ,  $0 \leq y \leq y_L$ ), with  $x - y$  pointing in, respectively, the cross-shore and alongshore directions. The red rectangle denotes the coupling zone ( $x_1 \leq x \leq x_2$ ). Bed levels  $z = z_{b_1}$ ,  $z = z_b$  and  $z = z_{b_2}$  denote the bottom levels of the nearshore, coupling zone and the shelf, respectively. Shoreline position  $x_s(y, t)$  marks the border between the dry ( $z_b > 0$ ) and wet beaches ( $z_b \leq 0$ ). Tidal forcing is imposed at the seaward boundary of the shelf ( $x_L$ ) as an  $M_2$  tidal wave that propagates from south to north along the coast. Furthermore, only mean wave conditions are prescribed, having a significant wave height  $H_{s0}$ , peak period  $T_{p0}$  and wave direction  $\theta_0$  (relative to the shore-normal, positive counter-clockwise).

On the shelf, the depth-averaged currents, waves and their interactions are computed with D3D-SWAN. Note that, unlike in Section 2.2, the original version of D3D-SWAN has been used here, without making any adjustments in the software code. A shelf bathymetry is considered that comprises an artificial field of sfcf (see next section). The water motion is forced by tides and waves. Here, tidal forcing is imposed at the seaward boundary of the shelf ( $x_L$ ) as an  $M_2$  tidal wave that propagates from south to north along the coast. Furthermore, only mean wave conditions are prescribed, having a significant wave height  $H_{s0}$ , peak period  $T_{p0}$  and wave direction  $\theta_0$  (relative to the shore-normal, positive counter-clockwise). In the nearshore zone, waves, sediment transport, as well as changes in bed level and position of the shoreline are calculated with Q2Dmorfo. Bed levels  $z = z_{b1}$ ,  $z = z_b$  and  $z = z_{b2}$  denote the bottom levels of the nearshore, coupling zone and the shelf, respectively. Shoreline position  $x_s(y, t)$  marks the border between the dry ( $z_{b1} > 0$ ) and wet beaches ( $z_{b1} \leq 0$ ). Initially, the beach has a width  $x_{s0}$ . Note that the shelf model is morphostatic, i.e., the bathymetry is kept fixed, whereas the nearshore model is morphodynamic. The coupling between the shelf and shoreline models is realized by 1) allowing the nearshore bed-level ( $z_{b1}$ ) inside the coupling zone to be affected by that of the shelf ( $z_{b1}$ ) (bed-level coupling) and by 2) imposing the wave parameters computed by the shelf model at  $x_2$  ( $H_{s1}, T_{p1}, \theta_1$ ) as wave forcing in shoreline model (wave-forcing coupling). Further details are given in Appendix 2.2.

### 2.3.2 Methodology

#### Model parameters

Dimensions of the coupled model domain, bathymetry, tides and waves were based on observations on the Belgian coast. Other parameter values were adopted from the work by Nnafie *et al.* (2021) and Arriaga *et al.* (2017). A list of all the values of model parameters is provided in Appendix 2.2 (Table 14). The dimensions of the coupled model domain are  $x_L \times y_L = 55 \times 75$  km. The coupling zone stretches between  $x_1 = 2.5$  km and  $x_2 = 5$  km. The dry beach has a width of 500 m (i.e.,  $x_{s0} = 500$  m) and its height is 1 m. Depths increases from 0 m at the shoreline ( $x_s$ ) to 43 m at the seaward end. The  $M_2$ -tidal forcing at the seaward boundary ( $x = x_L$ ) has amplitude  $\hat{\zeta}_2 = 1.8$  m and phase difference of  $31.5^\circ$  between the lateral boundaries,  $y = 0, y_L$ . This tidal forcing represents a propagating  $M_2$ -tidal wave in the negative  $y$ -direction. As for the waves, S-SW wave conditions were prescribed at the offshore boundaries (with parameters  $H_{s0} = 1$  m,  $T_{p0} = 5.7$  s,  $\theta_0 = 50^\circ$ ), which is a crude simplification of observed wave climate in the Belgian coastal region. The computational grid of the morphostatic shelf model has grid sizes of about 750 m in the cross- and alongshore directions, respectively, while the hydrodynamic time step is 1 minute. The alongshore grid size of the computational grid of the shoreline model is the same as in the shelf model. However, to resolve the surf zone processes, the cross-shore grid size is much smaller (20 m). Time step is set to 0.01 days. To establish the coupling between the shelf and shoreline models, data is being exchanged between the two models (see Figure 101), which is extremely time consuming. To avoid large computation times, these data is exchanged after 1 year (called coupling time), which is still much smaller than the morphodynamic time scale of the shoreline evolution (order 10 to 100 years).

#### Experiments

To explore potential impacts of onshore migrating sfcf on the Belgium shelf on the adjacent nearshore and the shoreline, three experiments ("Couple-Exp*i*",  $i = 1,2,3$ ) were carried out with the coupled model. An increasing  $i$  means that sfcf are located more onshore. An artificial field of sfcf was superimposed on the sloping bed of the shelf, having a height (crest-to-trough distance) of about 8 m and wavelength of 4 km (Figure 29). Note that the geometry of this artificial field of sfcf (dimensions, alongshore spacing, height, etc..) is based on that of observed sfcf on the Long-Island inner shelf and, thus, it does not reflect the geometry of observed sfcf on the Belgium inner shelf. The shoreline is initially straight and is situated at  $x_s = 500$  m.

As a reference case, a fourth experiment ("Couple-Exp0") was carried out in the absence of sfc<sub>r</sub> on the shelf (top panel in Figure 29). With this experiment, the relative impact of the presence of sfc<sub>r</sub> on the adjacent shoreline can be obtained by comparing the situations with and without their presence with each other. The experiments were run for 50 years.

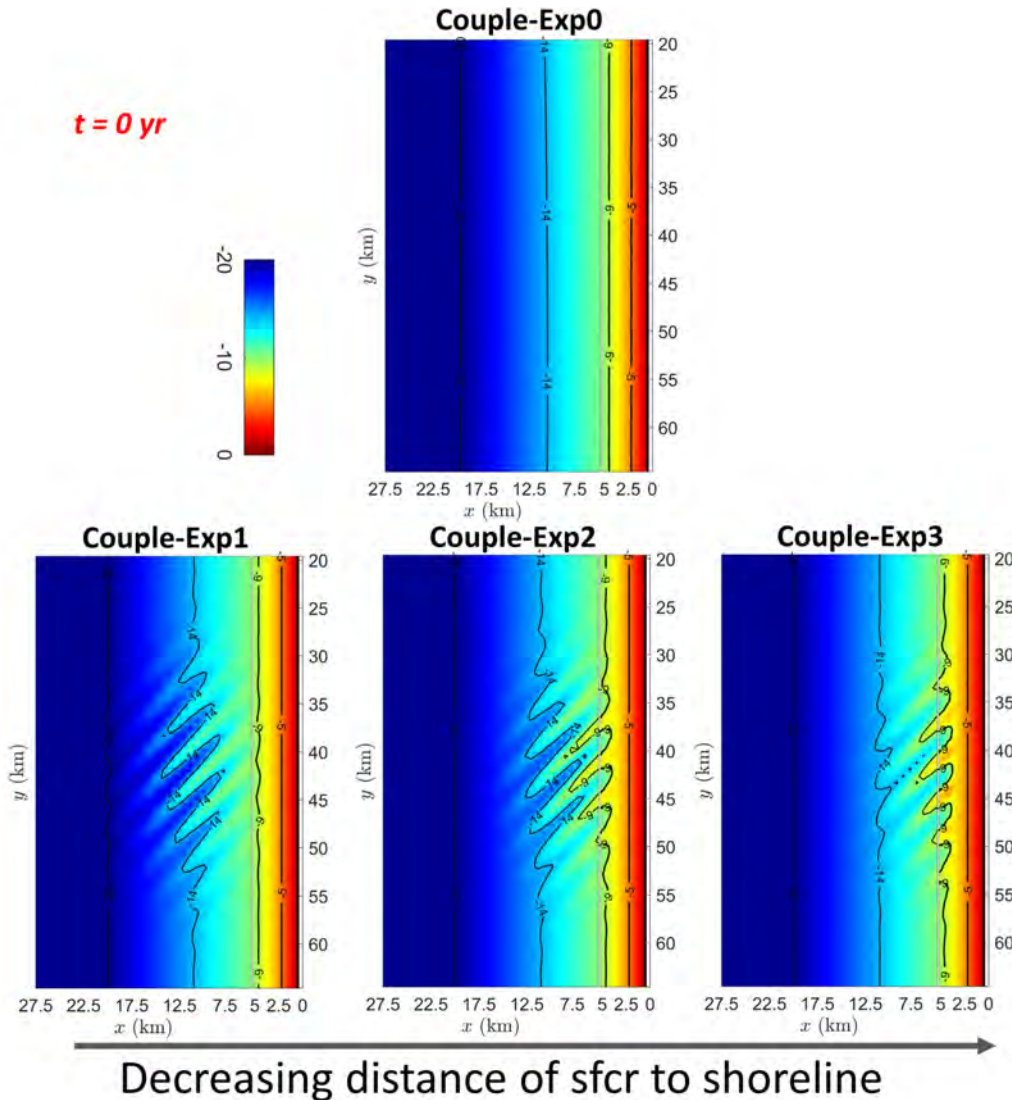


Figure 29 – Setup of run series "Couple-Exp $i$ ",  $i = 0,1,2,3'$ .

Note that no sfc<sub>r</sub> are present on the shelf in the reference case ("Couple-Exp0"). In each panel, the coast is located on the right. The thick black lines denote shoreline position  $x_s$ .

### 2.3.3 Results and discussion

Results from the experiments with the coupled model are presented in Figure 30, which shows snapshots of the shelf and nearshore bed-levels after 50 years of morphodynamic evolution for different offshore locations of the sfc<sub>r</sub> ("Couple-Exp $i$ ",  $i = 1,2,3'$ ). The reference situation (i.e., no sfc<sub>r</sub> on the shelf) is depicted in the top left panel. The simulated longshore profiles of shoreline positions  $x_s$  at  $t = 50$  years are presented in Figure 31. The initial positions of the shoreline ( $x_{s0}$ ) is situated at 500 m (thick black lines in Figure 29). These figures clearly demonstrate that the presence of sfc<sub>r</sub> on the shelf causes the formation of shoreline undulations along the adjacent shoreline, which are absent when there are no sfc<sub>r</sub>. The more onshore the bedforms are located, the stronger these undulations become. As was explained by Nnafie *et al.* (2021),

topographic wave refraction due to the presence of the sfc<sub>r</sub> leads to the focussing of wave energy density over the crests of the ridges and defocussing of energy in their troughs (see Figure 32). Consequently, alternating areas of high and low wave energy (white and dark areas, respectively) occur along the shoreline, which are associated with strong and weak longshore sediment transport. As a result, large alongshore gradients in the alongshore sediment transport occur, thereby creating localized areas of erosion and accretion along the shoreline. The more onshore the sfc<sub>r</sub> are located, the stronger are the alongshore gradients and thus the more distinct are these erosion/accretion areas. Note that the shoreline profile is asymmetric, meaning that, on average, it retreats (progrades) in the north (south) region (Figure 31, right panel). This is due to the fact that the height of the artificial sfc<sub>r</sub> used in the model was asymmetric in the alongshore direction (left panel). Consequently, as can be seen from Figure 32, highest ridges focus more wave energy than lower ones, causing the formation of stronger alongshore gradients in some areas than in others.

These results suggest that an onshore movement of sfc<sub>r</sub> is expected to induce stronger shoreline undulations along the shoreline. However, as this model is still under development, these results cannot be translated into projections of the impact of onshore migrating sfc<sub>r</sub> on the Belgium shoreline. The used wave forcing is crudely simplified, whose wave characteristics (wave height, wave angle and wave period) do not change in time. In reality, these characteristics continuously change in space and time. As was demonstrated by Nnafie et al. (2021) for the case of tidal sand ridges on the shelf, the use of a more realistic wave climate leads to the development of a relatively straight shoreline, which is a more realistic representation of the Belgium shoreline. Also, the geometry (offshore extent, orientation with respect to coastline, alongshore spacing) of the artificial sfc<sub>r</sub> used in the model does not reflect that of observed sfc<sub>r</sub> on the Belgium shelf. These two issues are proposed as key research topics for the second year of the project.

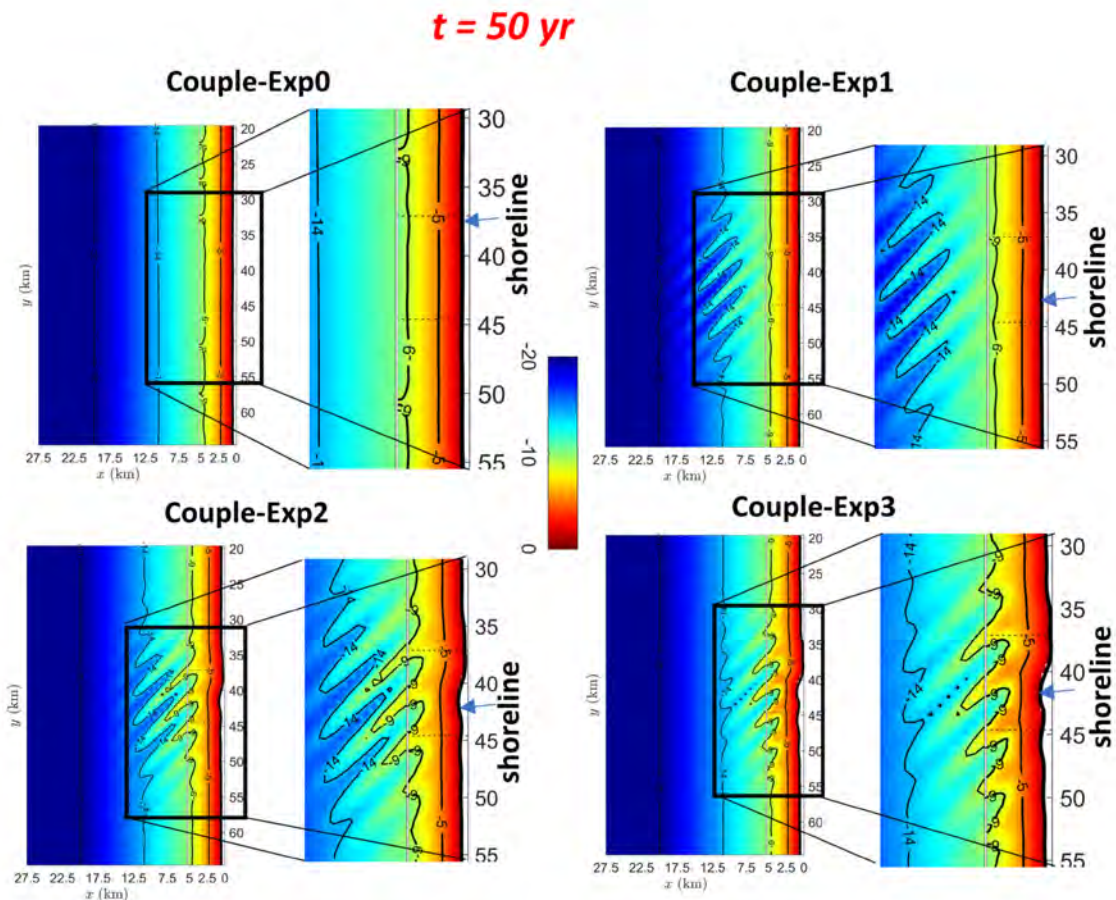


Figure 30 – Results of run series "Couple-Exp $i$ ",  $i = 0,1,2,3'$  (bathymetry).  
 Snapshots (with zoom-ins) of the shelf and nearshore bed-levels at  $t = 50$  yr. In each panel, the coast is located on the right.  
 The thick black lines denote shoreline position  $x_s$  at  $t = 50$  yr.

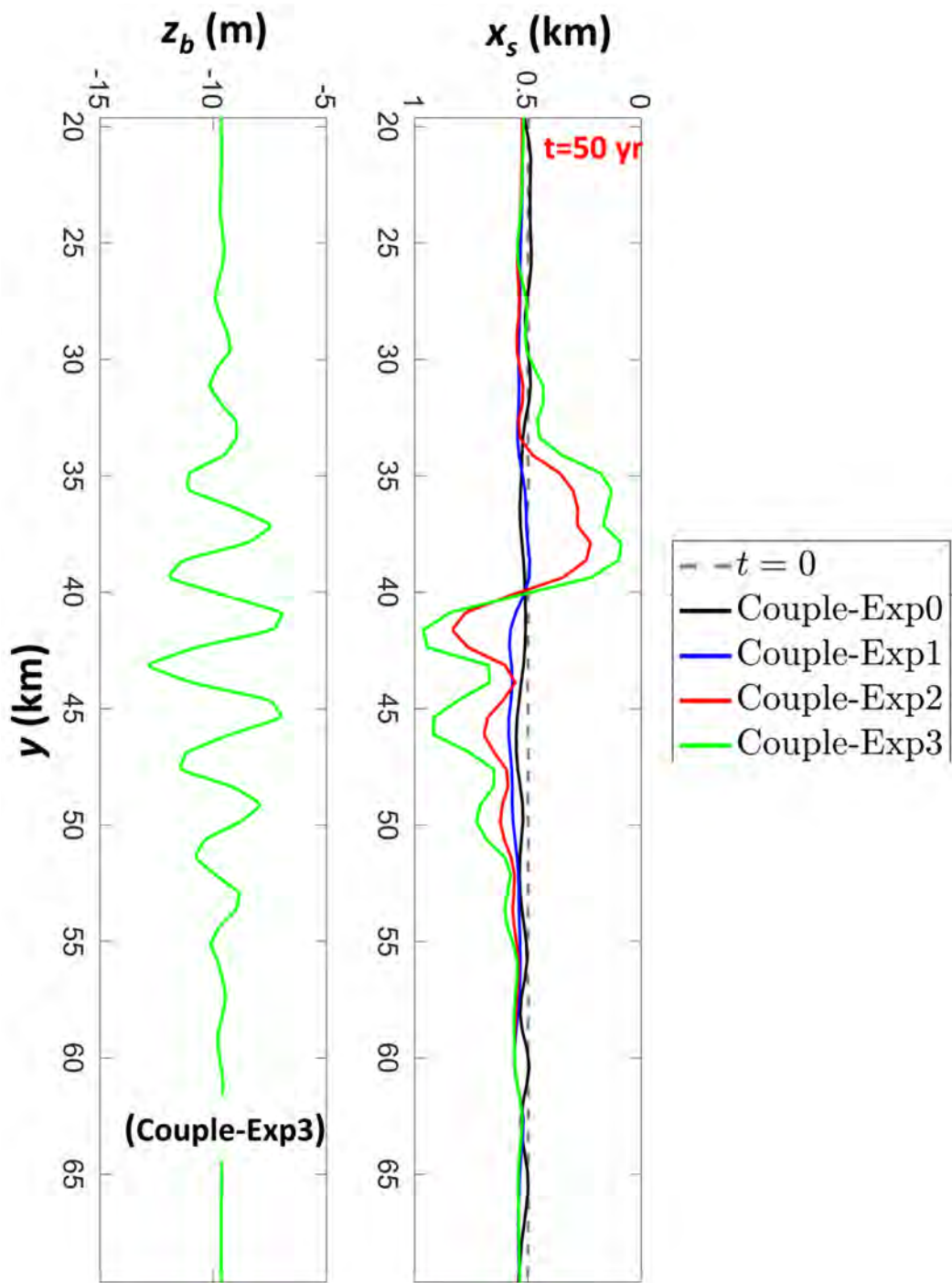


Figure 31 – Results of run series "Couple-Exp $i$ ",  $i = 0,1,2,3$ ' (shoreline evolution).

Left): Alongshore bed-level profile at  $x = 5$  km in the case of experiment "Couple-Exp3". Right) Alongshore profiles  $x_s$  after 50 years in the case of different offshore locations of the sfcrl (run series "Couple-Exp $i$ "). The initial shoreline positions is denoted by the dashed grey line.

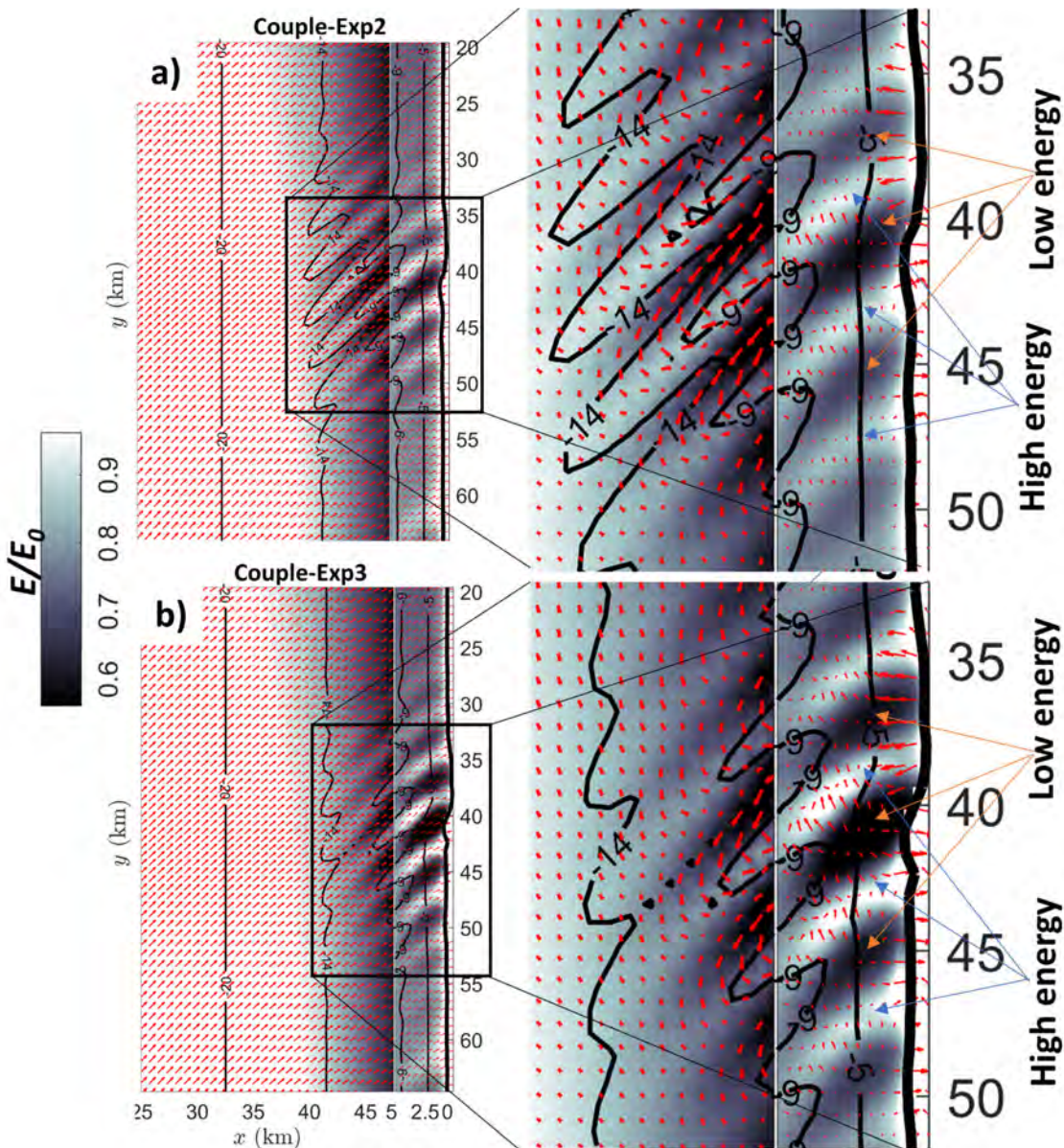


Figure 32 – Results of run series "Couple-Exp*i*",  $i = 0,1,2,3'$  (spatial distribution of wave energy density).

Left) Spatial distribution of the wave energy density  $E = \frac{1}{16} \rho g H_s^2$  (dark-white colours) in the shelf-shoreline system with superimposed the group velocity  $\vec{c}_g$  (red arrow, exact expression is given in the Appendix 2.2) at  $t = 50$  year in the cases of two different locations of the artificial sfc ("Couple-Exp2", panel a; "Couple-Exp3", panel b). Zoom-ins on energy  $E$  with superimposed the perturbed group velocity vector are presented in the right panels. The perturbed group velocity was computed by subtracting  $\vec{c}_g$  with its alongshore averaged value. Wave energy density  $E$  is normalized with the maximum value  $E_0 = 2.4 \cdot 10^3 \text{ Jm}^{-2}$ . Some hotspots of low (dark colours) and high (white colours) wave energy density in the nearshore are also indicated, which are due to focussing (defocussing) of wave energy density over crests (troughs) of the sfc.

## 2.4 Summary and outlook

Analysis of historical bathymetric data of the Belgium shelf (Chapter 4) reveals that the large-scale ridges on the inner shelf (so-called shoreface-connected sand ridges, sfc) migrate landward, which is expected to have effects on the decadal evolution of the adjacent nearshore and its shoreline. The overall aim of WP2 of the MOZES project is to investigate these effects by developing **a new (idealized) coupled shelf-shoreline model**, which couples a morphodynamic shelf model to a morphodynamic shoreline evolution model. The existing coupled shelf-shoreline model of Nnafie *et al.* (2021) was used as a starting point, in which a morphostatic (i.e., bed does not evolve in time) shelf model (Delft3D+SWAN) is coupled to a morphodynamic shoreline model (Q2Dmorfo). Chapter 2 of this report describes the specific activities of the first year of WP2, which comprise 1) the development of a **new morphodynamic shelf model** (Delft3D+SWAN) in which the bed evolves in time such that sfc spontaneously develop on the shelf on decadal and centennial time scales (Activity 1); and 2) the application of the coupled shelf-shoreline model of Nnafie *et al.* (2021) to the Belgium coast to explore potential effects of onshore migrating sfc on the evolution of the shoreline (Activity 2).

Following **three important milestones** were achieved so far:

1. The new morphodynamic shelf model has successfully reproduced the offshore (onshore) deflection of flow and transport fields over crests (troughs) of shelf ridges, which is considered as the growth mechanism responsible for growth of shoreface-connected sand ridges in micro-tidal conditions.
2. The new shelf model was capable of reproducing ridges with characteristics similar to those observed on the Long-Island shelf.
3. The adaption of the coupled model of Nnafie *et al.* (2021) such that it includes tides and its background bathymetry (without the artificial sfc that were imposed) is more representative for the Belgium coast. Preliminary results suggest that an onshore movement of sfc is expected to induce stronger undulations along the shoreline.

These milestones are considered significant steps forward towards establishing the ultimate tool to study the coupled shelf-shoreline morphodynamics in the Belgian coastal zone (see Figure 20). However, the new morphodynamic shelf model, as well as the coupled shelf-shoreline model **are not yet ready to be used** to make any statements on potential impacts of sfc on the Belgium shoreline. This is because many adjustments still have to be done, of which the most important ones are:

- **Morphodynamic shelf model**: inclusion of tides, use of more realistic waves, account for sea-level rise and the use of a background bathymetry that is more representative for the Belgium inner shelf. These adjustments are suggested as key topics for year 2 of the MOZES project.
- **Coupled shelf-shoreline model of Nnafie et al. (2021)**: the used artificial sfc were not representative for the observed ridges on the Belgium inner shelf. Instead, artificial ridges should be created that have similar geometries as the sfc that are present on the Belgium shelf (Figure 18). Furthermore, realistic waves should be considered whose characteristics (wave height, wave angle and wave period) reflect the wave climate of the Belgium coast. These two issues are suggested to be addressed in year 2 of the MOZES project.

Ultimately, once the morphodynamic shelf model would be able to successfully reproduce the gross characteristics of the observed sfc on the Belgium inner shelf, it will be also coupled to the shoreline evolution model. With this new (fully morphodynamic) coupled shelf-shoreline model, the impact of human interventions (e.g., construction of harbours, nourishments, ...) and sea-level rise on the evolution of sfc and the shoreline can also be investigated.

# 3 Research on natural feeding of the beach over shoreface-connected ridges

## 3.1 Introduction

Within Work Package 3 of the MOZES-project (**M**Orfolgische interactie kustnabije **Z**Eebodem en **S**trand), the hypothesis that shoreface-connected sand ridges naturally nourish the Belgian coastline is investigated. The research question is as follows: “Is the Belgian coastline naturally nourished by sediment transport from the three shoreface connected sand ridges (i) Trapegeer-Broersbank-Den Oever, (ii) Stroombank and (iii) Wenduinebank-Paardenmark (see Figure 33) to the beaches?”

This chapter presents preliminary results regarding this research question, forming the base for more detailed work in the coming project years. The research is based on a detailed numerical modelling approach using the Delft3D Flexible Mesh-Flemish Coast model (FM-FlemCo model) and the SedTRAILS software (Deltares) as well as the Telemac Scaldis-Coast model (Flanders Hydraulics).

First, the study area is presented with a focus on the local tides and wave climate as well as the geomorphology (Section 3.2). Subsequently, the approach and methodology used for the numerical modelling and literature review/data analysis are described. Section 3.3.1 summarizes the setup and features of the FM-FlemCo model and stresses the actual further development of the model compared to the first model version by Röbbke *et al.* (2020) and Grasmeijer *et al.* (2020). Section 3.3.2 presents the approach and methodology of the performed SedTRAILS analysis. In Section 3.3.3, the general setup and general features of the Scaldis-Coast model are described. Additionally, Table 12 gives a short overview of the differences and similarities between the FM-FlemCo model and the Telemac Scaldis-Coast model. The preliminary results of the numerical modelling are presented in Section 3.4. The discussion and conclusions section (Section 3.5) evaluates the presented results and makes suggestions for future research.

## 3.2 Study area

This study focuses on the Belgian coast located between the Belgian-French border (near De Panne) and the Belgian-Dutch border (near Cadzand-Bad) (Figure 33). The coast has a relatively straight outline and runs in a WSW-ENE direction. Except for the dune areas with maximum heights of around 30 m above NAP (Hoge Blekker, Koksijde, 32 m above TAW) the typical onshore elevations along the coast do not exceed few metres. In the nearshore zone, water depths are typically less than 10 m below NAP (-7.67 m TAW) but reach almost 18 m below NAP (-16.5 m TAW) in the area of the main navigation channel of the Western Scheldt mouth, which is divided into Scheur-West, Scheur-Oost and Wielingen (for this and the following see Figure 33). The harbour of Zeebrugge is connected to the main navigation channel by the Pas van 't Zand. Another dominant morphological feature can be found in the western part of the study area in the form of several offshore and shoreface connected sand ridges with depths of between 10 m and few metres below NAP (-7.67 m – 0 m TAW).

Of particular interest for the current study are the three shoreface connected sand ridges (i) Trapegeer-Broersbank-Den Oever, (ii) Stroombank and (iii) Wenduinebank-Paardenmarkt (see Figure 33). In 1866, i.e. the time before the construction of the harbour of Zeebrugge (the works started in 1896) and before dredging of the harbour navigation channels began, all three sand ridges were connected to the beach or to the upper shoreface (Figure 34). Nowadays, only the westernmost sand ridge, Trapegeer-Broersbank-Den Oever, is still directly connected to the beach, although showing a more elongated shape compared to 1866.

The other two sand ridges have been split into two parts by the navigation channel of Oostende and Zeebrugge harbours respectively and have decreased in size eastward of the channel/harbour in the area where they met the coastline in 1866 (cf. Figure 33 and Figure 34). Moreover, the Paardenmarkt is nowadays clearly separated from the beach by a distinct tidal channel called Appelzak. It is not exactly known, when this disconnection took place (Houthuys *et al.*, 2021).

Located in the southwestern North Sea, the area is exposed to wind, wave and tidal forces. Winds from the south-western sector are dominating, followed by winds from a north-eastern direction (Baeye *et al.*, 2010). In line with the wind climate, the main wave direction is south-west although the highest waves are associated with the north-western sector, which is related to the longer fetch in this direction and the typical path of extratropical cyclones during the storm season (Baeye *et al.*, 2010; Spencer *et al.*, 2015).

The average significant offshore wave height is of the order of 1 m with an associated peak period of circa 5.4 s (Westhinder station: MDK, 2022). The area is characterized by a semi-diurnal tide with a 28 day spring-neap tidal cycle. At Oostende – located in the centre of the Belgian coastline – the average tidal range amounts to ca. 3.9 m with a mean high water level of ca. 2 m above NAP/4.30 m above TAW (Vlaamse Hydrografie, 2011). The maximum storm surge level ever recorded at Oostende is 4 m above NAP (6.33 m TAW), which was on 1st February 1953 (Vlaamse Hydrografie, 2011).

According to van Lancker *et al.* (2012) and SHOM (2021), the nearshore seabed all along the Belgian coast (until ca. 15 km offshore) mainly consists of sediment with a grain size of between 125  $\mu\text{m}$  and 250  $\mu\text{m}$  ( $D_{50}$  equivalent diameter), i.e. fine to medium sand based on the grain size classification ISO 14688-1:2002 (ISO – International Organization for Standardization, 2002). Only in the area around Zeebrugge harbour, also silt ( $2 \mu\text{m} \leq D_{50} \leq 63 \mu\text{m}$ ) becomes a dominant sediment fraction in the bed (Figure 35). Ca. 15 km offshore from the Belgian coast, the average grain size increases to medium sand ( $200 \mu\text{m} \leq D_{50} \leq 630 \mu\text{m}$ ). While fine and medium sands in the study area are believed to originate from the cliffs of Calais and the English Channel and/or from riverine input from the Meuse and Rhine during the last ice age, muddy material is mainly associated with a Holocene source in the form of a submerged mudflat-marsh system in the area around Zeebrugge harbour as well as the sediment from the Western Scheldt (Fettweis *et al.*, 2007; Fettweis & van den Eynde, 2003; Vroom *et al.*, 2016; van Maren *et al.*, 2020). For a detailed treatise on the sediment dynamics in the study area the reader is referred to Trouw *et al.* (2015), De Maerschalck *et al.* (2017), Verwaest *et al.* (2022) and Houthuys *et al.* (2021 & 2022).

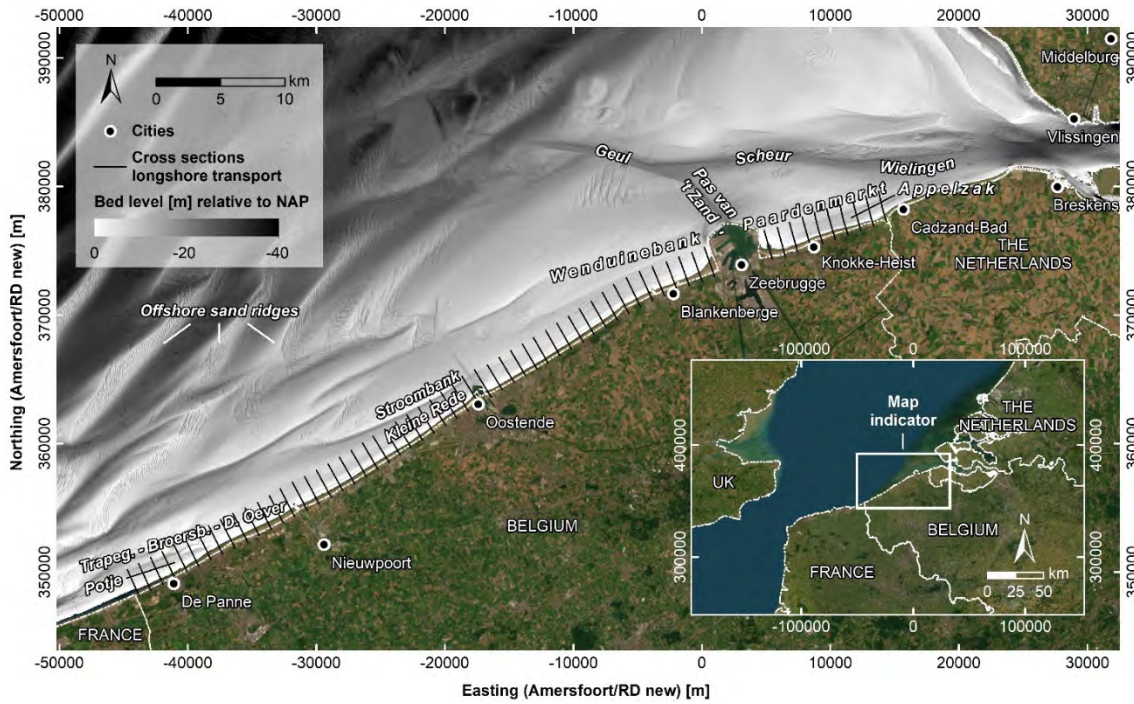


Figure 33 – Study area.

Satellite image (Esri 2022) and bathymetry of the Belgian (Flemish) coast and the Western Scheldt mouth including the main navigation channel Geul-Scheur-Wielingen and the connecting channel Pas van 't Zand to Zeebrugge harbour as well as the sand ridges in the western part of the study area. The coastal bathymetry is derived from several sources of data according to Table 11. The black lines indicate cross sections based on which the longshore sediment transport along the Belgian coast was simulated (Section 3.3.1, Section 3.4). The coordinates are given in km according to Amersfoort/RD New.

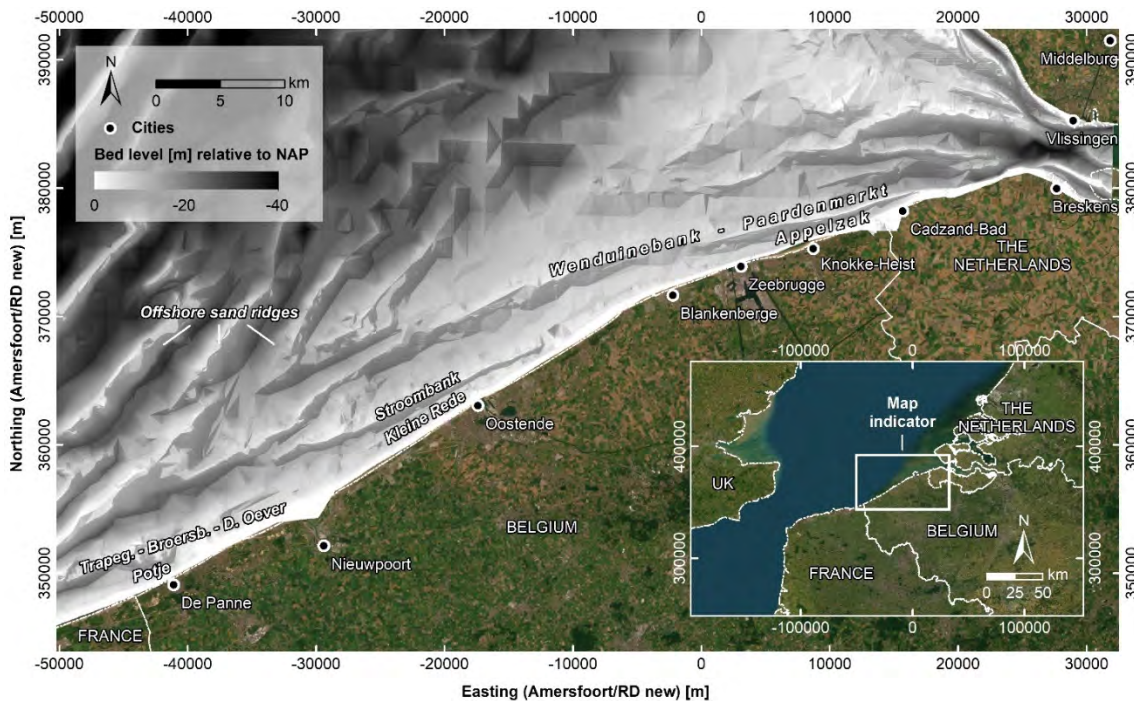


Figure 34 – Bathymetry of the Belgian coast and the Western Scheldt mouth of the year 1866.

TIN derived from the nautical chart by Stessels (1866) (cf. §1.3). At that time, i.e. the time before the construction of the harbour of Zeebrugge (started in 1896) and before dredging of the harbour navigation channels began, the three shoreface connected sand ridges (i) Trapegeer-Broersbank-Den Oever, (ii) Stroombank and (iii) Wenduinebank-Paardenmarkt were connected to the beach. The coordinates are given in km according to Amersfoort/RD New.

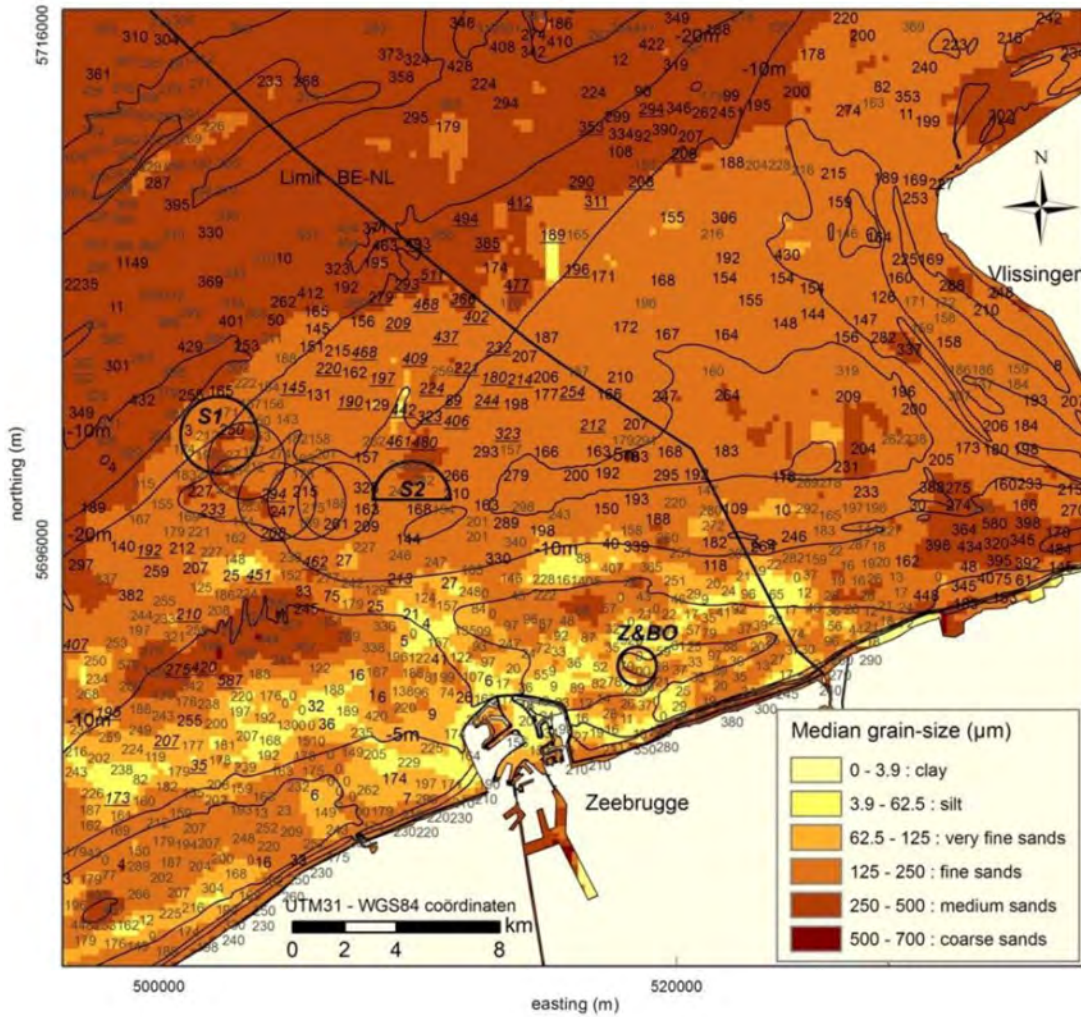


Figure 35 – Sedimentary composition of the seabed of the eastern Belgian coast and the adjacent Western Scheldt estuary mouth (according to van Lancker et al., 2012). The coloured areas indicate the median grain sizes ( $D$ ) based on samples taken between 1900 and 2005. For comparison, grey and black numbers show the median grain size based non-standarised data and samples taken after 2008 respectively. Please note that the grain size classification used here is not in line with the conventional classification ISO 14688-1:2002 (ISO – International Organization for Standardization, 2002; Ad-Hoc-AG Boden, 2005). The coordinates are given in km according to Amersfoort/RD New. For further details on the origin of the grain size data see van Lancker et al. (2012).

### 3.3 Methodology

#### 3.3.1 The FM-FlemCo model

The FM-FlemCo model was originally developed by Röbbke *et al.* (2020) and Grasmeyer *et al.* (2020) as part of the “Complex Project Kustvisie” (“Flanders Coast Vision”) initiated by the Flemish Government in 2014 with the aim to support studies on the protection of the Belgian coast against the effects of climate change. The model has been validated in terms of the hydrodynamics (Röbbke *et al.*, 2020) and applied for sediment transport and morphodynamic test simulations (Grasmeyer *et al.*, 2020). For the current study, the FM-FlemCo model has been further developed and applied with regard to the above-mentioned research question within Work Package 3 of the MOZES-project.

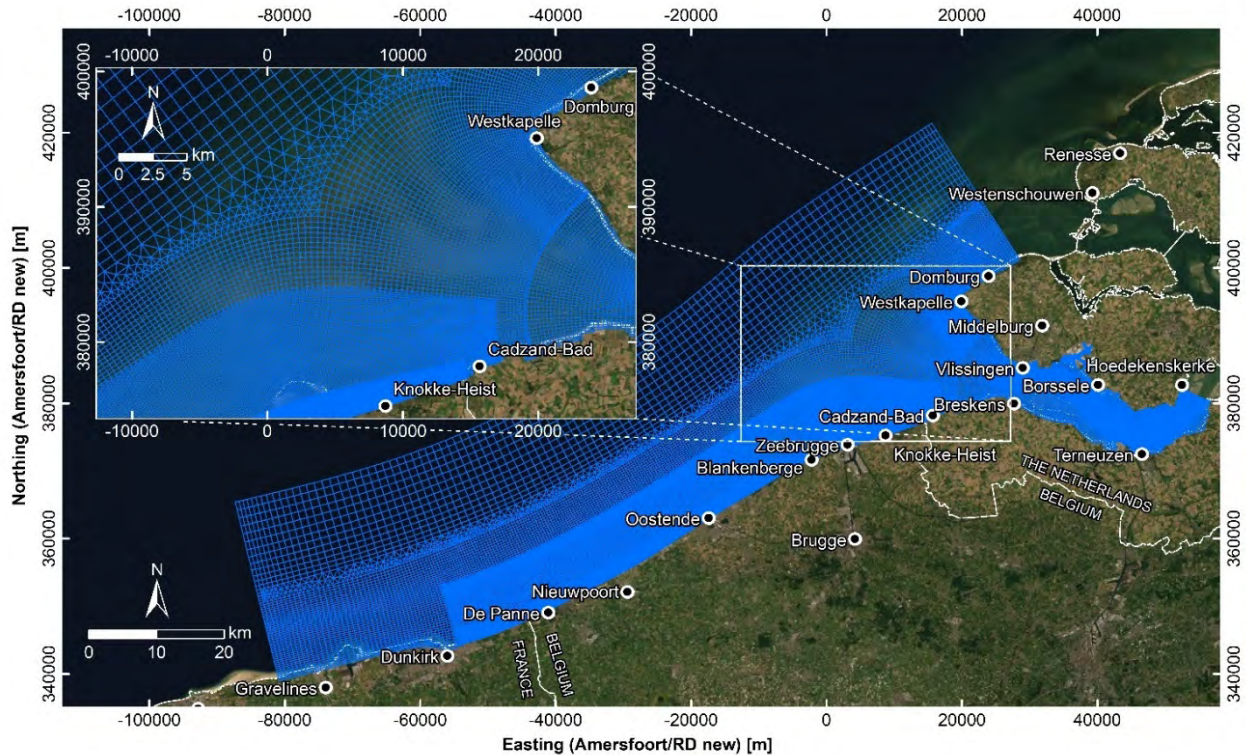


Figure 36 – Model domain and computational flow grid of the Delft3D Flexible Mesh-Flemish Coast Model.

Grid spacing ranges from circa 1,300 m by 1,300 m at the north-western offshore boundary to typically 45 m by 45 m along the Belgian coast. The maximum grid resolution in the Western Scheldt estuary is approximately 75 m by 230 m. The coordinates are given in km according to Amersfoort/RD New.

The following sections summarize the setup and features of the FM-FlemCo model and stresses the actual further development and differences of the current model compared to the its first version. This mainly concerns the sediment transport model, while the hydrodynamic model has hardly changed. For a detailed description of the hydrodynamic model, the reader is referred to the report by R bke *et al.* (2020).

### Model domain and computational grids

The FM-FlemCo model comprises a coupled flow and wave model. The computational flow grid stretches over a distance of 125 km from the French coast ca. 13 km east of Calais to Zeeland in the Netherlands ca. 5 km to the north-east of the village of Domburg (Figure 36). The grid reaches maximum 30 km offshore. The Western Scheldt estuary is covered by the grid up to the village of Hoedekenskerke.

In general, the flow grid is based on rectangular grid cells but uses triangular cells for connecting rectangular cells with different cell sizes and/or different orientation. The grid resolution ranges from about 1,300 m by 1,300 m at the north-western offshore boundary to typically 45 m by 45 m along the Belgian coast. The latter resolution is required in order to accurately capture wave breaking processes and associated longshore currents in the nearshore zone (see below). In total, the flow grid comprises 97,667 computational nodes.

In order to avoid shadow effects and ensure proper wave simulations for the area of the flow model domain, the domain of the wave model (based on the D-Waves module/SWAN) is significantly larger than the flow model domain. The overall wave grid measures approximately 150 km by 45 km and stretches from the French village of Sangatte to the mouth of the Eastern Scheldt in the Netherlands (Figure 37). The typical grid resolution at the north-western offshore boundary is circa 1,200 m by 1,200 m. The resolution increases towards the Western Scheldt mouth and reaches up to 280 m by 550 m at the Belgian-Dutch border (Table 10). In total, the overall wave grid comprises 12,450 cells.

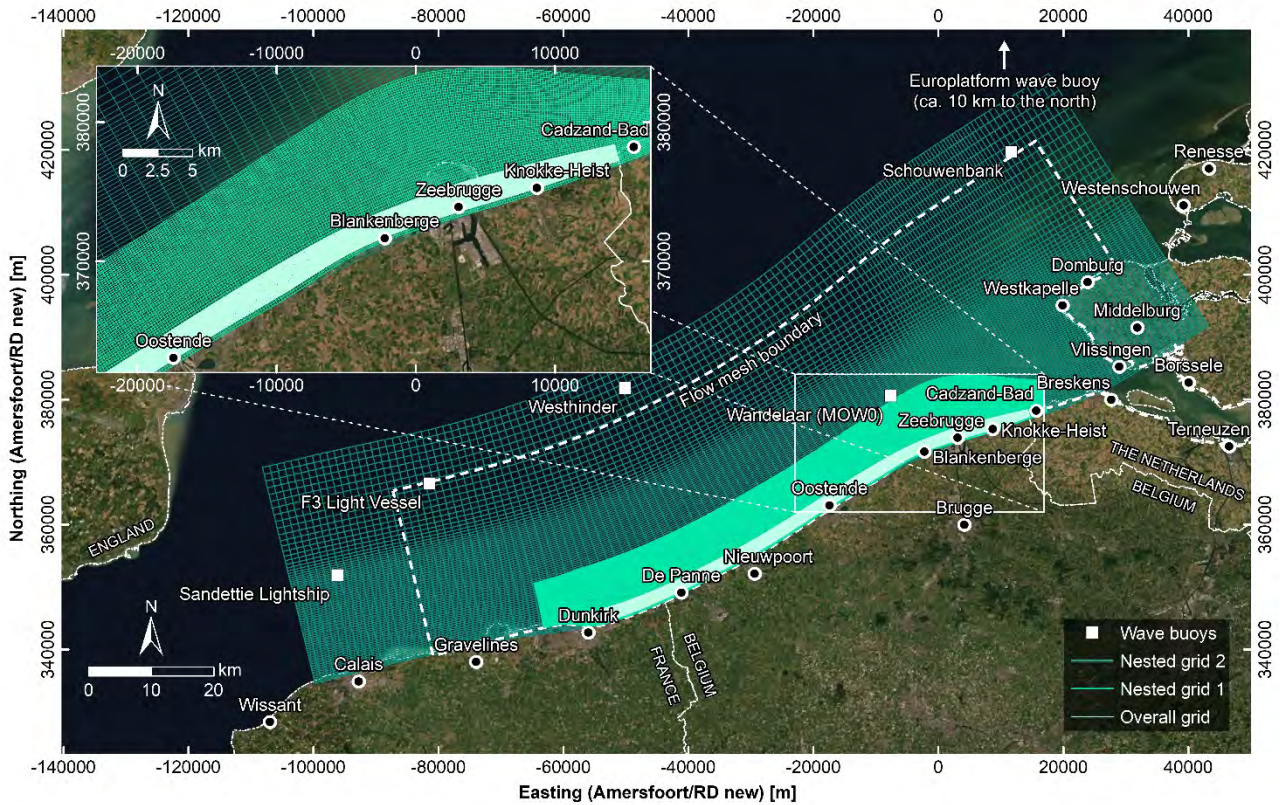


Figure 37 – Overall and nested computational wave grids of the Delft3D Flexible Mesh-Flemish Coast Model. Grid dimensions and resolutions are given in Table 10. The map indicates the locations of various wave buoys, which were considered to determine the boundary conditions of the wave model. The coordinates are given in km according to Amersfoort/RD New.

In order to accurately simulate wave behavior (in particular wave breaking) in the nearshore zone and the associated sediment transport in the flow model, the wave model comprises two additional nested wave grids, both covering the coastline between Dunkirk and Cadzand-Bad (Figure 37). The first nested wave grid (Nested grid 1) reaches almost 9 km offshore and it has a resolution of ca. 170 m by 170 m, resulting in a total number of grid cells of 23,706 (Table 10). In comparison to the former model version by R bke *et al.* (2020), this nested grid has been extended in a west-southwestern direction along the French coast by about 9 km in order to guarantee proper wave simulations in this area, which is characterized by a re-orientation of the coastline and a complex bathymetry. The second nested wave grid (Nested grid 2) reaches approximately 2 km offshore, with a typical resolution of circa 45 m by 45 m and a total of 61,400 cells. The cells of both nested grids are identical with the cells of the flow grid and by this are orientated parallel/orthogonal to the coast.

Table 10 – Size, spatial resolution and number of cells of the three employed wave grids.

| Wave grids    | Size [km] | Resolution [m]             | Number of cells |
|---------------|-----------|----------------------------|-----------------|
| Overall grid  | 150 x 45  | 1,200 x 1,200 to 275 x 255 | 12,450          |
| Nested grid 1 | 89 x 9    | 170 x 170                  | 23,706          |
| Nested grid 2 | 75 x 2    | 45 x 45                    | 61,400          |

## Model bathymetry

The bathymetry of the FM-FlemCo model (Figure 33) is compiled from various sources of data from different years (Table 11): (i) airborne Lidar data from the year 2015 (resolution: 1 m x 1 m), (ii) high-resolution harbour bathymetries from 2014 and 2015 provided by the Agentschap Maritieme Dienstverlening en Kust (MDK) (resolution: spatially varying), (iii) data provided by Vlaamse Hydrografie in 2016, referred to as Belgisch Continentaal Plaat (BCP) data (resolution: 5 m by 5 m), (iv) Vaklodingen data from 2015 for the Dutch part of the model domain provided by Rijkswaterstaat (resolution: 20 m x 20 m), (v) SHOM data from 2015 provided by the Service hydrographique et océanographique de la Marine (SHOM, 2015) covering the French part of the model domain (resolution: 20 m x 20 m) and (vi) EMODnet data from 2013 for the several offshore parts of the model domain (resolution: 230 m x 230 m). Depth measurements based on a differing vertical datum (e.g. such as TAW) were converted to the vertical datum of NAP. All bathymetric data was edited and compiled using ArcGIS, the Delft3D-QUICKIN tool and MATLAB.

Table 11 – Data sources used to create the model bathymetry of the Delft3D Flexible Mesh-Flemish Coast Model.

The data sources are listed with decreasing relevance. The bathymetry of the FM-FlemCo model is identical to the bathymetry of the Scaldis-Coast model (cf. Kolokythas et al. 2021; Wang et al. 2021). See text for further information.

| Sources of bathymetric data | Year of collection | Resolution        |
|-----------------------------|--------------------|-------------------|
| Lidar                       | 2015               | 1 m x 1 m         |
| MDK                         | 2014, 2015         | spatially varying |
| BCP                         | 2016               | 5 m by 5 m        |
| Vaklodingen                 | 2015               | 20 m by 20 m      |
| SHOM                        | 2015               | 20 m by 20 m      |
| EMODnet                     | 2013               | 230 m by 230 m    |

The bathymetric data listed above are the same as used for the Scaldis-Coast model (Kolokythas *et al.*, 2021; Wang *et al.*, 2021) and coincide with the bathymetry of the former version of the FM-FlemCo model by Röbbke *et al.* (2020) except for the SHOM data in the French part of the model domain. In this area, GEBCO data from 2014 were formerly used instead, which had a much lower resolution (577 m x 926 m) compared to the SHOM data (20 m x 20 m).

Besides the present bathymetry, the FM-FlemCo model also used the historical bathymetry of 1866. This bathymetry has been derived from the nautical chart by Stessels (1866) (Figure 34; for further information see §1.3). It has to be noted that the resolution and accuracy of the derived 1866 bathymetry is considerably lower compared to the present bathymetry (cf. Figure 33 and Figure 34; §3.2). This means that a direct comparison of simulation results based on both bathymetries is limited (see below).

## Hydrodynamic and wind forcing

The hydrodynamic boundary conditions of the flow model were derived from the validated hydrodynamic Simona DCSMv6-ZUNOV4 model (Zijl, 2013 & 2014) in the form of a time series for the year 2014 by means of nesting. The flow model has four open hydrodynamic boundaries — one seaward boundary, two cross-shore boundaries and one river boundary located in the Western Scheldt estuary near Hoedekenskerke (cf. Figure 36). The offshore boundary conditions are based on water levels, while the river open boundary uses discharge conditions. The water level conditions are specified at 118 locations along the offshore boundaries. In between these locations, the imposed water levels are interpolated linearly. The discharge is defined for two sections (ebb and flood channel) at the landward boundary near Hoedekenskerke.

For the meteorological forcing of the flow model, time- and space-varying wind and air pressure data (hourly) of the HIRLAM (High Resolution Limited Area Model) model (version 7.2; de Rooy & de Vries, 2017) are used; a time series for the year 2014 is extracted.

The boundary conditions of the wave model are based on the wave time series for 2014 (significant wave height  $H_s$ , peak wave period  $T_p$  and mean wave direction  $\theta_m$ ) measured at Westhinder buoy (uniform wave time series), which is located about 32 km offshore the Belgian-French border (for the location see Figure 37). Preliminary test simulations revealed that this wave time series yield the most accurate wave simulations along the Belgian coast compared to corresponding time series based on the measurements at (i) Wandelaar (MOWO) wave buoy (uniform wave time series), (ii) Europlatform wave buoy (uniform wave times series) and (iii) Sandettie Lightship, F3 Light Vessel, Westhinder and Schouwenbank (spatially varying time series; for locations see Figure 37). Also, spatially varying wave boundary conditions provided by the European Centre for Medium-Range Weather Forecasts (ECMWF) yielded less accurate results. The wave boundary conditions are imposed along the three offshore boundaries of the overall wave grid in the form of a time series for the year 2014. The wave input to the nested wave grids is derived online during the simulation from the results computed for the overall grid (input for nested grid 1)/nested grid 1 (input for nested grid 2).

The wave model uses the same meteorological forcing, i.e. wind and air pressure, as the flow model. Water levels computed by the flow model are communicated with the wave model every half hour (communication interval), allowing proper wave simulations in shallow water.

## Other model settings

Besides the model parameters described so far, the FM-FlemCo model uses further specific physical and numerical parameter settings. These parameter settings as well as other essential model features are shown in Table 12. For all remaining parameters available in the flow and waves module, default values are taken (see Deltares, 2022a & 2022b).

Table 12 – Overview of selected model parameter settings and essential features of the FM-FlemCo model and comparison with the Telemac Scaldis-Coast model (Wang et al., 2021; Kolokythas et al., 2020 &amp; 2021).

| Model feature               | FM-FlemCo   | Telemac Scaldis-Coast   |
|-----------------------------|---|---|
| Software                    | Delft3D Flexible Mesh/SWAN  | openTELEMAC-suite v7p2_cookie   |
| Solver                      | Finite Volumes on a staggered grid, solving shallow water equations           | Finite Element method, solving Saint-Venant equations (uni-directional shallow water equations) making use of generalized wave equation |
| Flow model domain           | see Figure 36   | see Figure 41   |
| Wave model domain           | see Figure 37   | see Figure 43   |
| Grid resolution nearshore   | ca. 45 m x 45 m   | ca. 20 m  |
| Bathymetry                  | Same as Scaldis-Coast coast but converted to NAP                              | see Figure 44 and Table 11  |
| Computational approach      | Two-dimensional (2DH)   | Two-dimensional (2DH)   |
| Origin of flow forcing      | Derived from Simona DCSMv6-ZUNOV4 model (Zijl, 2013 & 2014) for the year 2014 | Derived from Simona DCSMv6-ZUNOV4 model (Zijl, 2013 & 2014) for the year 2014   |
| Type of flow forcing        | Water level boundary conditions (sea) and discharge (Western Scheldt)         | Water level boundary conditions (sea); discharge (Western Scheldt) is possible, but not applied in the morphodynamic runs               |
| Tidal forcing               | Representative morphological period: 14-03-2014 to 13-05-2014                 | Representative morphological tide of 24 hours and 50 minutes: #137<br>25/05/2014 17:20 – 26/05/2014 08:10                               |
| Wind forcing                | Time and spatially varying wind and air pressure data from HIRLAM (2014)      | Time varying, spatially uniform wind data from Vlakte van de Raan time series (2014) for wave propagation model only                    |
| Wave forcing                | Time series measured at Westhinder buoy (2014)                                | Time series measured at Westhinder buoy (representative morphological year 30/11/2015 – 29/11/2016)                                     |
| Coupling interval flow-wave | 30 min  | 30 min  |
| Wave computational mode     | Non-stationary (time step: 30 min)  | Non-stationary (time step: 30 min)  |

|  |   |  |
|--|---|--|
| Secondary flow   | Switched on   | Switched off   |
| Salinity   | Switched off  | Switched off   |
| Maximum time step  | 30 s  | 10 s   |
| Horizontal eddy viscosity  | $1 \text{ m}^2 \text{ s}^{-1}$ (uniform)                                  | $1 \text{ m}^2 \text{ s}^{-1}$ (uniform)   |
| Horizontal eddy diffusivity  | $1 \text{ m}^2 \text{ s}^{-1}$ (uniform)                                  | $1 \text{ m}^2 \text{ s}^{-1}$ (uniform)   |
| Bottom roughness   | Manning's $n = 0.02$ [ $\text{s m}^{-1/3}$ ] (uniform)                    | Manning's $n = 0.022$ [ $\text{s m}^{-1/3}$ ] (uniform at sea), varying in Western Scheldt (Figure 45)   |
| Threshold depth wet/dry cells                                      | 0.1 m   | 0.0 m  |
| Morphological simulation period                                    | 1 year by using a morphological scale factor of 6 (6 x 2 months = 1 year) | 10 years by using a morphological scale factor of 10 (10 x 1 year = 10 years)  |
| Type of morphological model  | Morphostatic (only sediment transport, no morphodynamics)                 | Morphodynamic (sediment transport + bed update + dredging & dumping)   |
| Considered sediment fraction                                       | 200 $\mu\text{m}$   | 2 fractions: 200 $\mu\text{m}$ and 500 $\mu\text{m}$<br>The ratio of the fractions is calculated to mimic a corresponding sediment transport rate as the local observed grain size would |
| Initial sediment thickness   | 20 m (uniform), i.e. unlimited in a 1 year simulation                     | unlimited (10,000 m), except for sediment on top of groins   |
| Sediment transp. formulation                                       | Bijker (1971)/van Rijn (2007)   | Bijker (1968)  |
| Current-related suspended and bedload transport factors (Sus, Bed) | 1 [-]   | 1 [-]  |
| Wave-related suspended and bedload transport factors (SusW, BedW)  | 0.5 [-]   | 0.5 [-]  |
| Calibration coefficient b for shallow water (only Bijker 1971)     | 5 [-]   | 2 [-]<br>(no distinction between shallow and deep water in default SISYPHE)  |
| Calibration coefficient b for deep water (only Bijker 1971)        | 2 [-]   |  |
| Settling velocity (only Bijker 1971)                               | $0.02$ [ $\text{m s}^{-1}$ ]  | computed explicitly according to grain size  |

## Sediment transport model

Compared to Grasmeyer *et al.* (2020), several modifications of the sediment transport model have been performed. This mainly concerns the considered sediment fractions, sediment availability and the sediment transport formulations as described in the following.

Although the seabed in the study area is made up of various sediment fractions ranging from silt to middle sand (cf. Section 3.2), the sediment module of the FM-FlemCo model only considers a uniform grain size of 200  $\mu\text{m}$  (fine sand), which is the representative grain size for most parts of the Belgian coast (formerly two fractions, i.e. 100  $\mu\text{m}$  and 250  $\mu\text{m}$  were used). The initial sediment thickness in the model is uniform and amounts to 20 m, which means an unlimited sediment availability based on the morphological simulation time of the model of 1 year (see below). We apply two different sediment transport formulations — the formulation by van Rijn (2007) including the bottom roughness predictor and the formulation by Bijker (1971), which is used in the morphological Scaldis-Coast model (Kolokythas *et al.*, 2020). The parameter settings for both transport formulations are shown in Table 12. All sediment transport simulations performed with the FM-FlemCo model are morphostatic simulations, which means that the bed levels in the model domain are not updated during the simulations but only the sediment thicknesses.

With the aim of morphological mid- to long-term ( $\geq 1$  year) simulations and in order to avoid long computational times, the FM-FlemCo model uses a morphological scale factor — a so-called morfac — which scales up, i.e. multiplies the simulated erosion and deposition fluxes from the bed to the flow and vice-versa at each computational time step (Deltares, 2022a). In the case of the FM-FlemCo model, we apply a morfac of six and a representative hydrodynamic simulation period of two months (i.e. 14-03-2014 to 13-05-2014), resulting in a morphological simulation time of  $6 \times 2$  months = 1 year. The representative period was determined in an earlier study by R bke *et al.* (2018) based on a comparison of the regional wave climate of six preselected two-month periods of the years 2013 and 2014 with the average wave climate of both years. Subsequently, R bke *et al.* (2018) performed preliminary morphodynamic simulations based on the preselected two-month periods (morfac 60.83 = 10 year morphological simulation time) as well as on the entire year 2014 (morfac 10 = 10 year morphological simulation time) and compared the simulated cumulative erosion and sedimentation patterns. The patterns simulated based on the period 14-03-2014 to 13-05-2014 showed a good match with the patterns simulated based on the entire year of 2014 (R bke *et al.*, 2018). The morphological scale factor and the representative period applied for the FM-FlemCo model in the current study are the same as applied by Grasmeyer *et al.* (2000).

The sediment transport simulated with the FM-FlemCo model is validated based on the yearly longshore sediment transport in the nearshore zone (between the beach and approximately the -8 m NAP/-5.67 m TAW contour) of the Belgian coast. The simulated longshore sediment transport is determined based on the sum of the cumulative suspended and bedload sediment transport through 63 cross-sections along the Belgian coast, extending ca. 2 km seaward with an average water depth at the seaward end of about -8 m NAP / -5.67 m TAW (see Figure 33). For the preliminary validation of the model, the simulated longshore sand transports are compared with the transports determined in earlier studies for the Belgian coast (Figure 38). Such include studies in which the longshore sediment transport has been derived from (i) the analysis of measured bed level changes (i.e. the studies by Verwaest *et al.*, 2010; Trouw *et al.*, 2015), (ii) the application of empirical equations (i.e. the studies by Svasek, 2012; Vandebroek *et al.*, 2017) and (iii) the application of process-based numerical models (i.e. the studies by Wang *et al.*, 2012 & 2015). Moreover, the transports predicted by the FM-FlemCo model are also compared with those simulated with the Scaldis-Coast model (Kolokythas *et al.*, 2020; Section 3.3.3), based on the same 2 km long transects.

The comparison of the longshore sediment transport with earlier studies and the Scaldis-Coast model is based on two different FM-FlemCo model runs:

- Run038i: flow-wave coupled morphostatic simulation using the sediment transport formulation by van Rijn (2007);
- Run039b: flow-wave coupled morphostatic simulation using the sediment transport formulation by Bijker (1971).

The simulated sediment transport based on these two model runs is generally of the same order and shows a similar spatial variability as predicted by earlier studies (see yellow and green lines in Figure 38). Nevertheless, the following differences can be observed:

- both FM-FlemCo model runs, especially Run039b (which uses the formulation by Bijker (1971)) predict higher transport for most parts of the Belgian coast compared to the earlier studies, except for the study by Vandebroek et al. (2017) based on the CERC-equation;
- both FM-FlemCo model runs predict high transport peaks in the area of the Trapegeer-Broersbank-Den Oever sand ridge (east of De Panne) and west of Blankenberge where the coastline makes a bend (see Figure 33);
- east of Zeebrugge harbor, both FM-FlemCo model runs and Scaldis-Coast predict westward transport, while all earlier studies predict no or little eastward transport.

Although more analyses and additional model runs have to be performed to explain the observed differences, it is assumed that the three differences mentioned above are at least partly related to the following:

- The study by Vandebroek et al. (2017) based on the Kamphuis equation only considers wave related sediment transport and is therefore not representative for the total longshore sediment transport, which is probably much higher. Also the study by Vandebroek *et al.* (2017) based on the CERC equation only considers wave related sediment transport, however, it is doubted that the results of this study are reliable since the predicted wave related transport is up to factor 4 higher than the total transport predicted by all other studies (cf. Vandebroek *et al.*, 2017).

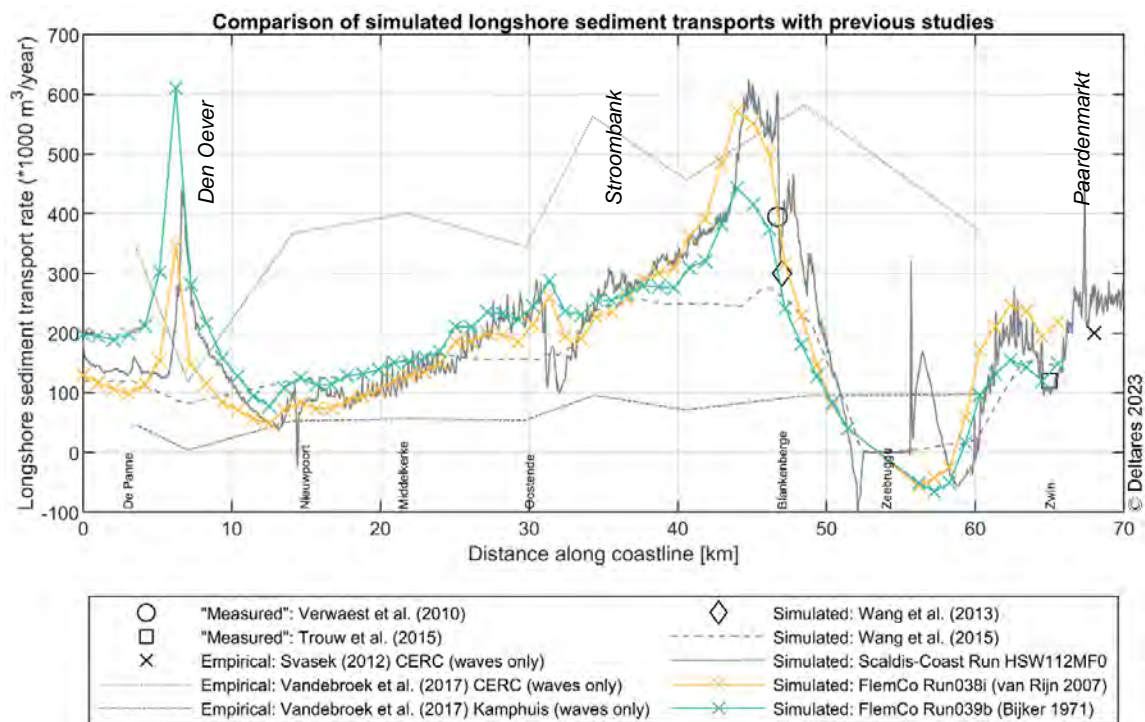


Figure 38 – Comparison of the longshore sediment transport, as simulated with the Delft3D Flexible Mesh-Flemish Coast model based on the sediment transport formulation by van Rijn (2007) and by Bijker (1971) and as published in previous studies. The longshore sediment transport indicated for the FM-FlemCo and Scaldis-Coast model runs is based on the 2 km long cross-sections shown in Figure 33. Positive transport rates indicate eastward transport, while negative rates indicate westward transport.

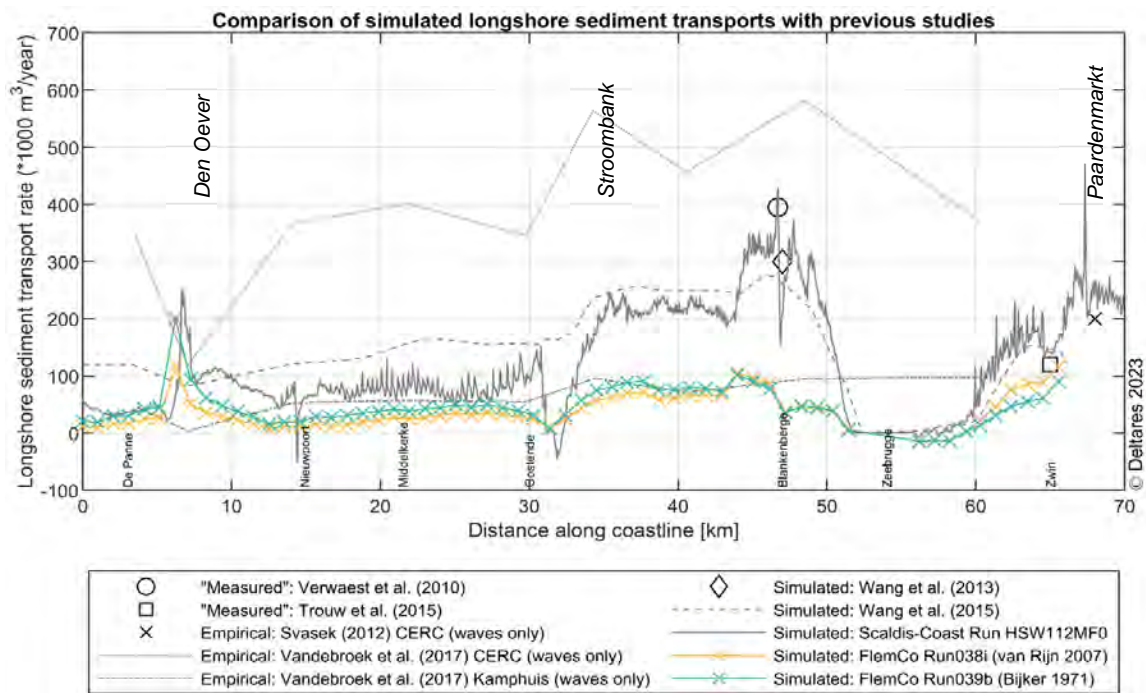


Figure 39 – Comparison of the longshore sediment transport, as simulated with the Delft3D Flexible Mesh-Flemish Coast model based on the sediment transport formulation by van Rijn (2007) and by Bijker (1971) and as published in previous studies. The longshore sediment transport indicated for the FM-FlemCo and Scaldis-Coast model runs is based on ca. 750 m long cross-sections with an average depth of ca. -5 m TAW at the seaward end. Positive transport rates indicate eastward transport, while negative rates indicate westward transport.

- All earlier studies (except for the one based on the Scaldis-Coast model) use shorter cross sections (max. 1,500 m long, until an average depth of -5 m TAW) than the FM-FlemCo model (2,000 m long with an average depth at the seaward end of -5.67 m TAW / -8 m NAP). This may explain why the earlier studies (i) generally predict lower longshore sediment transport, (ii) do not predict the two transport peaks since the cross sections are too short to account for the sediment transport occurring further offshore in the area of the Trapegeer-Broersbank-Den Oever sand ridge and the Wenduine sand ridge and (iii) do not predict westward sediment transport east of Zeebrugge harbour since the cross sections might be too short to account for westward transport occurring further offshore.
- The Scaldis-Coast model considers two sediment fractions (200  $\mu\text{m}$  and 500  $\mu\text{m}$ ) with a spatially varying initial availability of both fractions, while the FM-FlemCo model considers only one sediment fraction (200  $\mu\text{m}$ ) with a uniform initial availability. The coarser fraction (500  $\mu\text{m}$ ) in the Scaldis-Coast model domain is particularly present in the western part of the Belgian coast, while the finer fraction (200  $\mu\text{m}$ ) is dominant in the eastern part. The ratio of the two fractions is calculated to mimic a corresponding sediment transport rate as the observed local grain size would (cf. Figure 35). This might be the reason why the Scaldis-Coast model predicts slightly lower sediment transport than the FM-FlemCo model for the area west of Blankenberge, since in this area the coarser fraction limits the sediment transport simulated in the Scaldis-Coast model.

Although several studies on the longshore sediment transport along the Belgian coast do exist, a direct comparison with the simulated transport based on the FM-FlemCo model is limited due to the fact that all studies, except for the study based on the Scaldis-Coast model, use shorter cross distance and/or smaller water depth (the longer the cross section, the larger the transport) and some studies (i.e. the studies by Svasek (2012) and by Vandebroek *et al.* (2017)) do only account for wave related but not for both wave and flow related sediment transport (for details see the references in Figure 38). To enable comparison with the former, the longshore sediment transport in FlemCo (and Scaldis-Coast) is also calculated on shorter transects of ca. 750 m length and an average depth of -5 m TAW at the seaward end (Figure 39).

Remarkably the FlemCo results show much lower values of longshore sediment transport, although the peaks at Den Oever and west of Blankenberge can still be observed. The differences between Figure 38 and Figure 39 might indicate that the FlemCo model, relative to the Scaldis-Coast model, overestimates the contribution of the tidal currents to the longshore sediment transport and/or underestimates the contribution of waves.

Since the simulated longshore sediment transport based on the transport formulation by van Rijn (2007) (Run038i) shows a better match with the transport predicted by earlier studies in the western part of the Belgian coast and since the formulation by van Rijn (2007) is considered as the more advanced transport formulation compared to the one by Bijker (1971) (cf. Deltares 2022c), we applied the formulation by van Rijn (2007) in the current study.

In order to investigate the hypothesis of natural nourishment via shoreface connected sand ridges, the following FM-FlemCo model runs have been performed:

- Run038h: flow only morfostatic simulation based on the present bathymetry;
- Run038i: flow-wave coupled morfostatic simulation based on the present bathymetry;
- Run038o: flow-wave coupled morfostatic simulation based on the 1866 bathymetry.

In all runs the model is forced by the same windfield. Based on the first two runs, it is investigated whether – in the present situation – there is cross-shore sediment transport from the shoreface connected sand ridges (i) Trapegeer-Broersbank-Den Oever, (ii) Stroombank and (iii) Wenduinebank-Paardenmarkt towards the coastline and whether this transport is caused by tides only or by the combination of tides and waves. Run038o allows for a comparison of the sediment transport between the present situation and the situation in 1866. Based on this run it is particularly investigated whether or not there was more cross-shore sediment transport in 1866, when all three sand ridges were still connected to the beach. It has to be noted that the resolution and accuracy of the derived 1866 bathymetry is considerably lower compared to the present bathymetry (cf. Figure 33 and Figure 34), which makes it difficult to directly compare Run038i and Run038o.

### 3.3.2 SedTRAILS analysis

In order to evaluate the sediment transport simulated with the FM-FlemCo model, a preliminary analysis using the SedTRAILS (**S**ediment **TR**ansport visualisation and **L**agrangian **S**imulator) postprocessing tool (e.g. Elias & Pearson, 2020; Pearson, 2021; Pearson *et al.*, 2021) has been carried out. Elias & Pearson state that SedTRAILS translates the Eulerian sediment transport vector fields as simulated by a numerical process-based model (here FM-FlemCo model) into Lagrangian sediment pathways. However, it is important to note that SedTRAILS is not a particle tracking tool and has no physical meaning attached to the particle velocity; therefore SedTRAILS is merely a visualization tool, showing fictive pathways of hypothetical particles.

The principles of the SedTRAILS analysis are as follows (cf. Figure 40, Elias & Pearson, 2020; Pearson *et al.*, 2021):

1. From the Eulerian model, sediment velocity fields ( $u_{tr}$ ) are derived by dividing the computed volumetric suspended and bed load flux fields ( $S_v$ ) by a constant scaling factor (length scale factor  $h_{tr}$ , which, in SedTRAILS is introduced as so-called acceleration factor  $1/h_{tr}$ ).

$$S_v = \frac{S_m}{\rho_b} = \frac{\left[\frac{kg}{m \cdot s}\right]}{\left[\frac{kg}{m^3}\right]} = \left[\frac{m^3}{m \cdot s}\right] = \left[\frac{m^2}{s}\right] \qquad u_{tr} = \frac{S_v}{h_{tr}} = \frac{\left[\frac{m^2}{s}\right]}{\left[\frac{m}{s}\right]} = \left[\frac{m}{s}\right]$$

For a realistic approximation of the particle motion,  $h_{tr}$  should be related to a representative height in the water column over which material is transported, and varies depending on the mode of transport (suspended load and/or bed load). However, for visualization purposes,  $h_{tr}$  can be adjusted to increase the rate of particle motion, since sediment transport rates are often very small in magnitude. The length scale factor  $h_{tr}$  can only be adjusted until the point where particle trajectories begin to diverge with changes to  $h_{tr}$ .

To capture temporal variations in sediment transport (for example, over the course of a tidal cycle), the mean total sediment transport over a certain timestep (e.g. 10 minutes) is calculated from the simulated cumulative mean total transport. The use of the mean transport vector instead of the instantaneous transport vector has two advantages: firstly, instabilities that may occur in the instantaneous sediment transport field (for example in shallow areas) are averaged out over the selected time interval; secondly, the number of output/input intervals is reduced.

2. In SedTRAILS the Lagrangian model described by Storlazzi *et al.* (2017) is adapted to advect hypothetical particles through a changing vector field computed in the previous step (1.); it employs a similar methodology to sediment particle tracking modules such as the Lagrangian-based PTM (Macdonald *et al.*, 2006). Particle tracking models are often highly sensitive to the choice of the initial timestep (e.g. consider the release of a particle at the ebb versus flood phase of a tidal cycle), therefore the effective particle velocities ( $u_{tr}$ ) should be sufficiently small so the exact release time does not influence the ultimate trajectories. Diffusion is incorporated using a random displacement at each timestep. E.g. a diffusion coefficient of 0.1 corresponds to a random displacement equal to 10% of the particle's travel distance in the given timestep.
3. In a last step, a sediment connectivity analysis can be conducted, tracing particle pathways from every source and calculating its residence time in every cell it passes through.

During the first SedTRAILS time step, hypothetical particles from different source points are released, and then they are advected by the effective velocity fields ( $u_{tr}$ ). There are two ways of generating the sources points, with clusters or transects. To generate clusters, the area of interest of the domain is divided in  $k$  number of sources using the  $k$ -means algorithm depending on the characteristics of the bathymetry (below mean sea level), where the centroids of these subareas correspond to the source points. This way, more sources are created in the regions of complex bathymetry. For the use of transects, cross sections with equidistant number of source points are created, which is the approach applied in the current study (see below).

It is important to note that SedTRAILS is not a particle tracking tool and has no physical meaning attached to the particle velocity. Instead, it visualizes the morphodynamic connectivity between various elements of the considered morphological system. The time step for particle movement is based on numerical accuracy and not on the fictive particle velocity. Therefore, the lengths of the trajectories have to be analyzed qualitatively with a longer pathway indicating higher mobility of the sediment in the area compared to a shorter one (Elias & Pearson, 2020). This also means that SedTRAILS cannot be used to assess the change of sediment volume in a specific area.

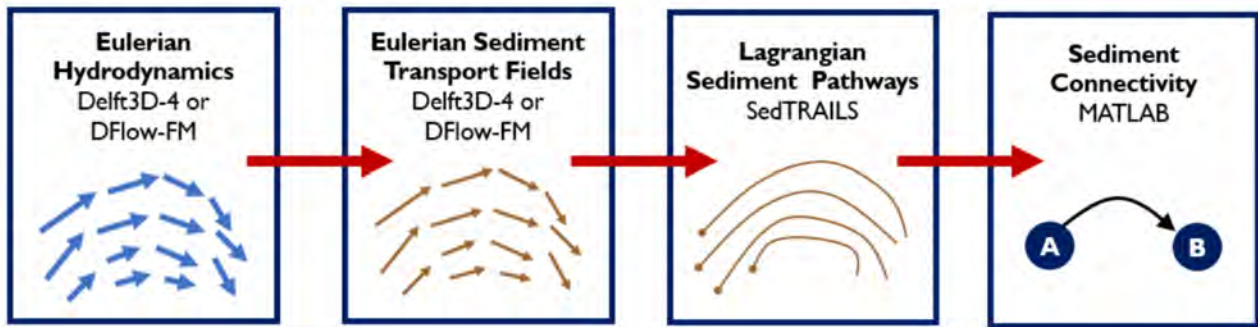


Figure 40 – Flow chart of the SedTRAILS modelling methodology.

Beginning with an Eulerian hydrodynamic and sediment transport model, hypothetical velocities are derived from the computed sediment transport. Pathways are then computed using SedTRAILS, which can then be used as input for connectivity analysis (from Pearson et al., 2021).

The usual procedure for the application of SedTRAILS is to first identify a morphologically representative period for the application of the process-based model (here FM-FlemCo model), which results in a sediment transport vector field representative for the annual (or longer) average conditions. Based on the output of the process-based model for the representative period, SedTRAILS is then run cyclically for a longer period of e.g. one year in order to determine representative hypothetical particle pathways (Elias & Pearson, 2020). In the current study, the FM-FlemCo model ran for the morphologically representative period from 14-03-2014 to 13-05-2014 (see Section 3.3.1), which forms the input for the SedTRAILS analysis. The sediment transport vector field used in SedTRAILS is the 1-hour incremental mean transport of the total load which is calculated from the time-averaged cumulative mean transport obtained as output from the FM-FlemCo model. The SedTRAILS analysis was performed for 16 cross-shore transects along the Belgian coast, each with a length of about 9 km and each with a resolution of 100 hypothetical particles along the transect (Section 3.4). Based on these transects, a sensitivity analysis was performed with regard to the applied acceleration factor and runtime in order to produce fully developed sediment particle pathways. This sensitivity analysis yielded an acceleration factor of 50 and a runtime of 365 days (for more details on the applied approach see Chaves, 2022).

### 3.3.3 The Telemac Scaldis-Coast model

The Scaldis-Coast model, developed by FH within the framework of the Complex Project Kustvisie (CPKV), simulates short and longer-term morphodynamics (up to 10 years) along the Belgian coast in the tidally driven offshore and wave driven nearshore zone. It is an integral coastal model build within the TELEMAC-MASCARET model suite, using direct coupling between the TELEMAC2D hydrodynamic module, the TOMAWAC wave propagation module and the SISYPHE sediment transport and bed update module.

The following sections summarize the setup and features of the Scaldis-Coast model. For a detailed description of the model, the reader is referred to Kolokythas *et al.* (2021), Wang *et al.* (2021) and Kolokythas *et al.* (2020) for reports on respectively hydrodynamics, waves and morphodynamic modelling.

### Model domain and computational grids

The so-called “Scaldis-Coast” model has an outline that resembles the corresponding one of the Scaldis-Coast model reported in Smolders *et al.* (2016). The most noticeable difference between the two outlines is the schematized upstream part of the Scaldis-Coast model.

The computational grid consists of > 250,000 nodes with a maximum resolution of 20 m along the Belgian coastline and a minimum resolution of 750 m in the open offshore boundary (Figure 41). In a second step of mesh building/refinement, the element size was inversely related to velocity gradients computed on the first base grid (Figure 42). Tidal (TELEMAC2D module) and wave (TOMAWAC module) driven forces are coupled, but computed on a different mesh. The TOMAWAC mesh has lower resolution in the nearshore area (ca. 50 m) and both Eastern and Western Scheldt estuaries have been removed from the computational domain (Figure 43).

### Model bathymetry

The topo-bathymetry consists of a patchwork of airborne LiDAR and bathymetric survey data collected between 2004 and 2015 as shown in Figure 44 (Kolokythas *et al.* 2021). For this project the same dataset was interpolated in the FM-FlemCo model (see §3.3.1). Figure 45 shows the imposed spatially varying bottom roughness field.

### Hydrodynamic and wind forcing

For the tidal forcing, a morphological representative tide has been selected. As for the FM-FlemCo model tidal boundary conditions were first derived from the validated hydrodynamic Simona DCSMv6-ZUNOV4 model (Zijl, 2013 & 2014) in the form of a time series for the year 2014 by means of nesting. Out of the whole year 2014 two successive tides (24) were selected, showing the best agreement between the mean sediment transport of the whole year 2014 and the tested subperiod. Depending on the sediment transport formula used, a different morphological representative tide should be considered (Kolokythas *et al.* 2020).

Although upstream discharge boundaries were applied in earlier runs of Scaldis-Coast, those are no longer applied in the final morphodynamic simulations.

The imposed wave climate corresponds to a time series at the measurement location Westhinder, from December 2015 till December 2016. This was believed to be the best approach to reproduce the mean annual wave climate for the period 2009 – 2018 and corresponding along-shore transport (Kolokythas *et al.*, 2020).

Wind forcing is only considered in the wave module of the model (TOMAWAC). It consist of a time series from Vlakte van de Raan for the year 2014, imposed uniformly throughout the models domain.

The three way coupled morphodynamic model was calibrated and validated against:

- the averaged alongshore sediment transport rates of 10 (morphostatic) sediment transport runs for the years 2009 – 2018;
- observed morphological changes between 1986 and 2005 at the mouth of the Western Scheldt (no dredging and dumping applied);
- observed morphological changes between 1986 and 196 in the Western Scheldt, including dredging and dumping works;
- alongshore sediment transport in the Wenduine – Blankenberge area, and observed sediment deposition in the access channel of Blankenberge marina after the Ciara storm (February 2020).

### Other model settings

Production run HSW112 showed the best overall performance (Kolokythas *et al.*, 2020). The Bijker formulation in combination with the proper calibration factor and grain size distribution is a good compromise to represent both the tidally driven offshore morphologic dynamics and the wave driven nearshore dynamics. An overview of its settings can be found in Table 12, along with the corresponding settings in the FM-FlemCo model. The HSW112 run and all its input- and additional source code files can be found in FH's subversion server

([https://wl-subversion.vlaanderen.be/svn/repoSpNumMod/TELEMAC/Scaldis-Kust/15\\_068\\_Complex\\_Model\\_Kustvisie\\_2021/3\\_MORPHODYNAMICS/HSW112](https://wl-subversion.vlaanderen.be/svn/repoSpNumMod/TELEMAC/Scaldis-Kust/15_068_Complex_Model_Kustvisie_2021/3_MORPHODYNAMICS/HSW112)).

Within this project the production run HSW112 is referred to as HSW112 MF10, as it has a morphodynamic acceleration factor of 10. This suffix was added to distinguish it from the morfostatic simulation (sediment transport without bed update) HSW112 MF0 where no bed update is imposed on the hydrodynamics after the calculation of the sediment fluxes.

Also a version of the model Scaldis-Coast model for the situation of 1866 is under development. Extra mesh nodes needed to be added, in order to surpass the seawards extending breakwaters (Dunkerke, Oostende, Zeebrugge) that were not present at that time.

### Calculation of sediment transport fluxes

The Scaldis-Coast model stores the cumulative sediment transport over time in every node of the model. In order to obtain figures comparable to previous studies (Wang *et al.*, 2015; Kolokythas *et al.*, 2020), the resulting sediment transport is interpolated on a curvilinear grid which follows the coastline. This curvilinear grid is ca. 2 km wide perpendicular to the coast (comparable to the cross-shore cross-sections defined in FlemCo, see Figure 33), and has a alongshore spacing of ca. 40 m. The resulting sediment transport is integrated over each of these cross-shore gridlines to get the yearly alongshore sediment flux for every location along the coastline (see Figure 46). The same is repeated for a subset of the interpolation grid, stretching ca. 750 m from the coast (Figure 47). These shorter cross-shore transects, with an average depth of -5 m TAW at their seaward end, are believed to be representative of the alongshore sediment transport in the breaker zone (longshore sediment transport *sensu stricto*). It was also this subset of the interpolation grid that was used to calculate the longshore sediment transport in previous studies like Wang *et al.* (2015) and Kolokythas *et al.* (2020).

In a similar way the cross-shore component of the resulting sediment transport can be calculated (see Figure 48).

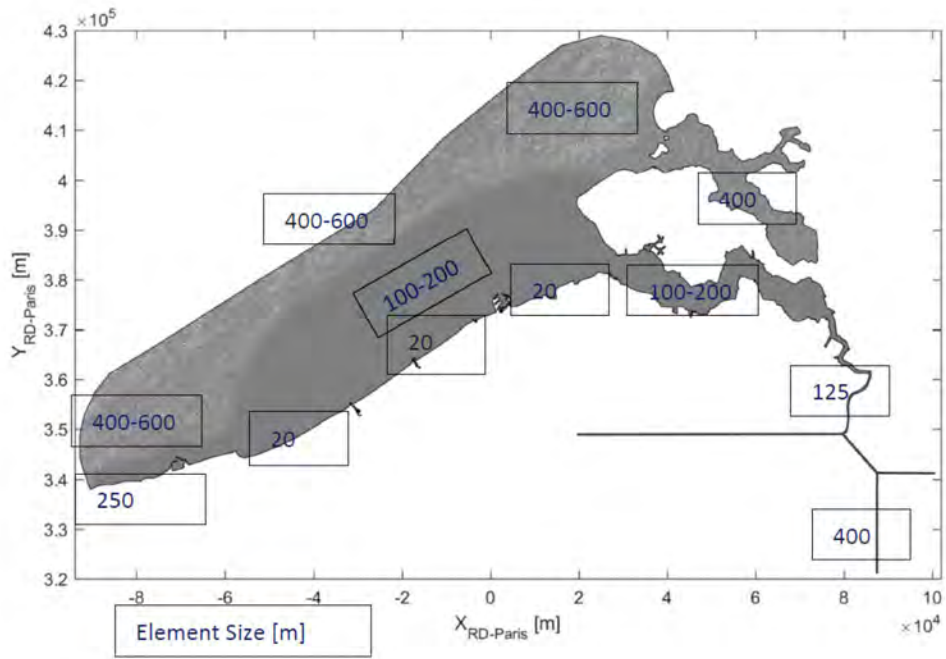


Figure 41 – Characteristic element sizes of the Scaldis-Coast TELEMAC2D base grid.

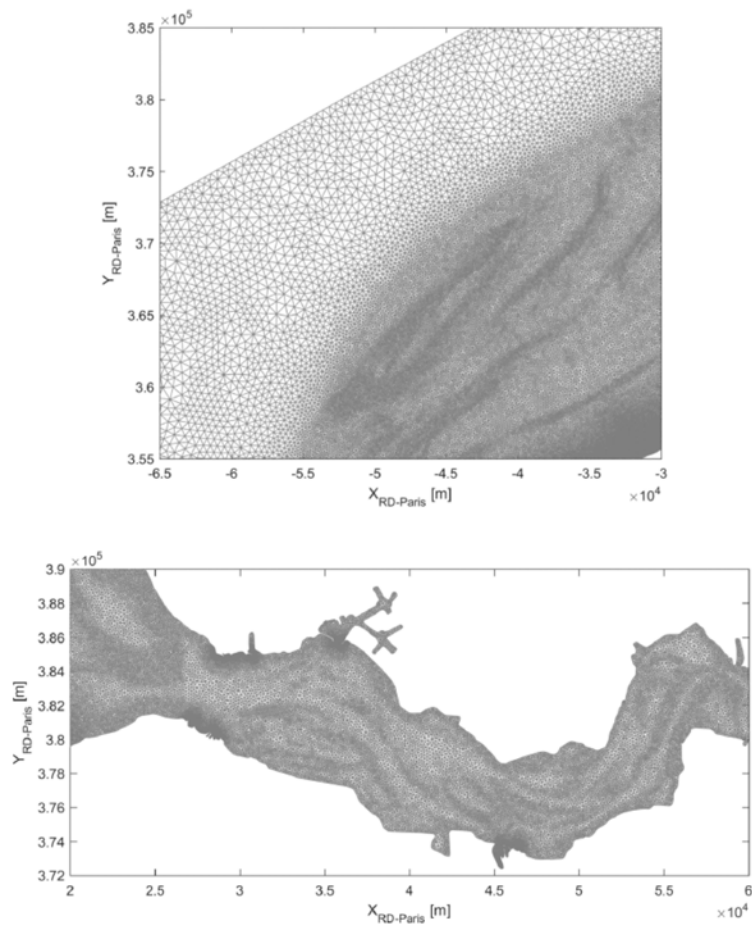


Figure 42 – Element size determination based on the local gradient of maximum velocity magnitude by use of GMSH Size Field options (Structured, Gradient, Threshold). Top figure: Focus on the coastal and offshore area (Nieuwpoort is located at the bottom right corner); Bottom figure: Focus on part of the Western Scheldt and its mouth.

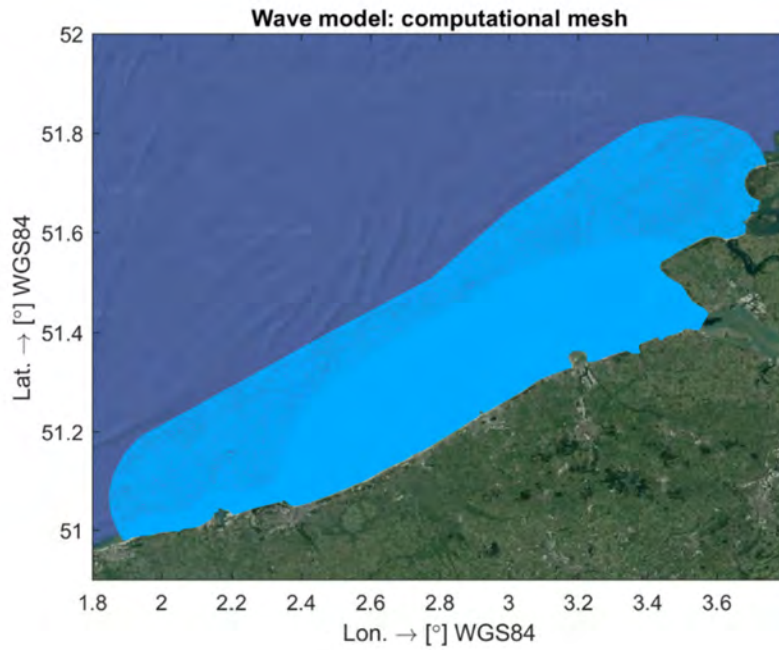


Figure 43 – Mesh layout of the Scaldis-Coast wave propagation model (TOMAWAC).

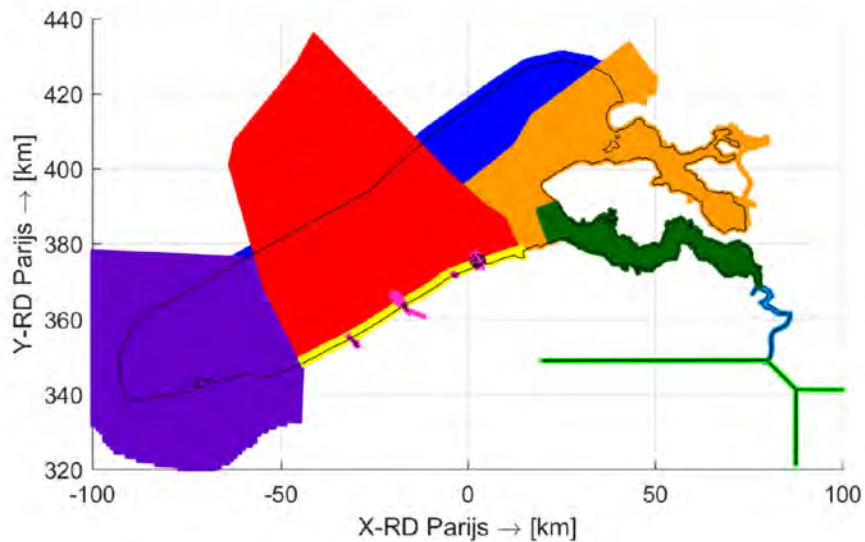


Figure 44 – Overview of the bathymetric data for the model domain  
 yellow – 1) Lidar data 2015; red – 2) BCP data 2004 – 2015; dark green – 3) WES data 2015; light blue – 4) BEZ data 2015; orange – 5) Vaklodingen data 2010 – 2015; purple – 6) French SHOM data; magenta – 7) Port data 2014 – 2015; blue – 8) EMODnet data; green – uniform values for the schematised part of the Scheldt Estuary.

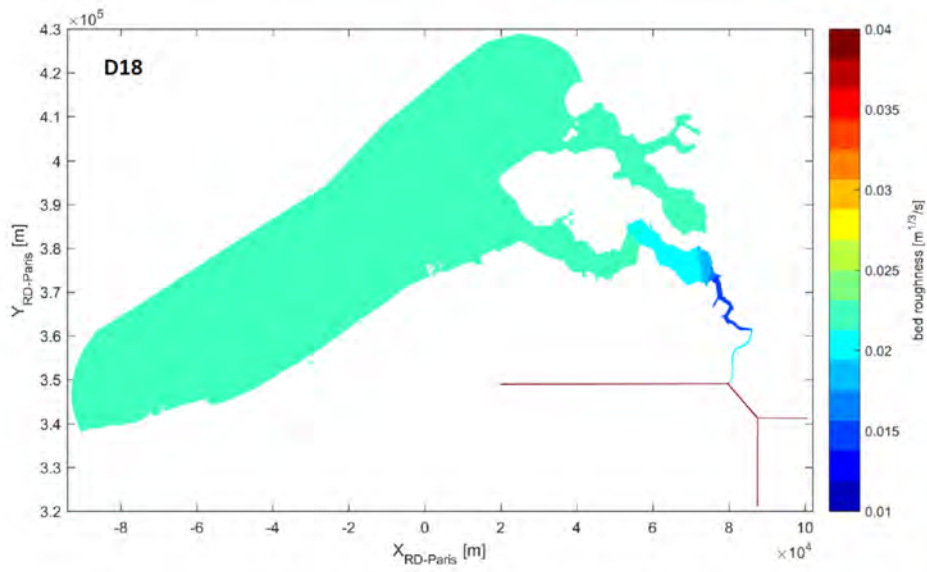


Figure 45 – Roughness field (Manning's law) on the computational domain of Scaldis-Coast model.

## 3.4 Results

### 3.4.1 Sediment transport

Figure 46 shows the longshore sediment transport within a 2 km wide stretch along the Belgian coast (longshore transport *sensu largo*) as simulated with the FM-FlemCo model based on three different models runs (cf. Section 3.3.1). The reference run, i.e. flow-waved coupled Run038i (yellow line) shows that the simulated longshore sediment transport ranges between  $-50,000 \text{ m}^3/\text{year}$  (westward transport) east of Zeebrugge harbour and almost  $600,000 \text{ m}^3/\text{year}$  (eastward transport) near Blankenberge. The model predicts two outstanding transport peaks – in the area of the Trapegeer-Broersbank-Den Oever sand ridge (east of De Panne) and west of Blankenberge where the coastline makes a bend (see Figure 33). Another, smaller peak can be observed directly east of Oostende harbour. Between Nieuwpoort and Blankenberge, the longshore sediment transport continuously increases and subsequently drops significantly towards Zeebrugge harbour. Here, the longshore sediment transport within the first 2 km of the coast is interrupted due to the presence of the two large harbour breakwaters (cf. Figure 33). Directly east of Zeebrugge harbour, the longshore transport changes its direction from earlier eastward to westward but subsequently becomes eastward orientated again (at a distance of about 58 km along the coastline) and increases significantly in the area of the tidal Appenzak channel.

In order to get insight into the role of tide and wave related sediment transport along the Belgian coast, the FM-FlemCo model has also been applied for a flow only simulation (only tides, no waves; Run038h). The simulated longshore sediment transport based on Run038h (green line in Figure 46) follows the same pattern as described above for flow-wave coupled Run038i. However, the transport predicted by Run038h is slightly lower compared to the transport predicted by Run038i. This means that – according to the FM-FlemCo model – the contribution of waves to the total longshore sediment transport within the first 2 km seawards the coastline (average water depth ca.  $-8 \text{ m NAP}$  /  $-5.67 \text{ m TAW}$ ) is limited, while the tide related longshore sediment transport clearly dominates. This is particularly true for the first 30 km of the Belgian coastline between the French-Belgian border and Oostende (except for the area of the Trapegeer-Broersbank-Den Oever sand ridge east of De Panne) and the area east of Blankenberge.

The simulated longshore sediment transport presented so far is based on the present bathymetry of the Belgian coast. The blue line in Figure 46 depicts the longshore transport as simulated in Run038o, which is using the bathymetry of 1866, i.e. the time before the construction of the harbour of Zeebrugge (the works started in 1977) and before dredging of the harbour navigation channels began. At that time, all three sand ridges (i) Trapegeer-Broersbank-Den Oever, (ii) Stroombank and (iii) Wenduinebank-Paardenmarkt were connected to the beach (Figure 34; Section 3.2). The longshore transport as simulated for the 1866 bathymetry and for the present bathymetry can be compared as follows:

- Between the French-Belgian border and De Panne, i.e. in the area of the sand ridge Trapegeer-Broersbank-Den Oever, the longshore transport simulated for the 1866 bathymetry is characterised by several peaks which are not observed for the present bathymetry.
- In the area between De Panne and Blankenberge, the simulated longshore sediment transport generally agrees well, although the transport peaks around the harbours of Nieuwpoort and Oostende are slightly more pronounced in the case of the 1866 bathymetry.
- Between Blankenberge and 't Zwin, the simulated sediment transport based on the 1866 bathymetry is clearly higher compared to the present bathymetry due to the absence of the breakwaters of Zeebrugge harbour. At Blankenberge, the sediment transport reaches its absolute maximum of almost  $700,000 \text{ m}^3/\text{year}$ , which is even higher than the absolute maximum predicted for the present bathymetry. In the area of 't Zwin, the sediment transport simulated for both bathymetries becomes similar again.

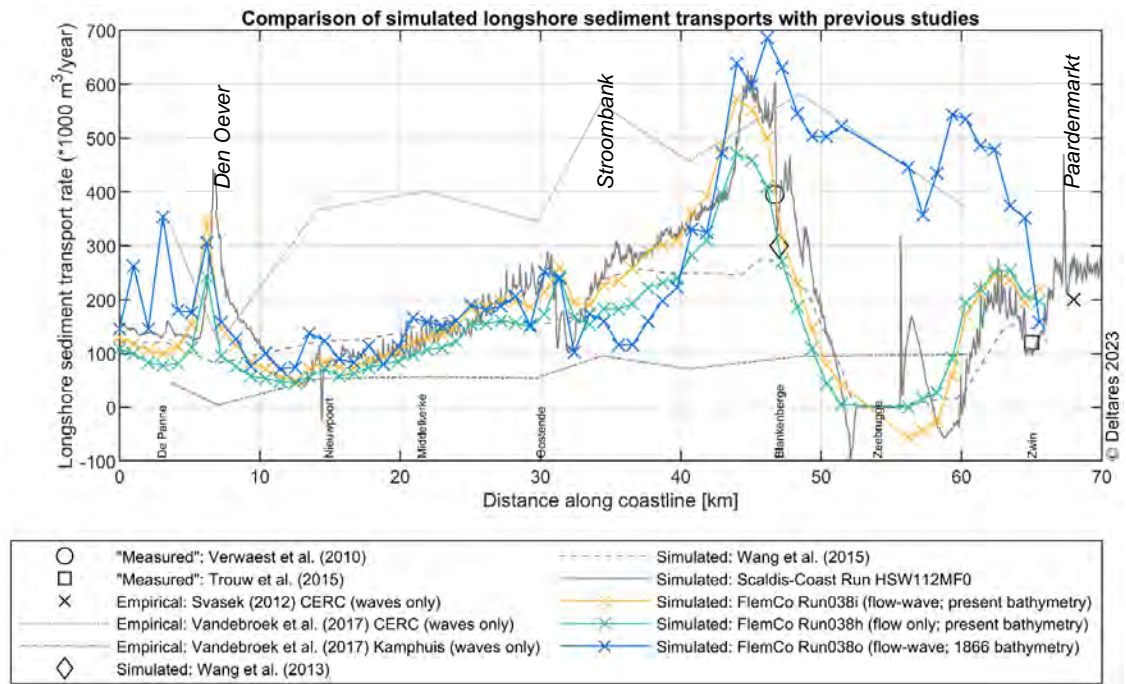


Figure 46 – Longshore sediment transport,

as simulated with the Delft3D Flexible Mesh-Flemish Coast model based on a flow only (Run038h) and on a flow-wave coupled run (Run038i) for the recent bathymetry as well as based on a flow-wave coupled run for the 1866 bathymetry (Run038o). All simulations are based on the sediment transport formulation by van Rijn (2007). For comparison, the longshore sediment transport as found in previous studies is illustrated as well. The longshore sediment transport indicated for the FM-FlemCo model runs is based on the cross-sections shown in Figure 33. Positive transport rates indicate eastward transport, while negative rates indicate westward transport.

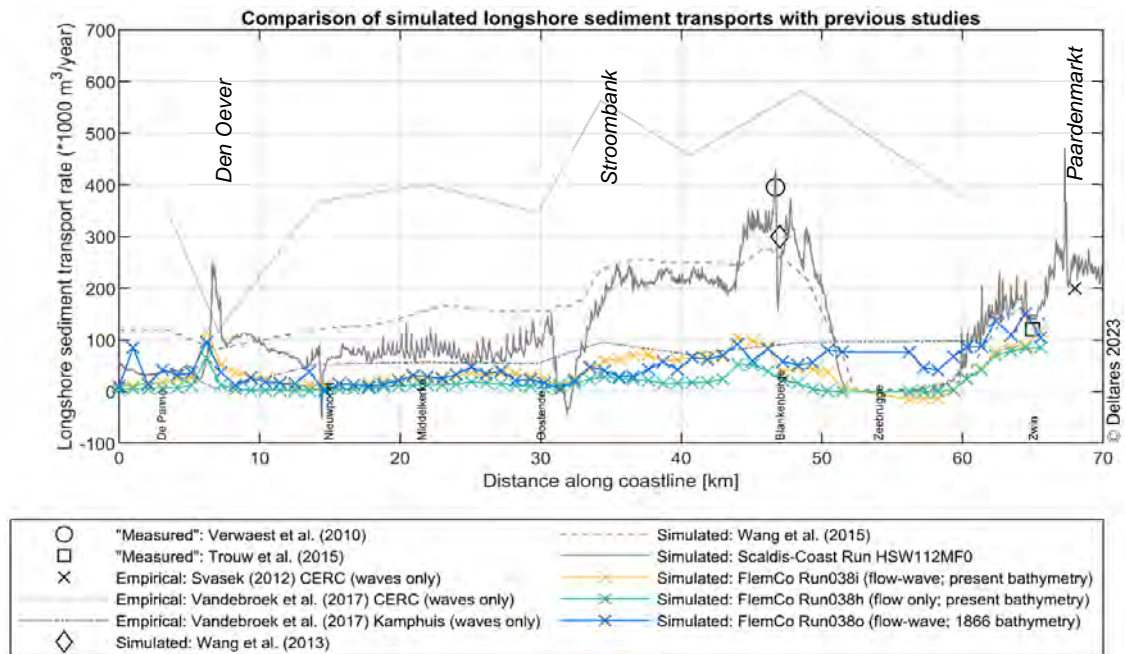


Figure 47 – Longshore sediment transport,

as simulated with the Delft3D Flexible Mesh-Flemish Coast model based on a flow only (Run038h) and on a flow-wave coupled run (Run038i) for the recent bathymetry as well as based on a flow-wave coupled run for the 1866 bathymetry (Run038o). All simulations are based on the sediment transport formulation by van Rijn (2007). For comparison, the longshore sediment transport as found in previous studies is illustrated as well. The longshore sediment transport indicated for the FM-FlemCo and Scaldis-Coast model runs is based on ca. 750 m long cross-sections with an average depth of ca. -5 m TAW at the seaward end. Positive transport rates indicate eastward transport, while negative rates indicate westward transport.

The alongshore sediment transport simulated by the HSW112MFO Scaldis-Coast run (grey line in Figure 46) follows the same pattern as those computed in the FlemCo runs, but is able to show a higher alongshore resolution due to the way post-processing was performed. The little but sharp fluctuations that can be observed are attributed to the presence of groin-fields: e.g. west of Den Oever no groins are present in the field and the resulting curve is smooth. The higher alongshore resolution also captures the drop in longshore sediment transport caused by the harbors (harbor access channels) of Nieuwpoort, Oostende, Blankenberge and Zeebrugge.

Figure 47 shows the longshore sediment transport within a ca. 750 m wide stretch along the Belgian coast; the average depth at the seaward side of this zone is ca. -5 m TAW, so the area corresponds with what is believed to be the breaker (surf) zone for the Belgian coast (longshore transport *sensu stricto*). Only between Oostende and Zeebrugge the FM-FlemCo model attributes an important component of the longshore transport in the breaker zone to the wave action; west and east of this zone there is little difference between the computed longshore sediment transport in the coupled flow-waves and the flow-only runs. This again might indicate that the FM-FlemCo model relatively underestimates the wave driven component and/or overestimates the tidal component of the longshore sediment transport. Between Blankenberge and km 60 the 1866 simulation shows a constant longshore transport due to the absence of the breakwaters of Zeebrugge harbour. East of km 60 the longshore transport simulated for 1866 is higher than for the present day simulations, but increases to the east at more or less the same pace as the present day simulations; so these higher base values can also be explained by the absence of the Zeebrugge breakwaters. Because the Paardenmarkt attaches to the shore east of Cadzand, where no output transect was defined, this influence cannot be seen in this figure.

Figure 48 shows the cross-shore component of the simulated sediment transport for two Scaldis-Coast runs: “MF = 0” is a morfostatic run, while “MF = 10” is the morphodynamic production run, including dredging and dumping. The influence of dredged sediment dumping can be seen on the transect 1500 m offshore, just east of Nieuwpoort, where a disposal site is located (km 16 – 18). Both alongshore transects show higher sediment transport towards the coast on top of the sand ridges Trapegeer – Den Oever, Stroombank and Paardenmarkt. Sudden drops in the curve of the sediment transport (orange circles 1, 2 and 3) might give an indication of the sensitivity of the calculation method for the difference in angle between the orientation of the transect and the direction of the sediment transport. After all, the latter is believed to be mainly tidal driven and oriented in an alongshore direction, so small differences in either transect orientation or direction of the sediment transport (due to local changes in bathymetry and/or influence of wave induced currents), can cause substantial fluctuations in the calculated cross-shore component of the sediment transport. As an example, the change in cross-shore sediment transport indicated by the dashed circle (4), might be attributed to the change in coastline orientation at Wenduine.

Closer to shore (Figure 49), at ca. 750 m offshore and at ca. -4 m TAW to -5 m TAW depth (an approximation for the depth of closure), most of the sediment transport seems to be oriented offshore. Positive values can be linked to the presence of groins, or are situated at the lee side of large harbour breakwaters. The highest offshore directed sediment transport is observed west of the harbours, for Oostende and Zeebrugge this can certainly be attributed to changes in flow direction upstream of the western breakwaters.

However, at least some of these negative values (e.g. at the long stretch of coast between Nieuwpoort and Oostende) might be due to an artifact induced by the model itself: in the morphologic run HSW112, during the first storm conditions a large quantity of sediment from the beach is dumped on the lower shoreface. This sediment is thereafter not, or only minorly, redistributed during calm weather conditions. The lack of cross-shore processes in large scale coastal models and the openTELEMAC-MASCARET suite was already pointed out by Kolokythas *et al.* (2020). The cross-shore sediment transport close to the beach and upper shoreface should thus be considered with care.

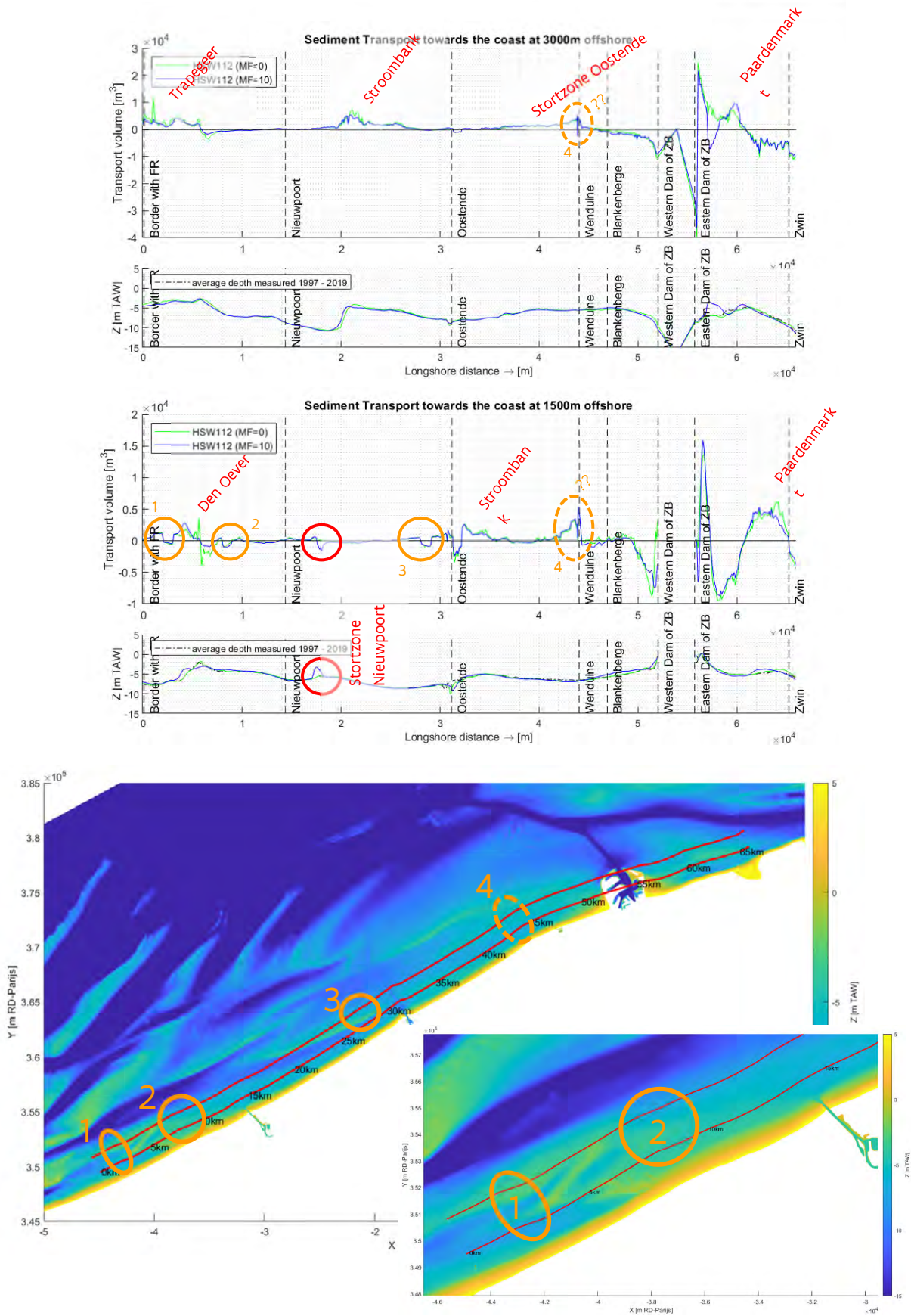


Figure 48 – Cross-shore component of the year-averaged sediment transport simulated by Scaldis-Coast. Top panel: fluxes at 3000 m offshore; Mid panel: transport at 1500 m offshore; Bottom panel: location of the alongshore transects from the French until the Dutch border; the inset shows a zoom of the area between the French border and Nieuwpoort. Orange circles show the sensitivity of the calculation method to the orientation of the transect.

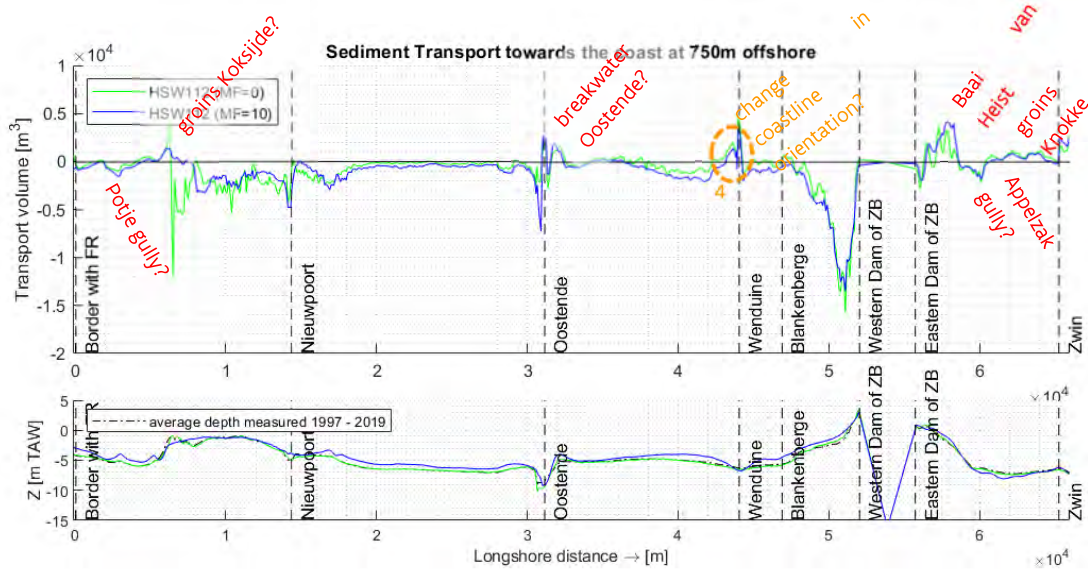


Figure 49 – Cross-shore component of the year-averaged sediment transport simulated by Scaldis-Coast at 750 m offshore.

Implementations of cross-shore processes, such as a modification of the depth-averaged flow velocities under the influence of Stokes drift and return flow and wave non-linearity, were already started by Kolokythas *et al.* (2020) but not yet thoroughly tested. It might be recommended to test these new developments in the openTELEMAC code made by the Scaldis-Coast team within the following year of the MOZES-project.

### 3.4.2 SedTRAILS

Figure 50 shows the results of the preliminary SedTRAILS analysis for the Belgian coast performed for FM-FlemCo model Run038i, which is based on a flow-wave coupling and the present bathymetry of the study area. The depicted pathways generally run parallel to the coastline and point towards the east-northeast, indicating – in line with the simulated longshore sediment transport presented in Figure 46 – mainly eastward longshore transport. East of Zeebrugge harbour, however, the hypothetical transport direction is less uniform and locally becomes westward orientated. Although the transects are about 9 km long, the sediment mobility does generally not decrease in a seaward direction, which is due to the relatively shallow water (of the order of about -10 m NAP (-7.67 m TAW), except for the deeper navigation channel Scheur-Wielingen) even 9 km seawards the coastline. As is indicated by the simulated longshore sediment transport shown in Figure 46, also the hypothetical pathways (Figure 50) imply an increasing sediment mobility from east to west along the Belgian coast. In the area of the shoreface the hypothetical pathways show a clear cross-shore component, which implies landward orientated sediment transport. This can be observed all along the Belgian coast but particularly in the areas where the sand ridges Trapegeer-Broersbank-Den Oever and Stroombank are connected to the shoreface/beach (see Figure 52a, Figure 53a). In the case of the Paardenmarkt sand ridge, however, the pathways run mainly parallel to the coastline and a clear landward component is missing (Figure 54a).

A comparison of the hypothetical pathways depicted in Figure 50 (based on a flow-wave coupled simulation; Run038i) and Figure 51 (based on a flow only simulation; Run038h) allows for a differentiation between tide and tide-wave related sediment transport along the Belgian coast. Generally, the pathways show very similar patterns, which confirms the earlier finding that tide related sediment transport clearly dominates the total longshore sediment transport (*sensu largo*) along the Belgian coast (see above and Figure 46). However, the following differences can be observed:

- The hypothetical pathways derived from the flow-only simulation (Run038h) are slightly shorter compared to the flow-wave coupled case indicating that the waves – even in larger distance to the coastline – contribute to the sediment transport magnitude.
- The flow-only simulation (Run038h) does not yield sediment pathways with a cross-shore/landward component. Instead, the pathways derived from Run038h run parallel to the coastline even close to the beaches. This can be observed all along the Belgian coast but particularly in the areas where the sand ridges Trapegeer-Broersbank-Den Oever and Stroombank are connected to the shoreface/beach (cf. Figure 52a, b and Figure 53a, b). In the case of the sand ridge Paardenmarkt, however, both simulations result in similar sediment pathways without a clear landward component (cf. Figure 54a, b). The fact that the cross-shore/landward transport component is missing in the case of the flow-only simulation implies that the landward sediment transport is caused by the presence of the waves.

Finally, the hypothetical pathways based on the present bathymetry (Run038i; Figure 50) and on the 1866 bathymetry (Run038o; Figure 55) are compared. Although a direct comparison between both simulations is limited due to the coarser resolution and lower accuracy of the digitized 1866 bathymetry (cf. Figure 33 and Figure 34; Section 3.2) the following observations can be made:

- Despite the considerable differences between the 1866 and the present bathymetry, the sediment pathways generally show similar patterns in both cases.
- Due to the absence of Zeebrugge harbour in 1866, the hypothetical pathways between Blankenberge and the Belgian-Dutch border are parallel to the coastline but do not bypass the harbour breakwaters as in the case of the present bathymetry. Moreover, the sediment mobility in this area is significantly larger in 1866, indicated by much longer hypothetical pathways in Figure 55 compared to Figure 50.
- Also in the case of the 1866 bathymetry, significant landward sediment transport occurs in the shallow zone of the shoreface all along the Belgian coast. In the areas, where the sand ridges Trapegeer-Broersbank-Den Oever and Stroombank meet the coastline, this landward transport is clearly intensified and spread over a larger area in the case of the 1866 bathymetry (cf. Figure 52a, c; Figure 53a, c). At the Paardenmarkt, however, the sediment transport from the sand ridge to the beach is limited, as is observed based on the present bathymetry (cf. Figure 54), although landward transport might occur further eastwards outside the area of high resolution of the FM-FlemCo model and the area of the SedTRAILS analysis.

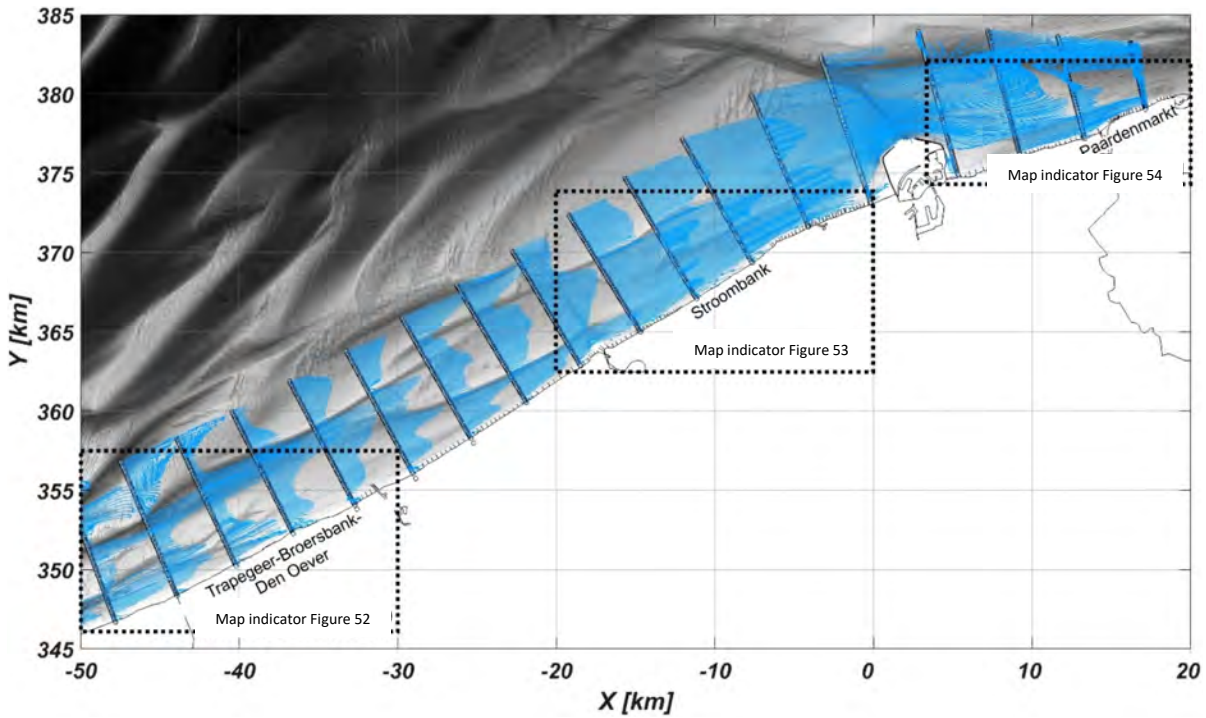


Figure 50 – Results of a preliminary SedTRAILS analysis for the Belgian coast, performed for FM-FlemCo model Run038i, which is based on a flow-wave coupled simulation using the present bathymetry of the study area. The blue lines indicate the fully developed pathways based on the representative period from 14-03-2014 to 13-05-2014 (see Section 3.3.1 and Section 3.3.2) for 100 fictive sediment particles along each transect. The sand ridge labels indicate the areas where the sand ridges are connected to the shoreface/beach. The coordinates are given in km according to Amersfoort/RD New.

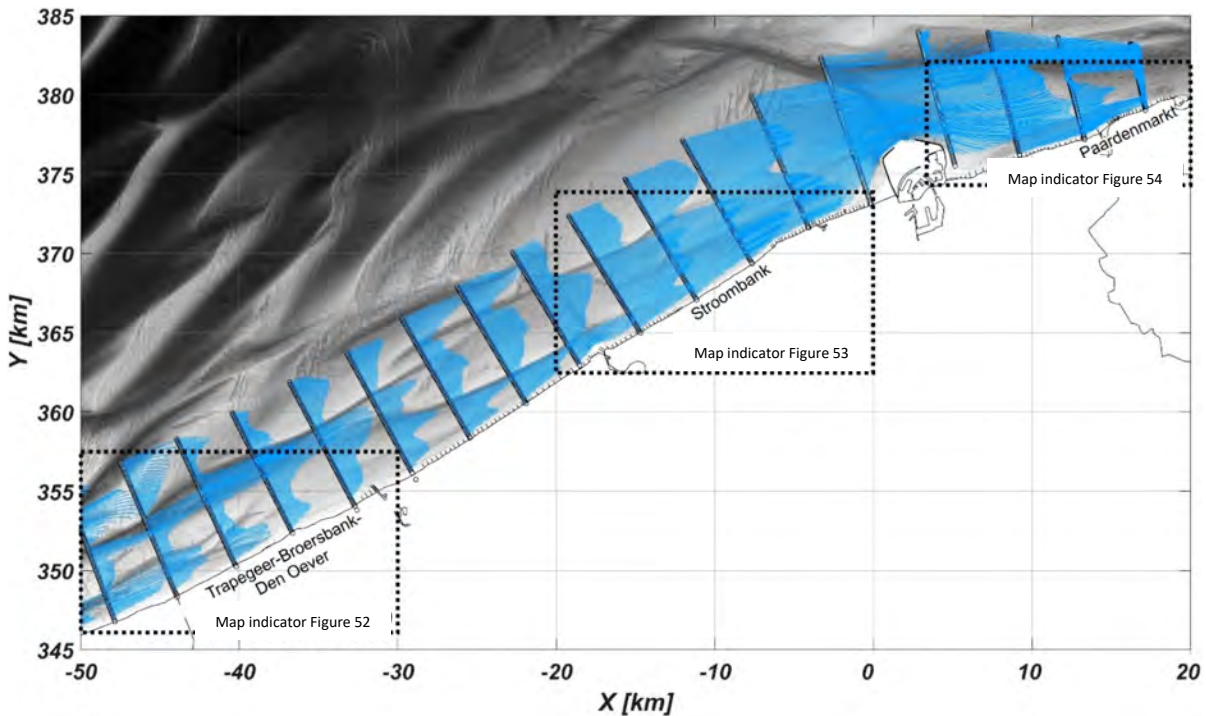


Figure 51 – Results of a preliminary SedTRAILS analysis for the Belgian coast, performed for FM-FlemCo model Run038h, which is based on a flow only simulation using the present bathymetry of the study area. The blue lines indicate the fully developed pathways based on the representative period from 14-03-2014 to 13-05-2014 (see Section 3.3.1 and Section 3.3.2) for 100 fictive sediment particles along each transect. The sand ridge labels indicate the areas where the sand ridges are connected to the shoreface/beach. The coordinates are given in km according to Amersfoort/RD New.

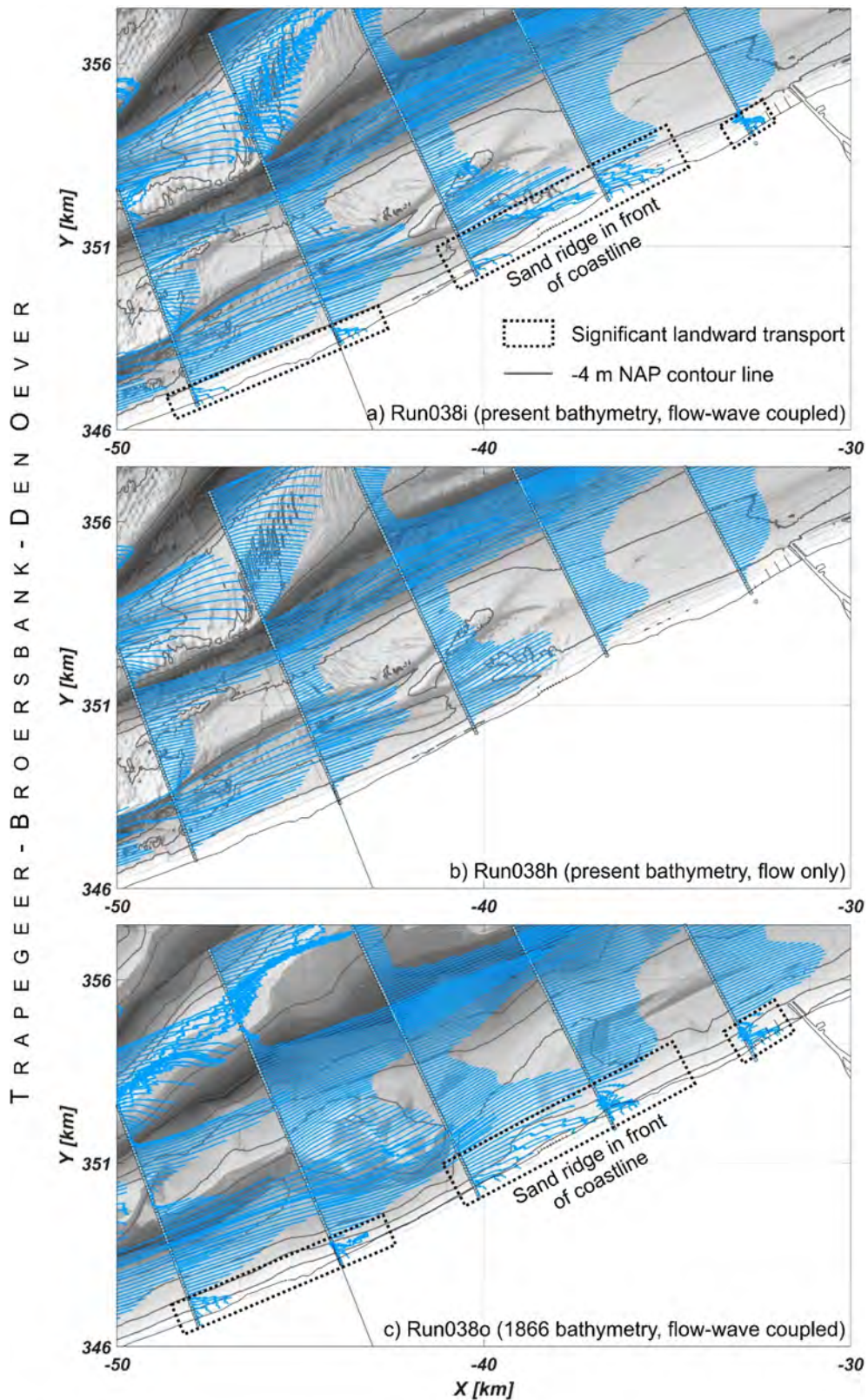


Figure 52 – Results of a preliminary SedTRAILS analysis for the area of the sand ridge Trapegeer-Broersbank-Den Oever (see map indicator in Figure 50) performed for FM-FlemCo model Run038i, Run038h and Run038o (Section 3.3.1). The blue lines indicate the fully developed pathways based on the representative period from 14-03-2014 to 13-05-2014 (see Section 3.3.1 and Section 3.3.2) for 100 fictive sediment particles along each transect. The dotted boxes indicate the areas where significant landward sediment transport can be observed. The coordinates are given in km according to Amersfoort/RD New.

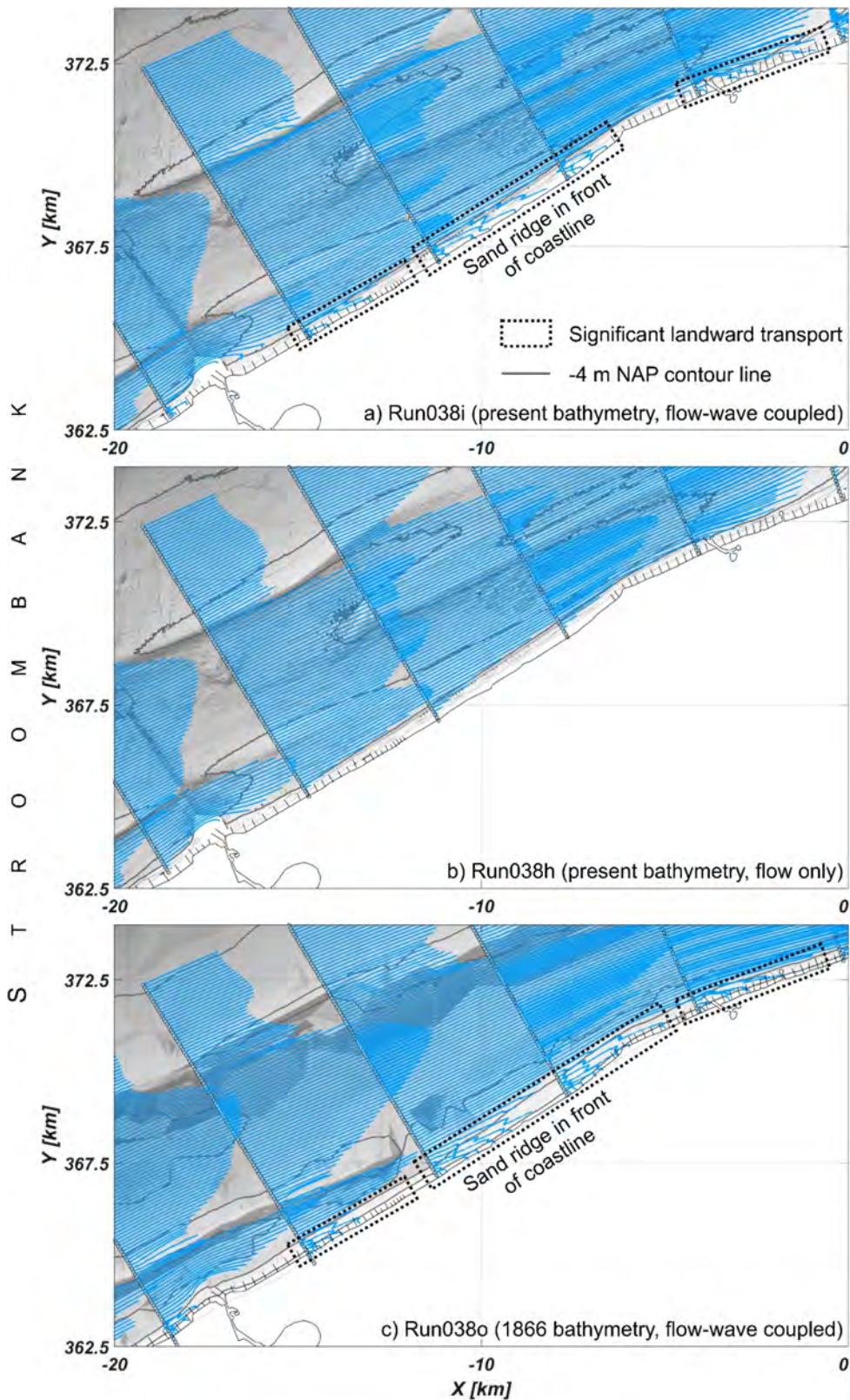


Figure 53 – Results of a preliminary SedTRAILS analysis for the area of the sand ridge Stroombank (see map indicator in Figure 50) performed for FM-FlemCo model Run038i, Run038h and Run038o (Section 3.3.1). The blue lines indicate the fully developed pathways based on the representative period from 14-03-2014 to 13-05-2014 (see Section 3.3.1 and Section 3.3.2) for 100 fictive sediment particles along each transect. The dotted boxes indicate the areas where significant landward sediment transport can be observed. The coordinates are given in km according to Amersfoort/RD New.

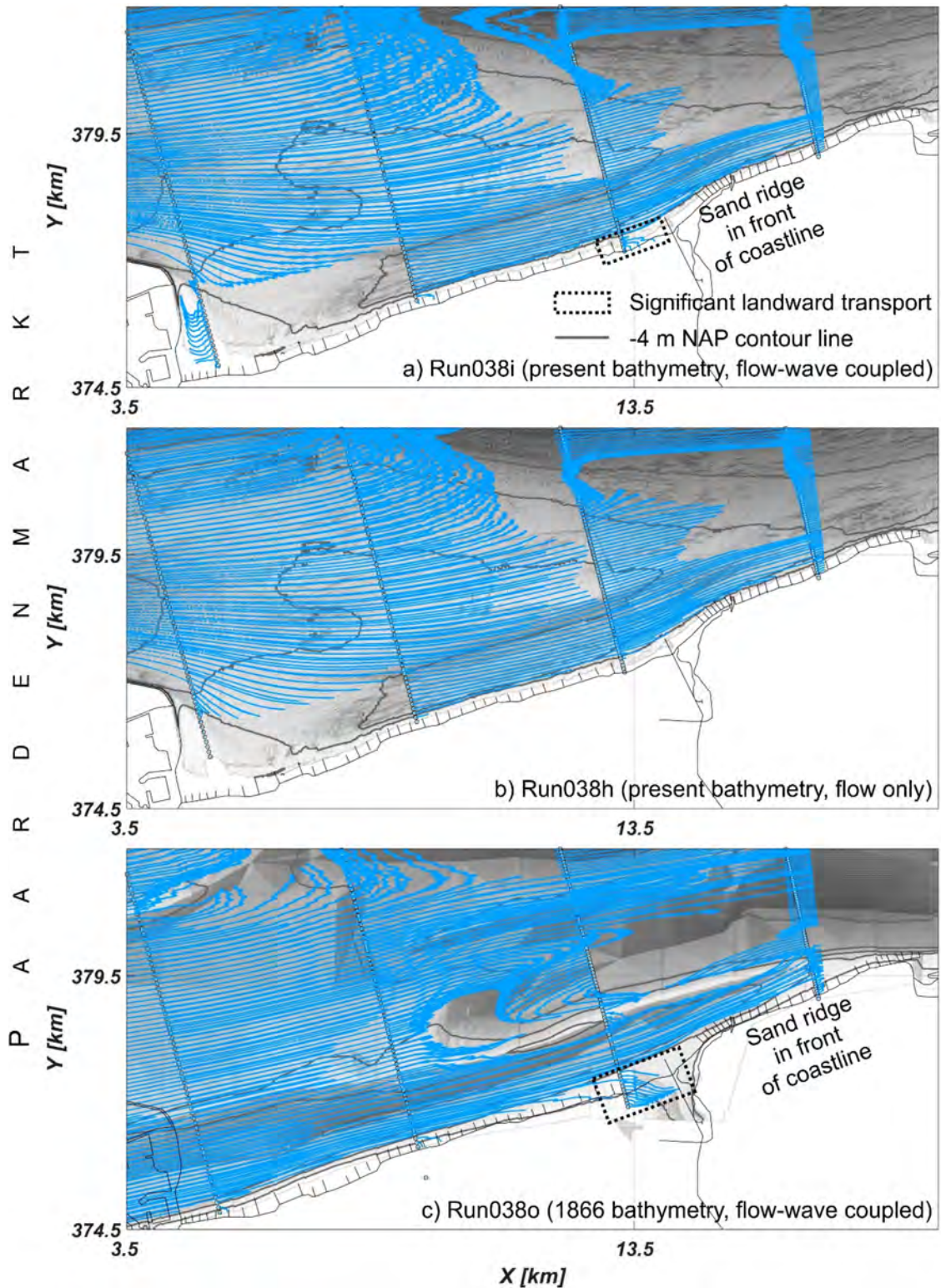


Figure 54 – Results of a preliminary SedTRAILS analysis for the area of the sand ridge (Wenduinebank-)Paardenmarkt (see map indicator in Figure 50) performed for FM-FlemCo model Run038i, Run038h and Run038o (Section 3.3.1). The blue lines indicate the fully developed pathways based on the representative period from 14-03-2014 to 13-05-2014 (see Section 3.3.1 and Section 3.3.2) for 100 fictive sediment particles along each transect. The dotted boxes indicate the areas where significant landward sediment transport can be observed. The coordinates are given in km according to Amersfoort/RD New.

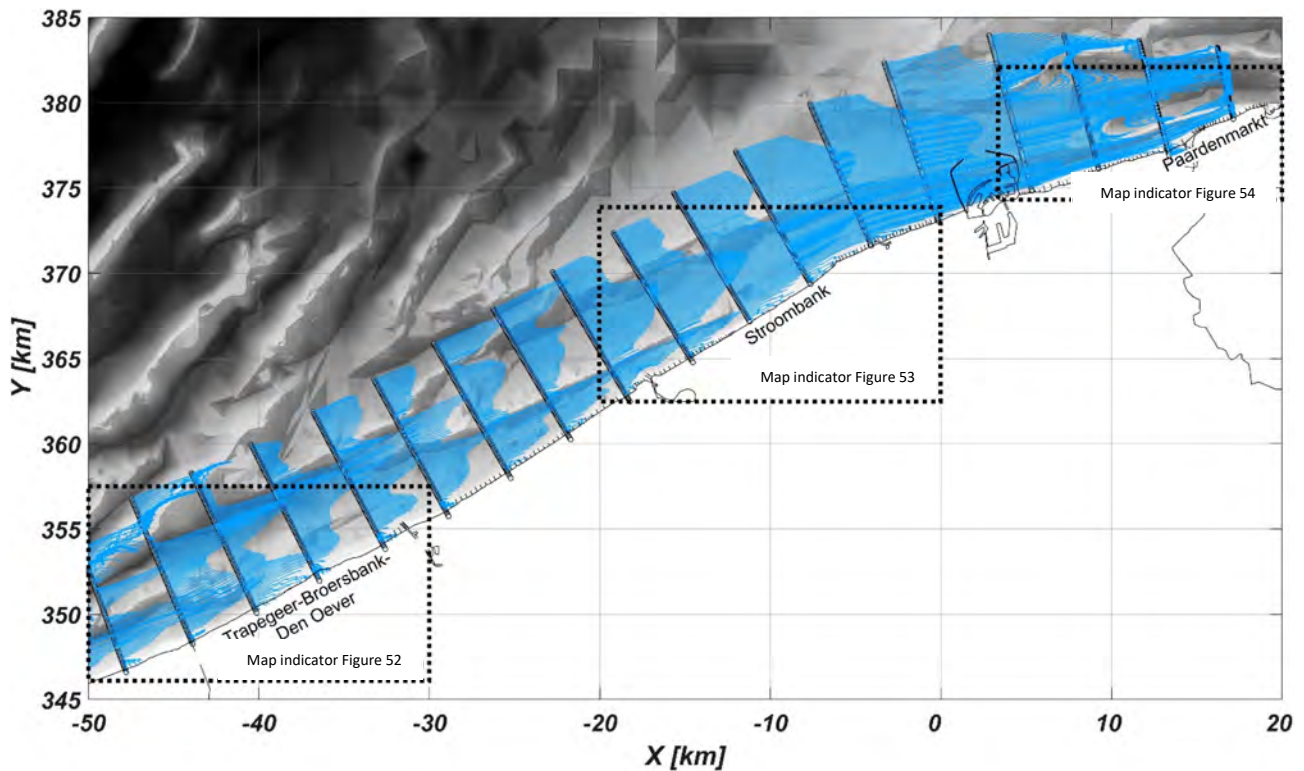


Figure 55 – Results of a preliminary SedTRAILS analysis for the Belgian coast performed for FM-FlemCo model Run038o which is based on a flow-wave coupled simulation using the 1866 bathymetry of the study area. The blue lines indicate the fully developed sediment pathways based on the representative period from 14-03-2014 to 13-05-2014 (see Section 3.3.1 and Section 3.3.2) for 100 fictive particles along each transect. The sand ridge labels indicate the areas where the sand ridges are connected to the shoreface/beach. Note that for the illustrated coastline is the present coastline, which allows a better comparison with the pathways shown in Figure 50 based on the present bathymetry. The coordinates are given in km according to Amersfoort/RD New.

### 3.4.3 Sediment transport in Scaldis-Coast

Figure 56 to Figure 58 show the yearly cumulative sediment transport in every node as calculated by the morphostatic Scaldis-Coast run HSW112MF0 (grey vectors). These vectors can also be interpreted as the yearly residual sediment transport. The “live streamlines cursor”-tool of BlueKenue (CHC, 2011), displays the resulting path of a particle within this vector field of yearly cumulative sediment transport (blue lines). Figure 56 to Figure 58 show the corresponding areas to the zooms on the SedTRAILS analysis (Figure 52 to Figure 54), based on the FlemCo runs.

As HSW112MF0 is a morphostatic run, and the vector field used is the cumulative sediment transport after one year, these streamlines shouldn't be interpreted as actual transport paths of a single sediment particle, but they rather show relative yearly residual sediment transport directions and intensities within the area. Longer streamlines demonstrate higher sediment transport intensity; diverging streamlines can indicate erosional areas, while converging streamlines can indicate areas of sediment deposition.

For all three locations sediment transport intensity is clearly the largest on the shoreface. Intensities also increase in the deeper parts of the tidal gullies between the sand ridges. On the seaward flank of the sand ridges transport intensities are generally lower. On top, and even more so on the steep landwards facing slope of the sand ridges Trapegeer – Broersbank – Den Oever (Figure 56), Stroombank and Wenduinebank (Figure 57) a sharp landwards deflection of the sediment transport paths can be observed. Within the tidal gullies the transport paths are again directed along the residual tide. Similar transport paths are observed on the Oostende bank and Nieuwpoortbank between the cities of Nieuwpoort and Oostende (not depicted in the figures).

The streamlines in the area of the Paardenmarkt (Figure 58) are more complex, showing influences of both the breakwaters of Zeebrugge and the mouth of the Western Scheldt. The scour pit in front of the harbor shows eastwards directed high transport intensities. On the shoreface and in the eastern most part of the Appelzak gully transport paths show that same direction. The slopes of the Paardenmarkt facing the Wielingen fareway channel show westwards directed transport paths, as does the westernmost part of the Appelzak gully. The diverging transport paths in the Appelzak gully in front of Knokke confirm the erosional character of the gully at this location. The converging transport paths on top of the Paardenmarkt are in confirmation with the observed sediment deposition in this area.

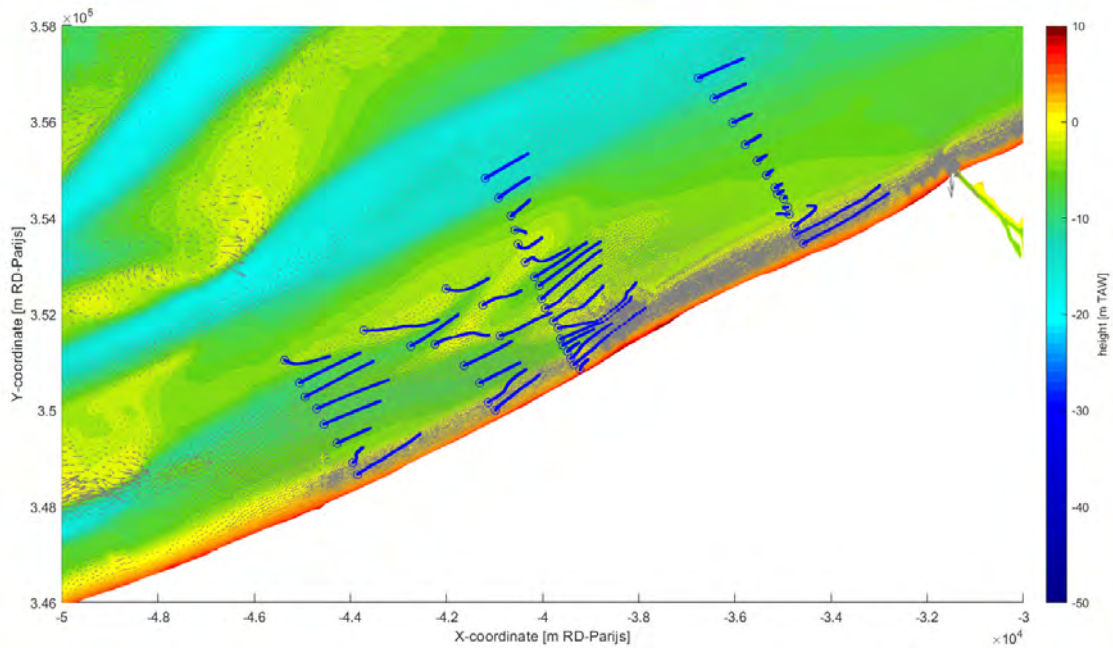


Figure 56 – Residual sediment transport streamlines at Trapegeer – Broersbank – Den Oever, as simulated by Scaldis-Coast. Starting position of the fictive particle is indicated by a circle. Grey vectors show the cumulative sediment transport after one year. The spatial density of the vectors is defined by the (varying) spatial density of the unstructured computational mesh of the model.

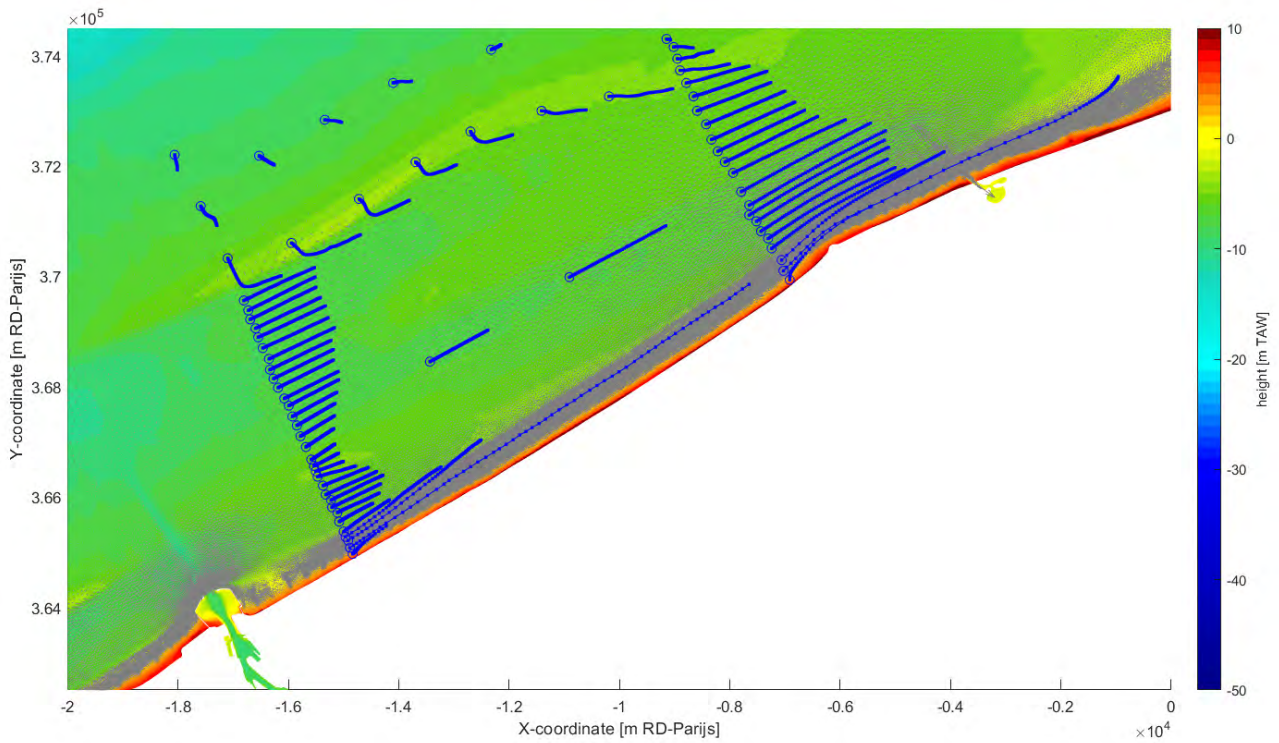


Figure 57 – Residual sediment transport streamlines at Stroombank, Grootere Rede and Wenduinebank, as simulated by Scaldis-Coast. Starting position of the fictive particles is indicated by a circle. Grey vectors show the cumulative sediment transport after one year. The spatial density of the vectors is defined by the (varying) spatial density of the unstructured computational mesh of the model.

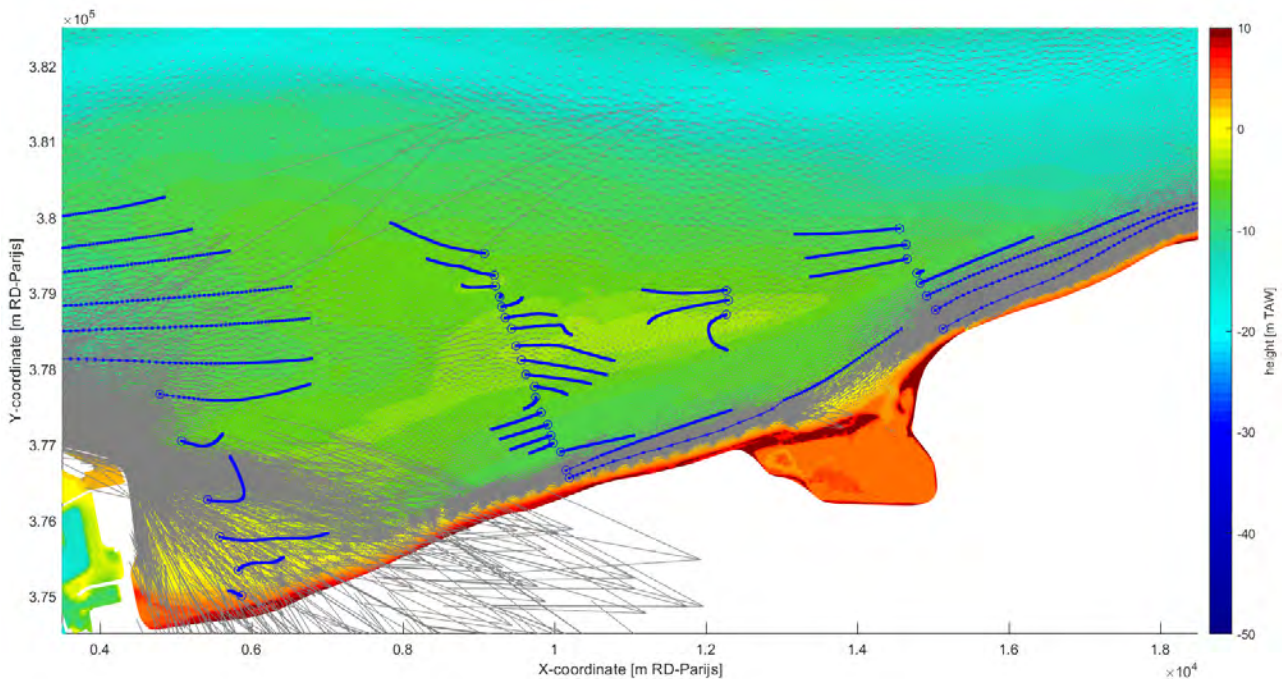


Figure 58 – Residual sediment transport streamlines at Paardenmarkt, as simulated by Scaldis-Coast. Starting position of the fictive particles is indicated by a circle. Grey vectors show the cumulative sediment transport after one year. The spatial density of the vectors is defined by the (varying) spatial density of the unstructured computational mesh of the model. The large grey arrows originating from the Zeebrugge breakwaters and other areas within the harbour are wetting/drying artifacts on the edges of the computational mesh, and should therefore not be considered.

### 3.5 Discussion

The simulation results based on the FM-FlemCo model and the preliminary SedTRAILS analysis (Section 3.4) indicate that significant longshore sediment transport occurs along the Belgian coast and that this transport is not limited to the upper shoreface but also occurs in deeper water several kilometers offshore. It is however important to distinguish between alongshore transport in the breaker zone (alongshore transport *sensu stricto*), and alongshore transport in a wider nearshore zone (alongshore transport *sensu largo*). The comparison between the flow-only (Run038h) and flow-wave coupled (Run038i) simulations demonstrates that the overall longshore transport within the first 2 km seawards the coastline (i.e. between the beach and approximately the -8 m NAP / -5.67 m TAW contour) is clearly dominated by tide related sediment transport, while wave related transport mainly occurs in the area of the upper shoreface within the first few hundred meters seawards the coastline. This is in contrast to the conclusions of earlier studies on the longshore sediment transport and the sediment dynamics along the Belgian coast (i.e. Svasek, 2012; Vandebroek *et al.*, 2017; Wang *et al.*, 2013 & 2015), who state that the longshore sediment transport in the nearshore zone (i.e. approximately the first 1.5 km seawards from the coastline) is mainly wave related. Although more analyses and additional model runs (e.g. based on an even higher cross-shore grid resolution of, for instance, 20 m instead of 40 m) have to be performed to explain the differences with earlier studies, it is assumed that the predicted dominance of tide related sediment transport along the Belgian coast is caused by the strong peak current asymmetry along the Belgian coast (the maximum flood flow velocities are significantly larger than the maximum ebb flow velocities; cf. Wang *et al.*, 2013) in combination with the relatively small average significant wave heights along the Belgian coast (the average significant wave height in the period 2010–2020 at Nieuwpoort, Oostende, Blankenberge and Cadzand was about 0.55 m; MDK, 2022; RWS, 2022).

Despite the importance of tide related sediment transport along the Belgian coast, the wave related transport seems to be crucial with regard to research question, whether the Belgian coastline is naturally fed by sand transport from the three shoreface connected sand ridges (Hypothesis natural feeding via shoreface connected sand ridges). The preliminary SedTRAILS analysis demonstrates that based on a flow-only simulation, the fictive pathways run generally parallel to the coast, while a cross-shore/landward component can only be observed when waves are added in the FM-FlemCo model (cf. Figure 50 and Figure 51). This effect is particularly obvious in the case of the sand ridges Trapegeer-Broersbank-Den Oever and Stroombank, while the pathways at the Paardenmarkt sand ridge are mainly parallel to the coastline even when waves are considered in the model. The comparison of the hypothetical pathways between the flow-only and the flow-wave coupled case implies that sediment is transported along the sand ridges Trapegeer-Broersbank-Den Oever and Stroombank and then – due to the presence of the waves – reaches the beach in those areas, where the sand ridges meet the coastline. Deposition of sediment near Den Oever is also indicated by the significant gradient of the longshore sediment transport as shown in Figure 46.

In the case of the Paardenmarkt sand ridge, the landward transport component can hardly be observed, which might be due to the facts that (i) in contrast to the other two sand ridges the Paardenmarkt is clearly separated from the coastline by a distinct tidal channel, i.e. the Appelzak channel and (ii) the wave heights at the Paardenmarkt are lower due to the protecting breakwaters of Zeebrugge harbours, the different coastline orientation and the smaller water depths in this area. The strong tidal flow in the Appelzak channel therefore seems to dominate the longshore sediment transport at the Paardenmarkt in a way that the local wave related cross-shore/landward transport is almost negligible and cannot contribute to significant landward orientated sediment transport. The clear dominance of the tide related longshore transport in the area of the Paardenmarkt/Appelzak is also indicated by Figure 46, which shows that the simulated longshore transport is almost the same in both the flow-only and the flow-wave coupled simulation.

The residual sediment transport streamlines as calculated with the morphostatic Scaldis-Coast run (Figure 56 to Figure 58) do not show the same deflection of sediment trajectories on the shoreface as in the SedTRAILS analysis of the FM-FlemCo model. This might be an indication of a lack of cross-shore wave induced processes in the openTELEMAC modelling suite, since in the SedTRAILS analysis these deflections could be attributed to wave action by comparing runs with and without wave forcing.

On top of, and on the landwards facing steep side of the sand ridges Trapegeer – Broersbank – Den Oever, Stroombank, Wenduinebank and Paardenmarkt the Scaldis-Coast simulation shows a strong landwards deflection of the streamlines. Within the tidal gullies the sediment transport paths are again aligned with the dominant tidal flow direction. The simulated residual sediment transport streamlines seem to be in line with the observed landward movement of these sand ridges (§4.1).

The SedTRAILS comparison of the hypothetical pathways based on the present and on the 1866 bathymetry (cf. Figure 50 and Figure 52 to Figure 55) shows that in both cases a clear landward orientated sediment transport occurs in the zone of the upper shoreface along the Belgian coast. Although a direct comparison between both simulations is limited due to the coarser resolution and lower accuracy of the digitized 1866 bathymetry (cf. Figure 33 and Figure 34; Section 3.2) it is implied that this landward transport in the areas where the sand ridges Trapegeer-Broersbank-Den Oever and Stroombank meet the coastline is more dominant based on the 1866 bathymetry. In the case of Trapegeer-Broersbank-Den Oever, this increase in landward transport might be related to the more compact shape and larger width of the sand ridge in the area where it merges into the beach in 1866 (cf. Section 3.2). More distinct landward transport in the area of the Stroombank might be due to the fact that no navigation channel existed in 1866 and splitted the sand ridge, which was much larger and closer connected to the coastline in 1866 (cf. Section 3.2). In contrast to the sand ridges Trapegeer-Broersbank-Den Oever and Stroombank, at the Paardenmarkt no significant landward sediment transport can be observed neither based on the present nor on the 1866 bathymetry. In both cases, the analysed sediment pathways run mainly parallel to the coast and clearly follow the tidal flow direction although the Paardenmarkt was directly connected to the beach in 1866. This stresses again the dominance of tide related longshore sediment transport in the area of the Paardenmarkt (see above).

The 1866 version of the Scaldis-Coast model is still in preparation. A comparison of the 1866 versions of both FlemCo and Scaldis-Coast could be conducted in the next working year.

### 3.6 Conclusions

With regard to the research question, whether the Belgian coastline is naturally fed by sediment transport from shoreface connected sand ridges to the beaches, the following can be concluded: The above described evaluation of the Scaldis-Coast model results, FM-FlemCo model results and the preliminary SedTRAILS analysis (Section 3.4) indicate that at the sand ridges Trapegeer-Broersbank-Den Oever and Stroombank landward directed sediment transport occurs, which potentially nourishes the adjacent coastline. On the shoreface this landward directed transport is particularly associated with wave related sediment transport, while the tide related sediment transport mainly occurs parallel the coastline. At the Paardenmarkt, no significant landward directed transport and by this no natural feeding of the coastline can be observed due to the dominance of tide related longshore transport even close to the coastline in the Appelzak gully. It can further be assumed that the landward directed sediment transport in the area of Trapegeer-Broersbank-Den Oever and Stroombank was more pronounced in 1866, when the sand ridges were wider/larger and closer connected to the coastline, respectively. At the Paardenmarkt, the FlemCo SedTRAILS show that landward directed transport is not significant neither in the case of the 1866 nor the present bathymetry, at least not in the investigated area. These conclusions regarding the 1866 situation are preliminary, as they still need to be investigated with the 1866 configuration of the Scaldis-Coast model.

For the Scaldis-Coast model, new developments in the openTELEMAC code made by the Scaldis-Coast team (Kolokythas *et al.*, 2020) in order to implement wave induced cross-shore processes like a modification of the depth-averaged flow velocities under the influence of Stokes drift and return flow and wave non-linearity, should be tested. These wave processes have a significant impact on the cross-shore sediment transport in the shoreface area and are thus essential to study the process of natural feeding of the beach by sediment transport over shoreface-connected sand ridges.

Although the current study implies landward directed sediment transport from the sand ridges towards the coast and by this indicates a potential natural feeding of the adjacent coastline, further research has to be carried out whether the landward transported sediment indeed feeds the beaches. Moreover, it has to be investigated what are the exact processes that lead to wave related landward direct sediment transport and in how far the interaction of tide and waves is relevant for this transport. A more in depth comparison of both process based numerical models should be conducted, to better understand the differences in the results. At this point it is not yet clear how much of these differences is induced by (i) parameter settings, (ii) the implementation of the physical processes in the model code and (iii) post-processing routines used.

Finally, it is suggested to apply a more advanced but also more expensive interpolation method (such as the kriging interpolation method) to generate the 1866 model bathymetry, which will result in a smoother bed and by this a more realistic representation of the actual 1866 bathymetry. The current, relatively angular model bathymetry, which was derived from a TIN (triangular irregular network) has, most likely, significant impact on the simulated sediment transport and derived fictive sediment pathways. Even after the application of a more advanced interpolation method, the accuracy and resolution of the (improved) 1866 bathymetry will still not be comparable with these of the present bathymetry. Therefore, it could be considered to use a coarsened model bathymetry for both the present and the (improved) 1866 bathymetry in the FM-FlemCo model in order to allow for a more direct comparison between both situations.

## 4 Effect of gradual deepening of nearshore tidal channels on beach erosion

Work Package 4 of the MOZES-project studies the influence of the (observed) deepening of the tidal channels near the coast on the nourishment intensity on the beaches. The research question asked is: “*What are the effects of the observed gradual deepening of the nearshore tidal channels, which separate the shoreface connected sand ridges from the coastline, on the beach erosion and on the intensity of (anthropogenic) nourishments required to maintain the (Belgian) coastline?*”

First, a literature review and data analysis will show the morphological evolution of the nearshore tidal gullies and (shoreface-connected) sand ridges for the Belgian coast on a time scale of decades to centuries. Then hotspots in shoreface and beach nourishment intensity will be defined. Secondly, again based on literature review and data analysis, similar case studies in the Netherlands will be explored for comparison.

Section §4.1 deals with the preliminary literature review, Section §4.2 shows data analysis performed for the morphodynamcis and nourishment volumes in the area of landward migrating channels along the Belgian coast and the preliminary results of the literature review/data analysis for the Dutch coast are presented in Section §4.3.

### 4.1 Literature quick-scan on the morphological evolution of the Belgian shelf and coastline

The following sections §4.1.1 and §4.1.2 are largely copied from earlier work by Houthuys *et al.* (2021), citing from Mathys (2009) and the work of Mathys (2009) respectively. Section §4.1.3 is copied from the work by Houthuys *et al.* (2021) and Janssens *et al.* (2012). The aim of this §4.1 is to give a brief introduction to the morphological evolution of the Belgian shelf, coastline and near shore sand ridges since the last ice age.

#### 4.1.1 Evolution of the Belgian shelf and coastline since the last ice age

During the Weichselian (116,000 to 11,650 BP), global sea level gradually dropped due to the fixation of water in ice caps. At the peak of this last ice age, around 20,000 years ago, the global sea level was maximally 120 m lower than today. The North Sea was reduced to a shallow proglacial lake situated in the centre of the present North Sea and separated from the Atlantic Ocean by an ice sheet that covered the northern part of the North Sea and joined the Northern British ice cover to the Scandinavian cover. To the south, a land area joined the European continent to southern England as the southern North Sea and the complete English Channel were emerged.

The limits of the Belgian Continental Shelf, at about 75 km from the present coastline, were, during the last stage of the Weichsel ice age (the Tardiglacial: 14,650 to 11,650 BP), only reached by the rising sea at about 12,500 BP.

Information on the Holocene (11,650 BP – now) flooding of the (present) nearshore area is primarily derived from sedimentary units recognized in this area (Mathys, 2009). Mathys (2009) interpreted 5300 km of high-resolution reflection seismic profiles, calibrated with data from more than 600 sediment cores, to establish a 3D-dataset of the patchy Quaternary sediment cover of the Belgian Continental Shelf. Seven seismic stratigraphic units were identified in the Quaternary deposits. After calibration of the seismic characteristics with the core data, these seismic stratigraphic units could also be assigned a lithological meaning (depositional and paleo-environmental setting).

The Holocene seismic stratigraphic units are:

- **U4:** a thin sand layer with internal channel fills. It contains also alternating clay-sand laminae, locally peat or peat lumps and shell layers. Interpretation: mud flats, sand flats, possibly in a back-barrier location, with tidal channels and marshes. Age: early Holocene. The unit covers a marine transgressive surface, largely dating back to the Eemian3 marine transgression.
- **U5:** truncated sand banks. Three long, parallel banks of which only the lower and middle part has been preserved. Internal reflectors dip landwards. The steeper slope is mostly the landward side, but is not steeper than 1°. Interpretation: storm-dominated shoreface connected ridges. They contain coarser sediment at their landward flank and finer on the top and at the seaward flank. A basal gravel or a sharp erosive lower surface is present underneath the unit: the environment that created U5 was erosional, and was accompanied by a receding coastal barrier. Age: around 9000 cal BP.
- **U6:** a thin deposit near the surface in the central and eastern part of the shelf near the present coast, with a dominance of black clay, often alternating with fine grey sand. Erosional base surface. Interpretation: deposit of eroded mud flats in sheltered swales between storm-dominated ridges and the coast.
- **U7:** uppermost unit. It consists of bank-like structures and thin sand sheets in the adjacent troughs. The unit makes up the top part of the most prominent features on the present-day seafloor: i.e. sandbanks and swales

### Start of the Holocene transgression

Around the start of the Holocene transgression the coastline in our area was formed by an open (exposed) tidal flat environment, not located behind a barrier, comparable to the present-day German Bight. The sea level was ca. 28 m lower than nowadays (Figure 59). What remains of these environments can be found in the seismic unit U4, at the base of the Oostdyck and Buiten Ratel sand banks.

### Development of coastal barriers

Depending on the scenario (connection with English Channel re-established or not), the first coastal barriers developed around 9000 or 9500 cal BP, with mean sea level at ca. 19 m lower than today. This age is dictated by the fact that the Southern Bight had to be sufficiently large to produce waves at its eastern shores capable of building a protective barrier behind which a complex of estuaries and tidal basins could develop.

The most offshore deposits of seismic unit U4 are located below the Kwintebank, at a depth of -19 m, and probably represent the first deposits formed behind the barrier. This means that the initial barrier was located at least 15 km offshore the present-day coastline (Figure 60).

### Retreat of the coastal barrier

During relatively fast sea-level rise (before 7500 BP), the back-barrier areas attracted sediment that was derived from the coastal barrier, causing it to erode and retreat. The coastal barrier sheltered tidal basins. Sand to fill the basins was derived from the shoreface adjacent to the tidal inlets and from the ebb-tidal deltas. As insufficient sediment was supplied to the shoreface by long-shore and cross-shore transport to compensate for this sediment loss, the shoreline was forced to recede, while eroding the underlying (U4) deposits.

Between De Panne and Nieuwpoort, the barrier had approximately reached the present day coastline; in the eastern part, the position of the coastline has been reconstructed using the -15 m contour of the Holocene transgressive surface (Figure 61). The result is a rectilinear connection between De Panne and the western tip of Walcheren, which seems a plausible coastline in the absence of the large Western Scheldt inlet, which only formed later.

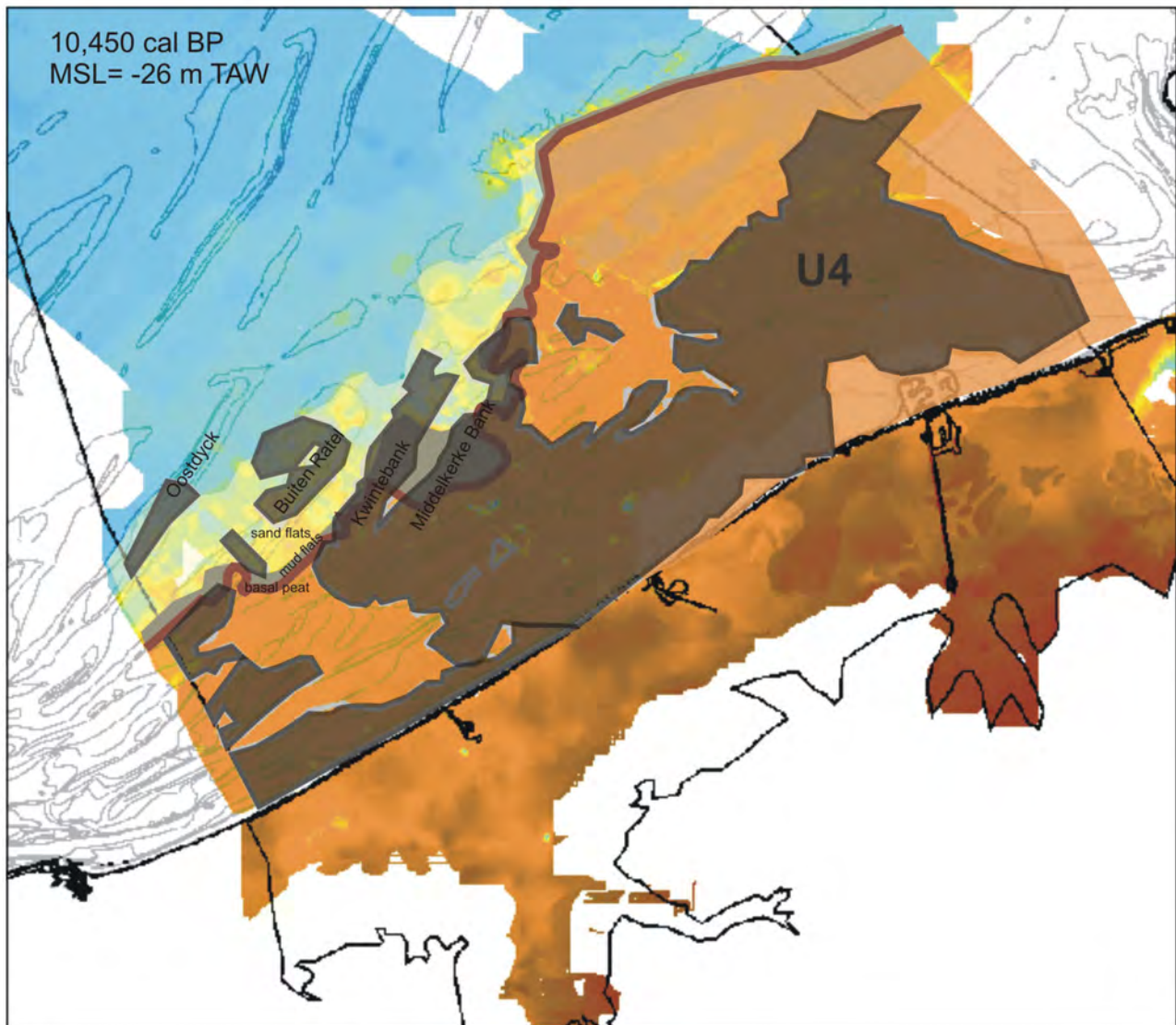


Figure 59 – Belgian coastline around 10,450 cal BP.

From Mathys (2009), Fig. 7.38. Paleo-reconstruction of the situation around 10,450 cal BP, when MSL was -26 m MLLWS. Part of the deepest (oldest) deposits of seismic unit U4, located below the Oostdyck and Buiten Ratel at -28 m MLLWS, have developed at that time. These deposits might represent remnants of an open (exposed) tidal flat environment, not located behind a barrier, comparable to the present-day German Bight. A fringe of basal peat (brown line) bordered the tidal flats (grey: mud flats and yellow: sand flats). Orange to brown area is land. The orange transparent overlay represents the presumed Pleistocene surface located higher than presently preserved (due to erosion in the swales between the presentday banks). The transparent dark grey area represents the position of seismic unit U4.

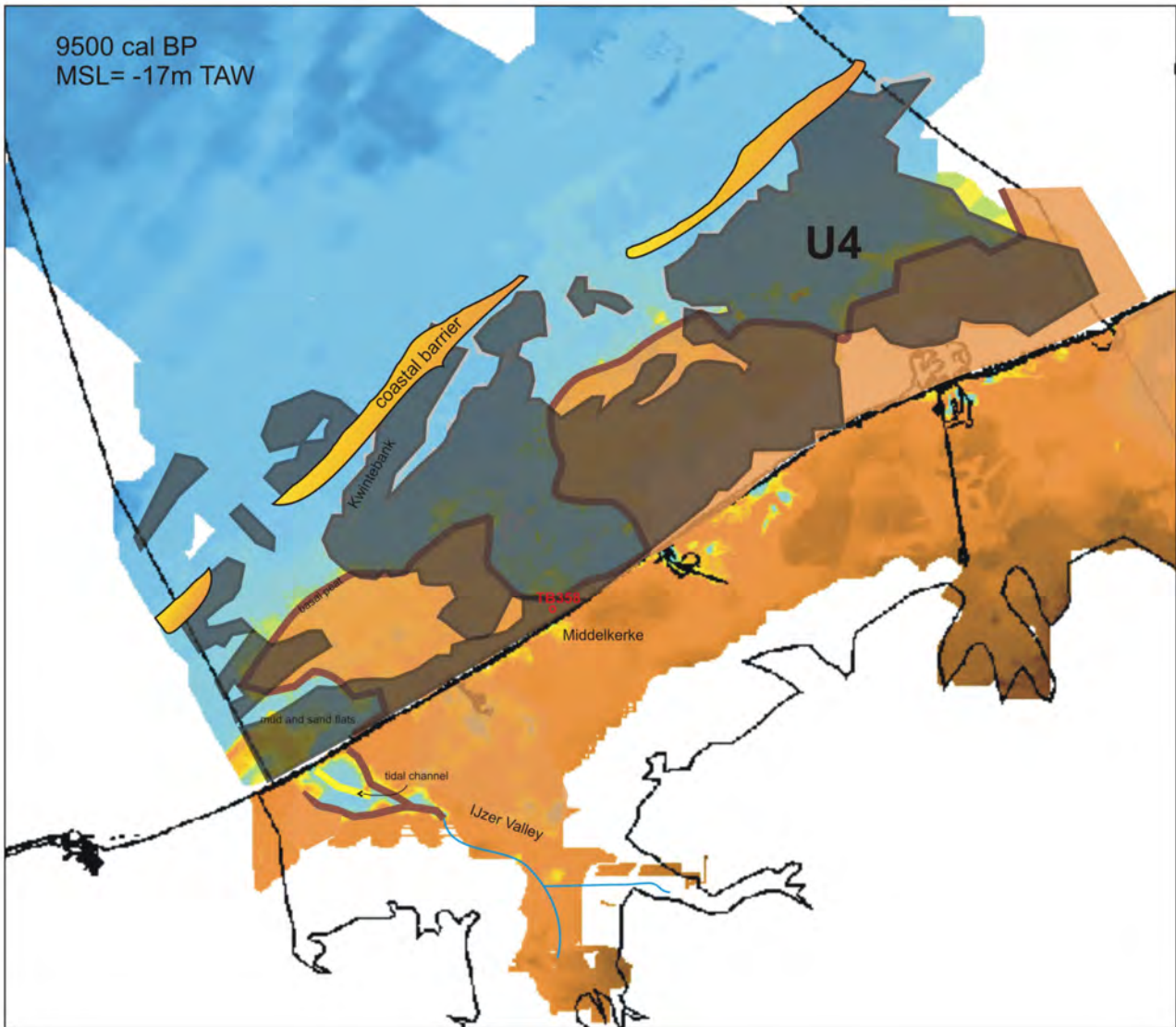


Figure 60 – Belgian coastline around 9,500 cal BP.

From Mathys (2009), Fig. 7.39. Paleo-reconstruction of the situation around 9500 cal BP, when coastal barriers started to form in the Southern Bight. Mean sea level at that time was about -17 m MLLWS. The first deposits formed behind the barrier (at a depth of -19 m) are located below the Kwintebank. So when the initial barrier developed, it was located (at least) 15 km off the present-day coastline. The isolated patches of U4 below the Oostdyck and Buiten Ratel have become at this stage drowned open tidal flats. The IJzer paleo-channels have been flooded since 9500 cal BP, but more to the east, offshore Middelkerke, the first evidence of flooding is probably around 8700 cal BP, which is evidenced from the presence of basal peat at a depth of -12 m in borehole TB358 (indicating a MSL of about -14 m). A fringe of basal peat (brown line) borders the tidal flats (in blue, distinction between mud and sand flats not specified here). Orange to brown area is land. The orange transparent overlay represents the presumed Pleistocene surface located higher than presently preserved. The transparent dark grey area represents the position of seismic unit U4.

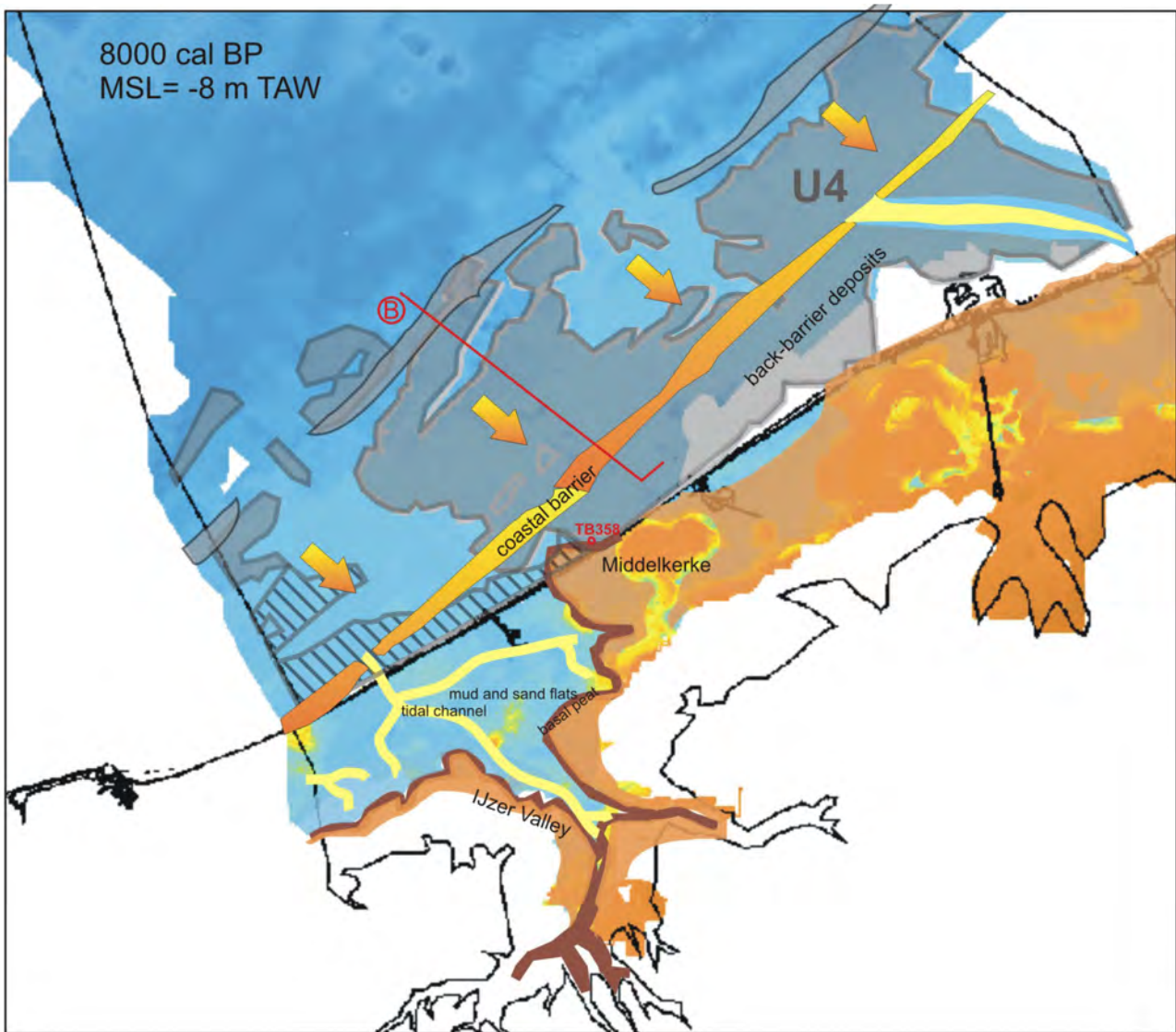


Figure 61 – Belgian coastline around 8,000 cal BP.

From Mathys (2009), Fig. 7.40A. Paleo-reconstruction of the situation around 8000 cal BP, when the coastal barrier reached the present-day coastline in the west for the first time. Mean sea level at that time was about -8 m MLLWS. Seaward of the barrier, former tidal flats have been eroded (in the west, they are even completely removed); landward of the barrier, the tidal environment is still developing. A fringe of basal peat (brown line) borders the tidal flats (in blue, distinction between mud and sand flats not specified here). Orange area is land. The orange transparent overlay represents the presumed Pleistocene surface located higher than presently preserved. The transparent grey area represents the position of seismic unit U4, the hatched areas are no longer interpreted as U4. The situation in the Western Coastal Plain is adapted after Baeteman (2005). In yellow, some reconstructed tidal channels.

### Barrier stabilisation and progradation

From 7500 BP the rate of sea-level rise decreased. Mean sea level was about -5 to -4 m MLLWS. Under equal sediment supply, the back-barrier basins silted up, allowing the barriers to first stabilize and then prograde seawards (Figure 62).

In the western Coastal Plain, the barrier started to prograde around 6800 cal BP. Mean sea level was about 1 m lower than today. Some tidal inlets, of which depositional evidence is found, pierced the barrier and extended seaward with its progradation. Since 5500 cal BP, this barrier had prograded seawards of the present-day coast. East of Nieuwpoort, the barrier still was more seaward than the modern coastline, as no remnants are found in the coastal plain, while seismic unit U5 is interpreted to contain tidal channel deposits, reworked ebb-tidal delta deposits and back-barrier coastal plain deposits (Figure 63).

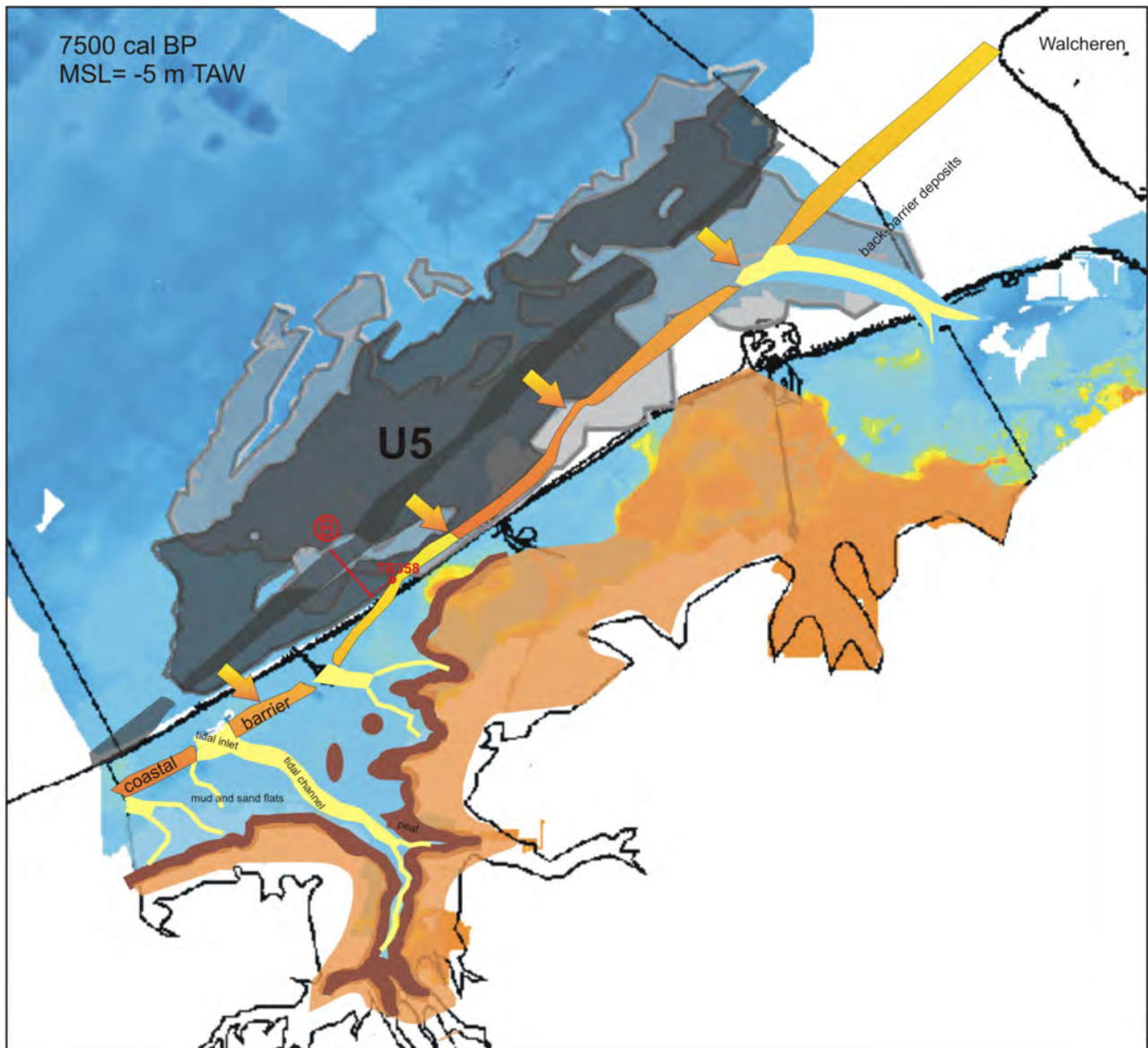


Figure 62 – Belgian coastline around 7500 cal BP.

From Mathys (2009), Fig. 7.41A. Paleo-reconstruction of the situation around 7500 cal BP, when the relative sea-level rise decreased, resulting in a sand surplus and consequently in the upsilting of the back-barrier tidal basins and the onset of stabilisation of the coastal barrier. The transparent grey areas represents the position of seismic units U4 and U5.

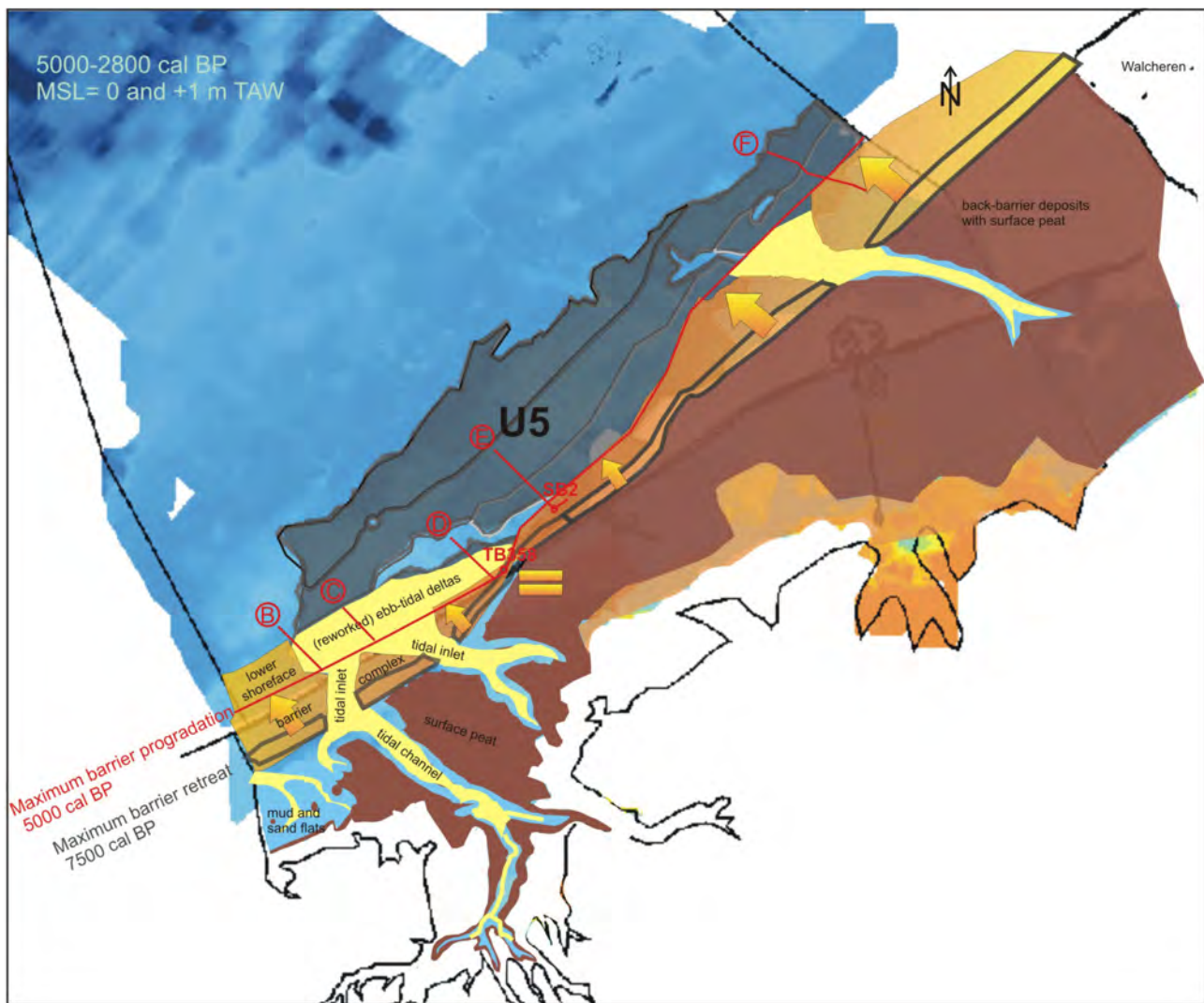


Figure 63 – Belgian coastline between 5000 and 2800 cal BP.

From Mathys (2009), Fig. 7.43A. Paleo-reconstruction of the situation between 5000 and 2800 cal BP, when the coastal barrier reached its maximal seaward extent since it started prograding around 6800 cal BP, and before a second barrier retreat set in. Mean sea level in that period rose from 0 m to +1 m MLLWS. The transparent grey area offshore represents the position of seismic units U5. The position of the coastline is reconstructed based on the height and the erosional character of the surface of seismic unit U5.

### Formation of storm-generated sand ridges

Either during stabilisation or retreat of the coastal barriers, sand ridges developed with sand sourced from ebb tidal deltas or transgressive shelf sand, i.e. the debris of shoreface erosion after barrier passage. This involved scour and down-cutting in the troughs between the ridges, eroding the underlying deposits of U4, with simultaneous aggradation of the ridge crests. The sand ridges are locally erosional rather than constructional responses to the hydraulic regime, as is clear from the coarse-grained shell lag at the base of U5, and the sometimes deep imprints of U5 in U4.

Seismic unit U5 shows remnants of three ridges in the direction perpendicular to the coast (Figure 64). Around 7700 cal BP, when the outer bank stopped developing, the coastline was already located about 6 km landward from the bank, and around 7000 cal BP the coastline was located 2 – 4 km from the middle bank.

Most likely, the start of the bank development began much earlier, when the presumed coastline was closer to the position of the outer and middle ridges. This could have been at around 8400 cal BP for the outer ridge, and at around 8000 cal BP for the middle ridge, based on the position of the reconstructed coastlines of 9500 and 8000 cal BP. These are, of course, rather rough estimations. Most likely, the development continued until the barrier prograded over the central and western nearshore sand ridge.

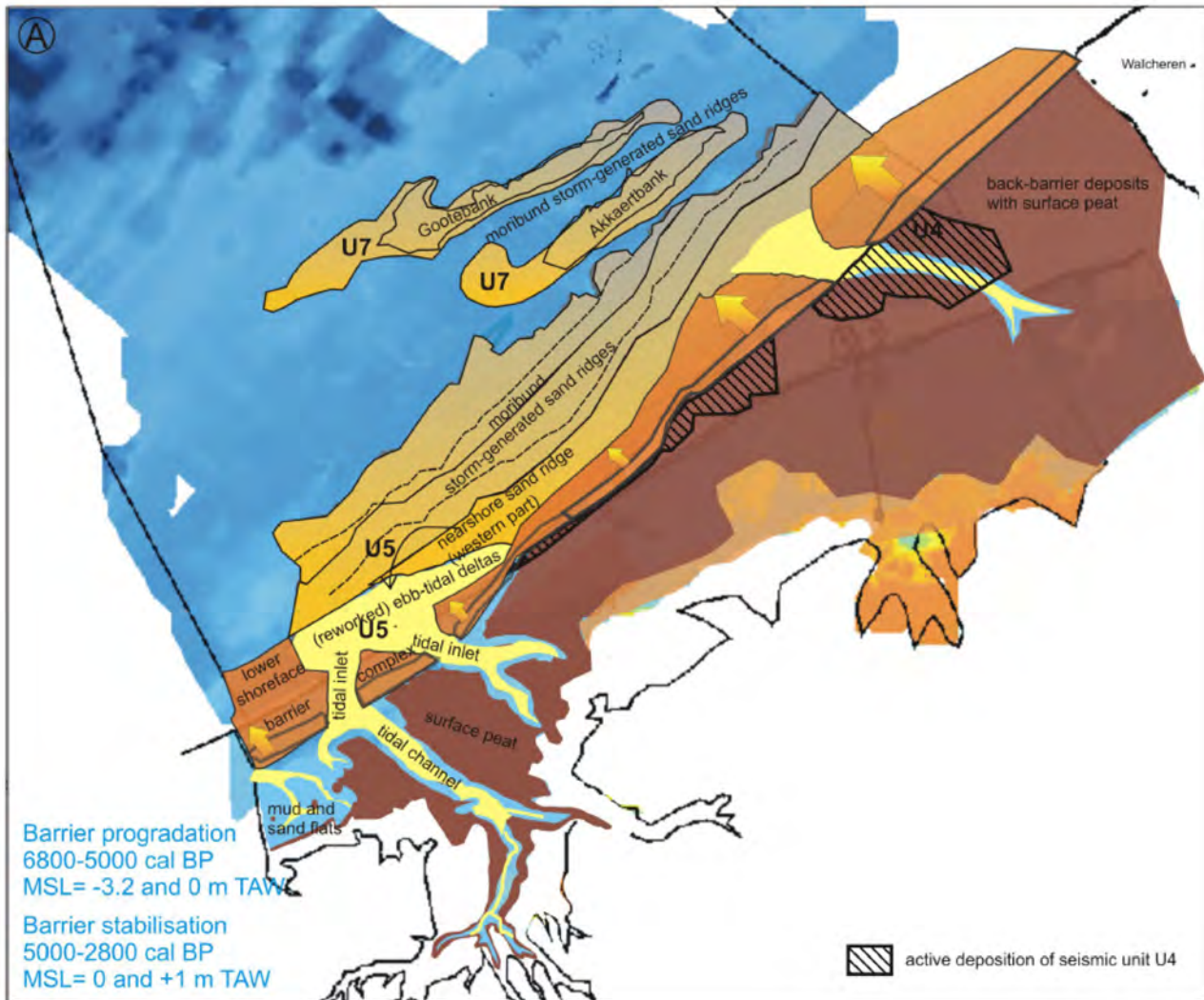


Figure 64 – Paleogeographic reconstruction of the Belgian shelf between 5000 and 2800 cal BP.

From Mathys (2009), Fig. 9.8A. Paleo-reconstruction of the situation between 5000 and 2800 cal BP, when the coastal barrier reached its maximal seaward extent since it started prograding around 6800 cal BP, and before a second barrier retreat set in. Offshore storm-generated sandridges are formed. Mean sea level in that period rose from 0 m to +1 m MLLWS.

### Barrier retreat before 1300 AD

Re-entrance of the tidal system was probably induced by the cleaning of older channels due to increased rainfall and excessive run-off from the continent, related to a climatic change around 2800 cal BP, and human activity. Due to compaction of the peat and collapse of the channel banks, a lowering of the ground level occurred, which induced oxidation and compaction to take place on a large scale. This generated an increase of the tidal prism of the tidal channels and, consequently, deep vertical incision. The renewed tidal action of the inlets gave rise to sediment demand, as a consequence of which the coastal barrier eroded. This resulted in a landward migration of the coastline (barrier retreat) and erosion of the tidal flats in the present-day offshore area. It was not until 1400-1200 cal BP (550-750 AD) that sediment supply and tidal prism reached an equilibrium with the sea-level rise in the western Coastal Plain. The newly formed channels came in intertidal position (infilling phase), and the major part of the plain evolved again into a supra-tidal environment. By 1000 cal BP (900-1000 AD), most of the tidal-flat areas between the channels were silted up to high-tide level and people started to build dikes to protect the newly formed salt marshes.

Most likely the back-barriers in the central and eastern Coastal Plain (including the present-day offshore parts) started evolving in a similar way and with a comparable timing as in the western Coastal Plain, since the driving force for the barrier retreat was of climatic origin and can therefore be supposed to have had a regional impact. The exact timing of the further development, however, depended on the timing, the degree and the extension of the collapse of the surface peat, which in turn depended on the incision of tidal channels and peat digging during the Roman occupation. These two controlling factors were not identical over the entire plain. Another factor that generated a spatial variability along the coastline might have been the position and sand transfer function of shoreface-connected ridges. At the locations where the ridges connected to the coastline a sand supply from offshore towards the coastline might have caused local progradation or have slowed down retreat.

In the area of Zeeland it is known that the time range for the renewed installation of the tidal environment is comparable to the one in the western Coastal Plain (2400 cal BP – 450 AD). The marine influence increased there locally around 2550 cal BP, and the peat areas on Walcheren and Zeeuws-Vlaanderen were flooded by the sea shortly after 300 AD, as indicated by the Middle Roman finds on the peat. Also the moment when the tidal channels came in intertidal position again (around 1200 cal BP or 750 AD in the western Coastal Plain) is the same in Zeeland. There, channels started silting up around 750 AD, a process which ended in the 9<sup>th</sup> and 10<sup>th</sup> century, similar as in the western Coastal Plain.

### Barrier retreat in the eastern Coastal Plain after 1300 AD

Where coastline shifts were initially of the same order regardless of the part of the coast, much more land was lost in the eastern part during historic time. The vast expanse of low-lying hinterland with peat in Zeeland is the ultimate reason for the development of deep and long tidal inlets, of which the Western Scheldt remains the most important. Seismic unit U6 is interpreted as the deposit of eroded mud flats in sheltered swales between storm-dominated ridges and the coast (Figure 65).

The further coastal retreat in the eastern Coastal Plain is believed to be human induced. In Flanders due to degradation of the dune areas since the 12<sup>th</sup> century (urbanisation, deforestation, conversion to farmland), construction of harbours, etc. (Augustijn (1995) in Mathys, 2009); and in Zeeuws-Vlaanderen due to mismanagement of dikes and embankments, present since the 11<sup>th</sup> century (Vos & van Heeringen (1997) in Mathys, 2009).

The actual Westerschelde originated in the early 12<sup>th</sup> century when during storm floods, a relatively small inlet, named Sincfal, got connected to a local river, named Honte, that drained eastwards into the Scheldt. Later inundations successively widened the inlet. Shipping traffic to Antwerp only started to use this route by the late 15<sup>th</sup> century.

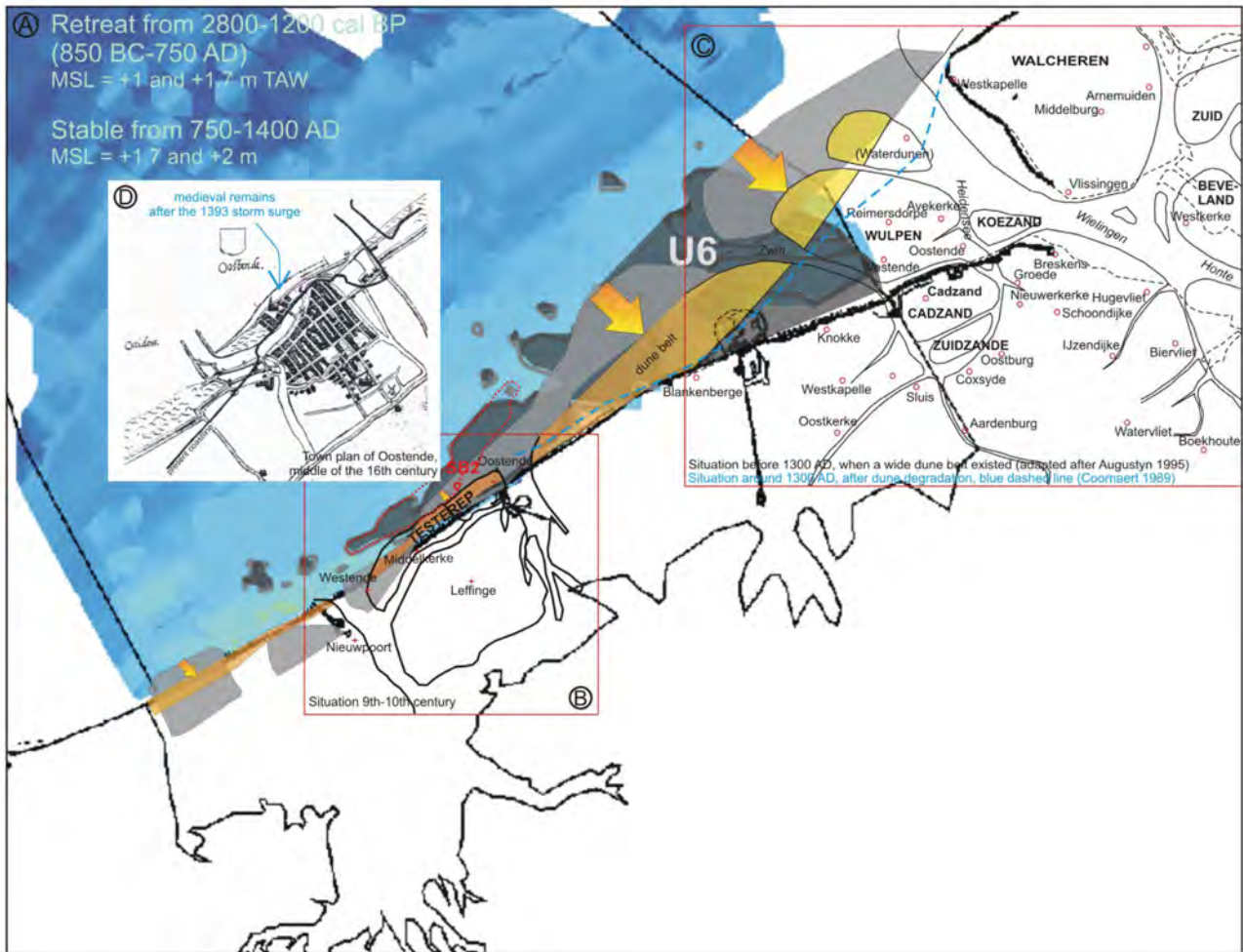


Figure 65 – Paleographic reconstruction of the Belgian coast between 2800 cal BP and 550 cal BP (1400 AD).

From Mathys (2009), Fig. 7.45 (A) Paleo-reconstruction of the situation between 2800 cal BP and 1400 AD. After 2000-3000 years of uninterrupted peat growth, a tidal system was again installed in the back-barrier area. Peat areas were transformed into sub- and intertidal flats and re-opened tidal channels incised vertically. The sediment needed to fill the deeply incised channels came from the early and mid-Holocene channels and the eroding shoreface. This resulted in a landward migration of the coastline (barrier retreat) and erosion of the tidal flats in the present-day offshore area. Around 1200 cal BP (750 AD), the back-barrier area had completely silted up again, and as almost no sediment was needed anymore for the further infilling of remaining tidal channels, the barrier retreat probably slowed down or even stopped. A wide dune belt formed in a gradual curve from Nieuwpoort to the western corner of the island Walcheren. Unit U6, which is for the major part located within the back-barrier area of 5000 cal BP, most likely represents remnants of the back-barrier deposits and surface peat of that time, which have been eroded during the natural barrier retreat since 2800 cal BP. And on the other hand, it represents remnants of newly silted-up areas since 1200 cal BP (750 AD), which have been eroded in the early 15<sup>th</sup> century by intense storm surges. (B) The situation in the Early Middle Ages (9th - 10th century) in the area of Oostende (<http://nl.wikipedia.org/wiki/Testerep>). The plain had silted up to high-tide level, except for a few tidal channels which remained open. In that period an 'island' surrounded by tidal channels, 'Testerep', was located near the present-day coastline on which the settlements of Westende (in the west), Oostende (in the east), and Middelkerke (in the middle) have been founded. The medieval town of Oostende remained located offshore the present-day coastline to at least the storm surge of 22 January 1394 AD, the St. Vincent Flood. (C) The map shows the situation in the east before 1300 AD, when the wide dune belt was still intact. The blue dashed line indicates the coastline around 1300 AD when the dune belt was largely degraded by human impact. Until eventually, in 1404, a north-westerly storm almost completely destroyed this chain of dunes. The large isle of Wulpen, situated off Cadzand, was engulfed by the sea, which resulted in irreversible hydrographic changes in the course of the Zwin and Westerschelde.

#### 4.1.2 Geology of the sand banks on the Belgian shelf

The following sections are almost fully based on the work of Mathys (2009).

##### Seismic unit U7

Seismic unit U7 makes up the top part of the most prominent features on the present-day seafloor: i.e. sandbanks and swales. Figure 66 shows the thickness of the U7 layer on the Belgian shelf (isopach map). In general the thickness of the U7 banks decreases in landward direction, and banks at similar distances from the shore have similar thicknesses (i.e. 12 m in the Kwintebank versus 14 m in the Akkaertbank and 21 m in the Oostdyck versus 18 m in the Thorntonbank). In the swales, the thickness of U7 ranges between 0 and 5 m. Probably most of the material of which the U7 banks are build up originates from local erosion of underlying sediments, what can be deduced from the often erosional character of the base of the banks and the presence of deeply incised swales in between. U7 in the Nieuwpoort Bank has a thickness of 12 m, U7 in the more landward located Stroombank has a maximum thickness of 10 m and U7 in the Wenduinebank is 7 m thick at most (Figure 66).

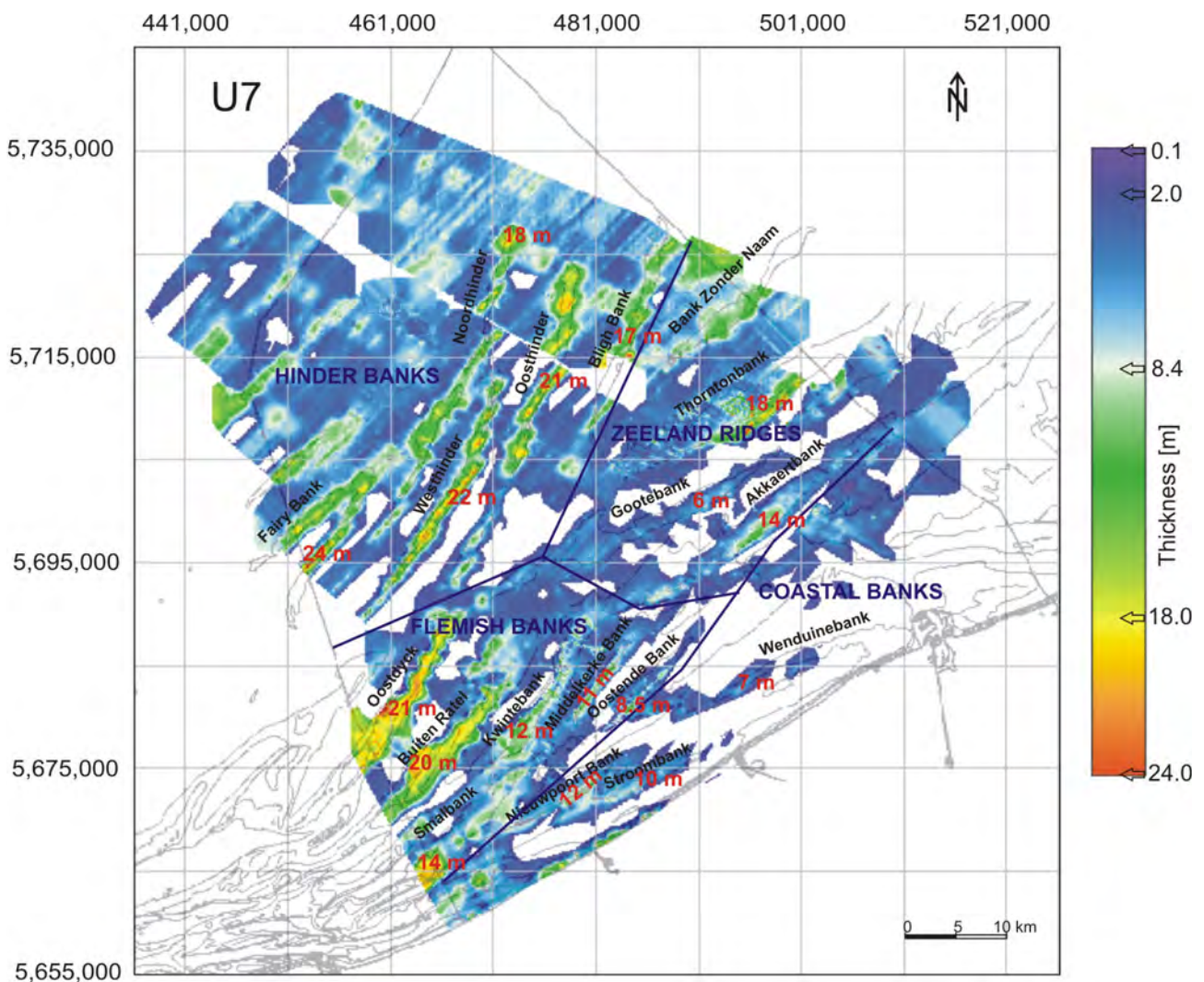


Figure 66 – Isopach map of seismic unit U7 (Mathys, 2009),

with indication of maximum thickness of each bank (number in red). In general, the thickness of the U7 banks decreases landward, and thickness of the U7 banks at similar distances from the shore have similar dimensions (12 m below the Kwintebank versus 14 m under the Akkaertbank, 21 m below the Oostdyck versus 18 m below the Thorntonbank). In the swales U7 ranges between 0 and 5 m.

The Coastal Banks occur close to the present-day coastline. The Wenduine Bank shows a clear connection to the shoreface on the bathymetric map. And also the Stroombank was connected to the present-day coastline before the digging of the harbour entrance of Oostende around 1900 AD. Only the Nieuwpoort Bank shows no direct link with the coastline. Shoreface-connected ridges can, however, become detached as the coast retreats to form fields of isolated ridges. At that stage, they are not connected to the coastline anymore, but they appear to retain the same characteristics and dynamics as the attached ones, although a reorientation can occur under the influence of the shelf hydraulic regime.

Nieuwpoort Bank, Stroombank and Wenduinebank, all consist of type-A cross-sections, meaning the banks *sensu lato* consist completely of the tidal sandbank U7 overlying a core of U5 sand ridges or of U6 deposits. The features of the U7 bank structures in the Coastal Banks closely resemble the characteristics of (active) shoreface-connected ridges, or of storm-generated ridges, in more general terms. The lithology of U7 in the Coastal Banks is in agreement with that expected in shoreface-connected ridges, which are generally coarsest in the landward through and become finer up the landward flank to the crest, where they are well sorted, and down the seaward flank where they become increasingly fine.

Although in the past the directions of asymmetric profiles of sandbanks have been used to define the large scale sediment transport pattern for the Southern Bight of the North Sea (Kenyon *et al.*, 1981), many arguments exist to prove that in fact the steep slope can be considered as an erosional surface and is merely created by the stronger tidal current along that flank (Houthuys, 1989; Van Lancker, 1999; Deleu, 2001; Lanckneus *et al.*, 2001). This is contradicted however with the observed landward movement of the Coastal Banks (see Houthuys *et al.*, 2021 and §4.2.1) and the sediment transport paths modelled within the first year of the MOZES-project (see §3.4).

### Time frame for the formation of the sandbanks on the Belgian shelf

Around 9500 cal BP, already all of the Hinder Banks, the Thorntonbank, Gootebank, Oostdyck and Buiten Ratel would have been located offshore the coastline of that time (Figure 67). Before that period, the sea invaded the Southern Bight rather fast, possibly leaving not much time for the formation of shoreface-attached ridges at the fast landward migrating coastline. Tidal regime was also microtidal, with negligible wind action, so there was little chance for the formation of these banks before that time. From 9500 cal BP onward, wave action was strong enough for the formation of a barrier, so also shoreface-connected ridges might have started forming. Around 8900 cal BP, also the Akkaertbank and Kwintebank would have been located offshore the coastline of that time. And by 8000 cal BP, the coastline had already migrated landward of the position of all of the present sandbanks, except for the Coastal Banks (Figure 67).

On the basis of their dimensions and morphology, the Akkaert and Gootebank have been interpreted as moribund shoreface-connected ridges or storm-generated ridges, which became detached when the coastline retreated. If their position stayed more or less the same while the shoreline receded, the Gootebank could have started to develop around 9500 cal BP when the shoreline was located in that region, and the Akkaertbank started developing around 8900 cal BP when the coastline had already retreated further landward. As the Akkaertbank lies more or less in line with the U5 outer ridge (Figure 67), the Akkaert and Gootebank might belong to the same group as the U5 storm-generated ridges.

The Middelkerke Bank, Oostende Bank, and Smalbank are located on top of the U5 outer and middle storm-generated ridges which have an age of 8400-7700 and 8000-7000 cal BP respectively, hence these banks could only have formed after that time. Therefore, it is most likely that the tidal sandbanks of the Flemish and Hinder Banks started to develop around 7000 cal BP, at a time when the tidal regime reached the present-day macrotidal range. This period was also characterised by a change in the net-sand transport pattern: before 7000 cal BP the sediment transport was mainly directed shoreward, while from that period on the tidal wave and related transport became alongshore (van der Molen and van Dijk, 2000).

This might explain the difference in orientation between the Zeeland Ridges which are more or less oriented coast-parallel and which were formed when the sediment transport was shoreward directed, while the Flemish Banks and Hinder Banks are oriented at an angle with the present-day coastline, and make a small oblique angle with the prevailing peak tidal flow direction (which is NE-ward in the near-coastal zone, and SW-ward along the Hinder Banks) (Lanckneus *et al.*, 2001), which is characteristically for a tidal sandbank (0-20° but mostly 7-15° in: Kenyon *et al.* 1981, Belderson 1986, Dyer and Huntley 1999). The Thorntonbank which lies parallel to the Goote and Akkaertbank, but which is clearly a tidal sandbank and not a storm-generated ridge, might have started to form when the sediment transport was still directed onshore, but when tidal currents were already strong enough to form tidal sandbanks in the deeper offshore areas (shortly before 7000 cal BP?).

The Coastal Banks have only formed in a final phase, on top of U6. So after a hydrodynamic equilibrium was reached following the widening of the Western Scheldt and the settling of the U6 sediments; meaning after the 16<sup>th</sup> century.

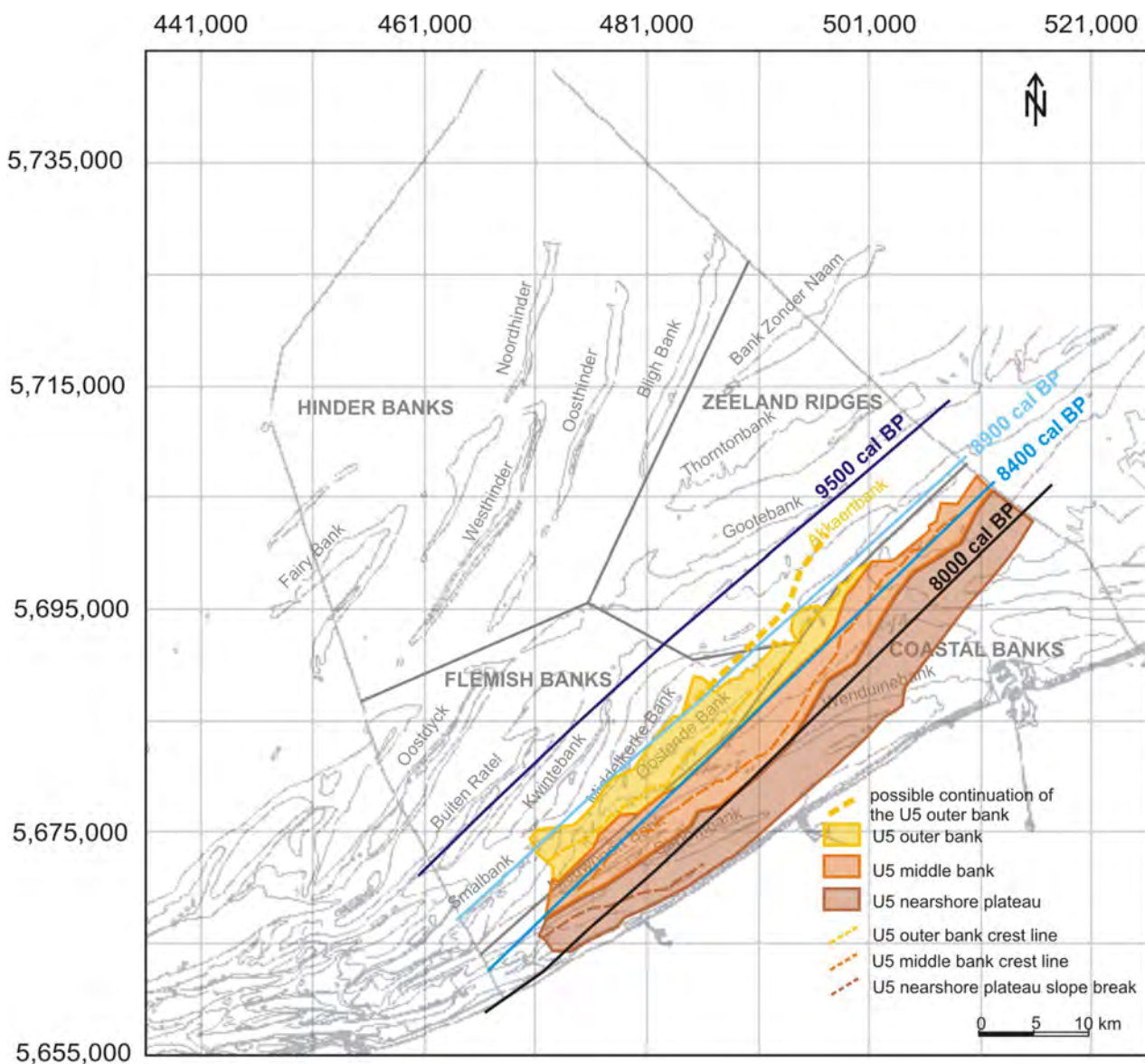


Figure 67 – Position of the sandbanks with respect to former coastlines.

From Mathys (2009), Fig. 8.20 Position of the sandbanks with respect to former coastlines. Note how the Akkaertbank lies in line with the U5 outer sand ridge. On the basis of their dimensions and morphological characteristics, the Gootebank and Akkaertbank are storm-dominated or former shoreface-connected ridges, and most likely belonged to the U5 sand ridge sequence.

#### 4.1.3 Evolution of the Coastal Banks and nearshore tidal gullies since the 16<sup>th</sup> century

Houthuys *et al.* (2021) studied a large set of scanned maps and bathymetric charts, dating back as far as the 16<sup>th</sup> century. They describe the occurrence and analyse the morphologic changes of the Coastal Banks, which is copied in full here below, with some additions of figures from Janssens *et al.* (2012) and Houthuys *et al.* (2022).

##### Trapegeer – Broersbank and Potje gully

The historic charts display several shallow banks near the coast between Dunkerque and Oostduinkerke. Often four banks are shown in a row, of which the westernmost was called "Brak Bank" or "Braeck Bank", the next one "Hills" or "Hiles", the following one "De Kams" or "De Cams" or "Cams Bank", while the easternmost was named "Broers Bank". The shallow sandbanks migrate to the east and show shape changes through time. Early on (or already at the time of the first charts?), "Braeck Bank" and "Hills Bank" were merged to one long coast-parallel ridge. A narrow channel named "Zuydcoote Pas" separated it from "De Kams", that on more recent maps, was named "Trapegeer". Beautemps-Beaupré (1800) used "Trapegeer" to cover all the shallow banks between the "Passe de Zuidcoote" and Nieuwpoort. Only a part of it, then situated 3 km off the coast at Oostduinkerke, was named "Broers banck".

"Broers Bank" is shown on early 17<sup>th</sup> century maps, e.g. Blaeu's 1635 map and Jansonius' 1666 map. The name refers to the Dune Abbey (Broers = Broeders = monks). The sandbank was further offshore than today. On van Keulen's 1680 map, a 4 (fathom?) deep channel separates it from the beach. It migrated shoreward and somewhat to SW during the 18<sup>th</sup> and 19<sup>th</sup> centuries and finally merged with the shallow shoreface "Den Oever". "De Kams", always shown as a complex shallow area, was around 1600 located at the present Belgian – French border and migrated eastwards. Its shallowest part was given the name of Broers Bank around 1900-1908 at the time when it had more or less occupied the position of the former Broers Bank that had merged with the shoreface (Desnerck *et al.*, 2007). Therefore, the present Broers Bank isn't the same as the 17<sup>th</sup> century's one, but it is at the same location along the coast, though closer to it than the older version.

Since around 1620, the shallowest parts of De Kams moved 8 km eastward, which yields a migration rate of 20 m/year. Since the more accurate 1866 Stessels map, the shallowest parts of Trapegeer and the tip of the Potje channel shifted about 3 km eastward (Figure 68). This shift corresponds to an about 20 m yearly migration rate, a figure still found in today's accurate coastal morphological monitoring (Houthuys *et al.*, 2022) (Figure 69). It can be concluded that the eastward migration was at a stable rate during the last 400 years and probably also before.

Some 17<sup>th</sup> and 18<sup>th</sup> century maps display a triangular westward protrusion of the coast at Lombardsijde. The 1800 Beautemps-Beaupré chart suggests it can be considered as the eastern tip of the Trapegeer Bank, there connecting to the shore. This shallow area disappeared during the 19<sup>th</sup> century. It appears to have moved westward, though more charts would have to be involved in order to be sure of this movement. It tallies with the movement of the former Broers Bank to the SW (from N of Oostduinkerke in the direction of the beach between Koksijde and Oostduinkerke) during the 19<sup>th</sup> century.

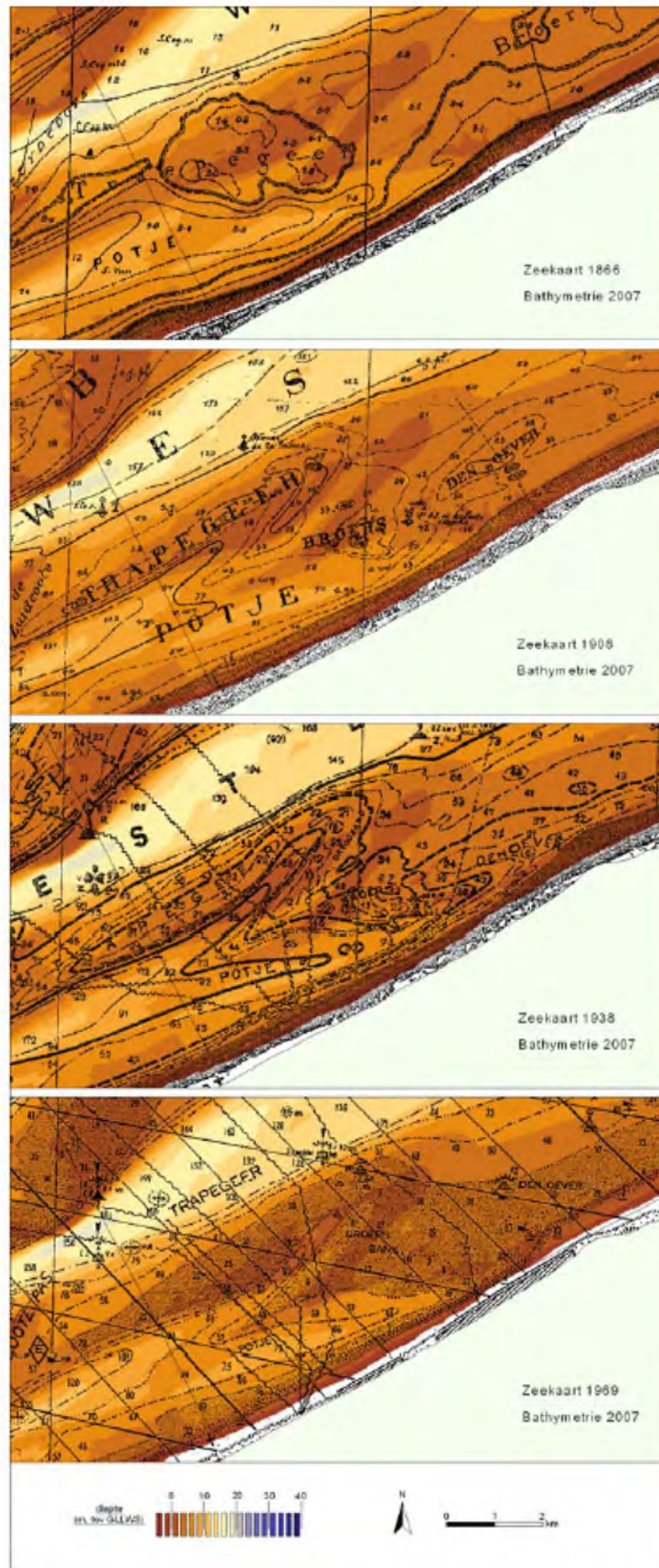


Figure 68 – Georeferenced bathymetric charts dating from 1866, 1908, 1938 en 1969 in the Potje gully – Trapegeer area. The colormap shows the 2007 bathymetry (Janssens et al., 2012).

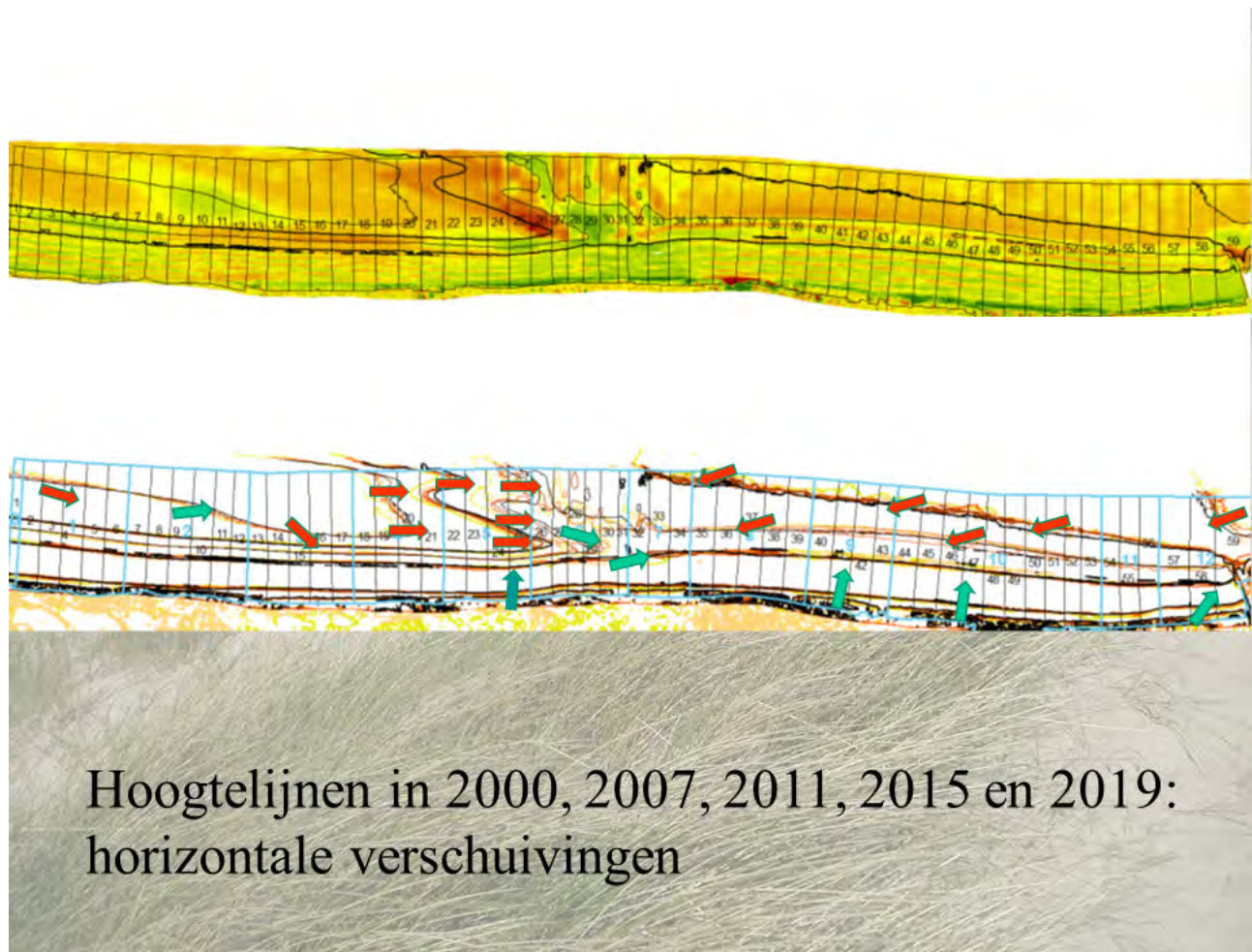


Figure 69 – Morphologic evolution of the Potje gully and Den Oever shoreface-connected sand ridge.

Upper panel – change in bathymetry between 2019 en 2000: red areas have deepened, green areas become more shallow. Lower panel – evolution of the isobaths between 2000 tot 2019. (Houthuys et al., 2022.)

### Stroombank and Kleine Rede gully

The 20 km long Stroombank gradually approaches the coast from Westende (at 4 km distance to the seawall) to the area of Bredene – De Haan, where it attaches to the shoreface. The bank was named "Geere" on 17<sup>th</sup> and 18<sup>th</sup> century charts (Devos *et al.*, 2014). Only around 1800, the name Stroombank, that also was used for other sandbanks, was attributed to this particular bank. The bank was both a blessing and a curse for Oostende: it protected the city from high waves, but hindered shipping and was a source for sand that continuously tended to smother the harbour (Devos *et al.*, 2014). Around 1880, dredging ships were efficient enough to clear the harbour entrance and to dredge a navigation channel across the Stroombank, called "Rechtstreekse Kil". Also around that time, another channel was dredged near Klemskerke to separate the sandbank from the shoreface. This was done to allow the tidal currents to sweep the area in front of Oostende harbour so that it wouldn't sand up (Devos *et al.*, 2014). Around 1880, even a plan was made to construct a breakwater on the southern edge of the Stroombank, so as to fix it. This plan was no longer needed as dredgers succeeded in keeping the shipping channel free.

The Stroombank moved both eastwards and landward through time. E.g., its western tip was situated off Nieuwpoort in 1776 and moved 3.5 km alongshore to the east and about 1 km shoreward to its present location. The eastern tip was probably near Oostende in the 17<sup>th</sup> century while it's attached to the shore just east of De Haan, almost 8 km more to the east, in 1866. The more recent behaviour was disrupted by the Oostende harbour dredging works.

Janssens *et al.* (2012) show eastwards and landwards movement of the Stroombank and an eastwards movement of the Kleine Rede gully since 1866 (Figure 70). The same pattern, as well as deepening of the Grote Rede, has been observed by Houthuys *et al.* (2022) for more recent times (Figure 71).

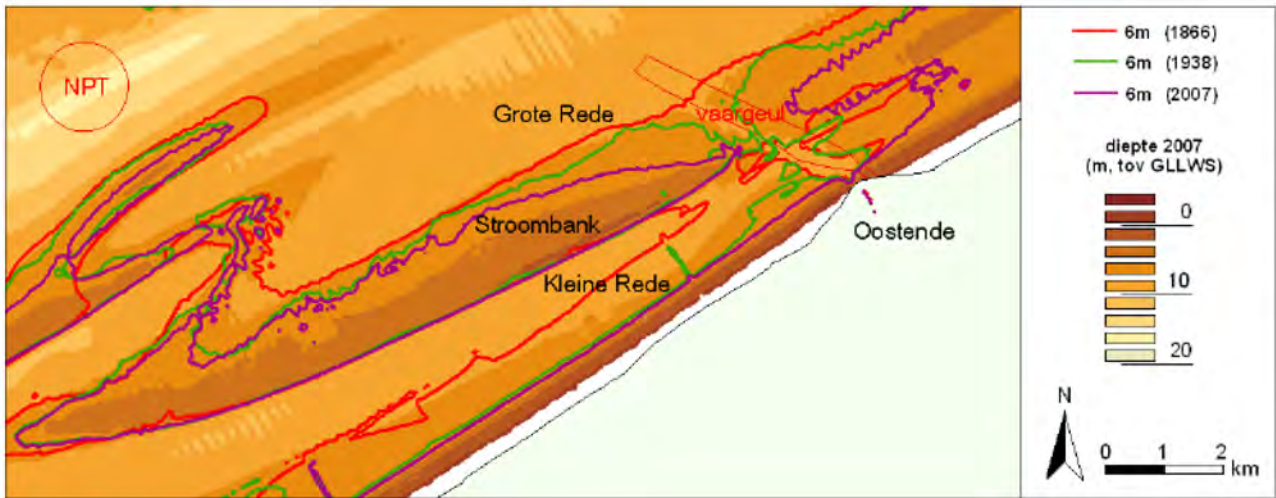


Figure 70 – Evolution of the Kleine Rede (gully) and Stroombank.

The 6 m-isobaths of the years 1866, 1938 en 2007 are shown. The colormap shows the 2007 bathymetry. A landward movement of the sand ridge as well as a NE-wards movement of the SW-tip of the bank can be observed. The NE-tip of the Kleine Rede gully migrated NE-wards. (Janssens *et al.*, 2012).

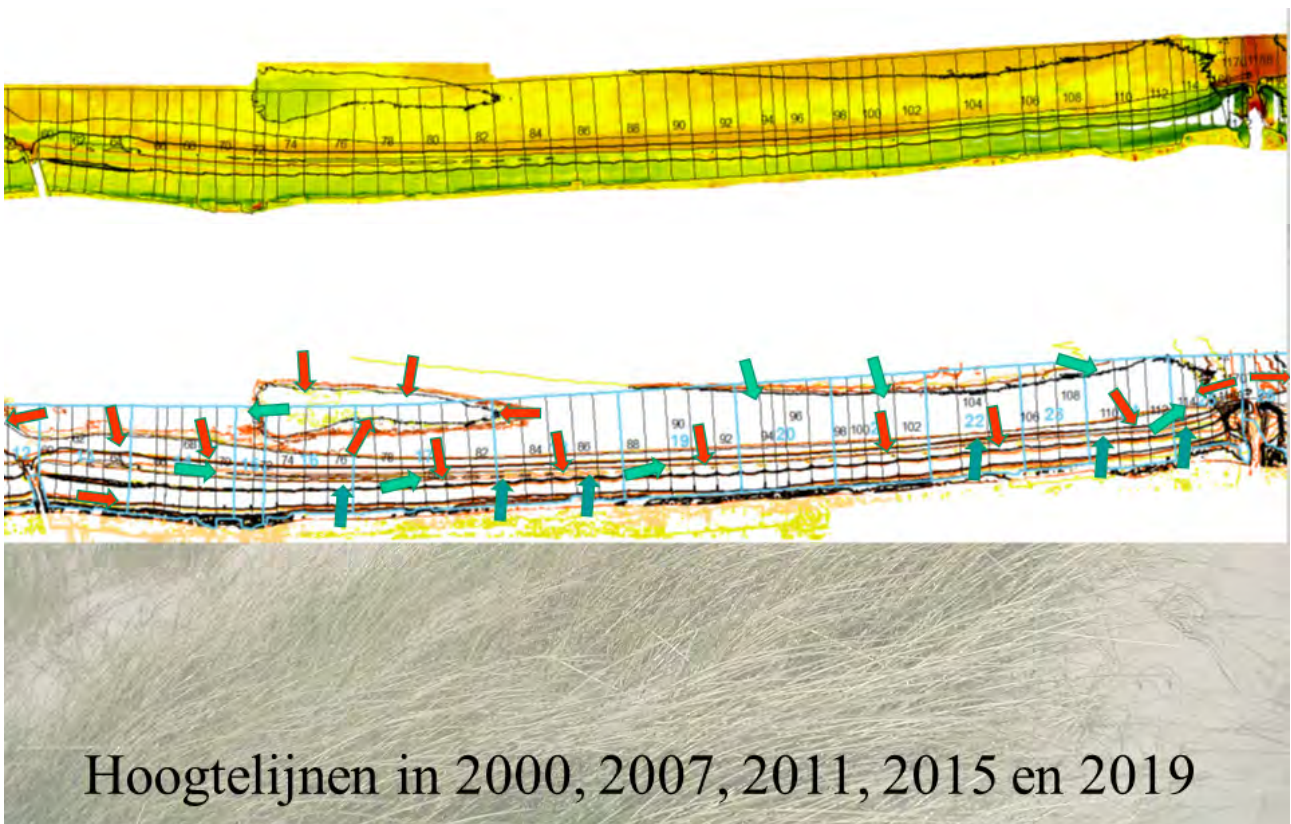


Figure 71 – Morphologic evolution of the Kleine Rede gully and Stroombank sand ridge.

Upper panel – change in bathymetry between 2019 en 2000: red areas have deepened, green areas become more shallow.  
 Lower panel – evolution of the isobaths between 2000 tot 2019. (Houthuys *et al.*, 2022.)

### Grote Rede gully, Wenduine Bank and Bol van Heist

Between Oostende and Wenduine, a long sandbank existed on some 16<sup>th</sup> century maps (Wib Sandt on the 1583 Waghenauer chart) and in the 17<sup>th</sup> century: the "Hard Zand" (Hardt Sandt, Hart Sant, ...). Like the other nearshore banks, it trended towards the coast. On the (trustworthy) Waghenauer chart, it continued eastward and touched the coast between Heist and the Zwin inlet; east of this, a prolongation was found, named "Wulpener Parde Merct". The situation is more or less similar on the 1639-1649 Hondius chart. The channel between "Hard Zand" and the coast was named "Binnen Sandt". Second half 17<sup>th</sup> century and first half 18<sup>th</sup> century charts show a wide shoreface – foreshore named "Schor van Blankenberge", which is no longer present on the around 1800 Beautemps-Beaupré map. Reference marks on the old charts are scarce; therefore the exact position of the "Hard Zand" is difficult to ascertain. Either it sat at the present Wenduine Bank position, or it sat in between the present Wenduine Bank and the shoreline. It is also possible that through time it migrated somewhat eastward keeping its western tip, originally near Oostende at some distance from the shore, at the same distance during its eastward journey.

A more offshore, long bank, of which the western tip near Oostende was named "Uit Bank" (Vytt Bank, Uytter Bank, Uitsandt, Wib Sandt, Wytter Bank, Witte Bank, Banc Blanc, ...), continued to east as De Ript ('t Ript Hart, Ript Hart Sant, De Rypt, Trix, Die Trijp, ...). De Ript was located some 2 km more offshore than the present Wenduine Bank. It gradually disappeared and seems to have moved eastward. It is named "Inner Bank" on the around 1800 Beautemps-Beaupré map and still smaller fragments are named "Banc de Heyst", "Banc de Knocke" and "Hompels" (Sluise Hompels) on the 1866 Stessels map. Today, remnants are still found in the Wandelaar, Ribzand and Bol van Heist.

Janssens *et al.* (2012) show an eastwards movement of the Grote Rede gully since 1866 (Figure 72). The Wenduine bank however seems to keep its offshore position, while its westernmost tip seems to be growing in western direction. Houthuys *et al.* (2022) observed a deepening of the Grote Rede for the whole area between Oostende and Blankenberge (Figure 71).

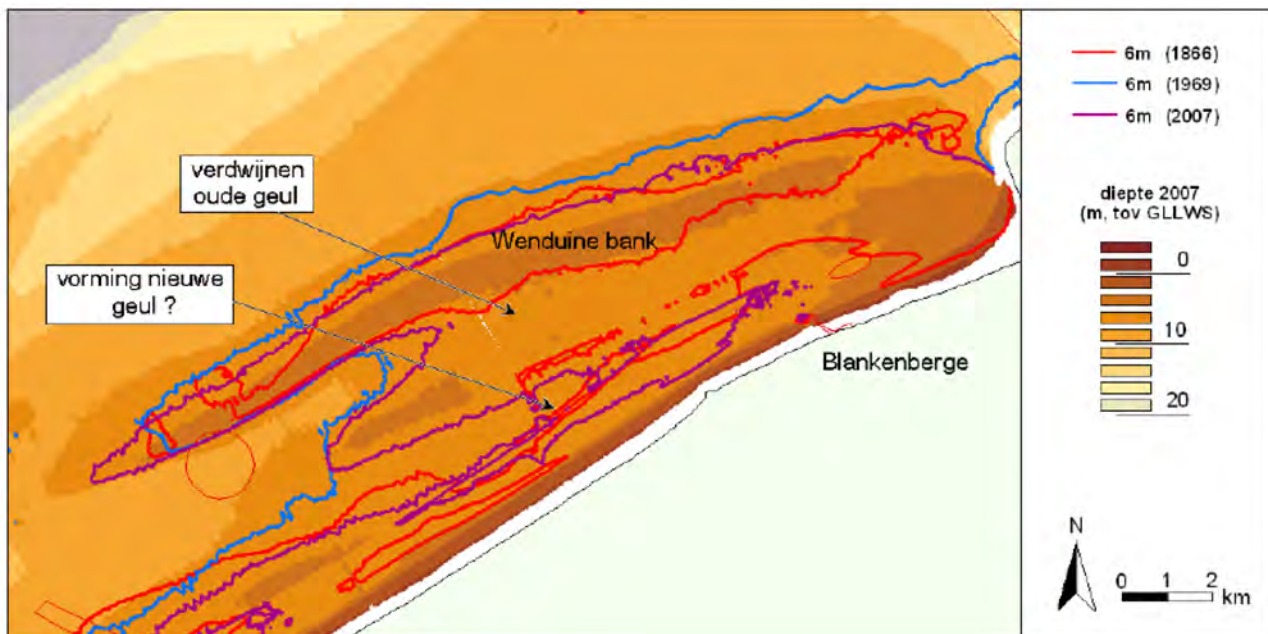


Figure 72 – Evolution of the Groote Rede (gully) and Stroombank.

The 6 m-isobaths of the years 1866, 1938 en 2007 are shown. The colormap shows the 2007 bathymetry (Janssens *et al.*, 2012).

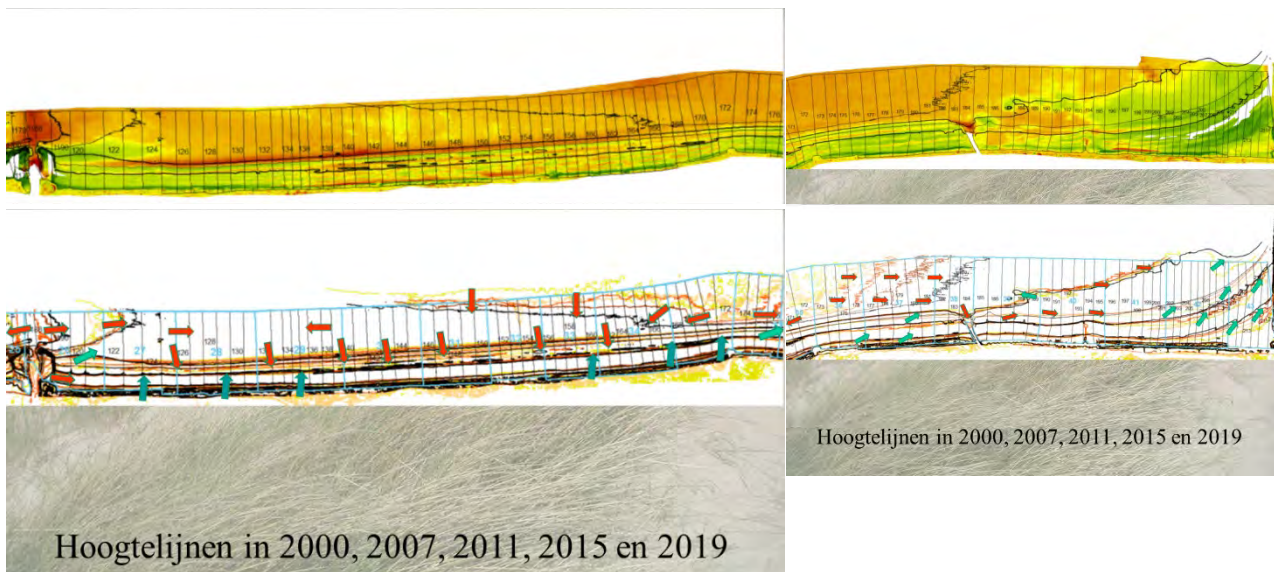


Figure 73 – Morphologic evolution of the Groote Rede gully between Oostende and Zeebrugge.

Left panels: Oostende – Wenduine; Right panels: Wenduine – Zeebrugge; Upper panels – change in bathymetry between 2019 en 2000: red areas have deepened, green areas become more shallow. Lower panels – evolution of the isobaths between 2000 tot 2019. (Houthuys *et al.*, 2022.)

### Paardenmarkt and Appelzak gully

The name of the sandbank refers to a horse trading area, possibly once located on the island of Wulpen, and in the 16<sup>th</sup> century a sand spit in the Zwin inlet mouth, connected to the beach at Cadzand (Desnerck *et al.*, 2005). Some 17<sup>th</sup> century maps connect it to the "Hard Zand" or Wenduine Bank. In 1660 (Visscher map), it was an isolated, large sand flat off Knokke and west of the Zwin mouth. In 1750 (de l'Isle map), it was again a long spit connected to the beach at Cadzand. Beautemps-Beaupré (1800) placed the name on part of the former "Hard Zand" from Blankenberge till Cadzand where the long sandbank still connected to the shoreface.

Around 1800, a northeastern branch of this bank extended towards the Westerschelde mouth and was situated at 3 km off the coast at Cadzand. This bank, also called "Paardenmarkt", moved steadily eastward, but disappeared gradually afterwards, probably in response to stronger tidal currents from the Western Scheldt (Van Cauwenberghe, 1966). The remaining, shallower part of the sandbank, then named "Binnen Paardenmarkt", was situated about 2.5 km off the beach at Zeebrugge, 2 km off Heist and only 1 km off Knokke. This sandbank was again simply called "Paardenmarkt" on Stessels' (1866) map. It was connected to the shore near Cadzand, making the channel "Appelzak" a closed trough-like depression between the sandbank and the shore. The channel extended from the vicinity of Blankenberge to Cadzand on the 1866 chart and was clearly a flood channel ("vloedschaar"), as shown by its funnel shape, while today it is an ebb channel ("ebschaar"). Probably, the morphological change occurred after the first mole was built at Zeebrugge around 1900. The Paardenmarkt connected to the shoreline at the east part of the beach at Cadzand. The connection to the shore moved 2 to 3 km eastwards between 1800 and 1925. After that, a channel junction appeared between Appelzak and Wielingen, thus severing the shoreface connection of the Paardenmarkt (Figure 74). The bank still exists, but lost sand at its northern flank (Van Cauwenberghe, 1966).

The bathymetric charts shown in Figure 74 illustrate that the Appelzak was gradually becoming more and more shallow (ca. 3 m between 1866 and 1986), while the crest of the Paardenmarkt deepened. Since the extension of the Zeebrugge harbour breakwaters however, the Appelzak channel is again deepening (ca. 0.5 m between 1986 and 2003). Houthuys *et al.* (2022) show a deepening of an extra 0.5 m in the Appelzak in recent times (2000 – 2019), and a shoreward migration of both the Paardenmarkt sand ridge and the channel (Figure 75).

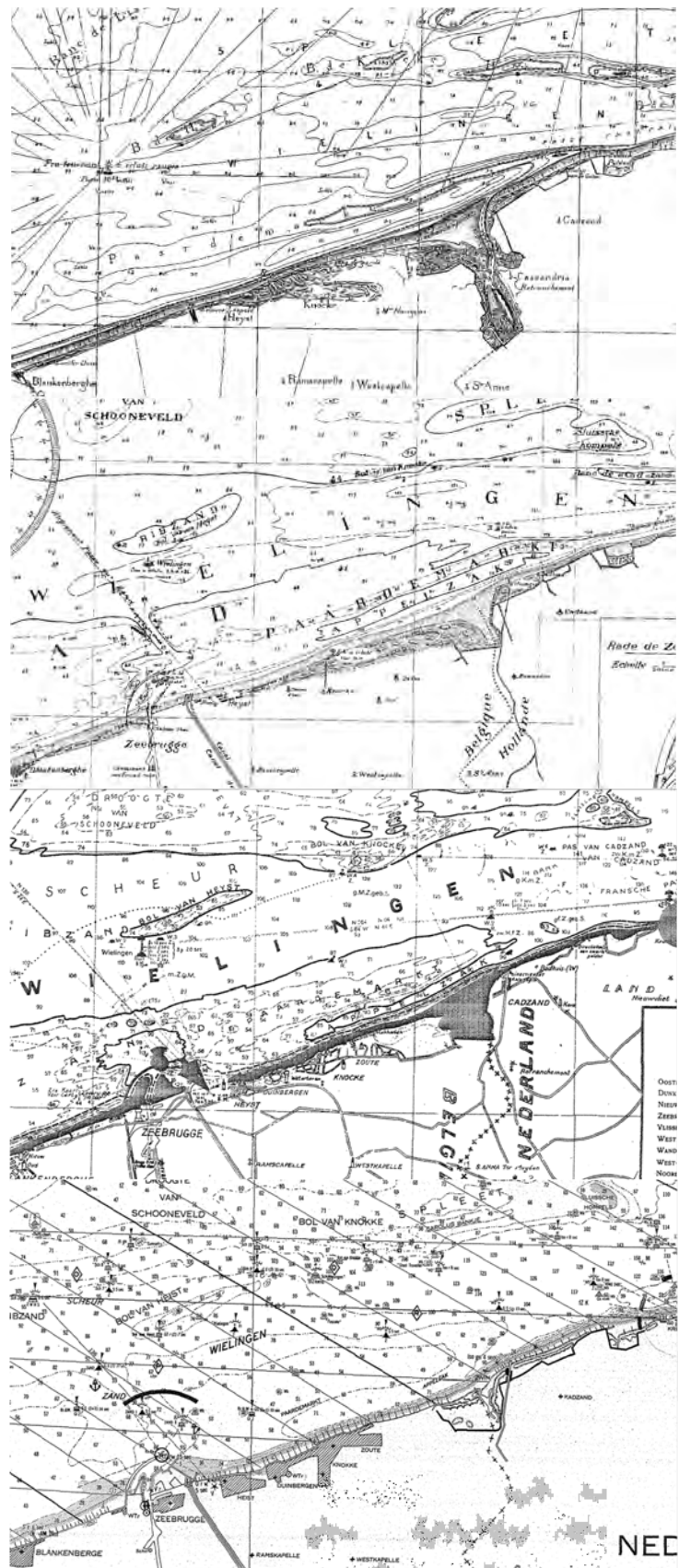


Figure 74 – Georeferenced bathymetric charts in the Paardenmarkt - Appelzak area.

The charts, dating (top to bottom) from 1866, 1908, 1938 and 1969, show the evolution for the Paardenmarkt from a shoreface-connected sand ridge (connecting to the shore near Cadzand) to a detached sand ridge after the building of the first breakwater of Zeebrugge (môle).

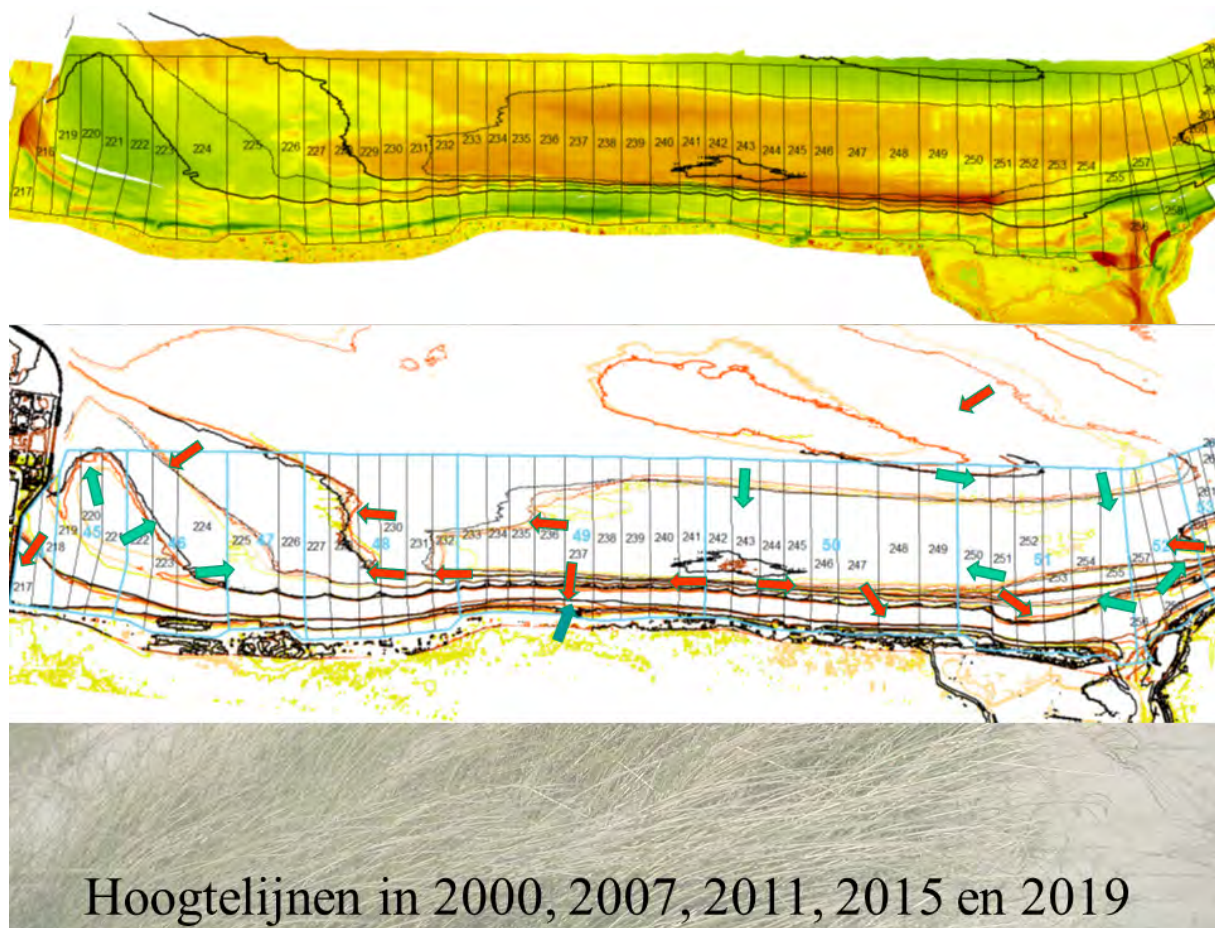


Figure 75 – Morphologic evolution of the Appelzak (gully) and Paardenmarkt sand ridge.  
 Upper panel – change in bathymetry between 2019 en 2000: red areas have deepened, green areas become more shallow.  
 Lower panel – evolution of the isobaths between 2000 tot 2019. (Houthuys *et al.*, 2022.)

#### 4.1.4 Summary

The described shallow nearshore sandbanks (Coastal Banks) all have an interior made up of sand. They may have originated from abandoned sand barrier coasts or ebb tidal deltas, remodelled by the currents and waves (Mathys, 2009). Ultimately the original sand source is river input to the exposed North Sea, mainly by Rhine and Meuse, during the Last Glaciation.

These banks seem to have migrated eastwards at a generalized, approximated rate of 1 to 2 km per century, and, at least locally, also shoreward, though at more reduced rates (Houthuys *et al.*, 2021). These morphological trends still exist today (Houthuys *et al.*, 2022).

## 4.2 Data analysis for the Belgian coast

Within this section, new work on already available data for the Belgian coastal zone is presented.

### 4.2.1 Large-scale morphological change of the inner shelf between 1984-87 and 2022

#### Introduction

This section describes the global morphological change between the 1984-1987-1986 survey and a recent survey composite (March 2022) of the inner part of the Belgian shelf. The description is carried out in relation to the well-documented change of the coastal and nearshore area, substantiated by volume time series per section since 1983/1992 and by map series since 2000 (Houthuys *et al.*, 2022). This section only compares the initial to the final bathymetry. Its observations will later be supplemented by earlier and intermediate surveys.

#### Method

The initial bathymetry is taken from the 1984, 1986 and 1987 bathymetric survey 1/20,000 map sheets map sheets of the Belgian inner shelf made by Coastal Division's Hydrographic Service. The inner shelf is defined here as the area covered by these maps, i.e. the nearshore area from the beach to 10/15 km offshore.

These paper maps are available as scanned images, with sufficient resolution to (mostly) clearly read the figures and texts in them. Use was made of the following maps: Sheet Zuydcoote – Westende, survey date March-June 1987; sheet Westende – De Haan, survey date March-May 1984; sheet Wielingen – Scheur, survey date April-August 1986. Together, they cover the Belgian inner shelf area. They have been digitized during the first year of the Mozes project. Digitization and DEM processing involved the following steps:

1. Georeferencing the scanned maps. Use was made of roughly every second coordinate cross of the UTM31 grids shown in the maps. The coordinates were converted to Belgian Lambert 1972 using cConvert version published by the NGI.
2. Vectorizing all depth points such as they are shown in the maps (i.e., depths in dm below GLLWS). The points are stored in a point shapefile. The depth value of each point is stored in an attribute.
3. Converting depths in dm to elevation in m.
4. Creating a TIN using all available depth points per map. The TIN was restricted to the data area using a manually drawn contour connecting the outer data points.
5. Interpolating a raster from the TIN with cell size 10 m.
6. Converting elevation in m GLLWS to elevation in m TAW using the conversion raster "gllws\_to\_taw\_vlaamsebanken\_172.tif" available on FH's GIS-server and has cell size 20 m. The latter is subtracted from the first, preserving the first raster's original cell size of 10 m. The result is the 1984/7 inner shelf raster in Lambert 72 and TAW.
7. Mosaicking the rasters of the three map sheets. The 1987 map overlapped the 1984 map: here, the 1987 values were preserved. Between the 1987 and 1986 map is a hiatus: this was filled using TIN interpolation between the outer data points of both maps.
8. This raster was displayed using 0.5 m elevation classes ranging from light blue near the beach over dark blue and purple at the depth of 12.5 m. Elevation contour lines were derived from the raster and a selection of the 0, -2, -4, -6, -8, -10 and -12 m contours was shown as full or dashed red lines on the map.

The final bathymetry was downloaded at a 10 m cell resolution on 9/09/2022 from <https://bathy.agentschapmdk.be/spatialfusionviewer/mapViewer/map.action>. The download is a Geotiff file in UTM31 and elevations in LAT; the depth values per cell are real depths at the nearest location of the cell.

The bathymetric map covers the complete Belgian continental shelf, i.e. also the inner shelf. However, it is restricted by the country boundaries. The map has the date of 2 March 2022. It is a mosaic of all most recent surveys. The area of the inner shelf in this mosaic consists of the most recent survey per survey area. DEM processing involved the following steps:

1. Projecting the map in GIS onto the Belgian Lambert 1972 coordinate system.
2. Converting elevation in m LAT to elevation in m TAW using a conversion raster with cell size 20 m made from "LATtoTAW\_VlaamseBanken\_v2.xyz " available on FH's GIS-server. The original cell size of 10 m was preserved. The result is the 2022 inner shelf raster in Lambert 72 and TAW.
3. This raster was displayed using 0.5 m elevation classes ranging from light blue near the beach over dark blue and purple at the depth of -12.5 m. Elevation contour lines were derived from the raster and a selection of the 0, -2, -4, -6, -8, -10 and -12 m contours was shown as full or dashed black lines on the map.

The change was studied in four cut-out zones together covering the Belgian inner shelf. They were selected from west to east with small overlaps. The easternmost zone could be shown at double scale (cfr. scale bar in each map). The change was displayed using different techniques:

1. By clicking back and forth, in a Powerpoint presentation, between the 1984/7 and 2022 bathymetric map of exactly the same cut out, shown in the same depth colours. This clearly reveals changes in bathymetry.
2. By displaying the selected 1984/7 and 2022 depth contours of each cut-out in one map, using red for the initial and black for the final situation. Thick arrows are added to highlight the most important contour line shifts. The arrows are coloured in red as the contour line shift represents bed erosion, in green as it represents bed accretion, and in pale blue as it represents a pure shift without overall depth change. It is remarked that the arrows merely show the direction of contour line movement between the initial and final map; they don't show sediment transport directions, although they in many particular locations they probably coincide with the long-term net sediment transport direction.
3. An elevation difference map was made by raster subtracting the final from the initial map. Negative values than represent erosion and are shown in classes of red, positive values represent accretion and are shown in classes of green. Change between -0.25 and +0.25 m is considered insignificant and is displayed in yellow. The thick arrows of contour line change are overlaid on this map.

Figure 76 shows the elevation difference map of the complete inner shelf area. It appears that erosion is the dominating change, although final morphological conclusions can only be made after an ongoing investigation will be completed to quantify the systematic difference between the two maps caused by differences in echosounding methodology and/or differences in used transformations from LAT/GLLWS to TAW and/or differences in x,y positioning at sea.

### **Caveat**

The overall depth change in the overlap area of the 1984/7 and the 2022 DEM is a depth increase of 0.32 m. This contrasts with an average 0.02 m depth decrease between 1866 and 1984/7. The depth increase over the last about 35 years would represent a very big loss of sediment of about  $0.32 \text{ m} \times 746.10^6 \text{ m}^2 = 239.10^6 \text{ m}^3$ . It is a huge amount of sediment erosion for which neither a straightforward explanation nor a clearly related destination area can be found.

In the past decades, substantial dredging has made the harbor entrance channels deeper and wider. However, if the dredging areas and disposal areas are left out of consideration, the overall depth change is still 0.27 m. So, the influence of these works is limited and can only explain 16% of the change.

A systematic bias in depth for the initial survey should thus be examined. The recent most survey dataset is taken to be more accurate, because of the generalized use of RTK dGPS systems yielding very precise positioning including satellite-based vertical positioning since the late 1990s. Aerial coverage has also improved considerably around 2007, as surveys have since then been conducted using MB. It is thought that the use of different sounding frequencies (33 or 200 kHz for SB systems and 200 or 400 kHz for MB systems) doesn't affect the depth measurement at least on sand, which is the main bed type in the area. There could be a small influence on bed morphology mapping of the gridding method. For classical navigation maps, MB point clouds are gridded using the minimum depth per grid cell. The mosaic raster on the bathymetric portal can be downloaded using a number of gridding methods; in this analysis, the real depth nearest to the cell centre was used.

The examination of the probably biased 1980s bed is proposed to be done in the second project year. The following topics would then be explored:

- depths determined using echosounding were recorded with respect to instantaneous still water level. Depths were converted to GLLWS manually or semi-automatically using their time stamp and a tidal reduction chart. The chart used in the 1980s was the 1972 Reduction chart. The correction raster `gllws_to_taw_vlaamsebanken_l72.tif`, used on the data set, is valid however for the 1990 Reduction chart. The influence of the transition from the 1972 to the 1990 Reduction chart will be examined.
- SB echosoundings result in closely spaced points on tracks that are often 100 or 200 m apart. The 1980s 1/20,000 maps show a selection of measured point, often one point every 20 to 30 m. The selection in this window picked out shallow points that were printed on their real position. As a result, a bed map based on these points tends to show a surface connecting all shallowest points. This may explain part of the shallow bias. This effect will be examined using a SB dataset where both the selected map points and all recorded points are available.

After addressing these points, it is hoped that a correction grid can be established and applied to the 1984/7 dataset. The following description of morphological change between 1984/7 and 2022 was based on the uncorrected 1984/7 dataset. The described features focus on regional, important elevation change, exceeding half a metre and sometimes several metres. The general trends are expected to remain valid, even if afterwards a depth correction will be applied. The description is subject to editing based on the results of the coming examinations mentioned here. And at this stage, it is too early to make sediment volume balances.

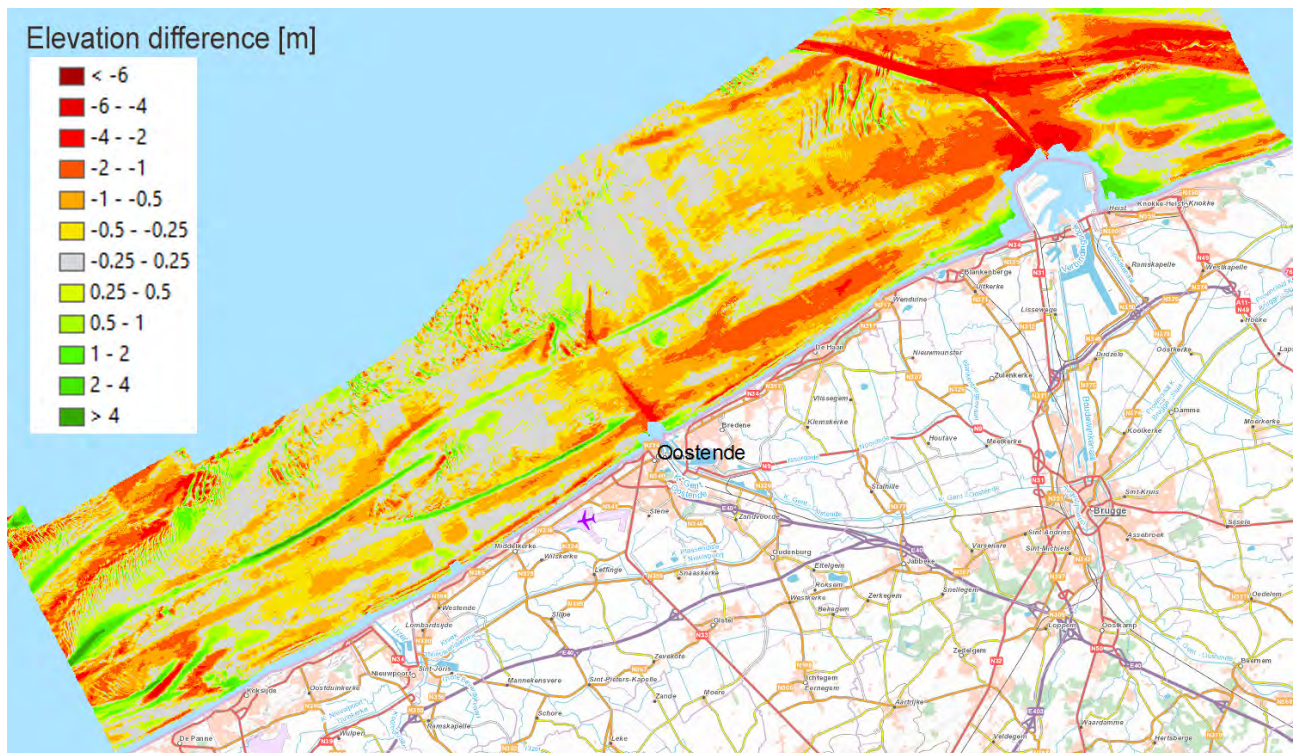


Figure 76 – Elevation difference map of the overlap area between the 1984/7 and the 2022 bathymetric maps.

### Observed large-scale morphological changes between 1984-87 and 2022 per zone

#### French border to Westende (Figure 77)

- the deepest part of the tidal channel Potje, the unnamed channel at about 1.75 km off the low-water mark that separates Broers Bank from Trapegeer, the shallowest parts of Trapegeer, the western flanks of Broers Bank and the secondary channel inside that flank at a distance of about 1 km of the low-water mark, as well as the shallow top area of Broers Bank, all migrated to the east, parallel to the coast, by about 700 m over 35 years, i.e. by 20 m per year on average.

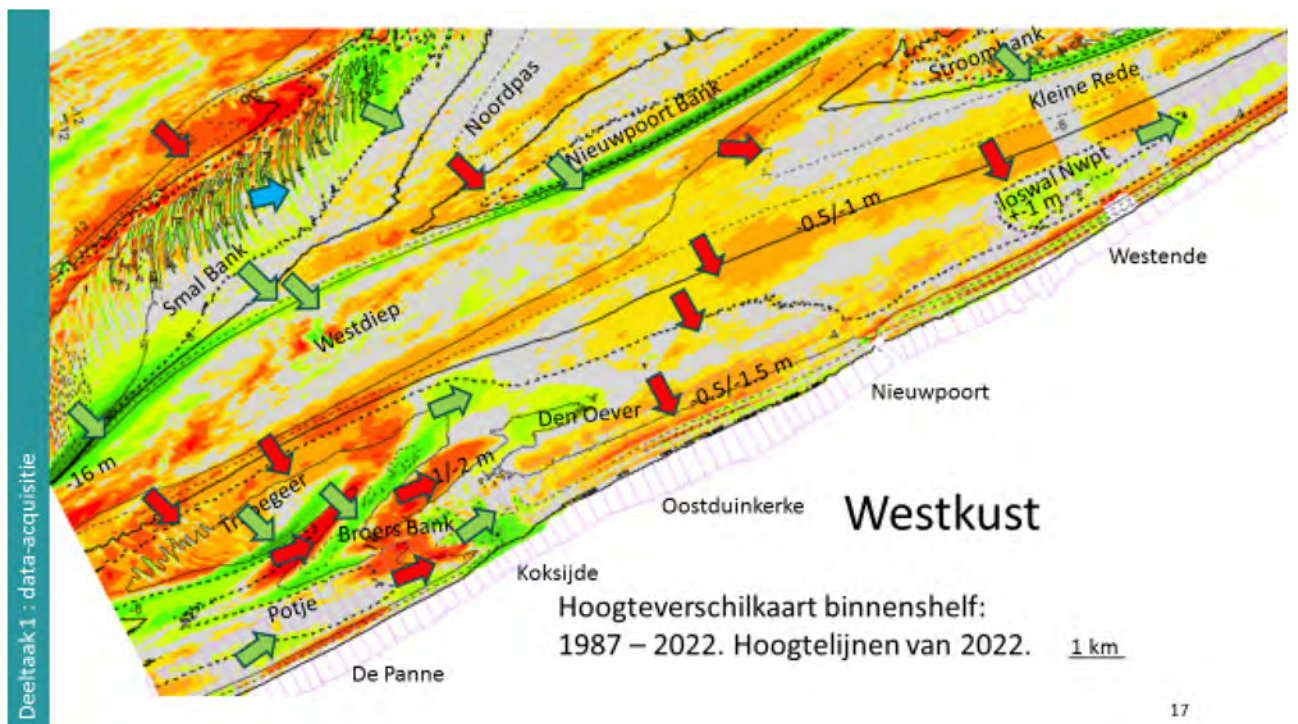
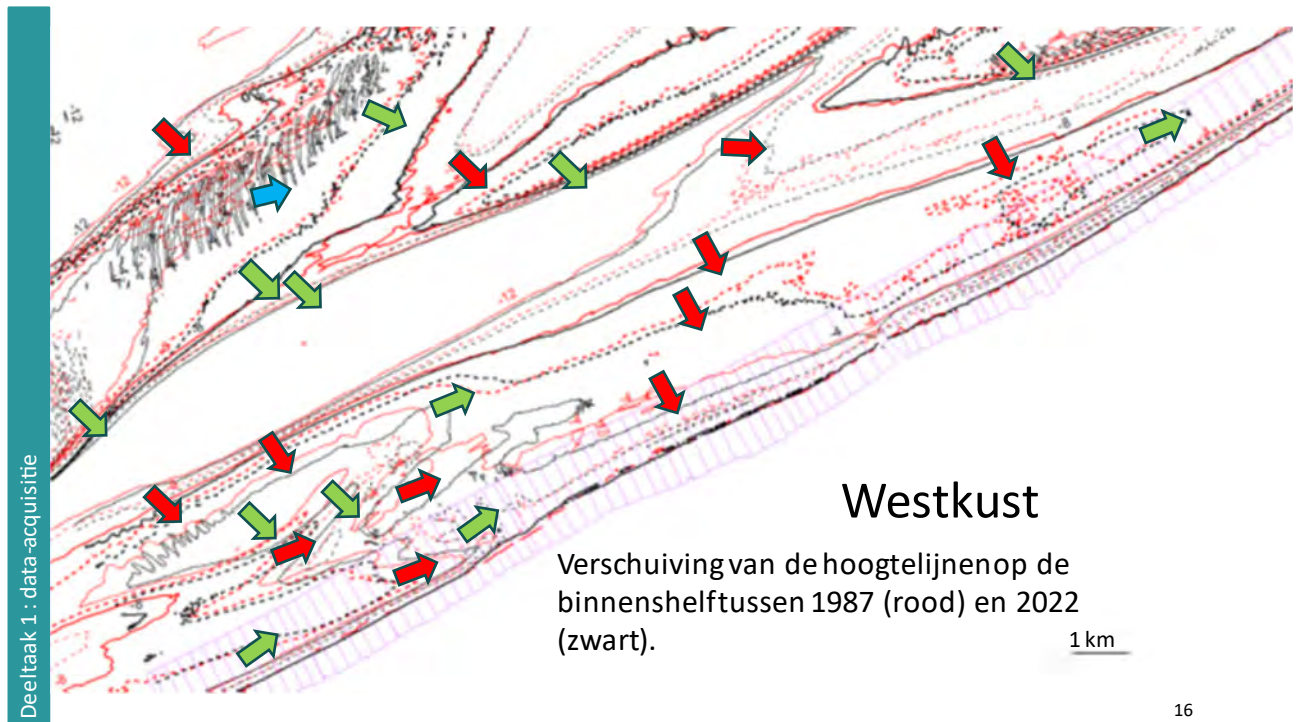


Figure 77 – West coast: Contour line shift (top) and elevation difference (bottom) between 1987 and 2022.

- the seaward flank of Trapegeer, near the Westdiep channel, migrated 150 m landwards.
- the eastern tip of Potje, that tapers out at Koksijde-Bad, shows a net sedimentation over 1987-2000 but afterwards deepened again (Houthuys *et al.*, 2022). This is seen as a morphological effect of the long groynes at Koksijde-Bad, built around 1985.
- the beach connection area of Broers Bank at Koksijde-Bad shoaled up.

- the shoreface base between Koksijde and Nieuwpoort deepened by 0.5 m to 1.5 m. This contrasts to the net beach and dune foot accretion observed in this area. The landward flank of the Westdiep channel migrated 120 m landwards.
- the focus of dumping activities at the discharge site "Ioswal Nieuwpoort", located on a shallow platform landwards of the Kleine Rede channel off Westende, clearly shifted by 2 km to the west. The dumped slurry tends to spread east at the foot of the shoreface.

#### **Middelkerke to De Haan (Figure 78):**

- the lower shoreface and the axial part of the Kleine Rede channel between Middelkerke and Oostende deepened by 0.5 to 1 m.
- the crest of Stroombank between Middelkerke and Oostende migrated by 120 m landward.
- the navigation passes to Oostende are now much deeper than in 1984, when the depth was at -6.5 m TAW.
- the attachment area of Stroombank to the shoreface near Bredene deepened by about 1 m.
- the shoreface base between Oostende and Bredene shifted by about 100 m landwards.
- the axis of the Grote Rede channel between Bredene and Wenduine shifted by about 150 m landwards.
- the shoreface between Bredene and Wenduine didn't shift. Major beach and shoreface nourishments have taken place here in the 1990s. The shoreface receded by about 25 m since 2000, though (Houthuys *et al.*, 2022).

#### **De Haan to Zeebrugge (Figure 79):**

- the crest of Wenduine Bank off Bredene-De Haan migrated over 250 m landwards. Beyond a central point that didn't move, the part between De Haan and Wenduine migrated over 250 m seawards. The entire bank crest line thus rotated anticlockwise.
- the shallow area in the centre of the Grote Rede channel, at about 2.8 km off the low-water mark near De Haan, didn't migrate in a coast-normal direction, but the shoal extended eastwards in a longshore sense by about 1 km. It is thought that these morphodynamics are related to dumping at the site "Bruggen en Wegen Oostende" that possibly was relocated more to the west in recent times. There may also be a link with the new flow configuration around Zeebrugge Outer Harbour.
- the branch of Grote Rede, landward of the preceding shallow area, remained at the same distance of the coast, but deepened considerably between Oostende and Wenduine, by 1.5 m increasing to 2 m just west of Wenduine. The shallow area in the centre of the Grote Rede channel seems to develop into a coast-parallel bank in its own. There may be a relation to (former) dumping activities. On the other hand, this recent sandbank attaches to the shallowing nearshore off Zeebrugge's western breakwater. So it might also represent a morphological adaptation to Zeebrugge's outer harbour.
- the nearshore area from about 4 km west to Zeebrugge's western breakwater is continuously shallowing, so that is now about 1.5 m shallower than in 1986.
- a little bit more offshore, at about 2.5 km off the low-water mark between Wenduine and Zeebrugge, a longshore channel deepened between 1986 and 2022 by 1 to 2 m. This appears to be a morphological response following the construction of Zeebrugge's outer harbour. Due to its appearance, the eastern tip of Wenduine Bank (at about 3 km from the low-water mark), is now more pronounced as a longitudinal sandbank than in 1986.
- around Zeebrugge's outer breakwaters, a wide coast-parallel depression is now at least 4 m deeper than in 1986, when the breakwaters were just constructed.

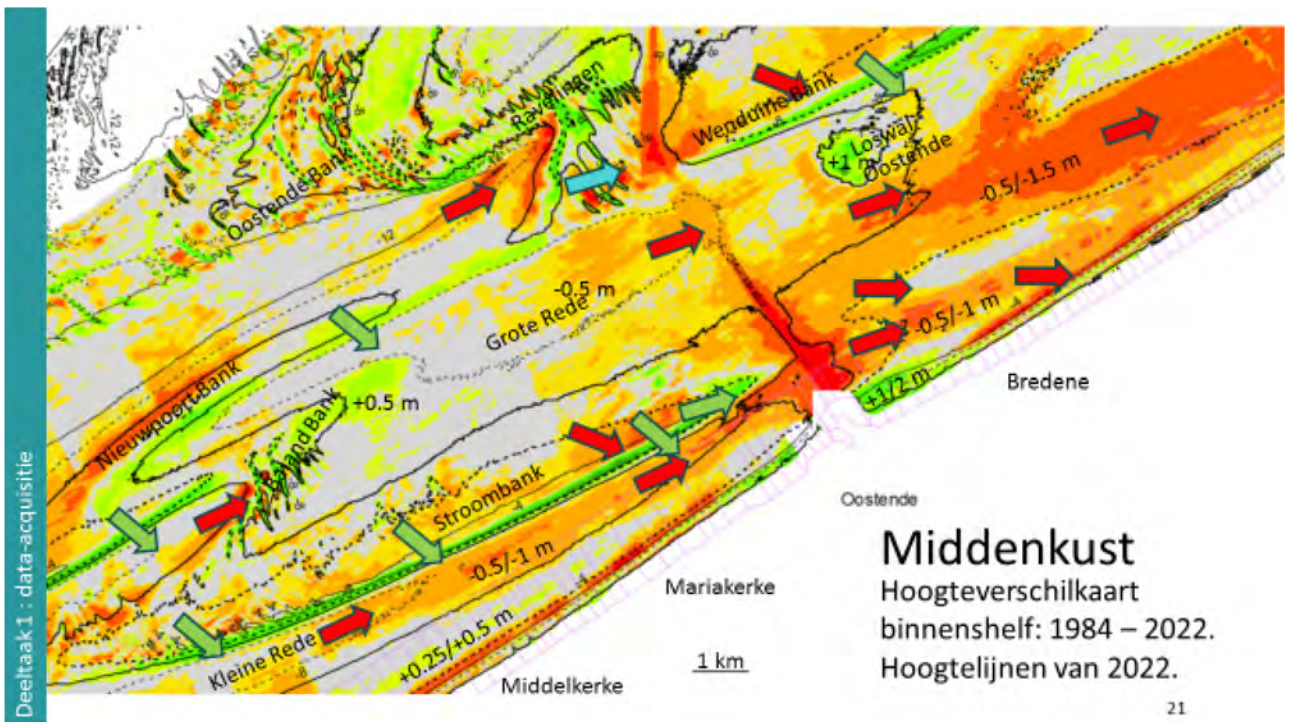
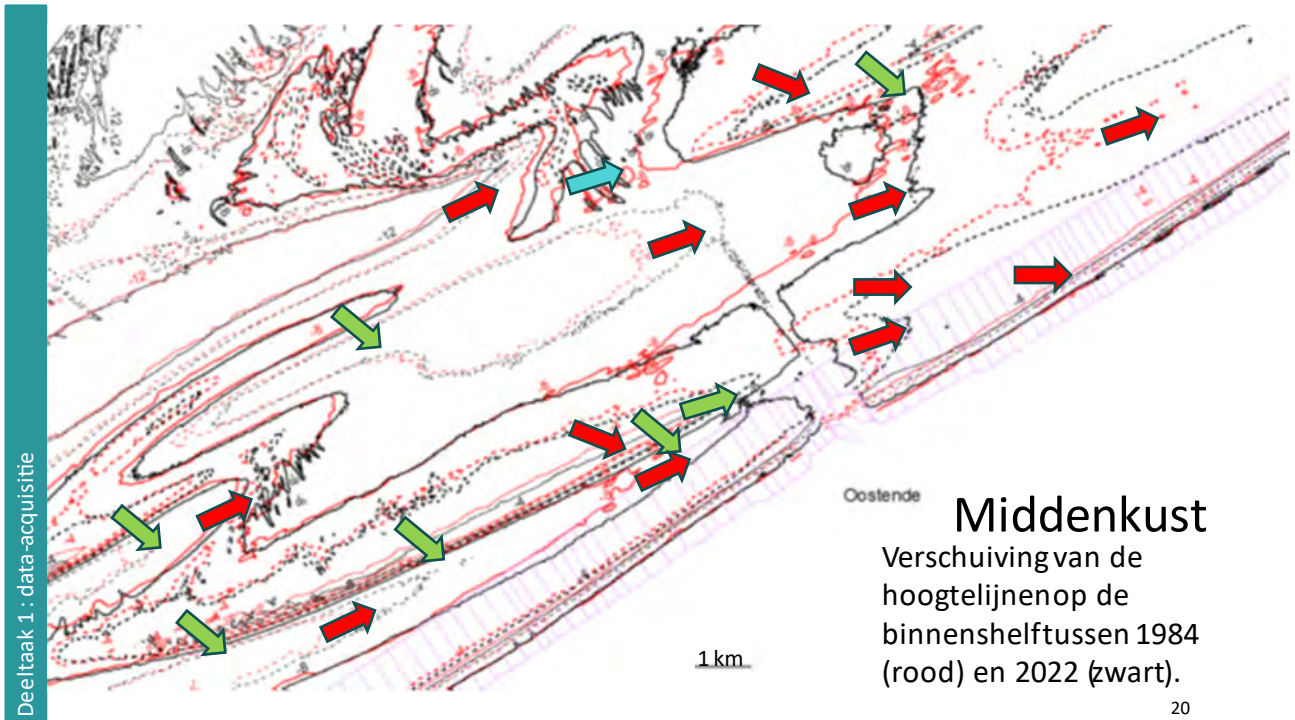


Figure 78 – Middle coast: Contour line shift (top) and elevation difference (bottom) between 1984 and 2022.

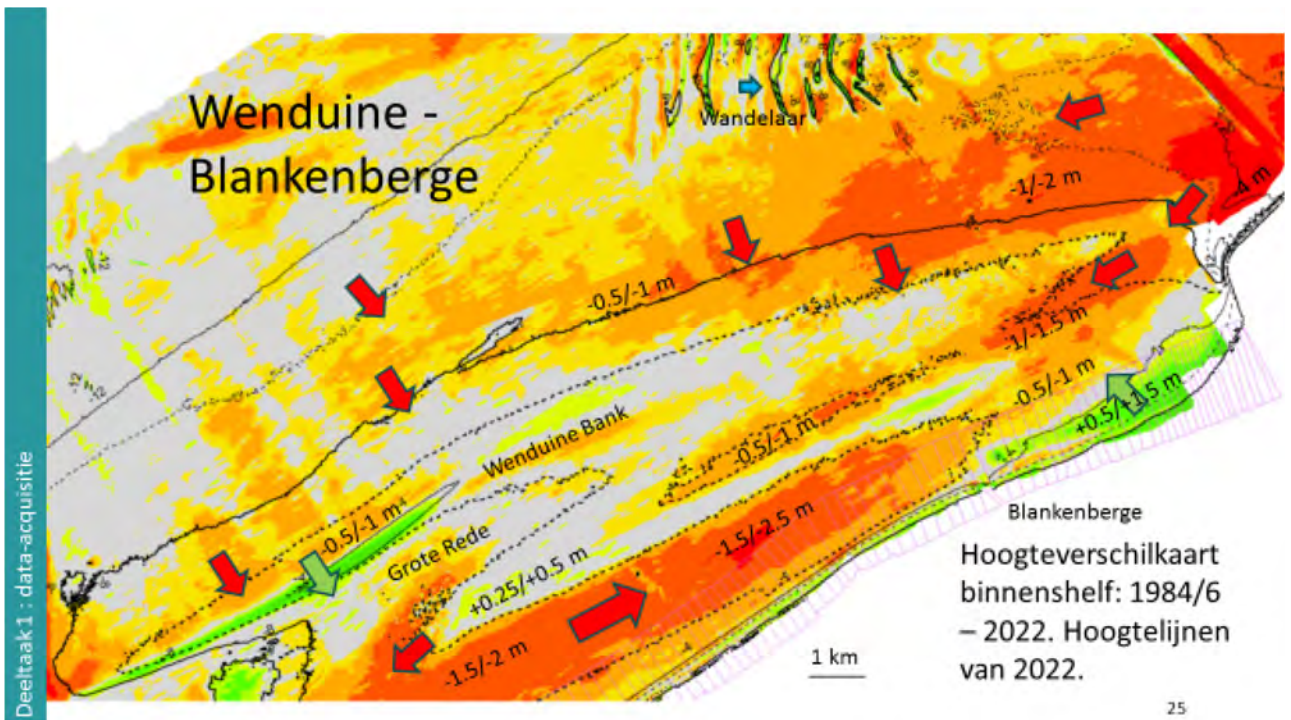
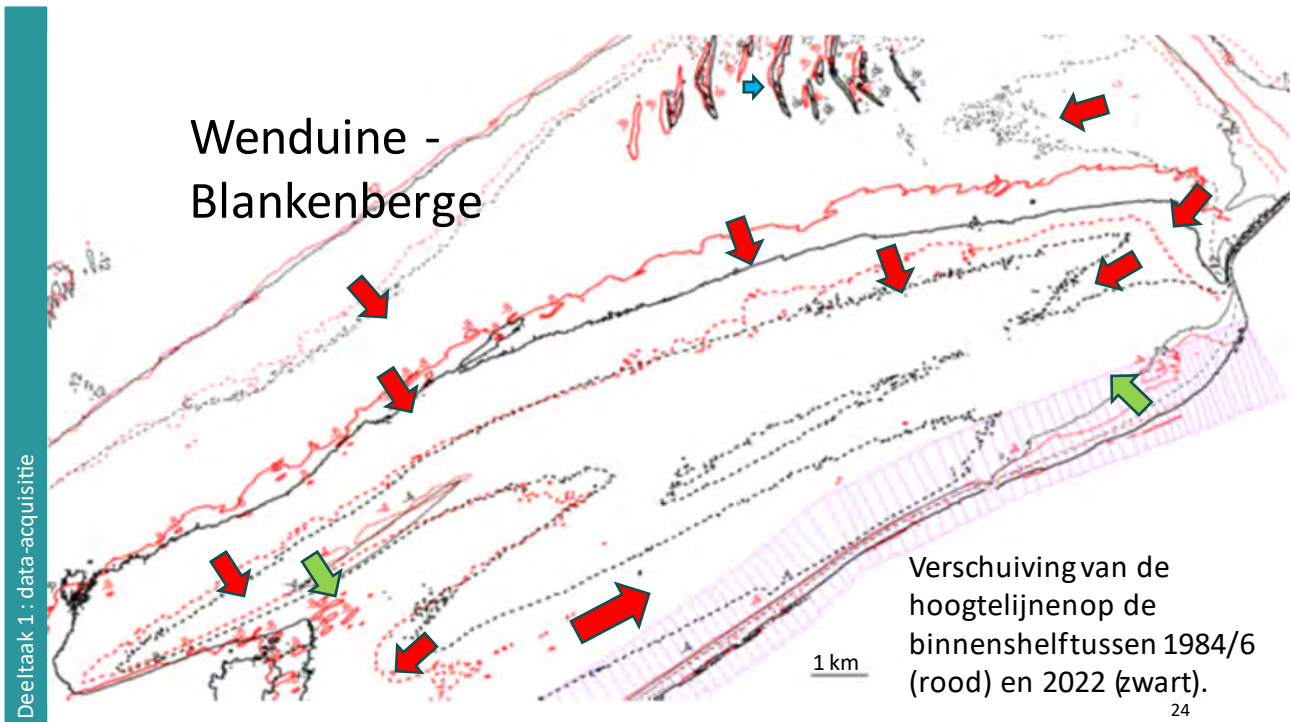


Figure 79 – De Haan to Zeebrugge: Contour line shift (top) and elevation difference (bottom) between 1984/6 and 2022.

- the big, coast-normal subaquatic dunes of Wandelaar migrated about 125 m eastwards between 1986 and 2022, i.e. on average 3.5 m a year. The surrounding area deepened by 0.5 to 1 m.

**East coast (Figure 80):**

- sedimentation in the eastern lee of Zeebrugge amounts vertically to 2 to 3 m since 1986.
- the shallowest area of Paardenmarkt sandbank migrated 2.5 km to the east and 250 m shorewards, while growing vertically over 1 m between 1986 and 2022.

- the deepest trace of Appelzak near Knokke remained at the same location, right at the shoreface foot, but was in 2022 1 m deeper than in 1986. A secondary trace developed 300 m more offshore, parallel to the deepest trace, seemingly as an adaptation to the new flow configuration east of Zeebrugge. These traces were dubbed “Tak 1” and “Tak 2” in Houthuys *et al.* (2022).
- the slope from Paardenmarkt to Scheur moved seaward by about 400 m. Sedimentation here is remarkable as the area is close to Zeebrugge outer harbour and the dredged fairway Scheur.

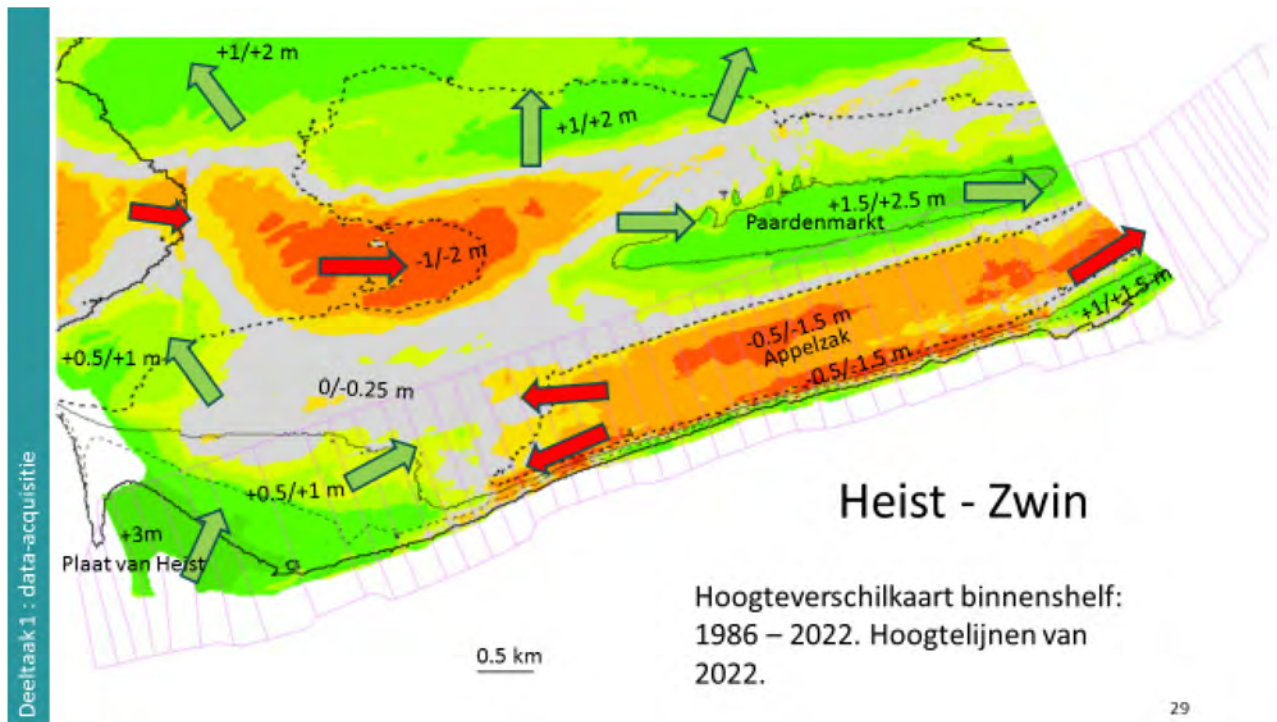
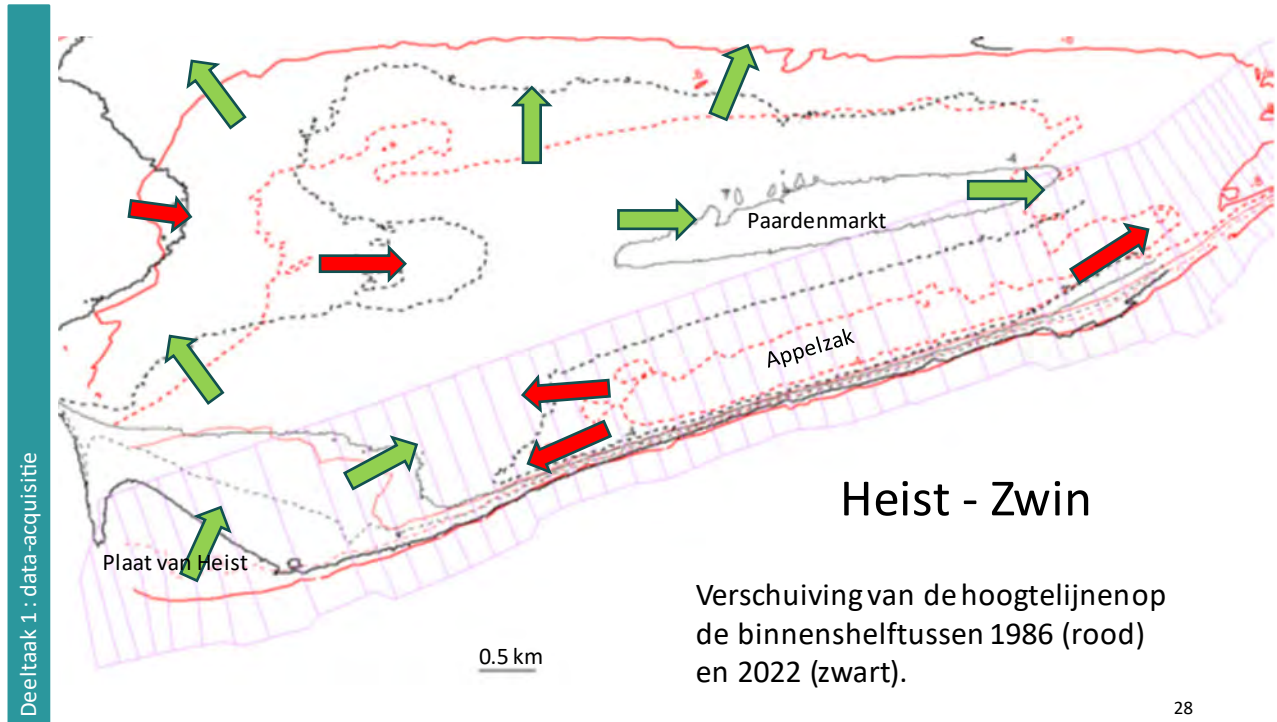


Figure 80 – East coast: : Contour line shift (top) and elevation difference (bottom) between 1986 and 2022. Note different scale to previous figures.

## Summary

All shoreface-connected ridges and the channels separating them from the beach migrated landwards and eastwards. Also, somewhat more offshore macro bedforms such as Nieuwpoort Bank, Baland Bank, Akkaert Bank, Ravelingen and Oostende Bank, and the channels between these banks, also migrated eastwards and shorewards between 1986 and 2022, but at slightly milder rates: about 100 m shorewards and 300 to 400 m eastwards over 1987-2022. In order to investigate the behaviour of these more offshore banks and channels more seaward bathymetric maps should be investigated as well.

In conclusion, all macroforms (banks and channels) along the Belgian shore migrate alongshore to the east and cross-shore to the coast. Morphological migration rates vary between 3 and 20 m/y. The morphological migration rates appear to decrease in offshore direction. The influence of dredge disposal extends a few hundred metres in cross-shore and a few kilometres in longshore direction. These sites are important supply points for the local area. It is clear that tidal currents rework and redistribute the disposed sediment to the east in the longshore direction. Zeebrugge's outer dams have significantly changed the surrounding morphology over several kilometres in all directions. While sedimentation characterizes the sheltered areas west and east of the dams, strong erosion is found in a wide area at the offshore side of the harbour. A similar response, but at the correspondingly smaller scale of that harbour, is found after the construction of Oostende's outer dams around 2010.

Based on a first comparison of the 1866 Stessels hydrographic map and the maps considered here, taking into account the low resolution of data in the Stessels map and the fact that this map probably favoured the representation of shallow points for safe navigation, there are good reasons to believe that the main described trends are persistent and have at least been going on for 1.5 century. A unique evolution however is noted for the Paardenmarkt sandbank: it was very prominent and shallow in 1866, almost completely absent in 1986 and almost regenerated in its 1866 position and depth in 2022.

More maps (time steps) will be added to the analysis.

After evaluating the echosounding accuracy and datum issues, volume balances will be established in relation to large regions that display similar behaviour.

### 4.2.2 Study of the (beach) nourishments at the Belgian coast since the 1980's

## Introduction

Within the project “Morfologische trends aan de Belgische Kust – Evolutie van de Vlaamse kust tot 2019” (Houthuys *et al.*, 2022) the volumetric and geographic changes in dunefoot, beach, shoreface and nearby seabed at the Belgian coast between 1979 and 2019 were analysed. These changes were calculated and mapped based on bathymetric and topographic surveys. Volumetric trends were corrected for human interventions like beach elevations for touristic purposes, shoreface and beach nourishments for coastal safety reasons, dredging works and sand mining. These human interventions were logged per coastal stretch (51 in total) in 5 excel files (one per coastal morphologic zone). Within the text of the report of Houthuys *et al.* (2022) a more precise description of the location of the nourishments along the coast can be found (on coastal section level). Table 13 shows the definition of the coastal morphological zones and the coastal stretches and sections they cover. Figure 81 shows the location of the stretches and sections along the Belgian coast.

Unfortunately no information exists on the volume distribution over the coastal sections within a nourishment, therefore the nourishment intensity is assumed to be uniform in the alongshore direction. Figure 82 shows the nourishment intensity over the 51 coastal stretches from 1979 until 2019 in three horizontal layers: the beach above low water (+1.39 m TAW), the shoreface between low water and - 4.11 m TAW, and the seabed below -4.11 m TAW. Figure 83 also shows the nourishment intensity for the beach and shoreface, but now showing the same scale on the y-axis for clarity. This however implies that

dredging works and disposal of dredged sediment on the foreshore at Blankenberge are out of range for the lower panel of this figure; for this we refer to the middle panel of Figure 82.

The morphological zones listed in Table 13 are mostly delineated by the access channels to the harbours (indicated by dashed lines in Figure 82 and Figure 83); only the border between zones 4 and 5 is not defined by the access channel to the marina of Blankenberge (stretches 38-39), but by the change in coastline orientation in Wenduine (stretches 36-37)

Table 13 – Definition of the coastal morphologic zones according to Houthuys et al. (2022).

|        | Name  | Coastal Stretches | Coastal Sections |
|--------|---|-------------------|------------------|
| Zone 1 | Natuurreservaat Westhoek – Nieuwpoort-Bad     | 01 – 12           | 002 – 059        |
| Zone 2 | Militair Domein Raversijde – Oostende-Centrum | 13 – 25           | 060 – 117        |
| Zone 3 | Oostende-Oost – Wenduine-West                 | 26 – 36           | 118 – 176        |
| Zone 4 | Wenduine-Oost – Zeebrugge Strand              | 37 – 43           | 177 – 216        |
| Zone 5 | Heist-Oostdam – Zwin                          | 44 – 51           | 217 – 255        |

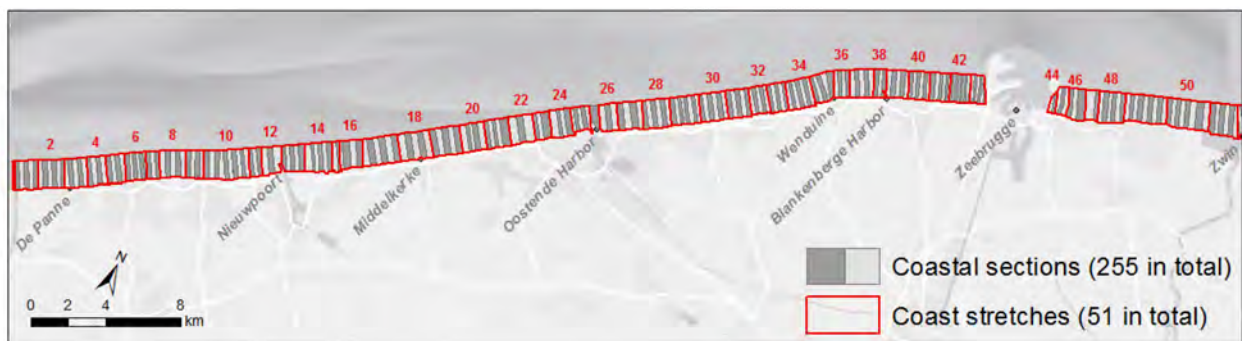


Figure 81 – Coastal sections and stretches along the Belgian coast (Vandebroek et al., 2017).

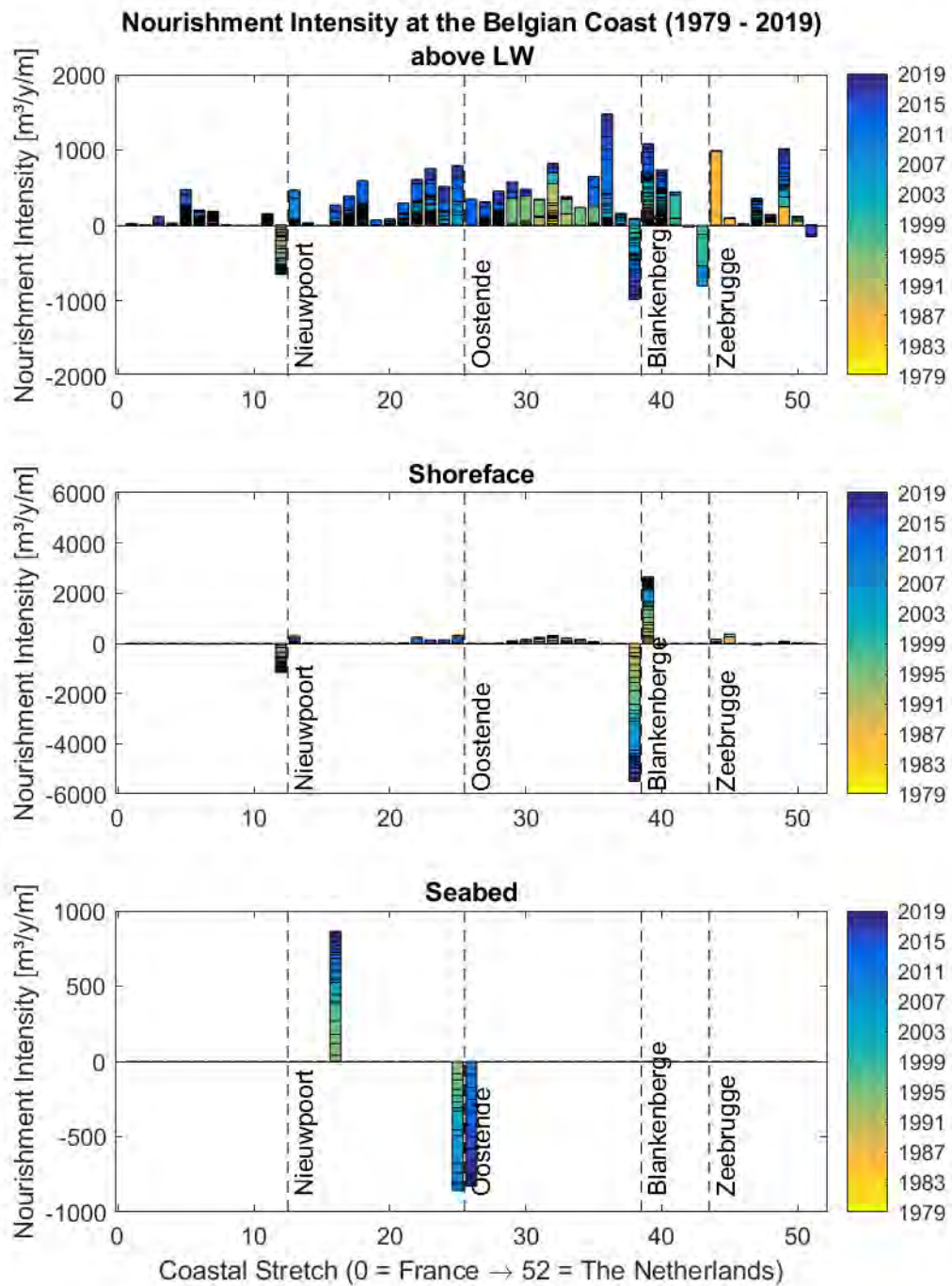


Figure 82 – Nourishment intensity at the Belgian coast, per stretch from 1979 until 2019.

Three vertical layers were defined: above Low Water (+1.39 m TAW), the shoreface between Low Water and -4.11 m TAW and the seabed below -4.11 m TAW. Negative values are related to dredging works. Please note the difference in scale on the y-axis.

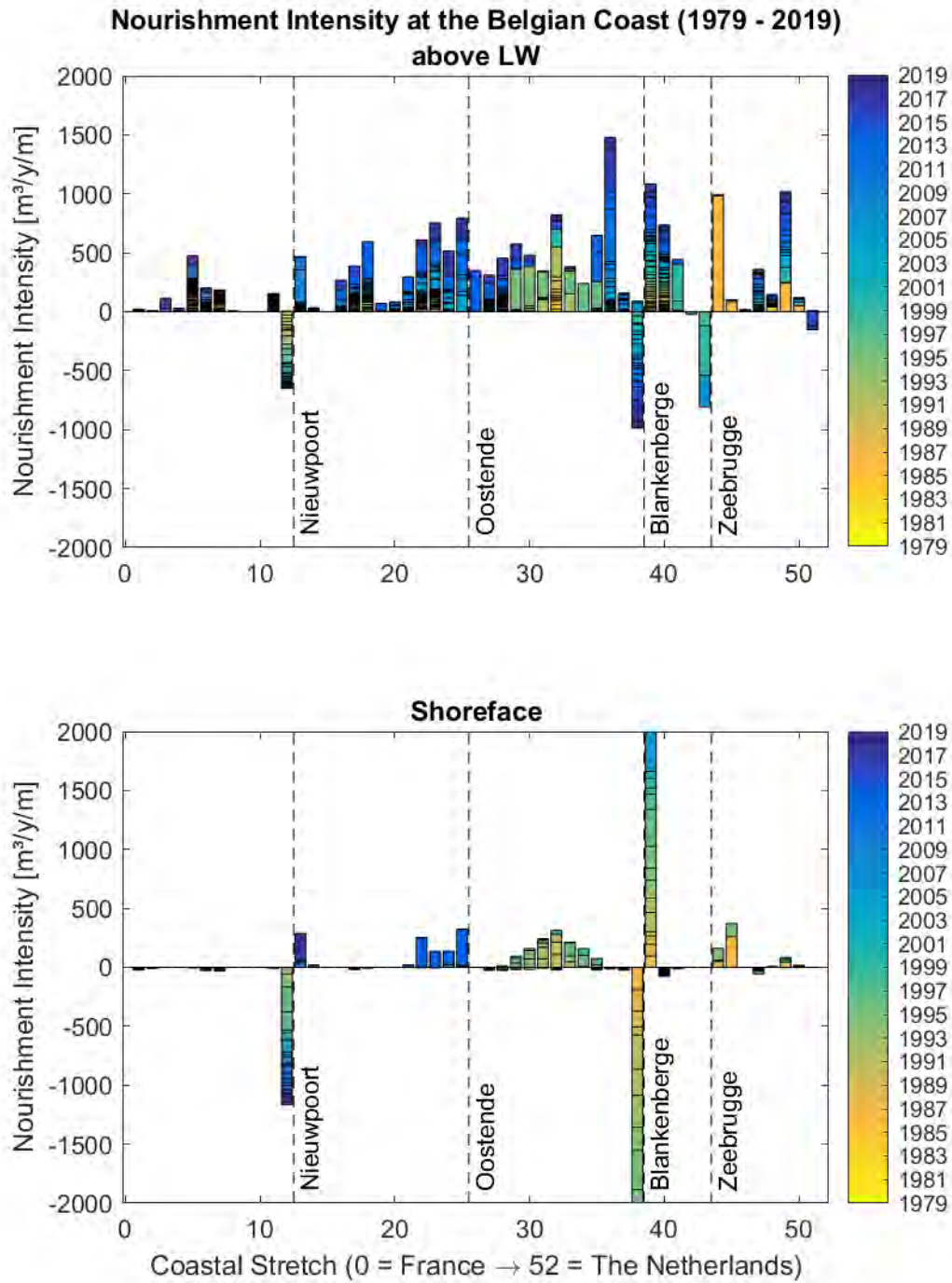


Figure 83 – Nourishment intensity at the Belgian coast, per stretch from 1979 until 2019. Three vertical layers were defined: above Low Water (+1.39 m TAW), the shoreface between Low Water and -4.11 m TAW and the seabed below -4.11 m TAW (not shown here). Negative values are related to dredging works. Dredging and dredged sediment disposal at Blankenberge are out of range in the lower panel, but can be observed in the middle panel of Figure 82.

## Dredging works and sand mining

All negative values shown in Figure 82 and Figure 83 are related to dredging works in the access channels to the harbours (illustrated by dashed lines), except for:

- the beach in stretch 43 (west of Zeebrugge) where sand mining was performed in April and December 1999 and in 2006;
- the beach in stretch 51 (Zwingeuil), where part of the dunes and Zwin gully were excavated in August 2016 and March 2017 within the framework of the extension of “Het Zwin” nature reserve.

In the seabed layer the dredging works in the old and new access channel to Oostende can be clearly observed. The sediment supply in stretch 16 is due to the presence the disposal site “Br&W Nieuwpoort”, where material from the maintenance dredging from the access channel of Nieuwpoort is dumped. The maintenance dredging in the access channel of Zeebrugge cannot be observed in this figure since the harbour areas of Zeebrugge are completely excluded from the coastal sections and stretches (because the breakwaters extent far beyond the beach and shoreface).

At the smaller harbours (marinas) of Nieuwpoort and Blankenberge, some sort of “sediment bypassing” seems to be conducted throughout the whole period 1979 – 2019: dredging in the coastal stretch comprising the access channel and nourishment in the neighbouring coastal stretch to the east. This “sediment bypassing” is not necessarily an intentional coastal management action, it can well be the co-occurrence of dredging works and beach nourishments in the adjacent zone in the same year, without an instant causality, nor the direct reuse of the same sediment.

## Nourishments

Except for stretch 39, directly east of the access channel to Blankenberge, nourishments are conducted mainly on the beach. Shoreface and beach nourishments were intensively conducted around stretch 32 (De Haan), and from stretch 22 (Mariakerke) till 25 (Oostende-Centrum).

### East coast

East of Zeebrugge large nourishments were carried out in 1977 – 1979 and 1986 (shown in yellow – orange in Figure 82 and Figure 83) to counter the expected erosion due to the interruption of the longshore drift after the extension of the harbour breakwaters. The nourishment was conducted in the area from the dunefoot till the upper shoreface. Between 1997 and 2003 small beach nourishments were conducted at stretch 47 – Duinbergen-Centrum by moving sand from the upper shoreface to the beach. From 2003 onwards these annual beach nourishments were carried out with marine sands. Also in the neighbouring stretches 48 till 50 (respectively Albertstrand, Knokke-Zoute and Lekkerbek) beach nourishments are carried out almost on annual basis from 2004 onwards. Nourishment intensities are highest in Knokke-Zoute. We assume the nourishment intensity in Albertstrand is lower than in the neighbouring stretches because it lies relatively more landwards, has a wider beach and the touristic platform in front of the seawall needs less maintenance.

In 2020 a shoreface nourishment was carried out (MDK, 2021).

### Blankenberge

As mentioned above, sand dredged from the access channel to the marina (stretch 38) is disposed of on the lower shoreface of the neighbouring stretch 39. Until 2008 the beach was elevated by moving sand from the shoreface to the (dry) beach; thereafter these elevations are conducted with sand originating directly from the dredging works in the access channel. In 2014 an additional nourishment was carried out within the framework of the “Masterplan Kustveiligheid”. Stretch 40 shows the same evolution/strategy, although with smaller nourishment volumes. Stretch 41 forms the border with the accumulation area against the western breakwater of Zeebrugge. In this stretch (stretch 41, sections 196-201) three nourishments were carried out in 1996 – 1999 after storms eroded the dune foot. In 2014 a fourth nourishment was carried out in its westernmost part to enhance the coastal safety level for Blankenberge (sections 196-198).

### **De Haan – Wenduine**

In the 1980's annual beach elevations were carried out in stretch 32 – De Haan-Centrum (yellow – orange in Figure 82). Severe winter/spring storms in 1990 caused beach erosion up till the toe of the seawall along the whole coastal town of De Haan. To increase safety, a large shoreface nourishment from Bredene-Oost (stretch 28) till Wenduine (stretch 35) was carried out in 1990 – 1991. In 1992 large beach nourishments were carried out in the same area (khaki green in Figure 82). In 2000 these nourishments on the beach and shoreface were renewed (green in Figure 82). Thereafter no additional nourishments were carried out; until in 2016 and 2019, smaller beach nourishments were conducted in the area (blue in Figure 82). This renewal might be related to the increase of coastal safety levels after the implementation of the “Masterplan Kustveiligheid” (2011). This is particularly clear in stretch 36 – Wenduine: from 1995 till 2011 small beach nourishments were conducted. Until 2005 this was mainly done by moving sand from upper shoreface to the beach; thereafter nourishments were carried out with marine sands. From 2012 on (after the implementation of the Masterplan Kustveiligheid) nourishment intensity increased largely in stretch 36.

### **Nieuwpoort – Oostende – Bredene**

In stretch 11 – Nieuwpoort-Bad annual elevations of the touristic beach platform were carried out from 1994 till 2012. These nourishments were done with marine sands. After 2012 no additional nourishments were needed.

In the coastal towns of Westende and Middelkerke (stretches 16 to 18) beach elevations were carried out from 1988 till 2007, either by moving sand from the lower beach to the upper beach (mainly Westende), either by nourishments with marine sands (mainly Middelkerke). From 2007 onwards only marine sands are used. Small nourishments for safety reasons were carried out in 2006 – 2010; after implementation of the Masterplan Kustveiligheid large nourishments were carried out in 2013 and 2014 (sections 17 and 18 only).

Also Mariakerke and Oostende-West (Wellington horse racetrack) have a history of small annual beach nourishments. Opposed to other locations these nourishments were almost always done with marine sands. In 2013 large nourishments were carried out from Mariakerke to Oostende-Centrum (stretches 22 till 25) in order to increase the safety levels in the framework of Masterplan Kustveiligheid. In 2018 this nourishment was replenished. In late autumn/early winter 2013 and late winter/early spring 2014 a large shoreface nourishment was conducted beginning from Oostende-Centrum (stretch 25) till Raversijde-Oost (stretch 21). East of the access channel to the harbour of Oostende only in 2014 a large beach nourishment was carried out.

In the coastal town of Bredene annual elevation of the beach was conducted since the 1990's, mostly with marine sands. In 2014 and 2017 large beach nourishments to increase the coastal safety level were carried out.

### **West coast**

A similar trend in nourishment strategy as in the area between De Haan and Wenduine can be seen in the area between Sint-Idesbald and Koksijde (stretches 5 till 7): in the 1990's beach nourishments were established by moving sand from upper shoreface to the beach, thereafter beach nourishments were directly carried out with marine sands. However the 1990's data need to be handled with care as these are estimates made by Houthuys *et al.* (2022) since the exact volumes were not documented during execution of the nourishment works. Between 2012 and 2019 no more nourishments were carried out; more recent nourishments are not yet included in our database.

## Summary

The analysis of the nourishment works shows how coastal authorities have a long history of elevating the beaches (and touristic sand platform) along the Belgian coast, either by moving sand from the upper shoreface to the beach (beach scraping) or by nourishing the beach with marine sands. The former was mainly used in the 1980's and 1990's until it was completely replaced by nourishing with marine sands in the years 2000. Only since 2011, after the introduction of the "Masterplan Kustveiligheid", this methodology of annual nourishments was abandoned. This might however be related to the increased safety levels defined by the Masterplan, the accompanying large nourishments carried out between 2011 and 2014, and the renewal/maintenance of the nourishments in 2017 – 2018; eliminating the need for annual maintenance.

This shift in maintenance strategy can be observed in 5 coastal town areas: Sint-Idesbald – Koksijde, Bredene, Mariakerke – Oostende, De Haan and Blankenberge. At the east coast this pattern of small annual nourishments only started in 1997, probably because there was less need for sand after the large nourishments of 1977 – 1979 and 1986, related to the extension of the Zeebrugge breakwaters.

Large nourishments can be related either to storm impacts (e.g. shoreface and beach in De Haan after 1990 or beach in Blankenberge after storms in 1990, 1993 and 1995), or – more recently – to the increased safety level defined by the "Masterplan Kustveiligheid".

### 4.2.3 Study of cross-shore profiles since the year 2000

## Introduction

In order to study the local impact of the nourishments (see §4.2.2), cross-shore profiles were analysed. The dataset was built by Bart Roest within the framework of the CREST-project and his PhD-thesis is used (Roest, 2019). The dataset consist of combined height measurements, derived from topographic and bathymetric measurements of the Belgian coast. It spans a 22 year time period, from spring 1997 until spring 2019. The raw point clouds are interpolated to arrays, transverse to the coast at the theoretical positions of the single-beam soundings. This data includes the Belgian coastal zone from the dunes down to 1500 m seawards from the coastline. Coverage of the dataset is limited to the actual coverage of the raw data (no extrapolation applied). The data is based on measurements made available by the Coastal Division of the Flemish Government.

## Evolution of the cross-shore profiles

### West coast

Transect 56 is located 1.7 km west of the coastal town of Koksijde, where the Trapegeer – Broersbank – Den Oever complex attaches to the coast. The transect itself shows the area where the Potje gully is eroding/moving to the north east (see §4.2.2). Figure 84 shows a progradation of the dry beach and upper shoreface since the last nourishment in 2012. Since 2007 the offshore seabed has decreased in height with 60 cm; the Potje gully closer to shore deepened with ca. 30 cm.

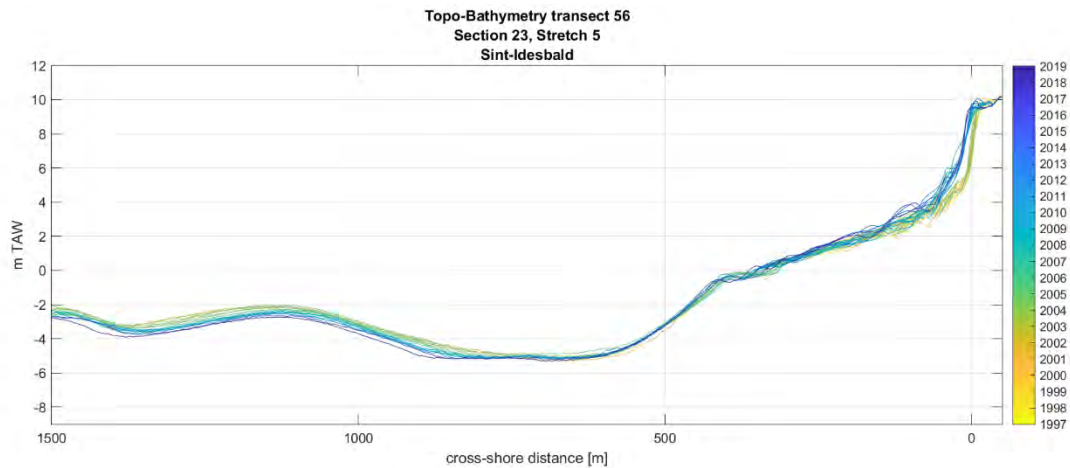


Figure 84 – Morphologic evolution of the Potje gully and shoreface west of Koksijde.

### Middelkerke – Oostende

The area from Middelkerke to Oostende is characterised by the Stroombank approaching the coastline; the gully between the sand ridge and the coast is called Kleine Rede. At Middelkerke the Stroombank is located ca. 2.7 km offshore, near the access channel to the harbour of Oostende the Stroombank is situated 1.7 km offshore.

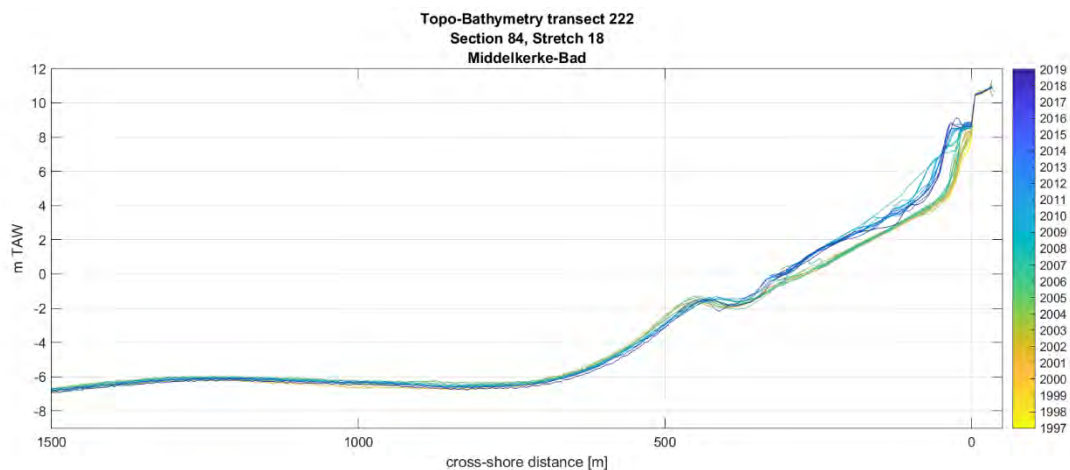


Figure 85 – Morphologic evolution of the Kleine Rede gully and shoreface at Middelkerke.

At Middelkerke the first annual shoreface sounding in the dataset is 2003. The seabed remained more or less stable, a slight landward movement of the bulge between 1500 and 750 m offshore can be seen (Figure 85). The lower shoreface however retreated ca. 20 m. The breaker bar, which divides the lower shoreface from the upper shoreface retreated with the same amount, but gained 20 cm in height.

The nourishment of 2013 – 2014 is clearly visible as an elevation and seaward movement of the whole profile above -1 m TAW. Erosion of the nourishments start at the upper beach in 2015 and the progresses towards the high water line over time. In the winter of 2018 – 2019 a large chunk is eroded around the high water line. On the intertidal beach the profile after nourishment remains more or less stable.

Transect 291 (Figure 86) is located ca. 2.5 km west of the harbour of Oostende; the Stroombank is situated ca. 1.75 km offshore. The first bathymetric record for this transect is 1999; remarkably the last record (May 2019) shows almost identical depth offshore. Between 1999 and 2011 the sea bottom gained ca. 60 cm in height; on the shoreface a breaker bar was formed. In winter 2013 a large nourishment was carried out on the shoreface and dry beach, which moved the whole profile 30 m seawards and ca. 1 m upwards, burying the breaker bar. In the next years the nourishment lost sand, first on the intertidal beach, later also on the upper shoreface; and a new breaker bar emerged. In 2018 the nourishment on the beach above the low water line was renewed. Since 2011 the sea bottom gradually deepened again with ca. 60 cm.

Directly east of the harbour of Oostende, since 2007, the sea bottom has been deepening, while the lower shoreface prograded (Figure 87). Both movements can be linked to the building of the new breakwaters, which changed the hydrodynamics in the area considerably. In front of the breakwaters a scour pit has formed, while at the leeside, sheltered from tidal currents and waves, the beach has moved seawards. In 2014 a beach nourishment was carried out; after initial erosion in the first year, the beach profile remained stable.

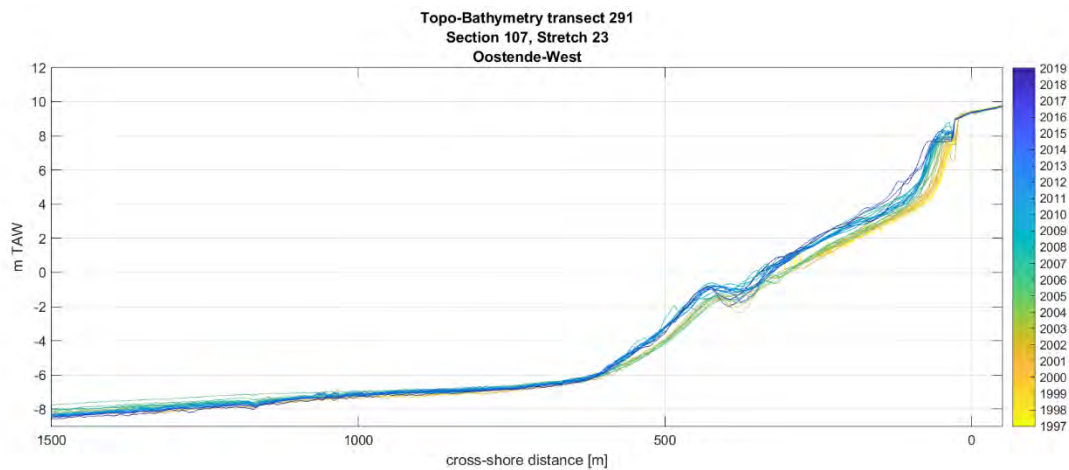


Figure 86 – Morphologic evolution of the Kleine Rede gully and shoreface at Oostende.

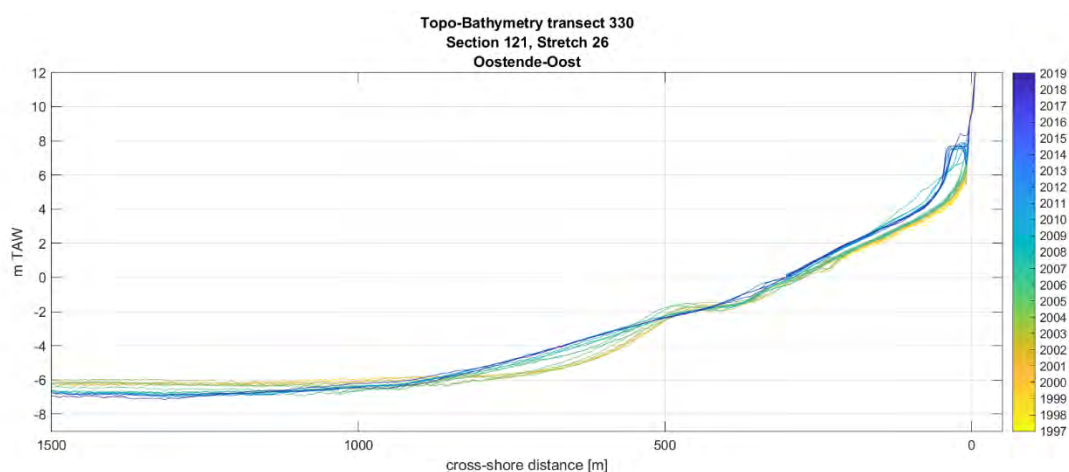


Figure 87 – Morphologic evolution of the Kleine Rede gully and shoreface 600 m east of Oostends eastern breakwater.

### De Haan – Wenduine – Blankenberge

In front of the coast between Oostende and Zeebrugge lies the Wenduine bank, situated ca. 5 km offshore. Between the sand ridge and the coastline lies the Grote Rede gully. At the coastal town of Wenduine the coastline changes orientation (65°N west of Wenduine and 70°N more to the east).

In De Haan, annual soundings of the shoreface only started after the large nourishments of the shoreface and beach in 1992 and 2000. Since then a series of bars have been moving over the profile: the two bars below low water have been moving landwards (70 and 30 m respectively) and lost a bit of height (ca. 5 cm); the bars on the intertidal beach seem to be moving seawards, back to their original position before the nourishment in 2000 (Figure 88). The bar that develops around high water however has been buried again by the beach nourishment of early 2019.

At De Haan, the offshore seabed level decreased with app. 40 cm to -6.40 m TAW. At Wenduine the sea bed gradually deepened with 80 to 90 cm to a depth of almost -7 m TAW (Figure 89). The coastal town of Blankenberge lies at the easternmost tip of the Grote Rede, here no clear evolution in sea bottom height can be observed (Figure 90); inter-annual variation in the seabed is calculated to be 14 cm.

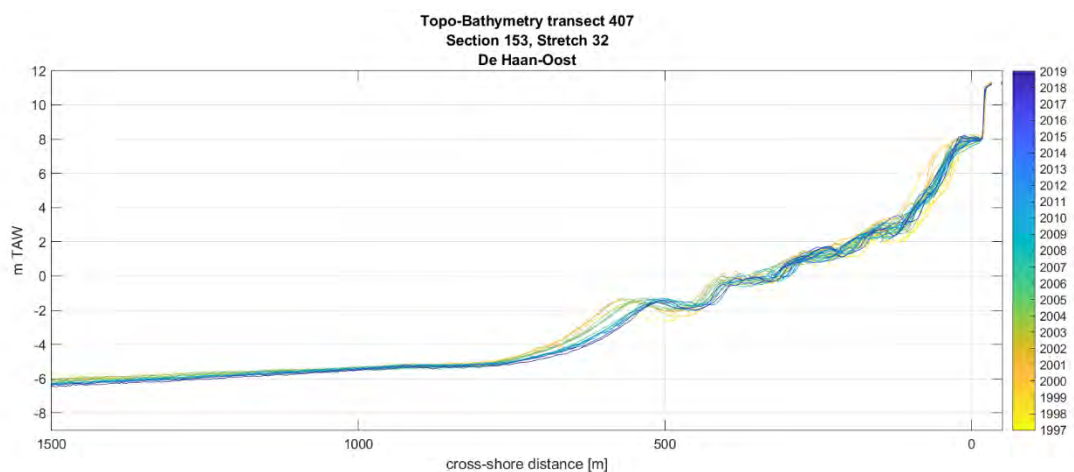


Figure 88 - Morphologic evolution of the Grote Rede gully and shoreface at De Haan.

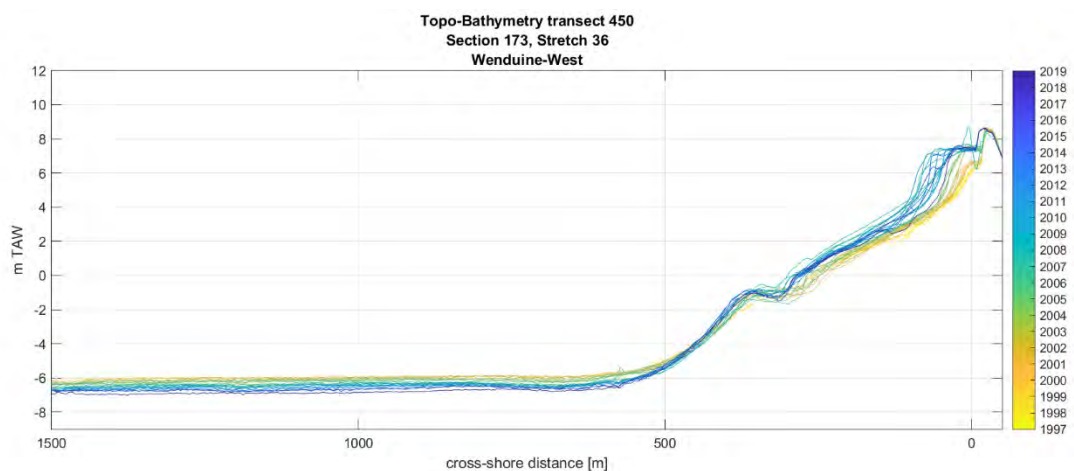


Figure 89 – Morphologic evolution of the Grote Rede gully and shoreface at Wenduine.

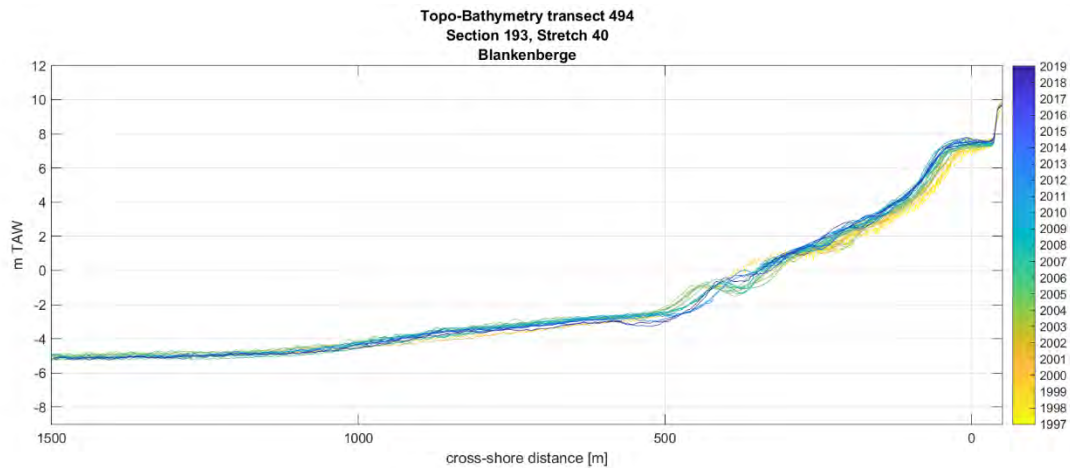


Figure 90 – Morfologic evolution of the Grote Rede gully and shoreface east of Blankenberge marina.

At Blankenberge (Figure 90) the lower shoreface shows large fluctuations, while the intertidal and dry beach are systematically moving seawards. The latter is caused by the trapping of sediment against the western breakwater of Zeebrugge; the former might be due to storms. At Wenduine (Figure 89) the elevation and seaward movement of the intertidal and dry beach is solely attributed to nourishments.

### East coast

In front of the coast of Knokke lies the Appelzak tidal gully; separated from the Wielingen – Scheur fairway channel by the Paardenmarkt sand ridge. Since 2003 the Appelzak in front of Knokke has deepened almost 1 m, most apparently at ca. 1000 m offshore and at the base of the shoreface (Figure 91). Annual nourishments caused a gradual seawards movement of the upper shoreface and beach, while the lower shoreface retreated ca. 5 m; the tipping point lying at ca. -4 m TAW depth.

Closer to the Western Scheldt mouth, in front of the Zwin nature reserve (Figure 92), the shoreface is not as steep as in Knokke, but here also the lower shoreface has been gradually retreating during the last decade. In total it moved 130 m landwards and deepened by almost 80 cm. From 1999 till 2015 the upper shoreface seemed to gain volume, until it suddenly dropped back to its 1999 level in 2018. This might be related to the excavations in the Zwin gully in 2016-2017. At ca. 900 m offshore the Appelzak gully gradually deepened 40 cm, while the Paardenmarkt sand ridge grew 1.8 m in height.

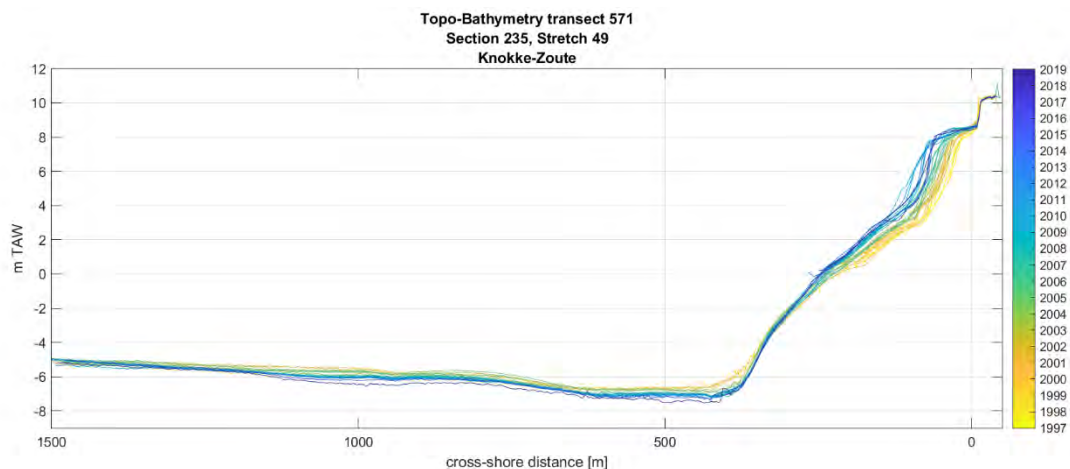


Figure 91 – Morfologic evolution of the Appelzak gully and shoreface at Knokke-Zoute.

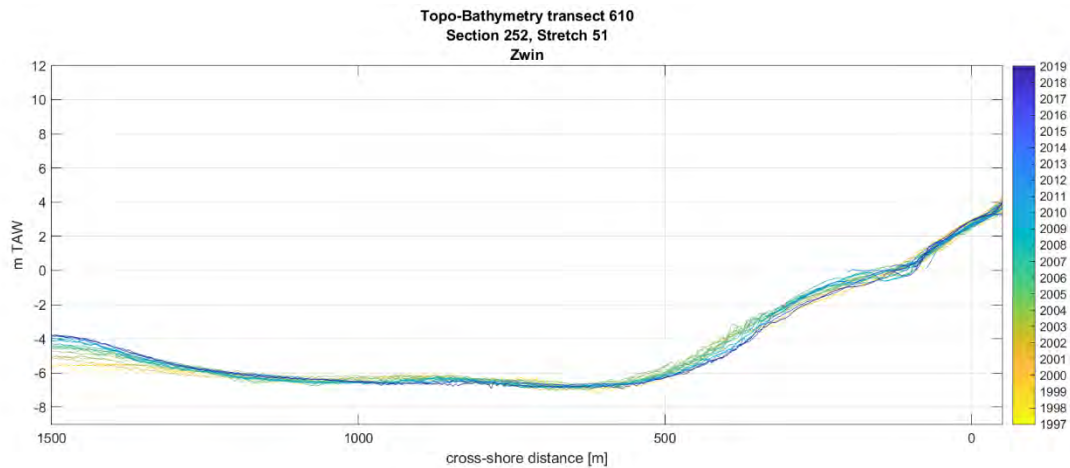


Figure 92 – Morphologic evolution of the Paardenmarkt sand ridge, Appelzak gully and shoreface in front of the Zwin.

## Summary

Deepening of the channels in front of the coastline have been shown here for Potje, Grote Rede and Appelzak. In the Kleine Rede, from to coastline till 1500 m offshore, sedimentation occurred between 1999 and 2011, thereafter the same amount of sediment was eroded again. The analysis on the inner shelf maps (§4.2.1) however showed that most of the erosion occurred in the deeper part of the channel, further offshore and thus can't be seen in the (semi-)annual beach and shoreface profiles (§4.2.3).

The profile at Sint-Idesbald (Potje gully) shows a stable lower shoreface, as does the profile at Middelkerke (Kleine Rede). In Oostende the seaward movement of the lower shoreface is caused by shoreface nourishments, while the retreat of the lower shoreface at De Haan is probably a return to the natural beach profile after the large shoreface nourishments in 1990 – 1991 and 2000. In Wenduine, where the Grote Rede approaches the shoreline, and where the Belgian coastline changes orientation, erosion can be observed at the base of the shoreface. Also in the Appelzak gully the lower shoreface is eroding.

None of the chosen profiles show a natural growth of the beach and (upper) shoreface, except for the one at Sint-Idesbald on the western part of the Belgian coast – showing progradation of the inter-tidal beach and upper shoreface since the last nourishment in 2012 – and the one in front of the Zwin at the easternmost part of the Belgian coast. For all other locations there's a clear relation between nourishments and the evolution of the beach and upper shoreface profiles. Fresh beach nourishments erode first at their highest point, thereafter erosion continues gradually until the low water line.

At some locations breaker bars can be observed in the profile; their crest position and shape varies through time. The breaker bars at Groenendijk have been studied in detail during the BelSPO project "RS4MoDy" (2017-2021) (see <https://eo.belspo.be/en/stereo-in-action/projects/remote-sensing-data-investigating-morphodynamics-belgian-multi-barred>). The correlation of this movement with nourishment intensity or volumes has not been studied here.

## 4.3 Literature review and data analysis for the Dutch coast

### 4.3.1 Introduction

In order to get additional insight into the effects of deepening nearshore tidal channels on beach erosion and on the intensity of (anthropogenic) nourishments to maintain the coastline, a quick scan study is performed for the Dutch coast. This quick scan includes an overview of the areas along the Dutch coast, in which deepening and/or landward migrating channels (according to the Beheerbibliotheek by Deltares 2022d) coincide with areas with large nourishment volumes. For this, overview maps of the Dutch coast are created showing the coastal bathymetry and the yearly beach and underwater nourishment volumes per JARKUS-transect (i.e. the name of the coastal transects along the Dutch coast for which yearly bathymetry measurements are being performed) averaged over the period 2000 to 2020 (i.e. 20 years). This period is representative for the current Dutch nourishment strategy in which underwater nourishments form an essential element to maintain the coastline. Underwater nourishments have been implemented at the Dutch coast in year 1999. For further details on how the yearly beach and underwater nourishment volumes per JARKUS-transect have been determined see Röbbke *et al.* (2021).

Beside this overview of the nourishment volumes along the Dutch coast, the quick scan study focusses on the morphological development of the Oostgat channel and the nourishment of the adjacent south-west coast of Zeeland (The Netherlands). The Oostgat channel is a typical example for a landward migrating tidal channel at the Dutch coast that coincides with intensive nourishing along the adjacent coast.

### 4.3.2 Quick scan of nourishments and morphological evolution of channels along the Dutch coast

Figure 93 to Figure 96 illustrate the yearly beach and underwater nourishment volumes per JARKUS-transect (i.e. the name of the coastal transects along the Dutch coast for which yearly bathymetric measurements are performed) averaged over the period 2000 to 2020 for the Dutch coast. There are several locations at the Dutch coast, where landward migrating/deepening tidal channel occur (Deltares 2022d) and – at the same time – large beach and/or underwater nourishments have been performed in the last 20 years. These areas are marked by red dotted lines in Figure 93 to Figure 96 and include (from north to south) the:

- west coast of Ameland,
- north-east coast of Vlieland,
- south-west coast of Texel,
- “head” of North-Holland near Den Helder,
- west coast of Schouwen-Duiveland (Zeeland),
- north coast of Walcheren (Zeeland),
- west coast of Walcheren along the Oostgat channel (Zeeland) and
- the coast between Cadzand and Breskens (Zeeland).

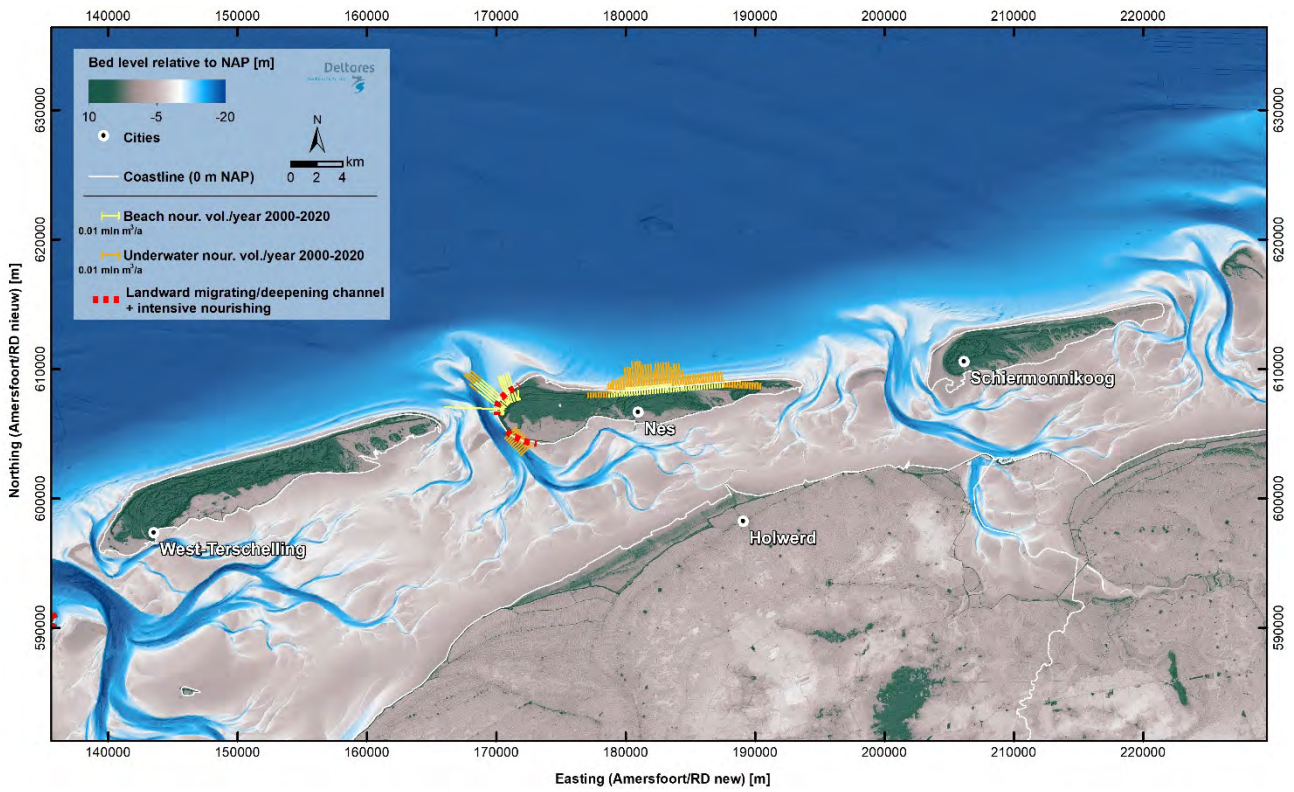


Figure 93 – Nourishments in the area of Terschelling, Ameland and Schiermonnikoog (The Netherlands).

On- and offshore topography and yearly beach and underwater nourishment volumes per JARKUS-transect (i.e. the name of the coastal transects along the Dutch coast for which yearly bathymetric measurements are performed) averaged over the period 2000 to 2020 for the area of Terschelling, Ameland and Schiermonnikoog (The Netherlands). For further details on how the yearly beach and underwater nourishment volumes per JARKUS-transect have been determined see Section 4.3.1 and Röbbke et al. (2021).

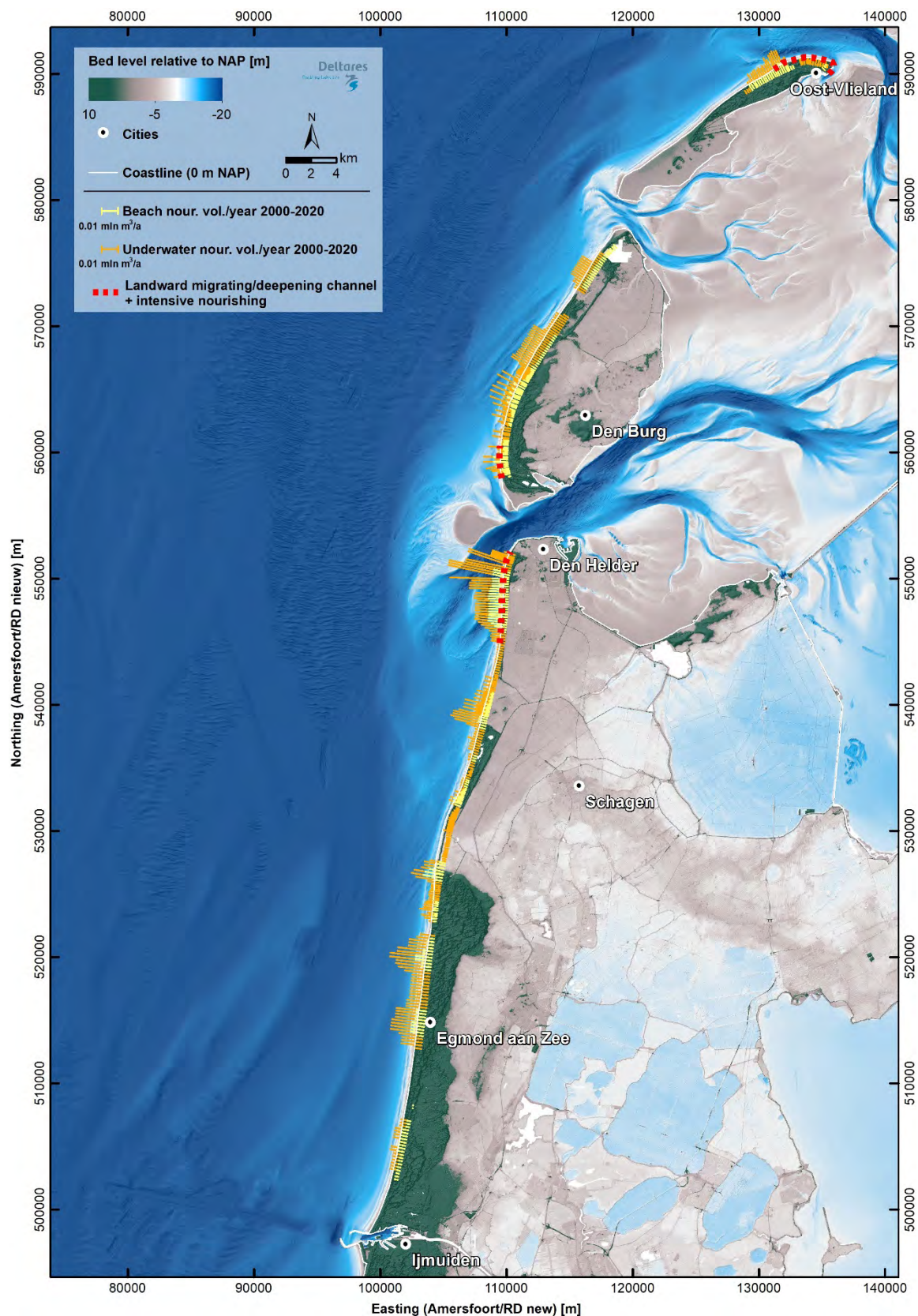


Figure 94 – Nourishments in the area of Vlieland, Texel and North-Holland (The Netherlands).

On- and offshore topography and yearly beach and underwater nourishment volumes per JARKUS-transect (i.e. the name of the coastal transects along the Dutch coast for which yearly bathymetric measurements are performed) averaged over the period 2000 to 2020 for the area of Vlieland, Texel and North-Holland (The Netherlands). For further details on how the yearly beach and underwater nourishment volumes per JARKUS-transect have been determined see Section 4.3.1 and Röbbke et al. (2021).

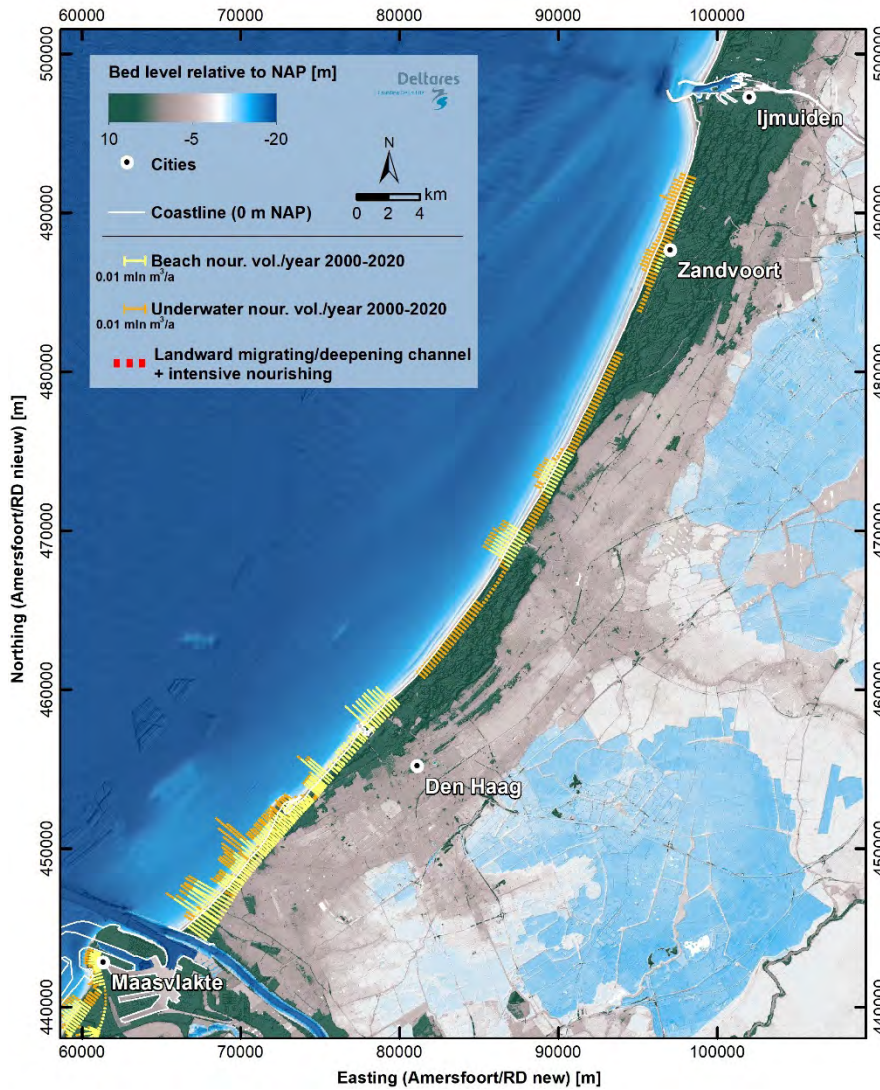


Figure 95 – Nourishments in the area of South-Holland (The Netherlands).

On- and offshore topography and yearly beach and underwater nourishment volumes per JARKUS-transect (i.e. the name of the coastal transects along the Dutch coast for which yearly bathymetric measurements are performed) averaged over the period 2000 to 2020 for the area of South-Holland (The Netherlands). For further details on how the yearly beach and underwater nourishment volumes per JARKUS-transect have been determined see Section 4.3.1 and Röbbke et al. (2021).

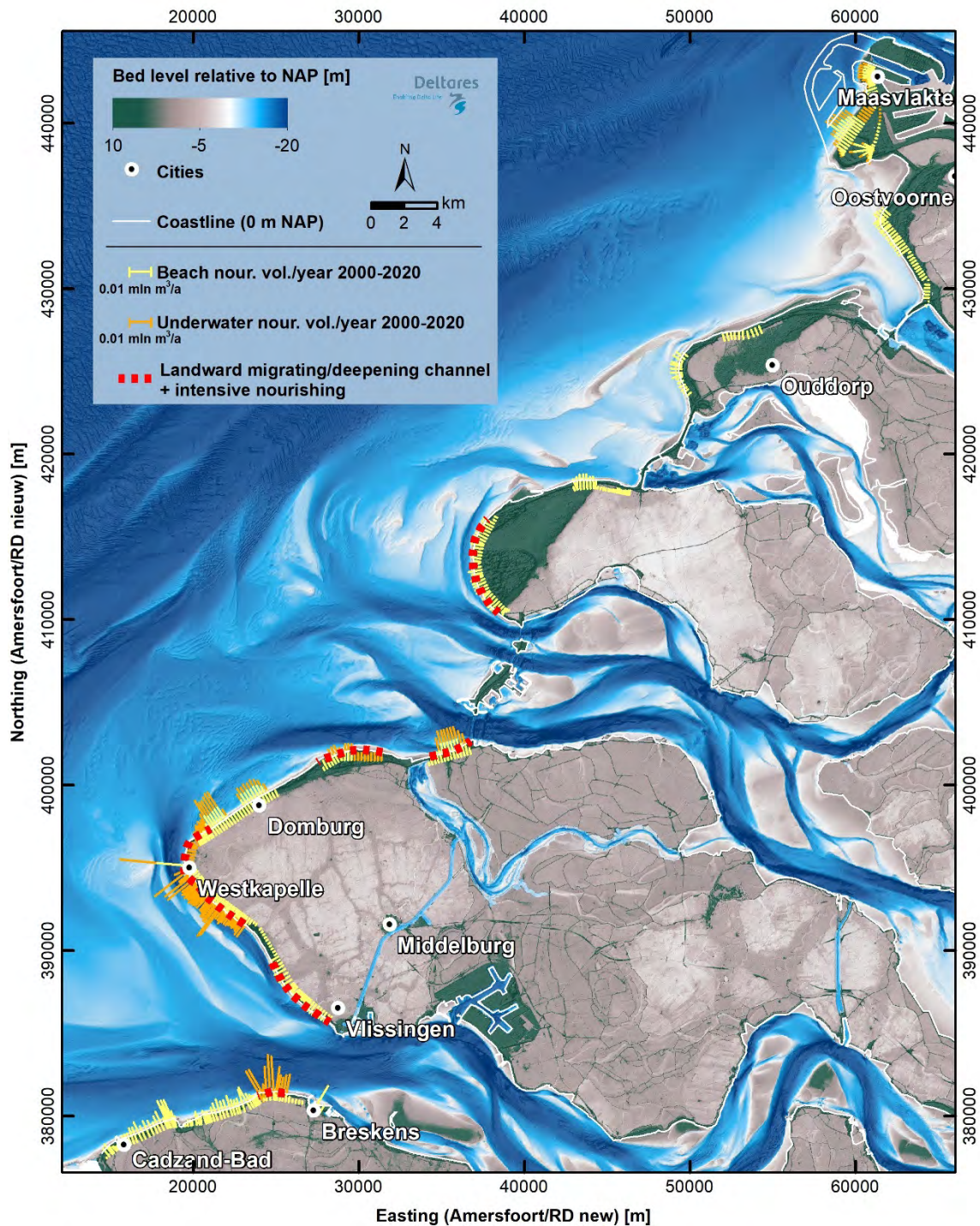


Figure 96 – Nourishments in the area of the Dutch Delta.

On- and offshore topography and yearly beach and underwater nourishment volumes per JARKUS-transect (i.e. the name of the coastal transects along the Dutch coast for which yearly bathymetric measurements are performed) averaged over the period 2000 to 2020 for the area of the Dutch Delta. For further details on how the yearly beach and underwater nourishment volumes per JARKUS-transect have been determined see Section 4.3.1 and R bke et al. (2021).

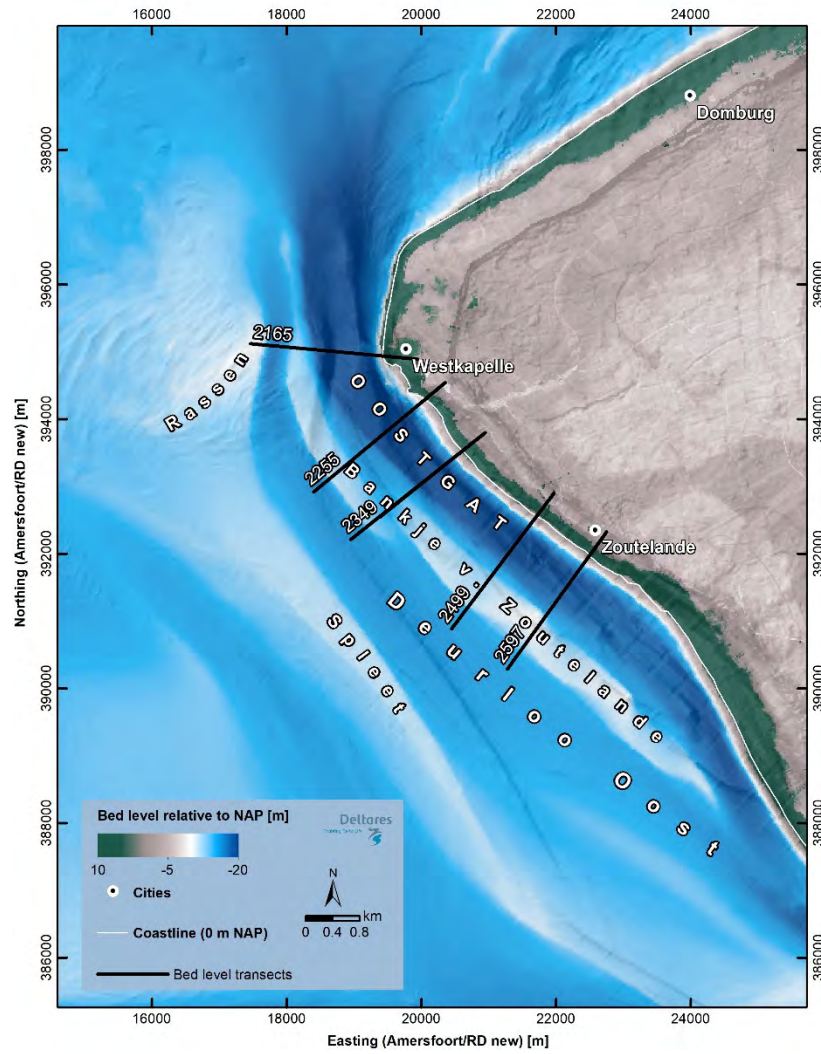


Figure 97 – On- and offshore topography in the area of the Oostgat channel east of Zeebrugge (The Netherlands) and location of the five bed level transects illustrated in Figure 98 to Figure 100.

### 4.3.3 Oostgat case study

In the following, the Oostgat channel – a landward migrating and deepening tidal channel along the south-west coast of Zeeland – is taken as an example to describe the morphological development of the channel and the nourishment volumes since the year 1970 in more detail.

The Oostgat tidal channel is located in the mouth of the Scheldt estuary along the west coast of Walcheren in the south-west of The Netherlands (Figure 97). The Oostgat channel is the second largest tidal channel of the Scheldt mouth after Wielingen and serves as a shipping route between Rotterdam and Antwerp. Seaward of the Oostgat channel there is a parallel and shallower tidal channel called Deurloo Oost. Both channels are separated from each other by the sand ridge Bankje van Zoutelande. The tidal flow in the Oostgat channel is primarily forced by a tidal range difference between Vlissingen (4.25 m) and Westkapelle (3.75 m) (van der Werf *et al.*, 2020). The most important tidal constituent is the semi-diurnal lunar tide (M2). The dominant wind direction is south-west, whereas dominant wave directions are south-west and north-west. Waves have a typical height between 0.5 m and 1.5 m.

The west coast of Walcheren along the Oostgat tidal channel suffers from structural erosion. Historically, the coast was protected by groins and – since around 1950 – by beach nourishments with an average yearly volume of about 0.2 million m<sup>3</sup>. Since these nourishments did not stop the landward migration of the Oostgat channel, an innovative scheme of channel-slope nourishments was designed. According to this scheme, sand nourishments with a total volume of 10.3 million m<sup>3</sup> have been performed along the Oostgat channel between 2005 and 2022. These nourishments have proven effective in maintaining the coastline position (Tonnon & van der Werf, 2014; van der Werf *et al.*, 2020). However, the physical processes causing the landward channel migration are not fully understood.

Figure 98 to Figure 100 illustrate the bed level evolution from 1970 to 2022 along five selected transects through the Oostgat channel (for the locations of the transects see Figure 97). All transects imply a clear migration of the shoal system towards the coast over time. The neighbouring channel Deurloo Oost has migrated landwards and the top of the Bankje van Zoutelande has steepened significantly. The erosion of the Oostgat channel is visible on the landward slope as well as a large nourishment of the channel slope in the year 2009. The landward slope of the Oostgat channel (between -5 and -15 m NAP) has been eroding with an average rate of about 0.2 m/year between 1975 and 2005 (before the channel-slope nourishments started). The erosion of both, the landward and the seaward slope of the Oostgat channel seem to accelerate after the 2005 and 2009 channel-slope nourishments (Tonnon & van der Werf, 2014). The persisting erosion and steepening of the landward slope pose a risk to the stability of the beach and dunes.

Previous studies have investigated and proposed potential mechanisms holding responsible for the erosion observed along the Oostgat channel. According to Steijn & van der Spek (2005), the dominant flood tidal flow is mainly responsible for sediment transport across the shore-parallel sand ridge Bankje van Zoutelande into the Oostgat channel with a smaller contribution by waves. This results in a slow migration of the Bankje van Zoutelande towards the coast. The landward side of the Oostgat channel needs to erode to keep its cross-sectional area to be able to discharge the water (Damen, 2014). Moreover, Steijn & van der Spek (2005) stress that the tide-dominated sand transport along the Oostgat channel diverges near Zoutelande.

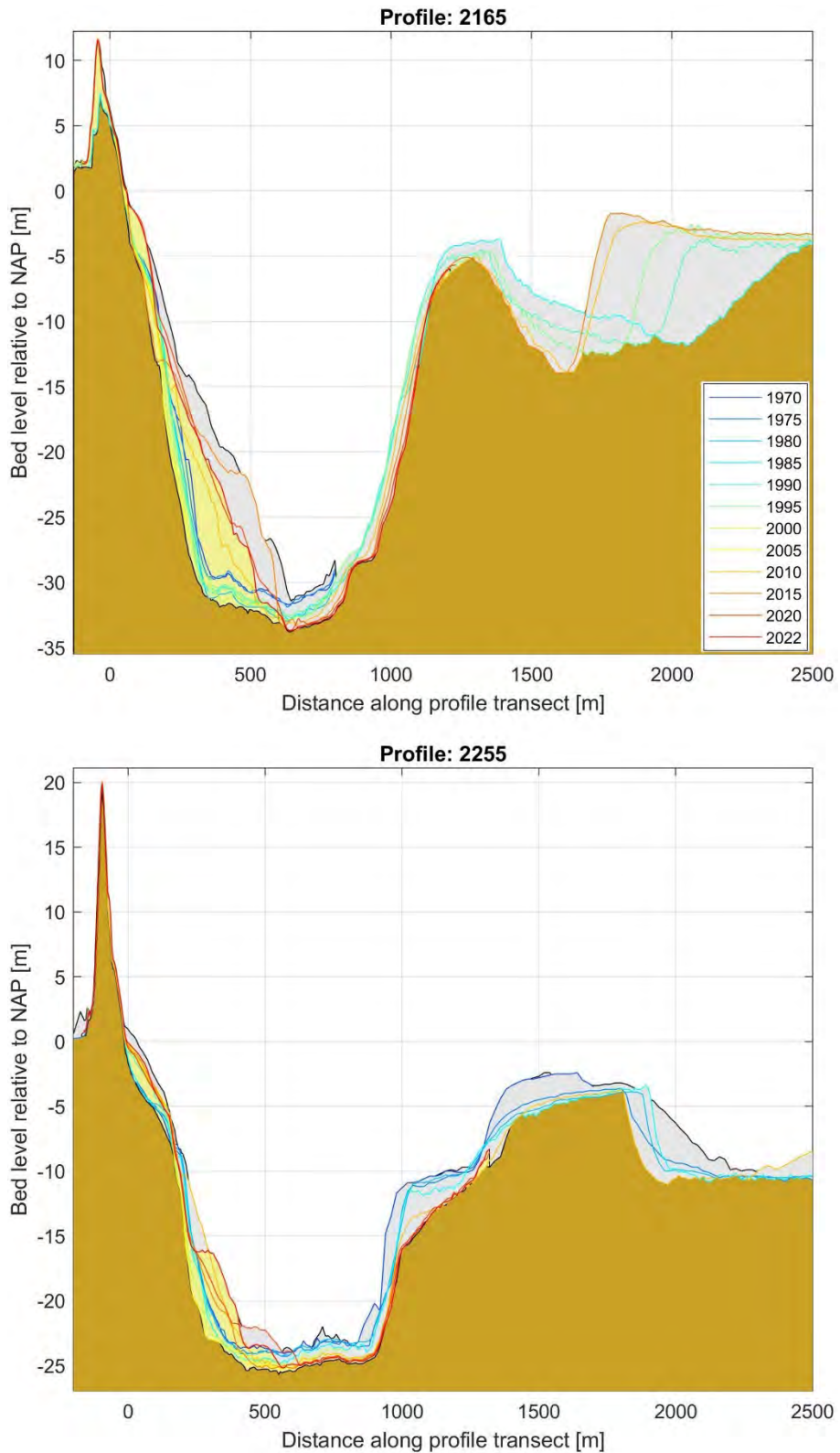


Figure 98 – Measured bed levels along the JARKUS-transects 2165 (top) and 2255 (bottom) located in the Oostgat channel (Zeeland, The Netherlands) in the period 1970 to 2022. The dark yellow area illustrates the minimum, the light grey area the maximum bed level through all illustrated measurements. The bright yellow area illustrates the most recent, i.e. the 2022 bathymetry.

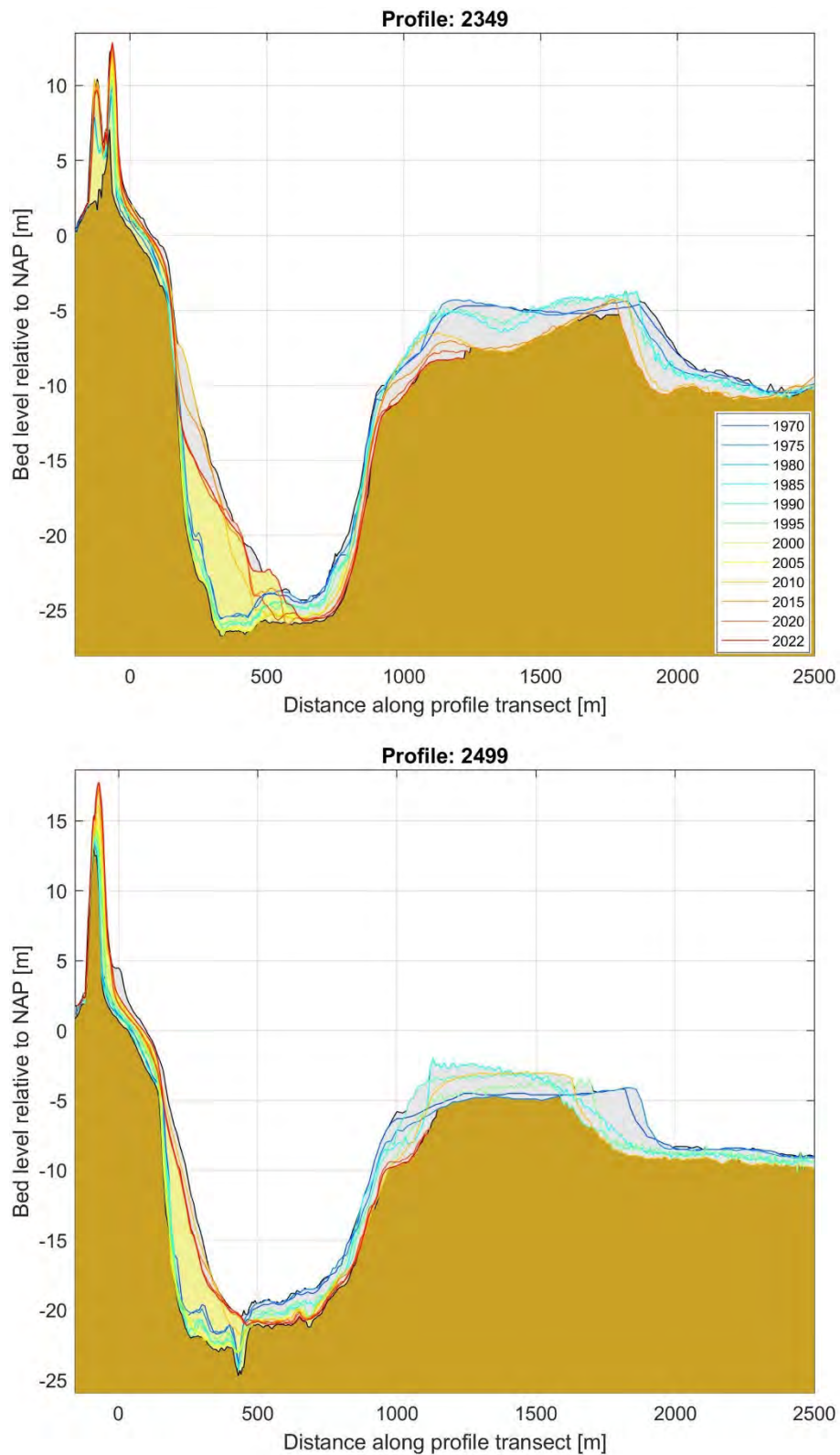


Figure 99 – Measured bed levels along the JARKUS-transects 2349 (top) and 2499 (bottom) located in the Oostgat channel (Zeeland, The Netherlands) in the period 1970 to 2022. The dark yellow area illustrates the minimum, the light grey area the maximum bed level through all illustrated measurements. The bright yellow area illustrates the most recent, i.e. the 2022 bathymetry.

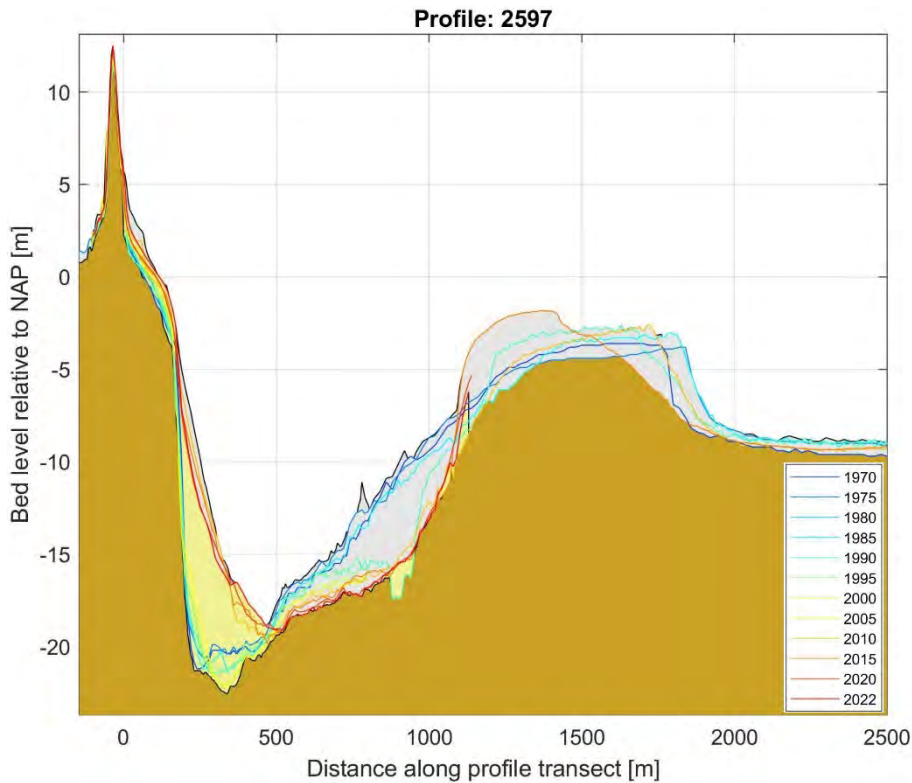


Figure 100 – Measured bed levels along the JARKUS-transect 2597 located in the Oostgat channel (Zeeland, The Netherlands) in the period 1970 to 2022. The dark yellow area illustrates the minimum, the light grey area the maximum bed level through all illustrated measurements. The bright yellow area illustrates the most recent, i.e. the 2022 bathymetry.

## 4.4 Conclusion

Geological evidence (Mathys, 2009) shows that shoreface-connected ridges and tidal sandbanks have been forming on the Belgian shelf from the moment the hydraulic regime (tides and waves) allowed. The offshore banks are interpreted as moribund shoreface-connected ridges or storm-generated ridges, which became detached when the coastline retreated under the influence of Holocene sea level rise. The present day Smalbank, Middelkerke Bank and Oostende Bank all lie on top of older storm generated ridges. The Coastal Banks, closest to the present day coastline, can only have developed since the 16<sup>th</sup> century since they overlie sediment deposits consisting of mud flats eroded by the opening and widening of the Western Scheldt mouth.

Houthuys *et al.* (2021) report that several shoreface-connected ridges appear on bathymetric maps since the 17<sup>th</sup> century. However, older charts are scarce and often didn't map the shallows. Exact positions are difficult to assess on pre-19<sup>th</sup> century maps. Only in the 19<sup>th</sup> century more reliable maps came available. Janssens *et al.* (2012) and Houthuys *et al.* (2021) showed that the nearshore banks seem to have migrated eastwards at a generalized, approximated rate of 1 to 2 km per century, and, at least locally, also shoreward, though at more reduced rates. These morphological trends still exist today (Houthuys *et al.*, 2022).

In this first working year of the MOZES-project the dataset of Houthuys *et al.* (2022) is extended with maps for 1984 – 1987. All shoreface-connected ridges and the channels separating them from the beach migrated landwards and eastwards during the past ca. 40 years. Somewhat more offshore macro bedforms such as Nieuwpoort Bank, Baland Bank, Akkaert Bank, Ravelingen and Oostende Bank, and the channels between these banks, also migrated eastwards and shorewards between 1986 and 2022, but at slightly milder rates: about 100 m shorewards and 300 to 400 m eastwards over 1987-2022. In order to investigate the behaviour of these more offshore banks and channels more seaward bathymetric maps should be investigated as well.

Based on a first comparison of the 1866 Stessels hydrographic map and the maps considered here, taking into account the low resolution of data in the Stessels map and the fact that this map probably favoured the representation of shallow points for safe navigation, there are good reasons to believe that the main described trends are persistent and have at least been going on for 1.5 century. A unique evolution however is noted for the Paardenmarkt sandbank: it was very prominent and shallow in 1866, almost completely absent in 1986 and almost regenerated in its 1866 position and depth in 2022.

The analysis of the nourishment works since the 1980's, shows how coastal authorities have a long history of elevating the beaches (and touristic sand platforms) along the Belgian coast, either by moving sand from the upper shoreface to the beach (beach scraping) or by nourishing the beach with marine sands. The former was mainly used in the 1980's and 1990's until it was completely replaced by nourishing with marine sands in the years 2000. Only since 2011, after the introduction of the "Masterplan Kustveiligheid", this methodology of annual methodology was abandoned. This might however be related to the increased safety levels defined by the Masterplan, the accompanying large nourishments carried out between 2011 and 2014, and the renewal/maintenance of the nourishments in 2017 – 2018; eliminating the need for annual maintenance. This shift in maintenance strategy can be observed in 5 coastal town areas: Sint-Idesbald – Koksijde, Bredene, Mariakerke – Oostende, De Haan and Blankenberge. At the east coast this pattern of small annual nourishments only started in 1997, probably because there was less need for sand after the large nourishments of 1977 – 1979 and 1986, related to the extension of the Zeebrugge breakwaters. Large nourishments can be related either to storm impacts (e.g. shoreface and beach in De Haan after 1990 or beach in Blankenberge after storms in 1990, 1993 and 1995), or – more recently – to the increased safety level defined by the "Masterplan Kustveiligheid".

The study of cross-shore profiles showed deepening of the Potje, Grote Rede and Appelzak tidal channels. In the Kleine Rede, from the beach until 1500 m offshore, sedimentation occurred between 1999 and 2011, thereafter the same amount of sediment was eroded again. The analysis on the inner shelf maps however showed that most of the erosion occurred in the deeper part of the Kleine Rede channel, further offshore and thus can't be seen in the (semi-)annual beach and shoreface profiles. The profile at Sint-Idesbald (Potje gully) shows a stable lower shoreface, as does the profile at Middelkerke (Kleine Rede). In Oostende the seaward movement of the lower shoreface is caused by shoreface nourishments, while the retreat of the lower shoreface at De Haan is probably a return to the natural beach profile after the large shoreface nourishments in 1990 – 1991 and 2000. In Wenduine, where the Grote Rede approaches the shoreline, and where the Belgian coastline changes orientation, erosion can be observed at the base of the shoreface. Also in the Appelzak gully the lower shoreface is eroding.

None of the chosen profiles show a natural growth of the beach and (upper) shoreface, except for the one at Sint-Idesbald on the western part of the Belgian coast and the one in front of the Zwin at the easternmost part of the Belgian coast. For all other locations there's a clear relation between nourishments and the evolution of the beach and upper shoreface profiles. Fresh beach nourishments erode first at their highest point, thereafter erosion continues gradually until the low water line.

We can thus conclude that storm events, changes in (safety) policy or nourishment method and other human factors (e.g. building the breakwaters of Oostende, excavating works at the Zwin) are the main drivers behind nourishment intensity and obscure the possible relation with the deepening of nearshore tidal channels. This human influence is further illustrated by the Dutch Oostgat case study: traditional beach nourishments proved insufficient to stop coastline retreat at the west coast of Walcheren. Large scale channel-slope nourishments were introduced, and these have proven effective in maintaining the coastline position. However, now the channel-slope on the seaward side is also eroding.

The lack of sustained periods without changes in the nourishment method during the last decades – be it due to storm events, changes in policy or construction works – made it impossible to correlate nourishment intensity to the gradual deepening of the tidal channels. Therefore, we suggest to analyze this question further by the use of numerical models in the next working years. Changes in model bathymetry might show changes in transport paths and increase or decrease of sediment fluxes to the beach.

## 5 Conclusions and outlook

### 5.1 Data acquisition

A selection of pre-2000 maps of the beach, shoreface and inner shelf has been vectorised by a subcontractor (Sparks bvba) during the second half of 2022. Three maps covering the inner shelf area from the French till the Dutch border and 10 – 15 km offshore in the period 1984 – 1987 were given priority; followed by several nearshore and beach maps. This will enable the construction of a DEM for the whole Belgian coastal area, describing the situation just after the extension of the Zeebrugge breakwaters was completed.

A preliminary analysis of the large-scale morphological changes between 1984 – 1987 and 2022 showed a much larger than expected loss of sediment (see § 4.2.1). So much that a systematic bias of the 1980's maps is suspected. The examination of the probably biased 1980's bed is proposed to be done in the second project year. The following topics would then be explored:

- depths determined using echosounding were recorded with respect to instantaneous still water level. Depths were converted to GLLWS manually or semi-automatically using their time stamp and a tidal reduction chart. The chart used in the 1980s was the 1972 Reduction chart. The correction raster `gllws_to_taw_vlaamsebanken_172.tif`, used on the data set, is valid however for the 1990 Reduction chart. The influence of the transition from the 1972 to the 1990 Reduction chart will be examined.
- SB echosoundings result in closely spaced points on tracks that are often 100 or 200 m apart. The 1980s 1/20,000 maps show a selection of measured points, often one point every 20 to 30 m. The selection in this window picked out shallow points that were printed on their real position. As a result, a bed map based on these points tends to show a surface connecting all shallowest points. This may explain part of the shallow bias. This effect will be examined using a SB dataset where both the selected map points and all recorded points are available.

After addressing these points, it is hoped that a correction grid can be established and applied to the 1984/7 dataset.

The Stessels map, a bathymetric chart much like the current nautical chart series “Vlaamse Banken”, dating from 1866, has now been fully vectorized. This map describes the situation of the Belgian coastal area before harbour breakwaters and fairway channels were introduced. Three shoreface-connected sand ridges appear on it: (i) Trapegeer – Broersbank – Den Oever, (ii) Stroombank and (iii) Wenduine bank – Paardenmarkt. Nowadays only the first is still connected to the shoreface; Stroombank is cut by the access channel to Oostende, while the outer port of Zeebrugge cuts the Wenduine bank and Paardenmarkt. This map is used to model and compare 1866 and present-day hydrodynamics and sediment transport.

Furthermore, an inventory is made of other historic data that might be of interest for the MOZES-project.

### 5.2 Modelling long-term morphodynamics

The overall aim of WP2 of the MOZES project is to investigate effects of onshore migrating shoreface-connected sand ridges (sfcr) on the Belgium shoreline by developing **a new (idealized) coupled shelf-shoreline model**, which couples a morphodynamic shelf model to a morphodynamic shoreline evolution model. The existing coupled shelf-shoreline model of Nnafie *et al.* (2021) was used as a starting point, in which a morphostatic (i.e., bed does not evolve in time) shelf model (Delft3D+SWAN) is coupled to a morphodynamic shoreline model (Q2Dmorfo). Chapter 2 of this report describes the specific activities of the first year of WP2, which comprise 1) the development of a **new morphodynamic shelf model** in which the bed evolves in time such that sfcr spontaneously develop on the shelf on decadal and centennial time scales (Activity 1); and 2) the application of the coupled shelf-shoreline model of Nnafie *et al.* (2021) to the Belgium coast to explore potential effects of onshore migrating sfcr on the evolution of the shoreline (Activity 2).

**The conclusions are:**

1. The new morphodynamic shelf model has successfully reproduced the offshore (onshore) deflection of flow and transport fields over crests (troughs) of shelf ridges, which is considered as the growth mechanism responsible for growth of shoreface-connected sand ridges in micro-tidal conditions.
2. The new shelf model was capable of reproducing ridges with characteristics similar to those of observed sfc on the Long-Island inner shelf.
3. The adaption of coupled model of Nnafie *et al.* (2021) such that it includes tides and its background bathymetry (without the artificial sfc that were imposed) is more representative for the Belgium coast. Preliminary results suggest that an onshore movement of sfc is expected to induce stronger undulations along the shoreline.

These achievements are believed to be great steps forward towards establishing the ultimate tool to study the coupled shelf-shoreline morphodynamics in the Belgium coastal zone. However, the new morphodynamic shelf model, as well as the coupled shelf-shoreline model **are not yet ready to be used** to make any statements on potential impacts of sfc on the Belgium shoreline. This is because many adjustments still have to be done, of which the most important ones are:

- **Morphodynamic shelf model**: inclusion of tides, use of more realistic waves, account for sea-level rise and the use of a background bathymetry that is more representative for the Belgium inner shelf. These adjustments are suggested as key topics for year 2 of the MOZES project.
- **Coupled shelf-shoreline model of Nnafie *et al.* (2021)**: the used artificial sfc were not representative for the observed ridges on the Belgium inner shelf. Instead, artificial ridges should be created that have similar geometries as the sfc that are present on the Belgium shelf (Figure 18). Furthermore, realistic waves should be considered whose characteristics (wave height, wave angle and wave period) reflect the wave climate of the Belgium coast. These two issues are suggested to be addressed in year 2 of the MOZES project.

Ultimately, once the morphodynamic shelf model would be able to successfully reproduce the gross characteristics of the observed sfc on the Belgium inner shelf, it will be also coupled to the shoreline evolution model. With this new (fully morphodynamic) coupled shelf-shoreline model, the impact of human interventions (e.g., construction of harbours, nourishments, ...) and sea-level rise on the evolution of sfc and the shoreline can also be investigated.

### 5.3 Natural feeding of the beach

With regard to the research question, whether the Belgian coastline is naturally nourished by sediment transport from shoreface connected sand ridges to the beaches, the following conclusions can be made:

- The evaluation of the Scaldis-Coast model results, FM-FlemCo model results and the preliminary SedTRAILS analysis indicate that landward directed sediment transport occurs over the sand ridges Trapegeer-Broersbank-Den Oever and Stroombank, which potentially nourishes the adjacent coastline.
- The FM-FlemCo model shows that the landward directed transport on the shoreface is particularly associated with wave-related sediment transport, while the tide-related sediment transport mainly occurs parallel to the coastline. This landward-directed transport on the shoreface is however not observed in the Scaldis-Coast model, which might be an indication of a lack of cross-shore wave induced processes in the openTELEMAC modelling suite. New developments in the openTELEMAC code made by the Scaldis-Coast team (Kolokythas *et al.*, 2020) in order to implement wave induced cross-shore processes like a modification of the depth-averaged flow velocities under the influence of Stokes drift and return flow and wave non-linearity, should be tested.

- The streamlines based on the simulated cumulative yearly sediment transport in the Scaldis-Coast model show converging sediment paths on top of the Paardenmarkt and diverging sediment paths in the Appelzak gully. This can indicate sedimentation – respectively erosion – zones, which is in accordance with the observed morphological changes: the Paardenmarkt sand ridge has consistently been gaining height since the 1980's, while the Appelzak has deepened. In the SedTRAILS analysis from the FM-FlemCo results, no landwards transport on top of the Paardenmarkt is observed.

The observed differences between both complex process based numerical models should be studied in more detail, to better understand how these processes work and how they are implemented. The use of other process based models renowned for nearshore and beach morphology, like e.g. XBeach, in future working years should not be ruled out a priori.

Although the current study implies landward-directed sediment transport from the sand ridges towards the coast and by this indicates a potential natural nourishment of the adjacent coastline, further research has to be carried out whether the landward transported sediment indeed nourishes the beaches. Moreover, the exact processes that lead to wave-related landward direct sediment transport have to be investigated further, as well as the extent of the interaction of tide and waves influencing this transport.

Finally, it is suggested to apply a more advanced and extensive interpolation method (such as the kriging interpolation method) to generate the 1866 model bathymetry, which will result in a smoother bed and by this a more realistic representation of the actual 1866 bathymetry. The current, relatively angular model bathymetry, which was derived from a TIN (triangular irregular network) has, most likely, significant impact on the simulated sediment transport and derived sediment pathways. The 1866 version of the Scaldis-Coast model is still in preparation. A comparison of the 1866 versions of both FlemCo and Scaldis-Coast (with improved representation of the bathymetry, if possible) should be conducted in the next working year.

## 5.4 Effects of gradual deepening of nearshore tidal channels on beach erosion and nourishment intensities

Thanks to the addition of the 1984 – 1987 DEM, the geographical base dataset of Houthuys *et al.* (2022) is extended backwards in time with almost 20 years. More maps (time steps) will be added to the analysis as soon as they will be available during the MOZES-project. After evaluating the echosounding accuracy and datum issues for the 1980's maps, volume balances will be established in relation to large regions that display similar behaviour.

Summarizing the first (preliminary) observations, all nearshore tidal channels have deepened, and all macroforms (banks and channels) along the Belgian shore migrate alongshore to the east and cross-shore to the coast. Morphological migration rates vary between 3 and 20 m/y. The morphological migration rates appear to decrease in offshore direction. The influence of offshore dredge disposal on bed morphology extends a few hundred metres in cross-shore and a few kilometres in longshore direction. These sites are important supply points for the local area. It is clear that tidal currents rework and redistribute the disposed sediment to the east in the longshore direction. Zeebrugge's outer dams have significantly changed the surrounding morphology over several kilometres in all directions. While sedimentation characterizes the sheltered areas west and east of the dams, strong erosion is found in a wide area at the offshore side of the harbour. A similar response, but at the correspondingly smaller scale of that harbour, is found after the construction of Oostende's outer dams around 2010.

The analysis of the nourishment works shows how coastal towns along the Belgian coast are the location of a long history of (touristic) beach replenishment (elevation), either by moving sand from the upper shoreface to the beach (beach scraping) or by nourishing the beach with marine sands. The former was mainly used in the 1980's and 1990's until it was completely replaced by nourishing with marine sands in the years 2000.

Only since 2011, after the introduction of the “Masterplan Kustveiligheid”, this methodology of annual nourishments was abandoned. This might be related to the increased safety levels defined by the Masterplan: the accompanying large nourishments carried out between 2011 and 2014, and the renewal/maintenance of those nourishments in 2017 – 2018; eliminating the need for annual maintenance. Large nourishments can be related either to storm impacts (e.g. shoreface and beach in De Haan after 1990 or beach in Blankenberge after storms in 1990, 1993 and 1995), or – more recently – to the increased safety level defined by the “Masterplan Kustveiligheid”.

The literature review and data analysis for the Dutch coast showed several locations at the Dutch coast, where landward migrating/deepening tidal channel occur and – at the same time – large beach and/or underwater nourishments have been performed in the last 20 years. The case study of the Oostgat showed how large-scale channel-slope nourishments have proven effective in maintaining the coastline position. However, at the same time the channel-slope nourishments at the landward side of the channel seem to have increased the erosion on the slope at the seaward side of the channel.

The analysis of beach and shoreface nourishment intensity showed that storm events, changes in (safety) policy or nourishment method and other human factors are the main drivers behind nourishment intensity and obscure the possible relation with the deepening of nearshore tidal channels. The case study of the Oostgat even showed how human intervention can influence the morphological behaviour across the whole tidal channel. Therefore, we suggest to analyze this research question further by the use of numerical models in the next working years. Changes in model bathymetry might show changes in transport paths and increase or decrease of sediment transport toward the beach.

## 6 References

- Ad-Hoc-AG Boden** (2005). *Bodenkundliche Kartieranleitung*. 5<sup>th</sup> edition. Schweizerbart Science Publishers: Hannover.
- Antia, E. E.** (1996). Shoreface-connected ridges in German and US Mid-Atlantic Bights: similarities and contrasts. *Journal of Coastal Research* 12 (1): 141–46.
- Arriaga, J.; Rutten, J.; Ribas, F.; Falqués, A.; Ruessink, G.** (2017). Modeling the Long-Term Diffusion and Feeding Capability of a Mega-Nourishment. *Coastal Engineering* 121: 1–13. <https://doi.org/10.1016/j.coastaleng.2016.11.011>
- Baeye, M.; Fettweis, M.; Voulgaris, G. & van Lancker, V.** (2010). Sediment mobility in response to tidal and wind-driven flows along the Belgian inner shelf, southern North Sea. *Ocean Dynamics*, 61, pp. 611–622. doi: 10.1007/s10236-010-0370-7.
- Bijker E.W.** (1968). Mechanics of sediment transport by the combination of waves and current. In *Design and Reliability of Coastal Structures*, pages 147–173. 23rd Int. Conf. on Coastal Engineering.
- Bijker, E.W.** (1971). Longshore transport computations. ASCE, J. Waterw., Harbours Coastal Eng. Div., 97 (WW4).
- Bliek, B.; de Gelder, A.; Gautier, C. & Les, B.** (1998). De rol van het getij in de morfologische ontwikkeling van de Westerscheldmond. Een modelmatige onderbouwing. Eindrapport getijreconstructie Westerscheldmond. in: Svasek (Ed.). Svasek rapporten. Vol. K2000\*KOP.
- Bolle, A.; Wang, Z.; Amos, C. & Ronde, J.** (2010). The influence of changes in tidal asymmetry on residual sediment transport in the Western Scheldt. *Continental Shelf Research*, 30, pp. 871– 882. doi: 10.1016/j.csr.2010.03.001
- Calvete, D.; Falqués, A.; de Swart, H. E.; Walgreen, M.** (2001). Modelling the formation of shoreface-connected sand ridges on storm-dominated inner shelves. *Journal of Fluid Mechanics* 441: 169–93. <https://doi.org/10.1017/S0022112001004815>.
- Chaves, M.A.** (2022). Sediment Pathways on the Voordelta. Deltares report 11208035-004. Delft, The Netherlands.
- CHC** (2011). Blue Kenue – Reference Manual – Sept. 2011. Canadian Hydraulics Centre/Centre d’Hydraulique Canadien, National Research Council, Ottawa, Ontario, Canada.
- Damen, J.** (2014). Coastal Erosion Processes in Tidal Channel Oostgat. Master’s thesis. University of Twente, The Netherlands.
- Deltares** (2021). SuperTrans – MATLAB toolbox for coordinate transformation. OpenEarthTools, revision 17309 d.d. 26/05/2021; Deltares.
- Deltares** (2022a). D-Flow Flexible Mesh. D-Flow FM in Delta Shell. User manual, version 1.5.0. <https://www.deltares.nl/app/uploads/2020/01/Documentation-Delft3D-FM-Suite-2020.02-1.6.1.zip>. 2020-01-30.
- Deltares** (2022b). D-Waves. Simulation of short-crested waves with SWAN. User manual, version 1.2. <https://www.deltares.nl/app/uploads/2020/01/Documentation-Delft3D-FM-Suite-2020.02-1.6.1.zip>. 2020-01-30.
- Deltares** (2022c). D-Morphology, 1D/2D/3D. D-Morphology in Delta Shell. User manual, version 1.5. <https://www.deltares.nl/app/uploads/2020/01/Documentation-Delft3D-FM-Suite-2020.02-1.6.1.zip>. 2020-01-30.

- Deltares** (2022d). Beheerbibliotheken: alle kustkennis samengevat. <https://publicwiki.deltares.nl/display/BOK/III.+Producten++Communicatie>. 2022-11-01.
- De Maerschallck, B.; van der Werf, J.; Kolokythas, G.; Qutaert, E.; van Oyen, T.; Dijkstra, J.; Vanlede, J. & Mostaert, F.** (2017). Modelling Belgische Kustzone en Scheldemonding, Deelrapport 2 — Morfologische analyse scenario's Vlaamse Baaien. in: Waterbouwkundig Laboratorium Antwerpen (Belgium) (Ed.). WL Rapporten. Vol. 15\_068\_2.
- de Rooy, W. & de Vries, H.** (2017). Harmonie verification and evaluation. in: KNMI — Royal Netherlands Institute (Ed.). Technical Report. Vol. 70.
- Duane, D. B.; Field, M. E.; Meisburger, E. P.; Swift, D. J. P.; Williams, S. J.** (1972). Linear Shoals on the Atlantic Inner Continental Shelf, Florida to Long Island. Edited by D. J. P. Swift D. B. Duane, Hutchinson O. H. Pilkey; Dowden, and Stroudsburg Ross. In: *Shelf Sediment Transport: Process and Pattern*, 447–98.
- Esri** (2022). World Imagery. <https://www.arcgis.com/home/item.html?id=10df2279f9684e4a9f6a7f08febac2a9>. 2022-11-25.
- Elias, E.P. & Pearson, S.** (2020). SedTRAILS - Sediment TRANsport visualization & Lagrangian Simulator: A novel method to visualize and analyse sediment transport pathways. Deltares report. Delft, The Netherlands.
- Fettweis, M.; Nechad, B. & van den Eynde, D.** (2007). An estimate of the suspended particulate matter (SPM) transport in the southern North Sea using SeaWiFS images, in situ measurements and numerical model results. *Continental Shelf Research*, 27, pp. 1568–1583. doi: 10.1016/j.csr.2007.01.017.
- Fettweis, M.; van den Eynde, D.** (2003). The mud deposits and the high turbidity in the Belgian-Dutch coastal zone, southern bight of the North Sea. *Continental Shelf Research*, 23, pp. 669–691. doi: 10.1016/S0278-4343(03)00027-X
- Geopunt Vlaanderen** (2022). Orthofotomozaïek, middenschalig, winteropnamen, kleur, meest recent, Vlaanderen. Laatste wijziging: 2022-04-13. Vlaamse Overheid - Metadata Vlaanderen. <https://metadata.vlaanderen.be/srv/dut/catalog.search#/metadata/418e8e4a-12c1-80a8-8306-fcf4-799c-581d-c4e38594>
- Grasmeijer, B.; Röbbke, B.R.; van der Werf, J.** (2020). The Delft3D-FM Flemish Coast Model. Set-up of sediment transport and morphology and first steps towards calibration and validation. Deltares report, vol. 1210301-001-ZKS-0014. Delft, The Netherlands.
- Houthuys, R.; Vos, G.; Dan, S.; Verwaest, T.** (2021). Long-term morphological evolution of the Flemish coast: Holocene, Late Middle Ages to present. Version 1.0. FHR Reports, 14\_023\_1. Flanders Hydraulics Research: Antwerp.
- Houthuys, R.; Verwaest, T.; Dan, S.** (2022). Morfologische trends aan de Belgische Kust: Evolutie van de Vlaamse kust tot 2019. Versie 3.0. WL Rapporten, 18\_142\_1. Waterbouwkundig Laboratorium: Antwerpen.
- Huthnance, J. M. (1982).** On One Mechanism Forming Linear Sand Banks. *Estuarine, Coastal and Shelf Science* 14 (1): 79–99.
- IGN** (2022). Ressources de services web. République Française, Institut National de l'Information Géographique et Forestière (IGN) – géoservices. [https://geoservices.ign.fr/documentation/services/tableau\\_ressources](https://geoservices.ign.fr/documentation/services/tableau_ressources)
- ISO — International Organization for Standardization** (2002). ISO 14688-1:2002. Geotechnical investigation and testing — identification and classification of soil — part 1: identification and description. <https://www.iso.org/standard/25260.html>. 2017-08-30.
- Janssens, J.; Reyns, J.; Verwaest, T.; Mostaert, F.** (2012). Morfologische evolutie van het Belgisch continentaal plat gedurende de laatste 150 jaar: Deelrapport in het kader van het Quest4D-project. Versie 2\_0. WL Rapporten, 814\_02. Waterbouwkundig Laboratorium: Antwerpen, België.

- Kadaster** (2022). TOPNL – administrative and spatial data on property and rights involved. The Netherlands' Cadastre, Land Registry and Mapping Agency. <https://www.kadaster.nl/zakelijk/producten/geo-informatie/topnl>
- Kato, T.** (2016). Chapter 4 - Prediction of photovoltaic power generation output and network operation. in: FUNABASHI, T. (Ed.). Integration of distributed energy resources in power systems. pp. 77–108. Academic Press: London. doi: 10.1016/B978-0-12-803212-1.00004-0.
- Kolokythas, G.; De Maerschack, B.; Wang, L.; Fonias, S.; Breugem, A.; Vanlede, J.; Mostaert, F.** (2021). Modelling Belgian coastal zone and Scheldt mouth area: Sub report 12: Scaldis-Coast model – Model setup and validation of the 2D hydrodynamic model. Version 4.0. FHR Reports, 15\_068\_12. Flanders Hydraulics Research: Antwerp.
- Kolokythas, G.; Fonias, S.; Wang, L.; De Maerschack, B.; Vanlede, J.; Mostaert, F.** (2020). Modelling Belgian Coastal zone and Scheldt mouth area: Sub report 14: Scaldis-Coast model – Model setup and validation of the morphodynamic model. Version 0.1. FHR Reports, 15\_068\_14. Flanders Hydraulics Research: Antwerp.
- Macdonald, N.; Davies, M.; Zundel, A.; Howlett, J.; Demirbilek, Z.; Gailani, J.; Lackey, T.; Smith, J.** (2006). PTM: Particle Tracking Model. Report 1: Model Theory, Implementation, and Example Applications. 168.
- Mathys, M.** (2009). The Quaternary geological evolution of the Belgian Continental Shelf, southern North Sea. PhD thesis, Ghent University, Belgium.
- MDK – Maritieme Dienstverlening en kust** (2022). Meetnet Vlaamse Banken. Wave measurements at Westhinder station. <https://meetnetvlaamsebanken.be/Download#> 2022-07-01.
- NGI** (2022a). CartoWeb.be: WMTS/WMS, schaal 1:2.500 tot 1:4.000.000. Nationaal Geografisch Instituut België. <https://www.ngi.be/website/aanbod/digitale-geodata/cartoweb-be/>
- NGI** (2022b). cConvert – Hulpmiddelen voor transformatie van coördinaten. Nationaal Geografisch Instituut België. <https://www.ngi.be/website/hulpmiddelen-voor-transformatie-van-coordinaten/>
- Nnafie, A.; de Swart, H. E.; Falqués, A. & Calvete, D.** (2021). Long-term morphodynamics of a coupled shelf-shoreline system forced by waves and tides, a model approach. *Journal of Geophysical Research: Earth Surface*, 126 (12).
- Nnafie, A.; de Swart, H. E.; Garnier, R.; Calvete, D.** (2014a). Modeling the Response of Shoreface-Connected Sand Ridges to Sand Extraction on an inner Shelf. *Ocean Dynamics* SC: 1–18. <https://doi.org/10.1007/s10236-014-0714-9>.
- Parker, G.; Lanfredi, N. W.; Swift, D. J. P.** (1982). Seafloor response to flow in a southern hemisphere sand-ridge field: Argentine inner shelf. *Sedimentary Geology* 33 (3): 195–216.
- Pawlowicz, R.; Beardsley, B. & Lentz, S.** (2002). Classical tidal harmonic analysis including error estimates in MATLAB using T\_TIDE. *Computers & Geosciences*, 28, pp. 929–937. doi: 10.1016/S0098-3004(02)00013-4.
- Pearson, S.G.** (2021). SedTRAILS Development. User manual.
- Pearson, S.G.; Elias, E.P.; van Ormondt, M.; Roelvink, F.E.; Lambregts, P.; Wang, Z.B. & van Prooijen, B.C.** (2021). Lagrangian sediment transport modelling as a tool for investigating coastal connectivity. In: Coastal Dynamics 2021. Delft, The Netherlands.
- Ribas, F.; Falqués, A; de Swart, H.E.; Dodd, N; Garnier, R.; Calvete, D.** (2015). Understanding Coastal Morphodynamic Patterns from Depth-Averaged Sediment Concentration. *Reviews of Geophysics* 53. <https://doi.org/10.1002/2014RG000457>.
- Röbke, B.R., Gawehn, M. & van der Werf, J.** (2018). The morphodynamic Delft3D-Vlaamse Baaien model. Deltares report, vol. 1210301-001-ZKS-0007. Delft, The Netherlands.
- Röbke, B.R.; Grasmeyer, B.; van der Werf, J.** (2020). The Delft3D-FM Flemish Coast Model. Model set-up and hydrodynamic validation. Deltares report, vol. 1210301-001-ZKS-0009. Delft, The Netherlands.



- Trouw, K.; Zimmermann, N.; Wang, L.; De Maerschack, B.; Delgado, R.; Verwaest, T. & Mostaert, F.** (2015). Scientific support regarding hydrodynamics and sand transport in the coastal zone: literature and data review coastal zone Zeebrugge–Zwin. WL Rapporten, 12\_107. Flanders Hydraulics Research/IMDC: Antwerp.
- Van Cauwenberghe, C.** (1971). Hydrografische analyse van de Vlaamse banken langs de Belgisch-Frans kust. Hydrografische Dienst van de Kust, Oostende, Belgium.
- Van de Meene, J. W. H.; Boersma, J. R.; Terwindt, J. H. J.** (1996). Sedimentary structures of combined flow deposits from the shoreface-connected ridges along the central Dutch coast. *Marine Geology* 131 (3-4): 151–75.
- van der Werf, J.; Damen, J.M.; Roos, P.C.; Vroom, J.; Elias, E. & Hulscher, S.J.** (2020). Erosion mechanism of the landward Oostgat tidal channel slope, The Netherlands. *Continental Shelf Research*, 193, pp. 1–10. doi: 10.1016/j.csr.2019.104027.
- van der Wegen, M.; van der Werf, J.; de Vet, P. & Rübke, B.R.** (2017). Hindcasting Westerschelde mouth morpho- dynamics (1963–2011). Deltares report, vol. 1210301-001-ZKS-0006. Delft, The Netherlands.
- Van Lancker, V.; Baeye, M.; Du Four, I.; Janssens, R.; Degraer, S.; Fettweis, M.; Francken, F.; Houziaux, J.S.; Luyten, P.; Van den Eynde, D.; Devolder, M.; De Cauwer, K.; Monbaliu, J.; Toorman, E.; Portilla, J.; Ullman, A.; Liste Muñoz, M.; Fernandez, L.; Komijani, H.; Verwaest, T.; Delgado, R.; De Schutter, J.; Levy, Y.; Vanlede, J.; Vincx, M.; Rabaut, M.; Vandenberghe, N.; Zeelmaekers, E.; Goffin, A.** (2012). Quantification of Erosion/Sedimentation patterns to Trace the natural versus anthropogenic sediment Dynamics “QUEST4D”. Final Report Brussels: Belgian Science Policy Office 2012 – 103 p. SD/NS/06 Research Program Science for a Sustainable Development.
- van Maren, D.S.; Vroom, J.; Fettweis, M. & Vanlede, J.** (2020). Formation of the Zeebrugge coastal turbidity maximum: the role of uncertainty in near-bed exchange processes. *Marine Geology*, 425, pp. 1–18. doi: 10.1016/j.margeo.2020.106186.
- van Rijn, L.** (2007). Unified view of sediment transport by currents and waves. I: Initiation of motion, bed rough- ness, and bed-load transport. *Journal of Hydraulic Engineering*, 133, pp. 649–667. doi: 10.1061/(ASCE)0733-9429(2007)133:6(649).
- Vandebroek, E.; Dan S.; Vanlede, J.; Verwaest, T. & Mostaert, F.** (2017). Sediment Budget for the Belgian Coast: Final report. Version 2.0. FHR Reports, 12\_155\_1. Flanders Hydraulics Research: Antwerp & Antea Group.
- Verwaest, T.; Dan, S.; De Maerschack, B.; Sol, S.** (2021). Onderzoek van de morfologische interactie tussen de kustnabije banken en geulen en de strandzone. WL Projectplan WL2021P20\_079\_1.
- Verwaest, T.; Delgado, R.; Janssens, J.; Reyns, J.** (2010). Longshore sediment transport along the Belgian coast. Paper abstract submitted for the Coastal Sediments conference, Miami, US, 2-6 May 2011.
- Verwaest, T.; Delgado, R.; Janssens, J.; Reyns, J.** (2011). Longshore sediment transport along the Belgian coast, in: Coastal sediments 2011: "Bringing Together Theory and Practice", May 2-6, Hyatt Regency Miami, Miami, Florida, USA: proceedings. pp. 1528-1538
- Verwaest, T.; Dujardin, A.; Montreuil, A.-L.; Trouw, K.** (2022). Understanding Coastal Resilience of the Belgian West Coast. *Water*, 14, 2104. <https://doi.org/10.3390/w14132104>
- Vis-Star, N. C.; de Swart, H. E.; Calvete, D.** (2008). Patch behaviour and predictability properties of modelled finite-amplitude sand ridges on the inner shelf. *Nonlinear Processes in Geophysics* 15: 943–55.
- Vittori, G.; Blondeaux, P.** (2022). Predicting Offshore Tidal Bedforms Using Stability Methods. *Earth-Science Reviews* 235: 104234. <https://doi.org/doi.org/10.1016/j.earscirev.2022.104234>.
- Vlaamse Hydrografie** (2011). Overzicht van de tijwaarnemingen langs de Belgische kust. Periode 2001–2010 voor Nieuwpoort, Oostende en Zeebrugge. Ministrie van de Vlaamse Gemeenschap: Oostende (Belgium).

- Vroom, J., van Maren, B., van der Werf & van Rooijen, A.** (2016). Zand-slib modellering voor het mondingsgebied van het Schelde-estuarium. in: Deltares Delft (Netherlands) (Ed.). Deltares report, vol. 1210301-002-ZKS-002. Delft, The Netherlands.
- Wang, Z., Jeuken, M., Gerritsen, H., de Vriend, H., Kornman, B.** (2002). Morphology and asymmetry of the vertical tide in the Westerschelde estuary. *Continental Shelf Research*, 22, pp. 2599–2609. doi: 10.1016/S0278-4343(02)00134-6.
- Wang, L.; Zimmermann, N.; Trouw, K.; Delgado, R.; Bolle, A.; Toro, F.; Verwaest, T. & Mostaert, F.** (2013). Scientific support regarding hydrodynamics and sand transport in the coastal zone. Longshore modelling: Realistic Blankenberge case. Version 2\_0. WL Rapporten, 00\_072. Flanders Hydraulics Research & IMDC: Antwerp, Belgium.
- Wang, L.; Zimmermann, N.; Trouw, K.; De Maerschalck, B.; Delgado, R.; Verwaest, T.; Mostaert, F.** (2015). Scientific support regarding hydrodynamics and sand transport in the coastal zone: Calibration of a Long term morphological model of the Belgian shelf. Version 4.0. WL Rapporten, 12\_107. Flanders Hydraulics Research & IMDC: Antwerp, Belgium.
- Wang, L., Kolokythas, G., Fonias, S., De Maerschalck, B., Vanlede, J., Mostaert, F.** (2021). Modelling Belgian coastal zone and Scheldt mouth area: Sub report 13: Scaldis-Coast model – Model setup and validation of the wave propagation model. Version 4.0. FHR Reports, 15\_068\_13. Flanders Hydraulics Research: Antwerp.
- Zijl, F.** (2013). Development of the next generation Dutch continental shelf flood forecasting models. Set-up, calibration and validation. Deltares report, vol. 1205989-003-ZKS-0002. Delft, The Netherlands.
- Zijl, F.** (2014). Noordzee modellen – release 2014. In Deltares Delft (Netherlands), ed., Deltares report, vol. 1209448-003-ZKS-0002. Delft, The Netherlands.

# Appendix 1 Documents on the outsourced vectorization work

## Location of pdf documents

[p:\20\\_079-MorfoInteract\3\\_Uitvoering\Deeltaak1\\_DataAcquisition\VectorisatieKustplannen\UitbestedingVectorisatie](p:\20_079-MorfoInteract\3_Uitvoering\Deeltaak1_DataAcquisition\VectorisatieKustplannen\UitbestedingVectorisatie) and then subfolders per grouped task.

## Work description

See pdf document: Vectorisatie Kustplannen.pdf

## Selection report

See pdf document: EvaluatieOffertesVectorisatie.pdf

## Acceptation reports

See pdf documents:

- EvaluatieLeveringDeelopdr1.pdf,
- EvaluatieLeveringDeelopdr2.pdf,
- EvaluatieLeveringDeelopdr3.pdf

## Appendix 2 Supplementary info on the setup of the longterm morphodynamic models

### Appendix 2.1 Supplementary info on §2.2 (WP 2, Activity 1)

#### Wave orbital velocity $u_{rms}$

The rms amplitude of the wave orbital velocity is computed using the parametrization of Calvete *et al.* (2001):

$$u_{rms}(y) = u_{rms0} \left( \frac{H_0}{H(y)} \right)^{m/2}. \quad (A1)$$

Here,  $u_{rms0}$  is the orbital velocity at the landward side of the domain ( $y = L_y$ ) and  $m$  is a constant parameter.

#### Initial bed-level profile

The chosen initial bed-level profile,  $z_b(x, y, 0) = -H(y)$  (Figure 22b), is uniform in the alongshore direction. In the seaward direction (negative  $y$ -direction),  $H(y)$  increases linearly over a distance  $L$  (width of the inner shelf,  $L_y - L \leq y \leq L_y$ ), according to the formula

$$H(y) = \begin{cases} \beta(L_y - y) + H_0, & \text{if } L_y - L \leq y \leq L_y \\ H_L & \text{if } 0 \leq y \leq L_y - L, \end{cases} \quad (A2)$$

with  $H_0$  the depth at the landward side ( $y = L_y$ ),  $\beta = (H_L - H_0)/L$  is the slope of the inner shelf. A constant depth ( $H_L$ ) on the outer shelf ( $0 \leq y \leq L_y - L$ ) is assumed.

#### Characteristics of simulated bedforms

The characteristics of the simulated bedforms by the morphodynamic shelf model were analysed in terms of their root-mean-square (rms) height  $\|h\|$ , global growth rate  $\sigma$ , global migration speed  $V_m$  and their longshore dominant spacing (wavelength). The global growth rate  $\sigma$  is defined as

$$\sigma \equiv \frac{1}{\|h\|^2} \overline{h \frac{\partial h}{\partial t}}, \quad (A3)$$

where the overline " $\overline{\quad}$ " denotes an averaging over the entire model domain. The global migration of the bedforms which is given by

$$V_m \equiv - \frac{1}{\left( \frac{\partial h}{\partial y} \right)^2} \overline{\frac{\partial h}{\partial y} \frac{\partial h}{\partial t}}, \quad (A4)$$

Finally, the longshore dominant spacing (wavelength) of the ridges that develop on the shelf is analysed. To this end, the discrete Fourier transform of bottom perturbations  $h$  are computed along the longshore transect  $y = 8$  km.

## Appendix 2.2 Supplementary info on §2.3 (WP 2, Activity 2)

### Domain coupled model

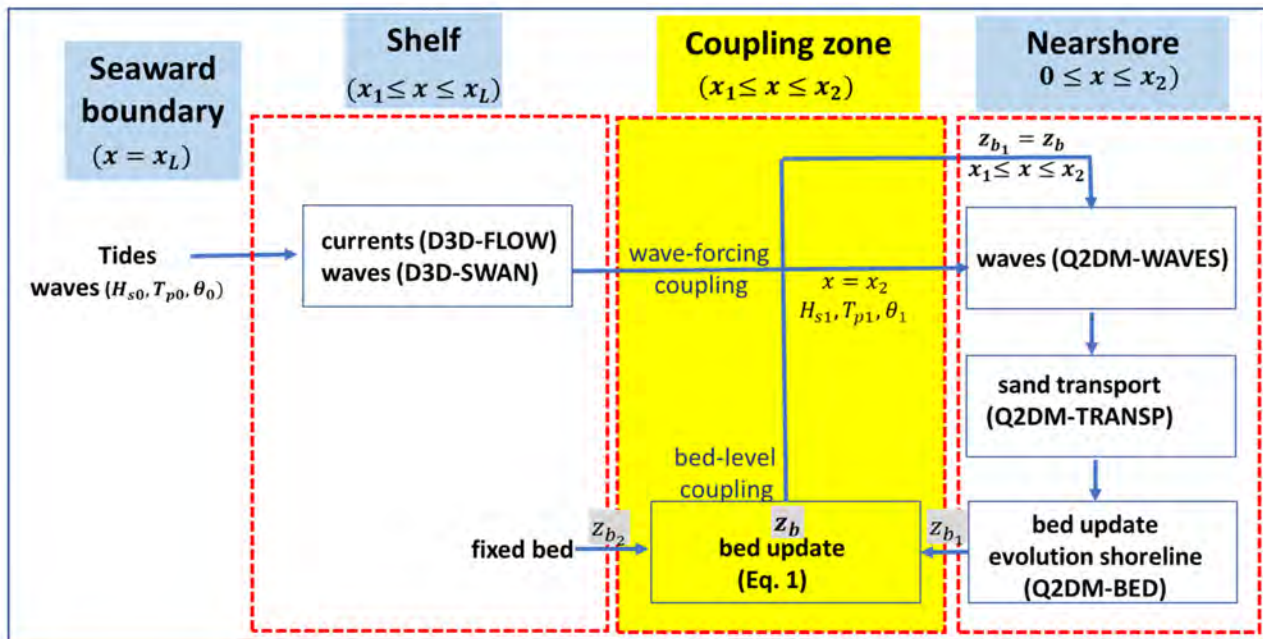


Figure 101 – Schematic view of the structure of the coupled shelf-shoreline model.

The shelf model (D3D + SWAN) computes currents and waves. At the seaward boundary ( $x_L$ ), a propagating  $M_2$ -tide and obliquely incoming waves with significant wave height  $H_{s0}$ , peak period  $T_{p0}$  and wave direction  $\theta_0$  (relative to the shore-normal, positive counter-clockwise) are prescribed. The shoreline model (Q2DM = Q2Dmorfo) computes waves, sand transport and the resulting changes in nearshore bottom and shoreline. At the offshore boundary ( $x_2$ ), wave parameters  $H_{s1}$ ,  $T_{p1}$ ,  $\theta_1$  computed by the shelf model are imposed. The coupling between the shelf and shoreline models is realized by 1) allowing the nearshore bed-level ( $z_{b1}$ ) inside the coupling zone to be affected by that of the shelf ( $z_{b2}$ ) (bed-level coupling) and by 2) imposing the wave parameters computed by the shelf model at  $x_2$  as wave forcing in shoreline model (wave-forcing coupling).

The coupled shelf-shoreline model consists of rectangular shelf and nearshore domains (Figure 28). A Cartesian coordinate system is used, with  $x$  a cross-shore,  $y$  an alongshore and  $z$  a vertical coordinate. The shelf and nearshore domains cover areas  $\{x_1 \leq x \leq x_L, 0 \leq y \leq y_L\}$  and  $\{0 \leq x \leq x_2, 0 \leq y \leq y_L\}$ , respectively,. Furthermore, a coupling zone is defined in the interval  $\{x_1 \leq x \leq x_2, 0 \leq y \leq y_L\}$  (red rectangle in Figure 28) by allowing the seaward part of the nearshore and the landward part of the shelf to overlap each other. Bed-levels  $z = z_{b1}$ ,  $z = z_b$  and  $z = z_{b2}$ , which are defined with respect to a reference level  $z = 0$  (mean sea level, MSL), denote the bottom levels of the nearshore, coupling zone and nearshore, respectively. The shoreline is situated at position  $x_s(y, t)$ , which depends on longshore coordinate  $y$  and time  $t$ . The shoreline domain is divided in a dry beach ( $z_{b1} > 0$ ) and wet beach areas ( $z_{b1} \leq 0$ ). The former area is located between 0 and  $x_s$  and the latter between  $x_s$  and  $x_2$ .

## Structure coupled model

The structure of the coupled model is depicted in Figure 101. The Delft3D (D3D) and SWAN models are used to solve the (2DH) hydrodynamics (currents and waves) on the shelf. Bed-level  $z_{b_2}$  of the shelf is kept constant in time (morphostatic). Shoreline model Q2Dmorfo solves 1) waves (based on linear wave theory), 2) sediment transport (based on empirical formulations that use the wave field), 3) the evolution of the nearshore bed-level  $z_{b_1}$  (based on spatial gradients in the sediment transport) and 4) the evolution of shoreline position  $x_s(y, t)$ . The latter position is determined using a linear interpolation between the cross-shore locations of the first wet cell and the last dry cell of the nearshore domain. The coupling between the shelf and shoreline models is realized by, first, allowing the nearshore bed-level ( $z_{b_1}$ ) in the coupling zone to be affected by that of the shelf ( $z_{b_2}$ ) (bed-level coupling). This is established by computing a new bed-level of the coupling zone  $z_b$  as the weighted average of the shelf and nearshore bed-levels according to

$$z_b = g(x)z_{b_1} + [1 - g(x)]z_{b_2}, \quad \text{for } x_1 \leq x \leq x_2, \quad (\text{A5})$$

$$g(x) = \frac{1}{2} \left[ 1 + \tanh\left(\frac{x-x_0}{w}\right) \right],$$

with  $g(x)$  a weight function,  $w$  a decay width and  $x_0$  the centre of the coupling zone. Second, the wave parameters computed by the shelf model at  $x_2$  (significant wave height  $H_{s1}$ , peak period  $T_{p1}$  and wave direction  $\theta_1$ ) are used as wave forcing to drive the shoreline model (wave-forcing coupling).

## Initial bottom topography

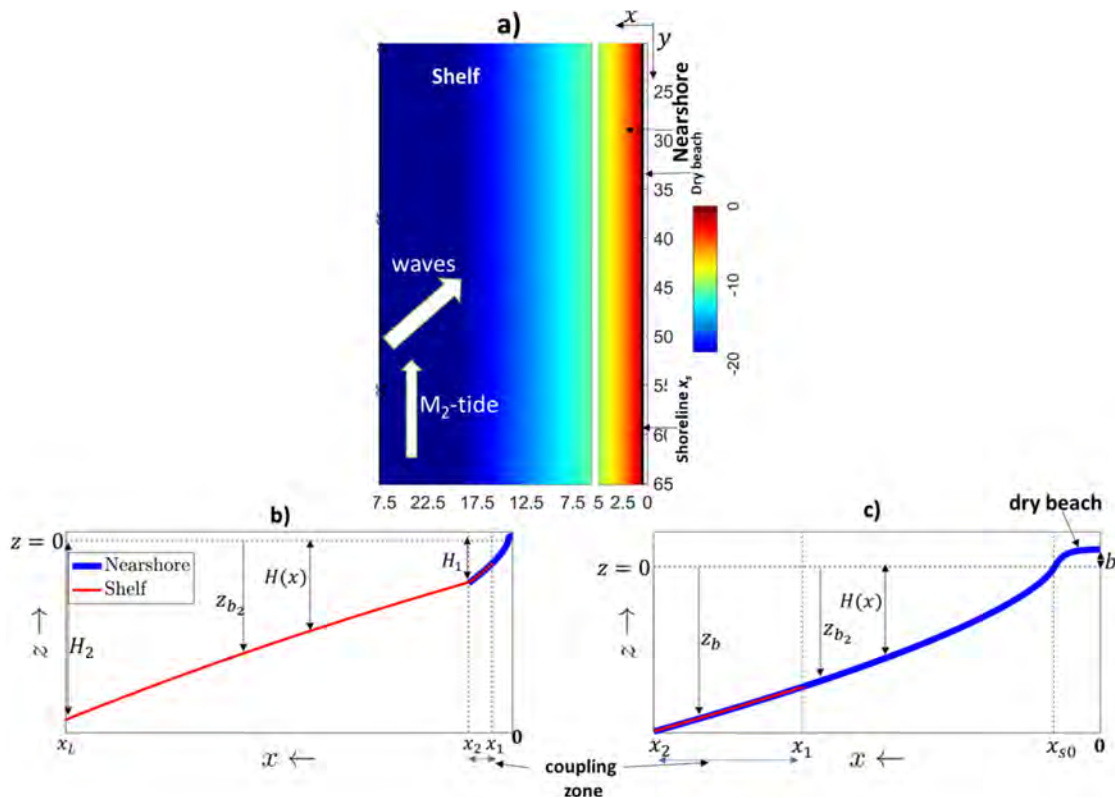


Figure 102 – Setup of the coupled shelf-shoreline model.

a) Initial bathymetry in the coupled model system. b) View of the cross-shore profile of depth  $H(x)$  of the coupled shelf-shoreline model, which is described by Eq. A6. A zoom-in on the region between 0 and  $x_2$  is displayed in panel c. The shelf-shoreline system comprises a dry beach ( $0 \leq x \leq x_{s0}$ ), whose height gradually decreases from  $b$  at  $x = 0$  to 0 at  $x = x_{s0}$ . In the area  $x_{s0} \leq x \leq x_2$  (including the coupling zone between  $x_1$  and  $x_2$ ), depth  $H(x)$  is governed by a shifted Dean equilibrium profile, while further offshore,  $H(x)$  increases linearly from  $H_1$  at  $x = x_2$  to  $H_2$  at the seaward boundary ( $x_L$ ).

As initial bottom topography, the shelf and nearshore are assumed to have a longshore uniform depth  $H(x)$  that depends only on the cross-shore coordinate  $x$  as follows (Figure 102):

$$H(x) = \begin{cases} -b \left(1 - e^{-\frac{\beta(x-x_{s0})}{b}}\right) & \text{if } 0 \leq x \leq x_{s0}, \\ \frac{3}{2}\beta\alpha^{1/3}[(x-x_{s0}+\alpha)^{2/3} - \alpha^{2/3}] & \text{if } x_{s0} \leq x \leq x_2, \\ \frac{H_2-H_1}{x_2-x_L}(x_2-x) + H_1 & \text{if } x_2 \leq x \leq x_L. \end{cases} \quad (A6)$$

According to the above expressions, the dry beach ( $0 \leq x \leq x_{s0}$ ) has a height that gradually increases from 0 at  $x_{s0}$  (initial position of the shoreline) to  $b$  at the landward end ( $x = 0$ ). Parameter  $\beta$  is the swash slope. The wet beach ( $x_{s0} \leq x \leq x_2$ ) is assumed to have a shifted Dean equilibrium beach profile. Constant parameter  $\alpha$  is obtained by imposing that  $H(x_2) = H_1$ . Further offshore, on the shelf, depth  $H(x)$  is assumed to increase from  $H_1$  at  $x = x_2$  to  $H_2$  at  $x = x_L$ .

### Overview coupled model parameters

Table 14 – Overview of the physical and numerical parameters of the coupled shelf-shoreline model.

| Parameter                      | Value                       | Description                                      |
|--------------------------------|-----------------------------|--|
| $x_L \times y_L$               | $55 \times 75 \text{ km}^2$ | Dimensions shelf-nearshore system.               |
| $x_{s0}$                       | 500 m                       | Initial shoreline position.                      |
| $[x_1, x_0, x_2, w]$           | [2500, 3950, 5200, 450] m   | Parameters transition zone.                      |
| $[b, \beta]$                   | [1 m, 0.01]                 | Parameters dry beach.                            |
| $[\alpha, H_1, H_2]$           | [13.7 m, 10 m, 43 m]        | Parameters initial depth.                        |
| $[\hat{\eta}_2, \Delta\psi_2]$ | [1.8 m, 31.5°]              | $M_2$ -tidal forcing.                            |
| $[H_{s0}, T_{p0}, \theta_0]$   | [1 m, 6 s, 50°]             | Wave forcing parameters.                         |
| $\Delta t_2$                   | 1 min                       | Time step in shelf model (in minutes).           |
| $[\Delta x_2, \Delta y_2]$     | [750, 750] m                | Grid size shelf model.                           |
| $\Delta t_1$                   | 0.01 d                      | Time step in shoreline model (in days).          |
| $[\Delta x_1, \Delta y_1]$     | [20, 750] m                 | Grid size in shoreline model.                    |
| $\Delta t_c$                   | 1 y                         | Coupling time between the two models (in years). |

### Group velocity

Magnitude of the group velocity vector  $\vec{c}_g$  is computed using following expression:

$$|\vec{c}_g| = \frac{\sigma}{2k} \left[ 1 + \frac{2kD}{\sinh(2kD)} \right], \quad (A7)$$

where  $\sigma$  is the wave frequency,  $k$  is the wavenumber and  $D$  is the depth.

## Appendix 2.3 Adjustments in the Delft3D model code

The state-of-the-art D3D shelf model is established through implementing following changes in the Fortran files of the original Delft3D code, which is the version 7545.

- *eroded.f90* → Main sediment file, calls *eqtran.f90* and *adjust – bedload.f90*
- *adjust – bedload.f90* → A new bedslope formulation has been added.
- *eqtran.f90* → a new option (*iform=7*) is added, which calls a Bailard type transport formula (defined in *tranb7.f90*).
- *tranb7.f90* → contains the advective sediment transport.
- *rdmor.f90* → A new option for *lslope* is added (*lslope=5*), which computes bedslope terms according to the bedload formulation.
- *rdtrafrm.f90* → Settings of new transport formulation (*iform=7*) adjusted.
- *morphology – data – module.f90* → additional models variables are defined.
- *wrsedm.f90* → Some additional model output ( $u_{rms}$ ,  $h$ ,  $\vec{V} \cdot \vec{q}_{tot}$ , etc.) is programmed.
- *taubot.f90* → New bedshear stress formulation added.
- *windtostress.f90* → Option of constant windshear stress added.
- *bott3d.f90* → This routine, which computes the divergence in sediment transport, has been simplified.

These new D3D shelf model can be found in the Mozes project folder.

[p:\20\\_079-MorfoInteract\3\\_Uitvoering\Deeltaak2\\_IdealizedModel\AdjustedD3DCode\](p:\20_079-MorfoInteract\3_Uitvoering\Deeltaak2_IdealizedModel\AdjustedD3DCode\)

DEPARTMENT **MOBILITY & PUBLIC WORKS**  
Flanders hydraulics

Berchemlei 115, 2140 Antwerp

**T** +32 (0)3 224 60 35

**F** +32 (0)3 224 60 36

[waterbouwkundiglabo@vlaanderen.be](mailto:waterbouwkundiglabo@vlaanderen.be)

[www.flandershydraulics.be](http://www.flandershydraulics.be)